

AMPA receptors in the development and treatment of epilepsy

Sophie Louise Williams

A thesis presented for the degree of
Doctor of Philosophy

University College London

Department of Clinical and Experimental Epilepsy
Institute of Neurology

April, 2017

Declaration

I, Sophie Louise Williams, confirm that the work presented in this thesis is my own. Where information has been derived from other sources, I confirm that this has been indicated in the thesis.

April 2017

Abstract

In this thesis I have determined the effects of seizures on AMPA receptors and examined the effects of AMPA receptor modulation, by medium chain triglycerides and derivatives, on seizures. AMPA receptors play a central role in synaptic transmission in the brain and are critical for the generation of seizure activity.

Recent work has indicated that prolonged seizures alter AMPA receptor transmission. Here I determined whether these changes occur in an acute *in vitro* seizure model, to aid exploration of the underlying mechanisms of these alterations. I demonstrated that, as observed *in vivo*, seizure activity changes the kinetics of AMPA receptor-mediated currents by increasing the proportion of GluA2-lacking, calcium permeable AMPA receptors. I next showed that this subunit switch is dependent on the activation of NMDA receptors and calcineurin.

In a separate set of experiments I determined the effects of a range of novel AMPA receptor antagonists on synaptic transmission and seizure activity. Decanoic acid, a key component of the medium chain triglyceride ketogenic diet used in refractory epilepsy, has recently been shown to act as a non-competitive AMPA receptor antagonist. Here I showed that a range of structurally related compounds which also act as AMPA receptor antagonists are effective in *in vitro* models of seizure-like activity. I have further explored the mechanisms underlying decanoic acid's action. Decanoic acid is synergistic with the AMPA receptor antagonist, perampanel, and is not use-dependent. Moreover, I have shown that decanoic acid has an action at voltage-gated sodium channels to decrease the intrinsic excitability of neurons. Decanoic acid reduces the persistent sodium current, without altering the transient sodium current. Surprisingly, decanoic acid has minimal effect on *in vivo* status epilepticus (prolonged seizure activity) possibly because of rapid and extensive metabolism by the liver. Lastly, I undertook preliminary experiments in human neurons. Decanoic acid effectively reduces induced seizure-like activity in slices from surgically-resected human neocortical tissue. It inhibits AMPA receptor-mediated currents but does not alter intrinsic excitability, as in rat CA1, possibly due to regional differences in neuronal properties.

My findings indicate that seizure activity rapidly changes the AMPA receptors expressed in the synapse and identify a range of compounds that target AMPA receptors, which are effective against seizure activity.

Contents

1	Introduction	16
1.1	Epilepsy	16
1.1.1	Epileptogenesis	16
1.1.2	Hippocampal networks in epilepsy	17
1.1.3	Receptors changes in epilepsy	18
1.1.4	Cell loss in epilepsy	19
1.2	Epilepsy treatments	20
1.2.1	Antiseizure drugs	20
1.2.2	Invasive treatments for epilepsy	22
1.2.3	The ketogenic diet	23
1.3	The ionotropic glutamate receptors: AMPA receptors	27
1.3.1	General structure of AMPA receptors	27
1.3.2	Auxiliary subunits regulate AMPA receptors	28
1.3.3	Post translational modifications of AMPA receptors	30
1.3.4	Location and function of CP-AMPA receptors	31
1.3.5	AMPA receptor trafficking and constitutive recycling	33
1.3.6	Regulated trafficking of AMPA receptors	34
1.4	AMPA receptors in epilepsy	40
1.4.1	Subunit expression is changed post-status epilepticus	40
1.4.2	Age-dependency of AMPA receptor composition	41
1.4.3	Toxicity due to CP-AMPA receptors	41
1.4.4	Action of AEDs at the AMPA receptor	44
1.5	Sodium channels	46
1.5.1	Sodium channels in epilepsy	47

1.6	Circuits of the hippocampus	49
1.7	Models of temporal lobe epilepsy	51
1.7.1	Human resected tissue slices	51
1.7.2	Acute slices	51
1.7.3	<i>In vivo</i> models	52
2	Materials and Methods	55
2.1	Animals	55
2.2	Acute rat hippocampal slices	55
2.3	<i>Ex vivo</i> induction of epileptiform activity	56
2.4	Single cell electrophysiology	59
2.4.1	Voltage clamp	60
2.4.2	Current clamp	63
2.5	Extracellular recordings	65
2.5.1	Epileptiform activity	65
2.5.2	Synergy between decanoic acid and perampanel	65
2.5.3	Use-dependence	67
2.6	Human surgically resected tissue	69
2.7	Computational models	70
2.7.1	Quantitative modelling of Schaffer collateral-CA1 synapse	70
2.7.2	Peak-scaled non stationary fluctuation analysis	70
2.8	Rodent model of epilepsy	73
2.8.1	Electrically-induced Status Epilepticus model	73
2.9	Statistics	77
3	AMPA receptor properties are altered after <i>in vitro</i> SE	78
3.1	Summary	78
3.2	Introduction	80
3.3	Results	82
3.3.1	Theoretical relationship between proportion of CP-AMPA receptors and rectification index	82
3.3.2	Comparison of epileptiform activity between <i>in vitro</i> models of seizure activity	82

3.3.3	0-Mg ²⁺ aCSF induces rectifying AMPA receptor-mediated currents . .	84
3.3.4	PTZ-aCSF induces rectifying AMPA receptor-mediated currents . . .	86
3.3.5	Pharmacological detection of CP-AMPA receptors using NASPM . . .	86
3.3.6	Variance analysis for estimation of conductance of synaptic AMPA receptors	89
3.3.7	Blocking CP-AMPA receptors with NASPM is insufficient to inhibit PTZ-induced epileptiform discharges	91
3.4	Discussion	95
4	Investigation into the mechanism of expression of CP-AMPA receptors	98
4.1	Summary	98
4.2	Introduction	99
4.3	Results	102
4.3.1	Inhibition of NMDA receptors blocks expression of CP-AMPA receptors in a seizure model	102
4.3.2	Inhibiting calcineurin reduces seizure-induced rectification of AMPA receptor-mediated currents.	103
4.3.3	Tyrosine phosphatase inhibition increases rectification in control slices to match the seizure model	106
4.4	Discussion	110
5	The action of decanoic acid and other MCTs at AMPA receptors	113
5.1	Summary	113
5.2	Introduction	115
5.3	Results	117
5.3.1	The anti-seizure effect of decanoic acid can be explained by its action at AMPA receptors	117
5.3.2	Modification of epileptiform activity by derivatives of medium chain triglycerides	117
5.3.3	Decanoic acid can not block status epilepticus <i>in vivo</i>	119
5.3.4	Decanoic acid has no effect on the kinetics of AMPA receptor EPSCs	119
5.3.5	The action of decanoic acid at AMPA receptors was not use-dependent	122

5.3.6	Perampanel and decanoic acid act synergistically to reduce epileptiform discharges	122
5.4	Discussion	124
6	Novel actions of decanoic acid on neuronal excitability	129
6.1	Summary	129
6.2	Introduction	130
6.3	Results	131
6.3.1	Neuronal intrinsic excitability is reduced by decanoic acid	131
6.3.2	Branched derivatives of octanoic acid also reduce neuron intrinsic excitability	132
6.3.3	Decanoic acid does require activation of PI3 kinase to reduce intrinsic excitability	132
6.3.4	Actions of decanoic acid on intrinsic excitability are TTX-sensitive	136
6.3.5	Decanoic acid did not change the transient sodium current	140
6.3.6	Decanoic acid reduced the persistent sodium current	140
6.4	Discussion	144
7	Comparison of experiments in rodent and human cortical tissue	147
7.1	Summary	147
7.2	Introduction	148
7.3	Results	151
7.3.1	Epileptiform discharges are inhibited by decanoic acid in a slice from human temporal lobe	151
7.3.2	Decanoic acid reduces AMPA receptor-mediated currents in human neurons	152
7.3.3	Decanoic acid does not reduce the intrinsic excitability of human neurons	154
7.3.4	No detection of CP-AMPA receptors at synapses on human cortical pyramidal neurons	154
7.4	Discussion	159
8	General Discussion	161
8.1	Excessive network activity causes a shift towards GluA2-lacking AMPA receptor expression at CA1 pyramidal neurons	162

8.2	The shift toward CP-AMPA receptor expression is blocked in the presence of NMDA receptor inhibitors	163
8.3	Specific CP-AMPA receptor inhibitors block epileptiform activity in a similar way to general AMPA receptor inhibitors	166
8.4	AMPA receptor inhibition by decanoic acid can explain the success of the ketogenic diet	166
8.5	Other neuronal targets of decanoic acid reduce network excitability	167
8.6	Recordings from human neocortical neurons can be compared to results obtained in rats	168
8.7	Future Directions	170
8.8	Conclusions and Perspectives	171

List of Figures

1.1	Schematic of common neuronal targets of current anti-epileptic drugs	21
1.2	Schematic of fatty acid metabolism	25
1.3	Binding sites of anti-epileptic drugs acting at the AMPA receptor	45
2.1	Brain dissection schematic for EC-hippocampal horizontal slices	57
2.2	Submerged and interface chambers	57
2.3	Position of stimulating electrodes and recording electrode in stratum radiatum of CA1, and the field response	66
2.4	Estimation of single-channel conductance by peak scaled non-stationary fluctuation analysis	72
3.1	<i>In silico</i> models of the synapse show that CP-AMPA receptors must be present in high proportion to be detected by rectification index	83
3.2	Representative extracellular recordings from stratum radiatum in CA1	85
3.3	General experiment outline	85
3.4	AMPA receptor-mediated currents in the 0-Mg ²⁺ slice model of seizures	87
3.5	AMPA receptor-mediated currents in the PTZ slice model of seizures	88
3.6	Pharmacological inhibition of CP-AMPA receptors in CA1 pyramidal neurons	90
3.7	Estimation of single-channel conductance by peak-scaled NSFA	92
3.8	Inhibition of CP-AMPA receptors by NASPM was not sufficient to inhibit epileptiform activity	94
4.1	Epileptiform activity is both sustained and initiated in the presence of a NMDA receptor antagonist	104
4.2	Inhibition of NMDA receptors blocks rectification of AMPA receptor-mediated currents	105

4.3	Inhibition of calcineurin blocks rectification of AMPA receptor-mediated currents	107
4.4	Inhibition of STEP ₆₁ does not alter rectification after seizures and increases rectification in the non-seizure group	109
4.5	Summary of the key findings in this chapter	112
5.1	The effect of AMPA receptor antagonism on epileptiform activity	118
5.2	Modified methyl-octanoic acid derivatives have anti-seizure properties in an acute slice model of epileptiform activity	120
5.3	Acute treatment with decanoic acid does not suppress electrically-induced SE	121
5.4	Decanoic acid reduces the AMPA receptor-mediated current but has no effect on eEPSC shape	126
5.5	Decanoic acid does not act at AMPA receptors in a use-dependent way	127
5.6	Decanoic acid and perampanel act synergistically to inhibit epileptiform activity in an acute slice model of epileptiform activity	128
6.1	Decanoic acid reduces neuronal intrinsic excitability	133
6.2	Phase plot showing that decanoic acid does not change the kinetics of action potentials	134
6.3	BCCA reduces neuronal intrinsic excitability	135
6.4	Decanoic acid continues to reduce intrinsic excitability of neurons with PI3 kinase blocked	137
6.5	Neuronal input resistance was not altered by decanoic acid	139
6.6	Decanoic acid does not change the transient sodium current	141
6.7	Decanoic acid reduces the persistent sodium current.	143
7.1	Epileptiform discharges are blocked by decanoic acid in one slice from human temporal lobe	153
7.2	Decanoic acid decreases AMPA receptor-mediated currents in neurons from surgically excised human cortex	155
7.3	Decanoic acid does not affect the intrinsic excitability of human neurons . . .	156
7.4	No CP-AMPA receptors were present in human cortical neurons outside the seizure onset zone	158

List of Tables

2.1	Compounds used in project, with standard concentration used.	58
2.2	Racine score: Behavioural classification of seizure severity	75
6.1	Application of decanoic acid does not alter G_{NaT}	141
7.1	Patient details of tissue included in this thesis	150
8.1	Supplementary information: Neuronal properties compared between treatment groups in slice models of status epilepticus	174
8.2	Supplementary information: Neuron properties and action potentials compared in the presence of decanoic acid	175
8.3	Supplementary information: Properties of neurons patched from human surgically resected tissue.	176

List of Abbreviations

ABP	AMPA receptor binding protein
AKAP	A-kinase anchor proteins
AMPA	α -amino-3-hydroxy-5-methyl-4-isoxazolepropionic acid receptor
Arc	Activity-regulated cytoskeleton-associated protein (also known as Arg3.1)
CaN	Calcineurin
CI	Calcium-impermeable
CICR	Calcium-induced calcium release
CP	Calcium-permeable
eEPSC	Evoked excitatory postsynaptic potential
E_{rev}	Reversal potential
EC	Entorhinal cortex
ER	Endoplasmic reticulum
fEPSP	Field excitatory postsynaptic potential
GABAR	γ -aminobutyric acid receptor
GRIP	Glutamate receptor interacting protein
HCN	Hyperpolarisation-activated cyclic nucleotide-gated
$I-V$	Current-voltage
LBD	Ligand binding domain
LTP	Long term plasticity
mGluR	Metabotropic glutamatergic receptor
NMDAR	N-methyl-D-aspartate receptor
NSF	N-ethylmaleimide sensitive fusion protein
NSFA	Non-stationary fluctuation analysis
PI3K	Phosphoinositide 3-kinase
PICK1	Protein interacting with C-kinase-1

PIP3	Phosphatidylinositol (3,4,5)-trisphosphate
PPS	Perforant path stimulation
RI	Rectification index
ROI	Region of interest
SE	Status epilepticus
SEM	Standard error of the mean
TARP	Transmembrane AMPAR regulatory proteins
TMB	Transmembrane domain
VG	Voltage-gated

Compounds

2PEA	2-(4-pentylcyclohexyl) ethanoic acid
4AP	4-aminopyridine
aCSF	Artificial cerebrospinal fluid
AED	Anti-epileptic drug
BCCA	trans-4-butylcyclohexane carboxylic acid
D-AP5	D-2-amino-5-phosphonopentanoic acid
DMSO	Dimethyl sulphoxide
EOA	4-ethyloctanoic acid
GYKI	GYKI-52466, 4-(8-methyl-9H-dioxolobenzodiazepin-5-yl)aniline
MNA	4-methylnonanoic acid
NASPM	1-naphthyl acetyl spermine trihydrochloride
NBQX	2,3-Dihydroxy-6-nitro-7-sulphamoyl-benzo[f]quinoxaline-2,3-dione
PBS	Phosphate buffered solution
PPEA	4-n-pentylphentylethanoic acid
PTX	Picrotoxin
PTZ	Pentylene-tetrazol
TTX	Tetrodotoxin

Publications from this thesis

Chang, P., Zuckermann, A. M. E., **Williams, S.**, Close, A. J., Cano-Jaimez, M., McEvoy, J. P., Spencer, J., Walker, M. C., and Williams, R. S. B. (2015). Seizure control by derivatives of medium chain fatty acids associated with the ketogenic diet show novel branching-point structure for enhanced potency. *Journal of Pharmacology and Experimental Therapeutics*, 352(1):43-52.

Chang, P., Augustin, K., Boddum, K., **Williams, S.**, Sun, M., Terschak, J. A., Hardege, J. D., Chen, P. E., Walker, M. C., and Williams, R. S. B. (2016). Seizure control by decanoic acid through direct AMPA receptor inhibition. *Brain: A Journal of Neurology*, 139(Pt 2):431-443.

Acknowledgements

This thesis has been completed thanks to the incredible patience, insight and support from my family, friends and colleagues.

Sincere thanks to Prof. Matthew Walker for guiding me through the field of epilepsy and synapses and to Dr. Ivan Pavlov for contribution throughout the project, both of which were critical for completion of this thesis. I am very thankful to all members of DCEE for their technical and academical expertise, as well as being great company at the Queens Larder.

I am especially appreciative to Dr. Vincent Magloire for helping me navigate all things electrophysiological and questioning everything I think I know about neuroscience. Thanks to Dr. Nicola Hamil for her patience whilst teaching me *in vivo* experimental techniques. Specific thanks to Jonathan Cornford for his input on Python and NEURON software, Drs. Tom Jensen and Ivan Pavlov for setting up human experiments and Dr. Gareth Morris for recording field potentials in human slices. Thanks to our collaborators at Royal Holloway university, especially Katrin Augustin for sharing her data on *Xenopus oocytes*. Thank-you also to Ramona, Aytakin, Amy, Tawfeeq, Pishan, Stjepana for all their advice and supportive discussions in lab.

I am enormously grateful that my parents and sister, Tasha, encouraged me to be curious about the world whilst I was growing up and thank Jonny for his enthusiasm and kindness, always.

Finally, I am thankful to the MRC Doctoral Training Account for allowing me to contribute this scientific research by funding my 4-year studentship.

Chapter 1

Introduction

1.1 Epilepsy

Historically, epilepsy has been described as a spectrum of disorders caused by hyper-excitabile networks in the brain. The physiologist Fritsch (1838-1927) and psychiatrist Hitzig (1838-1907) were the first to match the mechanism of epilepsy with hyper-excitability; in their paper entitled 'On the Electric Excitability of the Cerebrum' they presented experiments in which they provoked seizures by electric stimulation in the brain cortex of dogs (Fritsch, 1870; Magiorkinis et al., 2014).

Currently around two-thirds, of the 1% of the population with epilepsy, achieve complete seizure control with currently available AEDs. Temporal lobe epilepsy (TLE), the most common form of epilepsy, is defined by spontaneous recurrent seizures originating in the temporal lobe and is often accompanied by cognitive deficits (ILAE case report, 2004). Seizures may trigger neuronal cell death through excitotoxicity leading to hippocampal sclerosis (Meldrum, 1993), although whether sclerosis is the consequence or the cause of pathological activity is debatable (but see Uysal et al., 2003; Kobayashi et al., 2002). In this section I will describe some of the most clearly defined cellular and network changes that occur during epileptogenesis.

1.1.1 Epileptogenesis

Epileptogenesis is the gradual progression of the brain from a normal into an epileptic state following an initial insult such as brain trauma, stroke, tumour, infection and status

epilepticus (SE). During the latent period following a triggering insult to the brain there may not be spontaneous seizures. However, structural and functional changes occur, which increase the propensity for spontaneous seizures by altering the physiology of neuronal networks. There are changes at both the network and neuronal level after an initial insult; Neuronal death occurs via the necrotic and apoptotic pathways, rearrangement of circuits causes the formation of aberrant connections, and in some areas (e.g. dentate gyrus) there is increased neurogenesis (Bengzon et al., 1997; Parent et al., 1998). Surviving neurons often compensate for reduced connections through an increase in intrinsic excitability and axonal sprouting. New or dispersed granule cells are observed outside the usual dense layers, the extent of which is related to cell loss in the polymorph layer of the dentate gyrus (Houser, 1990).

1.1.2 Hippocampal networks in epilepsy

The hippocampus is a highly connected brain region with many properties that allow the generation of epileptic events. Due to intrinsically burst-generating cells and recurrent excitatory connections, the CA3 region relies upon inhibition for regulating network excitability (Colom and Saggau, 1994). Synaptic connections are readily strengthened or weakened with repetitive activation, and the possible presence of gap junctions increases the ability of hippocampal neurons to synchronise their firing.

Interictal and ictal activity can be initiated within the same neuronal network. Interictal activity is distinct from ictal events as it may have an anti-ictal effect (de Curtis et al., 2012), although there is often an increase in interictal activity prior to the transition to seizures. Synaptic mechanisms and key receptor contributions may vary during different stages of an epileptic event. Glutamatergic transmission through α -amino-3-hydroxy-5-methyl-4-isoxazolepropionic acid (AMPA) receptors is required for the spread of pre-ictal activity, which has a distinct initiation site, is high amplitude and spreads more quickly than interictal activity, at least *in vitro* (Huberfeld et al., 2011). The hyperpolarising actions of γ -aminobutyric acid (GABA)_A receptors are important for restraining excitation during interictal and pre-ictal stages of seizure development. During an ictal event however, GABA may become depolarising from intracellular chloride loading and the corresponding shift in driving force of the GABA_A receptor mediated currents (Sepkuty et al., 2002).

The dentate gyrus has been considered a gateway which controls the spread of seizures through the hippocampal network, via entry from the entorhinal cortex (Behr et al., 1998). From this entry point signals propagate to CA3, which is particularly important in synchronisation and in interictal discharge generation. Finally signals propagate to CA1, an area which can also directly receive perforant path input, and back out through the entorhinal cortex in a re-entrant loop. This loop may promote feed-forward propagation (Lu et al., 2016), which leaves the hippocampal network prone to runaway excitation. For more about basic hippocampal circuitry, see section 1.6.

Some evidence suggests that the hippocampus reverts to a morphologically younger developmental stage during epileptogenesis. Cajal-Retzius cells, which usually disappear during development, have been found in sclerosed hippocampi (Blumcke et al., 1996b). Increased dentate gyrus neurogenesis has also been reported particularly in tissue that was obtained from young patients (Blumcke et al., 2001).

1.1.3 Receptors changes in epilepsy

There are also alterations in both receptors and ion channels which change network excitability; for example there is a loss of the potassium channel $K_{V4.2}$ (Francis et al., 1997) and hyperpolarisation-activated cyclic nucleotide-gated 1 (HCN1; Shah et al., 2004) channels, but an up regulation of calcium channels such as $Ca_{V3.2}$ (Khosravani et al., 2005). Some of these changes have a clear pro-epileptic effect, whereas other are compensatory attempts to reduce excitation. Further, it is sometimes difficult to establish the functional consequences of epilepsy-induced alterations, for example with changes in HCN-mediated currents.

Many anti-epileptic drugs (AEDs) target synaptic receptors, which suggests that reducing transmission across the synapse may be a particularly effective way of controlling seizure activity (see Fig 1.1). Epileptiform activity can cause an up-regulation of the NR2B subunit of *N*-methyl-D-aspartate (NMDA) receptors; and NMDA receptors containing this subunit have been implicated in neuronal death by activating a range of apoptotic intracellular cascades (Hardingham et al., 2002). In response to epileptiform activity, there are changes

in the localisation of GABA receptors expression and subunit composition. This may occur to minimise damage.

Similarly, AMPA receptor activation is important for the spread of seizures through neuronal networks; changes in receptor expression and localisation is seen after seizures (see section 1.4). Also, variations in post-transcriptional processing, including alternative splicing and pre-mRNA editing of AMPA receptors have been seen during epileptogenesis. Expression of calcium permeable (CP)-AMPA receptors could contribute to the damage caused by Ca^{2+} overloading and a larger single-channel conductance (Liu and Zukin, 2007).

Receptor changes are not unique to neurons. Astrocytes also show alterations in glutamate transporters and receptors, as well as inwardly rectifying potassium channels (K_{ir} channels) and aquaporins (Binder and Steinhuser, 2006).

1.1.4 Cell loss in epilepsy

Cell death in response to seizures follows specific patterns depending on the seizure foci, or the model used *in vivo*. Status epilepticus is an extreme form of epilepsy, characterised by prolonged seizures, resulting in considerable cell loss (Meldrum, 1993). In the hippocampus, the CA1 pyramidal cell layer and dentate hilar cells are particularly at risk of cell loss. This pattern of cell loss can be matched in rodent models of epilepsy such as perforant path stimulation (PPS model) and to a lesser extent, the kindling model (Parent et al., 1998).

Neuronal death may occur by necrosis or apoptosis depending on the trigger, the time point after seizures and the cell type (Sloviter et al., 1996). Apoptosis from excitotoxicity is prominent in cells that are not used to a high calcium load such as CA1 pyramidal neurons. As well as increased calcium influx, the formation of reactive oxygen species (ROS) such as superoxide (O_2^-) by NADPH oxidase and xanthine oxidase (Kovac et al., 2014; Williams et al., 2015). Cell loss is partially compensated for by increased neurogenesis in the hippocampus, but many of the new neurons here form connections which may promote seizure propagation (Blumcke et al., 1996a). Glial cells respond to seizures by reactive microgliosis and then astroglial death. This disrupts the blood-brain barrier and is involved in formation of aberrant synaptic connections (Binder and Steinhuser, 2006).

Neuronal death can cause drug refractory epilepsy, as well as cognitive decline, memory loss and behavioural changes. If the cells targeted by AEDs are lost then the controlling effect is lost (Sisodiya, 2003).

1.2 Epilepsy treatments

The first-line of treatment for seizure control is always pharmacological. If multiple AEDs are tried without success, other treatments such as surgery or dietary change can prove effective for seizure prevention. However, epilepsy is not a static disorder. Patients can become refractory to treatments which have controlled seizures for many years previously. In this case, using an AED with a different molecular target can be effective or a non-pharmacological treatment option can be attempted (see Fig 1.1).

1.2.1 Antiseizure drugs

Many people achieve adequate seizure control from currently available AEDs. Common targets for AEDs are voltage-gated (VG) ion channels and synaptic receptors (Meldrum and Rogawski, 2007). Most AEDs have multiple mechanisms of action, and such drugs have also been reported to target synaptic receptors in addition to their action on VG sodium channels (Fig 1.1). Even though the drugs may be effective against seizures, it is common for AEDs to have significant side-effects that limit use, which may lead to non compliance in drug taking.

These AEDs are seizure blocking but not disease modifying, as they only provide symptomatic treatment and have not been demonstrated to alter the course of epilepsy. A number of factors affect the efficacy of AEDs including compliance and drug resistance. The cause of drug resistance is likely to be multifactorial; changes at the blood-brain barrier could reduce the concentration of drug reaching the brain and acquired changes at the target membrane could block effectiveness (Loscher et al., 2013). Animal studies suggest that treatment from the initial trigger causing epilepsy may prevent epileptogenesis (Walker et al., 2002).

Pre-clinical studies in which AMPA receptors are blocked have generally looked promising as epilepsy treatments. However, as AMPA receptors play a critical role in the mechanism

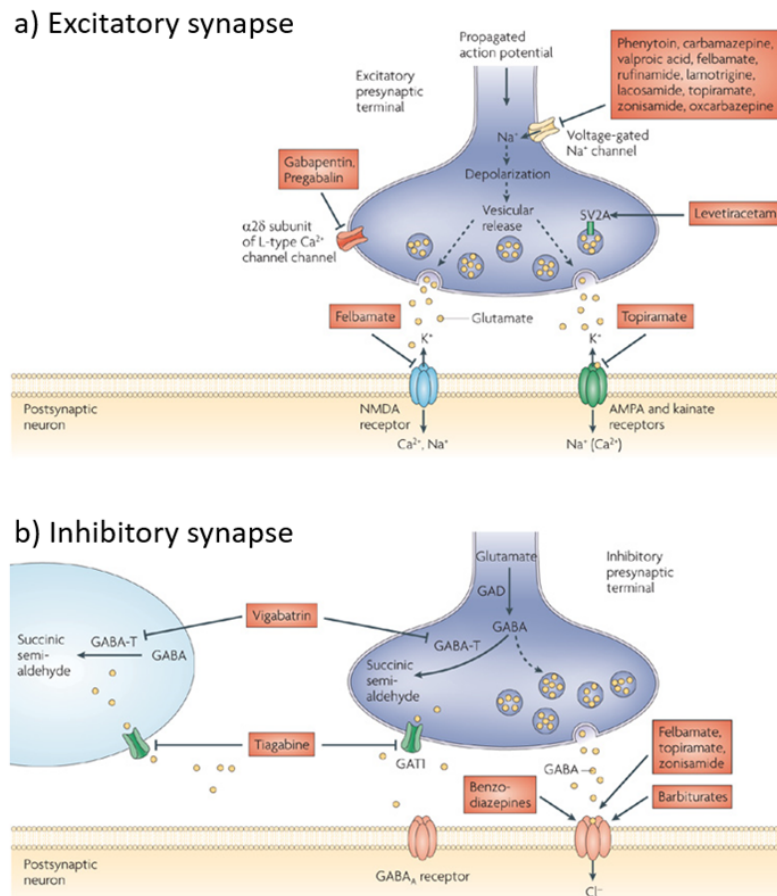


FIGURE 1.1: Schematic of common neuronal targets of current anti-epileptic drugs.

AEDs target synaptic proteins to (a) reduce excitatory transmission and (b) increase inhibitory transmission. A large class of drugs also target voltage-gated (VG) sodium channels which block the intrinsic excitability of neurons. Red boxes contain examples of drugs acting at these specific targets, for controlling seizures. Reused with permission from Bialer and White (2010).

of learning and memory, concerns have been raised about their clinical use. More recently, interest has been regenerated at targeting AMPA receptors in epilepsy (Rogawski, 2013). Perampanel is a newly approved AED which targets all subtypes of AMPA receptor. It acts as a selective negative allosteric AMPA receptor antagonist, which has slow kinetics, a high affinity and is concentration-dependent. Perampanel inhibits AMPA receptor-induced Ca^{2+} influx from the GluA2-lacking AMPA receptors, in cell cultures of cortical cells (Hanada et al., 2011).

Although not a prescribed treatment, post-seizure administration of AMPA receptor antagonists results in attenuation of AMPA receptor potentiation and phosphorylation in animal studies (Rakhade et al., 2008). This treatment was also found to prevent long term increases in seizure susceptibility and seizure-induced neuronal injury.

1.2.2 Invasive treatments for epilepsy

For those whose seizures can not be managed by AEDs alone, there are invasive treatments which can allow seizure control. Resection of the region generating seizures, or cutting connections from the onset zone to other brain areas can prevent seizures, but are only possible in focal epilepsy and carry the normal risks associated with brain surgery. Before surgery, patients undergo seizure monitoring, electroencephalogram (EEG), magnetic resonance imaging (MRI), and positron emission tomography (PET) examination to gain vital information about the location and size of the seizure focus. These tests determine if surgery is a possible option.

Neuromodulation therapy involves implanting a stimulating electrode to target specific areas, such as the epileptic foci. Deep brain stimulation and transcranial direct current stimulation are examples of neuromodulation. The hippocampus and thalamus are often targets for this (Morace et al., 2016). Although it is unclear how neurostimulation works, one hypothesis is that applying current to a certain structure will induce local inhibition to inhibit overexcitable tissue, or projections between hyperconnected networks.

Transcranial magnetic stimulation uses strong current stimulation at low frequency targeting the epileptic zone. It has long lasting effects and significantly reduces seizure frequency in a

randomised controlled study in humans (Sun et al., 2012). Electrical stimulation promotes plasticity, which could lead to the longer term benefits in epilepsy.

1.2.3 The ketogenic diet

Controlled dietary interventions represent another method of seizure control, which is particularly effective in children whose seizures cannot be controlled by medication alone. During the 1920s the effects of starvation, by induction of the ketogenic diet, and altered cerebral oxygen were of interest in seizure control (Lennox and Cobb, 1928). The ketogenic diet is a strict high-fat, low-carbohydrate diet commonly used in refractory epilepsy. It is a successful epilepsy treatment in 30% of patients after 12 months (Li et al., 2016), but there are difficulties relying on seizure control through this diet due to high attrition rates (Payne et al., 2011), as it is inflexible and difficult to tolerate. Adverse gastro-intestinal related effects are common, such as diarrhoea, vomiting, bloating, and cramps (Liu, 2008).

Several variations of the ketogenic diet exist, with the medium chain triglyceride (MCT) ketogenic diet allowing more flexibility, as some calorific intake from carbohydrates is allowed. In this diet a high percentage of daily calories are obtained from MCT oil, which is derived from coconut oil and contains 81% octanoic acid and 16% decanoic acid, both of which reach the brain at a clinically relevant concentration (Haidukewych et al., 1982).

1.2.3.1 Metabolic effects

The mechanism by which the ketogenic diet allows seizure control is not completely understood yet. Initially the fasting period of the ketogenic diet was thought to bring cessation from seizures by forcing the main method of metabolism to change. The primary source of energy for neurons is switched from glucose to ketone bodies, which are produced during the course of the diet (Lutas and Yellen, 2013). Later, ketone bodies were thought to be an active molecule in seizure control. Several other mechanisms exist that may be responsible for the antiepileptic action of the ketogenic diet, including disruption of glutamatergic synaptic transmission, inhibition of glycolysis, and activation of ATP-sensitive potassium channels (Lutas and Yellen, 2013).

Fatty acids are broken down by β -oxidation in the mitochondria (see Fig.1.2). This reaction

increases expression and activity of mitochondrial uncoupling proteins in the hippocampus of juvenile mice subjected to a high-fat ketogenic diet. The process also produces acetyl-CoA and co-enzymes that reduce ROS formation by the respiratory chain. This may constitute a neuroprotective mechanism aimed at reducing oxidative stress (Sullivan et al., 2004). In studies in which mitochondrial function is impaired, the ketogenic diet improves mitochondria respiratory chain function (Greco et al., 2015). Specifically, MCTs are used by the liver to produce β -hydroxybutyrate and acetoacetate, which are ketone bodies and can be used as an energy source. The MCT decanoic acid increases seizure threshold when administered alone in mice (Wlaz et al., 2015).

1.2.3.2 Synaptic targets

Recently it has been shown that decanoic acid acts via synaptic AMPA receptors as a non-competitive antagonist (Chang et al., 2016). Decanoic acid, a ten carbon, straight-chain fatty acid is present at higher concentrations in those on the ketogenic diet and is able to cross the blood-brain barrier (Haidukewych et al., 1982). A binding site has been proposed on the AMPA receptor from amino acid modelling, which is different to that of perampanel (see also section 1.4.4). In acute hippocampal slices, decanoic acid application can completely block epileptiform discharges in seizure models (Chang et al., 2013). Decanoic acid acts on all subunits of AMPA receptors, but favours GluA2 (Chang et al., 2016).

Reducing glutamatergic transmission onto excitatory pyramidal cells would logically reduce transmission of over-active signals. This same mechanism at inhibitory interneurons could disinhibit the circuits, although if GABAergic transmission during seizures becomes depolarising then a general toning down of synaptic transmission would be advantageous (see Cossart et al., 2005 for review).

Polyunsaturated fatty acids found in the typical ketogenic diet act at the A-type potassium channel and on the transient sodium current, to reduce intrinsic excitability (Tigerholm et al., 2012). It would be surprising for this, or any one of the mechanisms described above, to be the only anti-seizure mechanism that the ketogenic diet works via, as many patients achieve seizure freedom on the ketogenic diet even after failed attempts with con-

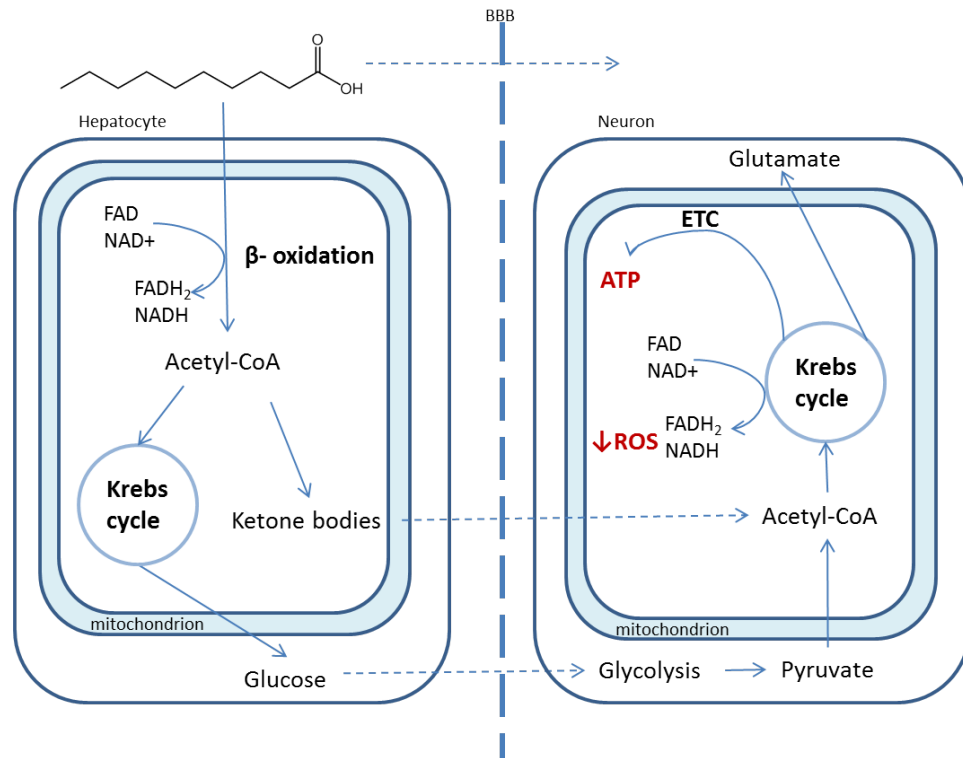


FIGURE 1.2: Schematic of fatty acid metabolism.

Medium chain triglycerides (such as decanoic acid) can move across the cell membrane and into the mitochondria without an carrier protein. Fatty acids are converted to acetyl-CoA in hepatocytes by β -oxidation. Acetyl-CoA is converted into ketone bodies, or used as a substrate in the Krebs cycle, where glucose is produced. Medium chain triglycerides, ketone bodies and glucose are all able to cross from blood capillaries through the blood-brain barrier (BBB) into the CNS. Glucose is converted to pyruvate by glycolysis inside the neuron. Pyruvate and ketone bodies can be converted back to acetyl-CoA, which can enter Krebs cycle, in a process that produces the energy substrate ATP via the electron transport chain (ETC), as well as glutamate. Krebs cycle co-produces Flavin adenine dinucleotide+H₂ (FADH₂) and Nicotinamide adenine dinucleotide+H (NADH). These redox cofactors can salvage ROS. Figure is based on Gano et al. (2014).

ventional AEDs. The benefit of the diet is likely to be a general facilitative effect of multiple mechanisms of action. The difficulty complying with the specific requirements for the ketogenic diet restrict its benefit for controlling seizures in the general population with epilepsy. By determining the targets through which molecules in the ketogenic diet act to control hyperexcitable networks, a new treatment might be found that would be based on the ketogenic diet but allow dietary flexibility.

1.3 The ionotropic glutamate receptors: AMPA receptors

As the main excitatory receptor in the brain, AMPA receptors are an obvious target for the control of seizures. The family of ionotropic glutamatergic receptors encompasses AMPA receptors along with NMDA receptors and kainate receptors. These are encoded by 18 genes, producing 18 individual subunits (Traynelis et al., 2010). AMPA receptors are expressed throughout the brain, on all known neuronal cell types as well as in glia.

1.3.1 General structure of AMPA receptors

AMPA receptors are tetramers, formed by the pairing up of two dimers of subunits. They can assemble with identical subunits (homomers) or as a combination of different subunits (heteromers) from the four AMPA receptor subunits (GluA1-4; Gan et al., 2014). The subunit configuration determines receptor kinetics, modulation and localisation via post translational modifications and interactions with other modulators. If a subunit combination is successfully formed, then the completed receptor is assembled with auxiliary subunits in the endoplasmic reticulum (ER) and exported to the target membrane.

At the synapse, following binding of glutamate or an agonist the AMPA receptors rapidly activates and allows Na^+ , K^+ and, depending on the channel selectivity, Ca^{2+} to pass before inactivating from the agonist unbinding or desensitising. From resting membrane potential (RMP) Na^+ entry depolarises the cell membrane from resting membrane potential; AMPA receptor-mediated currents reverse at 0mV.

All AMPA receptor subunits comprise 3 transmembrane domains (TMD) and 1 re-entrant loop, with an intracellular C-terminal, an extracellular N-terminal and ligand binding domain (LBD). Crystallisation of homomeric AMPA receptors, without the fluid C terminal, was achieved by Sobolevsky et al. (2009), with the addition of heteromeric receptor crystallisation more recently by Herguedas et al. (2016). The TMD forms the channel pore, and contains the Q/R RNA edit site, which is described below. An alternative splicing site on the LBD of AMPA receptor subunits results in flip/flop variants of each subunit. The flop variant has faster desensitisation kinetics and is more common in mature healthy neurons (Mosbacher et al., 1994). However, in the GluA1 homomer, both isoforms desensitise at equal rates (Quirk et al., 2004). The GluA1 subunit also contains a long carboxy (C) tail

with a PDZ binding motif that defines which scaffold and trafficking proteins it is able to interact with. This C-terminal domain contains many phosphorylation sites, as well as ubiquitination, nitrosylation, sumoylation and intracellular protein binding sites.

In the hippocampus, most principal cells express surface AMPA receptors containing both GluA1 and GluA2 subunits (Lu et al., 2009). Inclusion of the GluA2 subunit dramatically alters permeability of Ca^{2+} and Zn^{2+} through the pore, mediated by a post-transcriptional modification site (Q/R) on GluA2 mRNA (Sommer et al., 1991). After editing neutral glutamine (Q) to charged arginine (R), positively charged calcium ions are repelled by the positively charged pore lining. Therefore there is almost complete block of calcium permeability when the GluA2 subunit is present in the receptor. 99.99% of pre-mRNA receptors have this post-transcriptional modification by adenosine deaminase acting on RNA (ADAR2), which is protective against calcium-induced cell death. ADAR2 deficiency produces lethal seizures in mice (Peng et al., 2006). Another RNA edit site, the R-to-G site, is not fully edited when expressed functionally. This is also edited by ADAR2 and changes the kinetics of desensitisation (Hume et al., 1991).

Calcium permeable (GluA2-lacking) channels incur use- and voltage-dependent channel block from endogenous intracellular polyamines. Polyamines block the pore more strongly when the neuron is depolarised, so the channel is less able to pass outward current than inward current. The strong inward rectification of CP-AMPA receptors allows them to be easily distinguished from calcium impermeable (CI) subtypes by their current-voltage ($I-V$) relationship (Cull-Candy et al., 2006). Further, CP-AMPA receptors have markedly increased single-channel conductance (Swanson et al., 1997) and desensitisation rates (Hume et al., 1991).

1.3.2 Auxiliary subunits regulate AMPA receptors

Auxiliary subunits such as transmembrane AMPA receptor regulatory proteins (TARPs) increase the diversity of AMPA receptor properties by allowing specific protein interactions both within the cell and in the extracellular matrix (Schwenk et al., 2014). These subunits interact with synaptic proteins to dynamically regulate surface expression, calcium permeability, accumulation, localisation into and out of the synapse, pharmacology and kinetic

properties of the channel (Cuadra et al., 2004; Menuz et al., 2007; Bats et al., 2013; Studniarczyk et al., 2013).

TARPs are grouped into type I and atypical type II families. Stargazin (γ -2), a typical TARP and the most studied auxiliary subunit, slows channel deactivation and desensitisation (Tomita et al., 2007b), and greatly increases single-channel conductance (Soto et al., 2007). Both stargazin and γ -8 dramatically increase the magnitude of glutamate evoked currents from GluA1 cRNA injected oocytes (Chen et al., 2003). Furthermore, stargazin's presence markedly attenuates the block of CP-AMPA receptors by intracellular polyamines (Soto et al., 2007), while enhancing their sensitivity to extracellular philanthotoxin-433 (Jackson et al., 2011) and increasing their permeability to Ca^{2+} (Kott et al., 2009). Native AMPA receptors contain one to four TARPs, but there is little interaction between TARPs (Kato et al., 2007). A different set of auxiliary AMPA receptor subunits, the cornichons, do not additively increase conductance when expressed alongside TARPs, but may displace AMPA receptor binding to γ -8 (Kato et al., 2010).

TARPs are differentially expressed throughout the brain. In the hippocampus, mature synapses require GluA1 and γ -8 (Rouach et al., 2005) and genetic deletion of γ -8 selectively abolishes sustained depolarisations when bathed in AMPA. Other TARPs are likely to be important for anchoring AMPA receptors to PSD-95, and for reducing receptor desensitisation in response to synaptic glutamate. PSD-95 concentration at the synapse directly determines the number of synaptic AMPA receptors expressed, via their mutual interaction with TARPs.

For CP-AMPA receptors, interaction with an auxiliary subunit can double the average single-channel conductance, slow desensitisation and deactivation, and enhance calcium permeability without affecting open probability (Tomita et al., 2007a; Kott et al., 2009; Soto et al., 2014). Auxiliary subunits are also able to attenuate intracellular polyamine block across all voltages, reverting from inward rectification to a linear I - V relationship (Soto et al., 2007). The conductance of isolated CP-AMPA receptors is already double that of GluA2-containing AMPA receptors (Swanson et al., 1997), so modulation of CP-AMPA receptors by auxiliary subunits can substantially increase excitatory synaptic transmission.

AMPA receptors also interact with cornichons (Schwenk et al., 2009), CKAMP44, and GSG1L (Schwenk et al., 2014; McGee et al., 2015) which is found in dendritic spines of CA1 pyramidal cells and co-localises with GluA2- or GluA4-containing AMPA receptors.

1.3.3 Post translational modifications of AMPA receptors

The location and biophysical characteristics of AMPA receptors can be modulated by protein interactions at the PDZ tail of the C terminal. Throughout the intracellular domain, there are sites for phosphorylation by protein kinase A (PKA), protein kinase C (PKC), and the SRC family tyrosine kinase STEP₆₁ (Lu and Roche, 2012; Hayashi and Huganir, 2004). Proteins can be diversified by tagging with other small molecules at defined sites. Palmitoylation of GluA2 at C⁶¹⁰ increases the stability of CI-AMPA receptors (Yang et al., 2009). This adaptation shows subunit specific effects, and proteins can also be ubiquitinated, glycosylation, nitrosylated and sumoylated.

Phosphorylation patterns are dynamically regulated, and can affect the AMPA receptor-mediated currents differently depending on the sites phosphorylated. At GluA1, calcium entry activates CaMKII to phosphorylate S⁸³¹, which increases single-channel conductance in CI-AMPA receptors only (Derkach et al., 1999). CaMKII also acts at S⁵⁶⁷ in loop 1 to negatively regulate synaptic delivery (Lu et al., 2010). Further, phosphorylation of T⁸⁴⁰ on GluA1 by PKC may be important in LTD, for reducing the number of AMPA receptors present at the synapse (Delgado et al., 2007).

Altering the phosphorylation pattern on GluA2 subunits has a more complex effect. This subunit is not present in most CP-AMPA receptors, so phosphorylation will specifically affect CI-AMPA receptors. The S⁸⁸⁰ position is phosphorylated by PKC, causing internalisation of GluA2-containing receptors by regulating interactions with intracellular trafficking regulators (Chung et al., 2000). Conversely, phosphorylation at Thr⁹¹² leads to activity-dependent reinsertion of internalised GluA2-containing AMPA receptors, via the JNK1 pathway. Phosphorylation at tyrosine sites (including Tyr⁸⁶⁹, Tyr⁸⁷³, and Tyr⁸⁷⁶) also regulates receptor trafficking indirectly by changing GluA2's association with intracellular proteins. New phosphorylation sites by kinases are still being characterised.

Post-translational modifications are triggered by small molecule interactions at the PDZ domain of the C terminus of AMPA receptors, which is different in GluA1 subunits (type I) and GluA2 subunits (type II). This means the two subunits interact with separate proteins; different PDZ domains cannot even both bind to the same version of the scaffolding protein PSD95. 4.1N is required for GluA1 insertion into the membrane, and its action is enhanced by phosphorylation or palmitoylation (Lin et al., 2009). SAP97 is also required for trafficking; it interacts with myosin VI to form a trimeric complex with GluA1 to deliver it to the membrane. Conversely, ablation of Arc/Arg3.1 selectively recruits CP-AMPA receptors to the membrane for homeostatic scaling (Shepherd et al., 2006). A key modulator of AMPA receptor expression is Protein interacting with C-kinase-1 (PICK1), which clusters AMPA receptors and has a Ca^{2+} binding domain that could act as a trigger for AMPA receptor internalisation. Ca^{2+} enhances PICK1 binding to GluA2 and vesicle fusion proteins, to promote endocytosis of CI-AMPA receptors which have been phosphorylated by PKC at S⁸⁸⁰ (Hanley, 2008). This instability of phosphorylated CI-AMPA receptors is in contrast to the stabilisation of CP-AMPA receptor at perisynaptic sites by phosphorylation at S⁸⁴⁵ (He et al., 2009).

Small molecules can interact with mRNA to influence which subunits are translated, and act on nascent proteins at the ER to regulate which will reach the membrane. MicroRNAs are small non-coding RNA molecules which are a form of RNA silencing and post-transcriptional regulation of gene expression. They block the transcription or degradation of a target gene. miRNA124 blocks GluA2 expression by targeting the 3-UTR, leading to the formation of CP-AMPA receptors (Dogini et al., 2013; Dutta et al., 2013). MicroRNAs are dynamically regulated in disease states; for example, miRNA124 is upregulated in epilepsy.

1.3.4 Location and function of CP-AMPA receptors

Under physiological conditions, multiple brain regions have expression of CP-AMPA receptors. For example, in the cerebellum CP-AMPA receptors are expressed in stellate and basket cells, and are used to increase the fidelity of signal propagation along dendrites, since they have a higher conductance and faster channel kinetics than CI-AMPA receptors or NMDA receptors (Abrahamsson et al., 2012; Geiger et al., 1995).

In hippocampal CA1 neurons, the majority of excitatory synapses onto pyramidal neurons express heteromeric AMPA receptors containing GluA1-GluA2 subunits, with a smaller contribution of GluA2-GluA3 heteromers and $\sim 8\%$ GluA1 homomers (Wenthold et al., 1996). CP-AMPA receptors are present on specific interneurons (e.g. OLM interneurons; Lamsa et al., 2007) and glia (Schwenk et al., 2014). There is also age-dependent control of AMPA receptor expression. Early in development, GluA2 lacking AMPA receptors are also expressed at synapses in the neocortical principle cells and CA3 pyramidal neurons (Ho et al., 2007).

CP-AMPA receptors are physiologically interesting as they promote signal transfer close to resting membrane potential and are blocked by polyamines at near 0mV and positive potentials. This contrasts with NMDA receptors which pass more conductance at similar potentials. CP-AMPA receptors allow a unique form of LTP at O-LM interneuron synapses described as "anti-Hebbian", as it is induced by presynaptic activity but prevented by postsynaptic depolarisation (Lamsa et al., 2007).

The transient expression of CP-AMPA receptors at CA1 pyramidal neuron synapses during LTP induction and stabilisation has been described (Plant et al., 2006). However, others have also found CP-AMPA receptors are not necessary for initiation nor stabilisation of LTP (Gray et al., 2007); the requirement may be dependent on the protocol of LTP induction (Park et al., 2016). Silent synapses, the term given to synapses containing NMDA receptors but without AMPA receptors, may have incorporation of CP-AMPA receptors before maturation and the expression of CI-AMPA receptors (Morita et al., 2014). It has been suggested that CP-AMPA receptors are dynamically regulated globally, and removed during sleep. Increases in GluA1-containing AMPA receptor levels in are seen in synapses at both the cortex and hippocampus during wakefulness, and decreases during sleep (Vyazovskiy et al., 2008). Expression levels may also be dependent of the oestrogen cycle (Tada et al., 2015).

In pathological conditions, there have been many reports of CP-AMPA receptor expression in cells where they are not usually found. Ischemic insults trigger the long-lasting down-regulation of GluA2 mRNA and protein expression in CA1 pyramidal neurons, inducing a switch to CP-AMPA receptor expression (Gorter et al., 1997; Dias et al., 2013). In ischemia, the GluA2 subunit switch is PKC-dependent and involves dissociation of GluA2

from PICK1 (Terashima et al., 2004). PICK1 overexpression increases CP-AMPA receptors at pyramidal neuron synapses, possibly by blocking recycling of GluA2 subunits, and blocks LTP (Terashima et al., 2008). Phosphorylation of GluA2 at S⁸⁸⁰ by PKC is crucial for determining the GluA2 binding partner; it therefore regulates its interaction with GRIP (Glutamate receptor interacting protein)/ABP. GluA2 phosphorylation favours binding to PICK1 and hinders interaction with GRIP1.

After SE or spinal cord injury, and in those with Amyotrophic Lateral Sclerosis (ALS) and Alzheimers disease there is also evidence suggesting a decrease in GluA2 mRNA and an increase in CP-AMPA receptor expression (Grooms et al., 2000). These changes in expression are seen both on a local and on a global scale.

1.3.5 AMPA receptor trafficking and constitutive recycling

If the trigger causing an AMPA receptor subunit switch in pathological states were characterised, then the effect of blocking the switch could be studied. However, the precise mechanism of CP-AMPA receptor insertion and CI-AMPA receptor removal is not known. AMPA receptors at the synapse are highly mobile, with a basal turnover rate of 16% surface AMPA receptors endocytosed in 30 minutes (Ehlers, 2000). Trafficking occurs both in a constitutive and in an activity-dependent way, with different mechanisms required for each. AMPA receptors are removed from somatodendritic sites and replacements found from a pool of receptors in the dendritic spine in a one for one manner, at a rate independent to the activity level. This endocytosis requires clathrin, Arc, and binding of the GTPase dynamin-3 to the PSD-enriched protein Homer (Hanley et al., 2002). The endosome either fuses with a lysosome leading to degradation of the receptor, or transports it back to the membrane surface.

As well as leaving directly from the postsynaptic density (PSD), AMPA receptors can leave the synapse by lateral diffusion as has been observed in single-particle tracking experiments. At the perisynapse, the GluA1 subunit moves freely in the membrane. In contrast, it loses mobility at the synapse (Passafaro et al., 2001; Collingridge et al., 2004; Constals et al., 2015). This is because the long C-tail on the GluA1 subunit has a PDZ binding motif which defines the scaffold and trafficking proteins it interacts with, and this blocks its ability to

be directly inserted into the PSD in the absence of activity. Conversely, GluA2 contains a short C-tail, allowing it to be inserted directly into the PSD regardless of activity level. It can directly interact with N-ethylmaleimide Sensitive Fusion protein (NSF; Song et al., 1998) and PICK1 (Braithwaite et al., 2002) as is necessary for membrane fusion. GluA2-3 heteromeric CI-AMPA receptors replace (CP), GluA1-homomers at the synapse through this pathway.

The edited GluA2 subunit is present as a dimer and retained in the ER, to ensure a large pool is constantly available. Unedited subunits readily form tetramers and exit the ER, targeted to nascent or pre-existing synapses. This limits the level of unedited GluA2 subunits in AMPA receptors delivered to synaptic and extra synaptic sites. GluA2 binding to GRIP1 may be important for trafficking and targeting of CI-AMPA receptors (Setou et al., 2002). GRIP and PICK1 are in dynamic equilibrium; after phosphorylation of GluA2 by PKC, the GluA2-GRIP relationship is weakened but PICK1 is unaffected. This allows GluA2 to be inserted into the membrane, and internalised receptors can be captured by PICK1. PICK1 over-expression increases AMPA receptor-EPSCs and the appearance of synaptic CP-AMPA receptors in acute cultured hippocampal slices (Terashima et al., 2004).

Vesicles containing new or recycled AMPA receptors are trafficked to dendritic membranes by kinesin and dyneins. They are then exocytosed by the vesicular SNARE family of proteins and NSF (Araki et al., 2010).

1.3.6 Regulated trafficking of AMPA receptors

In response to activity, dynamin-dependent endocytosis and exocytosis of specific AMPA receptor compositions is triggered. Endocytosis is decreased by synaptic blockade, and increased by synaptic activity, via protein interactions and site directed phosphorylation. An estimated 60-70% of the AMPA receptor population are intracellularly localised, ready for delivery to the cell surface (Bredt and Nicoll, 2003). Further, it has been shown in culture that many dendrites contain GluA1 and GluA2 mRNA, allowing rapid receptor production when the activity level changes (Grooms et al., 2000).

Phosphorylated GluA1-containing AMPA receptors are transported to the membrane by

Ca^{2+} -sensitive, actin-based motor proteins myosin-Va/Vb. Conversely, dephosphorylation initiates the removal of receptors from the synapse. Dephosphorylation of GluA1 by calcineurin, a Ca^{2+} -dependent serine/threonine phosphatase, leads to the internalisation and degradation of CP-AMPA receptors. Reduced activity of calcineurin increases synaptic expression of CP-AMPA receptors by stabilizing GluA1 phosphorylation (Kim and Ziff, 2014).

STEP₆₁ is the tyrosine phosphatase present in CA1 pyramidal neurons, which dephosphorylates sites at AMPA receptor GluA2 subunits and at NMDA receptors. Dephosphorylation of GluA2 subunits causes internalisation of AMPA receptors (Zhang et al., 2008), as well as acting on NMDA receptors.

1.3.6.1 Hebbian Plasticity

AMPA receptors are trafficked to alter the strength of the synapse in different forms of plasticity. In classical Hebbian plasticity, NMDA receptor activation causes an influx of Ca^{2+} , which triggers dynamic AMPA receptor movement into or out of the membrane. Multiple kinases and phosphatases are involved. Simply, activity-dependent activation of PKA, CaMKII or SAP97 causes delivery of AMPA receptors to the perisynapse, and phosphorylation of synaptic AMPA receptors to increase their activity (Song and Huganir, 2002; Fox et al., 2007; Howard et al., 2010); whereas GluA1 dephosphorylation by calcineurin and PP1 signals for receptor internalisation (especially CI-AMPA receptors) and LTD. GluA1 phosphorylation increases the number (Hayashi et al., 2000) and clustering (Xie et al., 1997) of AMPA receptors, or decreases the rise time and decay time constant of synaptic potentials (Ambros-Ingerson et al., 1993). By contrast, phosphorylation of the GluA2 subunit generally leads to internalisation and its dephosphorylation is important in synaptic retention. As discussed above, CP-AMPA receptors may be necessary for stabilisation of LTP (Park et al., 2016), possibly via CaMKI (Guire et al., 2008).

A PKA and CaMKII independent, but PKC and NMDA receptor-dependent form of CP-AMPA receptor mediated LTP has recently been described (Kim et al., 2015b). This form of LTP can be induced when the post synaptic membrane is hyperpolarised in the CA1 of mice lacking GluA2 (Wiltgen et al., 2010). Decreased phosphorylation of IP3 receptors causes decreased Ca^{2+} release from the ER, activating less calcineurin. This stabilises phos-

phorylation of GluA1 subunits at S⁸⁴⁵, keeping them at the synapse to increase the number of CP-AMPA receptors. In addition, a CP-AMPA receptor and protein synthesis-dependent, but NMDA receptor-independent form of plasticity was also seen at CA1 synapses with this conditional knock-out (KO) mouse (Asrar et al., 2009). Calcium entry through the CP-AMPA receptor may be sufficient to induce some forms of LTP when NMDA receptors are blocked or not activated. Polyamine-dependent facilitation allows for selectively enhancing synaptic gain at CP-AMPA receptor expressing synapses following use-dependant relief of polyamine block during high-frequency stimulation (Rozov and Burnashev, 1999).

LTP at dentate gyrus granule cells and fast-spiking interneurons requires coincident activation of CP-AMPA receptors and group I mGluR, causing a strong intracellular Ca²⁺ elevation (Hainmuller et al., 2014) for PKC activation. The GluA1-S⁸⁴⁵ site is necessary for maintaining a perisynaptic pool of CP-AMPA receptors, and these could be recruited to participate in synaptic transmission upon Group 1 mGluR activation (He et al., 2009). This induction is NMDA receptor independent and similar to that seen in other interneurons (eg. O-LM interneurons). The pathway of synaptic strengthening has been studied *in vivo* (Clem and Barth, 2006). Whisker stimulation causes potentiation in a synapse specific manner via CP-AMPA receptor expression. This was seen only in cortical layer 4-2/3 neurons, so it may be the case that only certain synapses increase CP-AMPA receptor expression during potentiation, or that the expression is restricted only to active synapses.

In cerebellar stellate cells high frequency activity replaces the synapse population of CP-AMPA receptors with CI-AMPA receptors (Liu and Cull-Candy, 2000). This process involves PICK1 and NSF interaction with GluA2 (Gardner et al., 2005) and is a self regulating mechanism involving the subunit contribution of AMPA receptors, without affecting the number of receptors.

Conversely, in LTD the role of CP-AMPA receptors is unclear. Calcineurin dephosphorylates S⁸⁴⁵ and promotes AMPA receptor removal from synapses and endocytosis. CP-AMPA receptors are recruited to synapses by anchored PKA during LTD induction but are then rapidly removed by anchored calcineurin. Blocking CP-AMPA receptor activity, recruitment, or removal interferes with NMDA receptor signalling for LTD. Removal of GluA2-containing AMPA receptors is enough to induce some forms of LTD, but additional contributions from

CP-AMPA receptors are required for robust LTD expression. A-kinase anchor proteins (AKAPs) and calcineurin mediate removal of both versions of AMPA receptor (Sanderson et al., 2016).

1.3.6.2 Homeostatic plasticity

Homeostatic plasticity is a process to tune synapses within an optimal activity band, required to restabilise networks and maintain a constant output over time. Bidirectional changes in mini EPSC amplitude measure the scaling up of both synaptic CI- and CP-AMPA receptor numbers in conditions of low activity, and down in conditions of high activity (Wang et al., 2012; Turrigiano et al., 1998).

Over a longer time scale and at a more global level than LTP, initiation of homeostatic plasticity is thought to require CP-AMPA receptors. The loss of activity through L-type Ca^{2+} channels, AMPA receptors or by reduced firing, leads to increases in vesicle pool size and the addition of postsynaptic CP-AMPA receptors to the existing population of CI-AMPA receptors (Ju et al., 2004; Thiagarajan et al., 2005). Stimulated AMPA receptor endocytosis requires the GluA2 subunit, and reducing GluA2 levels with shRNA blocks synaptic scaling. Hou et al. (2008) used cultured neurons to look at site specific changes. CP-AMPA receptors are required for the early induction of homeostatic plasticity only, and PI3K activity was required as it initiates protein synthesis processes. CP-AMPA receptor inclusion may be in input specific scaling only, not global homeostatic plasticity (Hou et al., 2008). Molecular mechanisms are also dependent on the induction method and which synapse is involved.

Synaptic up-scaling of CP-AMPA receptors can be triggered by intracellular and glial-released molecules, for example retinoic acid and the cytokine $\text{TNF}\alpha$ (Poon and Chen, 2008; Ogoshi et al., 2005). *Arc/arg3.1* is an immediate-early gene regulated by neuronal activity, which mediates both global regulation and local homeostatic plasticity at individual synapses. Usually, *Arc/arg3.1* is involved in CP-AMPA receptor upscaling (Beique et al., 2011); at distal dendrites mRNA accumulates at sites of synaptic activity and is locally translated (Steward et al., 1998). *Arc/arg3.1* is co-ordinately induced in populations of neurons implicated in learning, such as hippocampal place cells *in vivo*.

Homeostatic plasticity can be distinguished from LTP/LTD by the activation of group 1 mGluRs. LTD is caused by activation of mGluR1 by agonist binding, whereas activity-dependent Homer1a expression switches mGluR1 from agonist-dependent to independent action. This causes widespread AMPA receptor down-regulation during homeostatic plasticity (Hu et al., 2012), via mechanism linked to the reduction of tyrosine phosphorylation at GluA2.

1.3.6.3 Metaplasticity

Metaplasticity is a higher order regulatory process, described as the plasticity of synaptic plasticity. It sets the threshold and direction of plasticity to keep synapses in a dynamically functional range and prevents the saturation of receptors (Abraham and Bear, 1996). Networks are primed over hours and days by situations such as environmental enrichment or stress; this affects subsequent induction and persistence of plasticity.

The adaptation of plasticity features changes on both sides of the synapse. Presynaptic increases in vesicle turnover are present as well as increases in homomeric GluA1 expression. CP-AMPA receptor recruitment confers a meta-plastic state that promotes LTD, which lasts for days and has a function in processes such as in memory consolidation or in response to prolonged inactivity of synapses as may arise with sensory impairment, stroke, and other forms of neural damage (Thiagarajan et al., 2005).

The mechanisms involved in metaplasticity may be important for synaptic changes observed in epilepsy. An induction protocol which caused depression of LTP in control slices failed to affect LTP amplitude in acute slices after febrile seizures, indicating a failure of metaplasticity mechanism (Zhang and Luo, 2011). Conversely, after a kindling protocol stimulation was less able to induce LTP in the CA1 than in control slices (Schubert et al., 2005).

The expression functional plasticity (FP) has been coined to describe those changes in stimulus-response relationships or in spontaneous patterns that are experimentally induced by electrical stimulation and lasting at least on the order of one hour (Wagenaar et al., 2006). However, this may depend of how strong the induction protocol is. This could be a

good time window in which to study seizure-induced changes.

1.4 AMPA receptors in epilepsy

As the most common fast excitatory receptors in the brain, AMPA receptors are important in epileptic synchronisation and the spread of epileptiform activity across networks. Increased excitability is temporally associated with a rapid increase in expression of AMPA receptor subunits GluA1 and GluA2 after seizures (Rakhade et al., 2008); this may indicate an increase in both CP- and CI-AMPA receptors.

Whilst mutations in AMPA receptors have not been identified as a cause for genetic epilepsies, the observation that mutations in TARPs do cause seizures is consistent with the view that AMPA receptors play a fundamental role in the disorder (Barad et al., 2012). Within the seizure onset area, the distribution of polyamines is differentially altered compared to propagation areas in tissue from MTLE patients (Laschet et al., 1999). Since polyamines are involved in the control of NMDA receptors and CP-AMPA receptors, this is likely to affect neuronal excitability within the network.

1.4.1 Subunit expression is changed post-status epilepticus

Pathophysiological networks states can allow expression of CP-AMPA receptors at synapses in which they are not usually seen, as discussed in section 1.3.4. When there is a switch in the subunit composition of AMPA receptors, this can be monitored at the level of mRNA and proteins. Changes at the AMPA receptor have an effect on synaptic function in models *in vitro*, *in vivo*, and in studies on humans with epilepsy (Loddenkemper et al., 2014). Specifically, Grooms et al. (2000) and Hu et al. (2012) found a marked decrease in both GluA1 and GluA2 expression 12-16 hours after SE. In different regions of the hippocampus both total mRNA content and protein levels were altered; this indicates that the changes were not limited to surface expression of the receptor. There could, however, still be a change in synaptic expression without change in mRNA levels (Cull-Candy et al., 2006). The general rule of GluA2 prevailing over other AMPA receptor subunits in normal adult pyramidal neurons changes 3 days post-SE. GluA2/3 receptors still predominate until 7 days after SE, when more CP-AMPA receptors are expressed (Hu et al., 2012). It has also been demonstrated that expression of GluA1 is elevated in the human epileptic hippocampus, and this positively correlates with axonal sprouting (Ying et al., 1998).

A study by Rajasekaran et al. (2012) found increased rectification of AMPA receptors after 10 minutes (modelling refractory-SE) and 60 minutes (modelling late-SE) of status, when recording evoked EPSCs from CA1 pyramidal neurons in pilocarpine injected adult rats. GluA2 internalisation and changes in internal Ca^{2+} levels were seen using immunocytochemistry and live cell imaging in hippocampal cultures in the 0-Mg^{2+} model of epileptiform activity (Rajasekaran et al., 2012).

Additionally, inhibition of Q/R editing by ADAR2 in GluA2 results in increased excitability of hippocampal neurons with associated spontaneous seizures (Krestel et al., 2004).

1.4.2 Age-dependency of AMPA receptor composition

There is age-dependence both in the AMPA receptor composition of healthy neurons, and in their response to epileptic insults. In the immature brain during peak synaptogenesis, CP-AMPA receptors are expressed at relatively high levels compared to adults (Kumar et al., 2002; Pandey et al., 2015). The highest risk of seizure occurs in the very young and in the very old, although immature brains are more resistant to seizure-induced neuronal damage. There are age-specific differences in structure, physiology and metabolism to allow effective development of networks in the brain, epileptic neurons reverting back to an immature state may be proepileptic.

Immature brains have reduced overall expression of AMPA receptors, and respond to kainic acid by increasing GluA2 expression. The reduced calcium permeability of these AMPA receptors is protective against excitotoxicity. Further, seizures in immature rats lead to transient increases in GluA1 phosphorylation with increased AMPA receptor-mediated currents, and blocking this phosphorylation decreased the susceptibility of mice to PTZ and hypoxia-induced seizures (Rakhade et al., 2012).

1.4.3 Toxicity due to CP-AMPA receptors

A change in the subunit configuration could enhance the toxicity of endogenous glutamate following neurological insult. Glutamate induces cell death by increasing $[\text{Ca}^{2+}]_i$ in neurons via NMDA receptors and CP-AMPA receptors, thereby leading to a rise in the generation of free radicals and activation of proteases, phospholipases and endonucleases. Post seizure,

NMDA receptor-induced apoptosis requires calcium entry through CP-AMPA receptors for transcriptional activation of the specific cell death programs (Friedman, 2006). Hippocampal pyramidal neurons do not express high levels of Ca^{2+} -binding proteins or fast, local calcium extrusion pumps, as they do not experience a high calcium load under physiological conditions. Therefore, acute loss of the GluA2 subunit would be expected to confer enhanced toxicity to endogenous glutamate and vulnerability to neuronal insults. Furthermore, CP-AMPA receptors are permeable to Zn^{2+} , which causes toxicity as it inhibits cellular energy production when it accumulates intracellularly, leading to cell death (Dineley et al., 2003). The c-Jun N-terminal kinase (JNK) signalling pathway, a subfamily of mitogen-activated protein kinase (MAPK), is activated by CP-AMPA receptors in a Ca^{2+} concentration-dependent manner (Vieira et al., 2010). MAPK signalling pathways are one of the major signalling systems that transduce extracellular signals into cells. Activation of this pathway, in response to Ca^{2+} increase or ROS activation, is important after an excitotoxic stimuli for inducing apoptosis (Cui et al., 2007).

Another way in which CP-AMPA receptors can be toxic to the cell is by their higher conductance level through each channel. This increases the risk of excitotoxicity. Ca^{2+} influx mediates a rapid increase in CaMKII, PKA, and PKC activity in hippocampal neurons which may lead to enhanced phosphorylation of both GluA1 and GluA2 subunits, and therefore increased conductance. As CA1 pyramidal neuron dendrites have a high input resistance compared to interneurons, the fidelity of signal transfer from dendrites to the soma is higher. The increased conduction creates an opportunity for summation of postsynaptic potentials (Spruston, 2008).

GluA2 is internalised upon phosphorylation of S⁸⁸⁰ by PKC γ . This process is facilitated by its interaction with the PICK1-PKC γ protein complex. Rakhade et al. (2012) demonstrated in a recent report that S⁸⁸⁰ phosphorylation of GluA2, following hypoxia-induced seizures in neonatal rat, was associated with enhanced functional expression of CP-AMPA receptors (Rakhade et al., 2012). Accelerated endocytosis of the GluA2 subunit may be mediated by seizure-induced expression of the immediate early gene, Arc. Arc expression is induced in both the dentate granule cells (DGCs) and CA1 neurons as early as 30 minutes following pilocarpine-induced SE. In an earlier report, Teber et al. (2004) demonstrated that even sub-convulsive doses of pilocarpine-induced a rapid expression of Arc in rat forebrain (Teber

et al., 2004).

S⁸³¹ phosphorylation of the GluA1 subunit increases the open probability of AMPA receptors, creating a feedforward loop that leads to membrane insertion of extrasynaptic CP-AMPA receptors. These receptors are trafficked laterally to the synaptic membrane, further strengthening this excitatory connection (Huie et al., 2015).

A different target which has been implicated in the expression of CP-AMPA receptors is Poly (ADP-ribose) polymerase 1 (PARP-1). PARP-1 alters protein expression at the nucleus by polyADP-ribosylation and is hyperexpressed in CA1 after SE (Kim et al., 2014). This reversible post-translational modification is a signal for intracellular stress which can induce apoptosis (Basello and Scovassi, 2015). PARP-1 activation has been associated with increased CP-AMPA receptor expression in CA1 but not CA3 pyramidal neurons (Gerace et al., 2014).

RE1-Silencing Transcription factor (REST/ NRSF) is a transcriptional regulator, involved in the switch of AMPA receptor phenotype and in the highly selective neuronal death seen in global ischemia. It suppresses gene expression in those neurons that are destined to die. After SE there is a transcriptional repression of GluA2 by upregulation of REST; acute knockdown of REST prevents GluA2 suppression and rescues CA1 neurons (Noh et al., 2012).

Mice with a knock out (KO) of the TARP γ -8 display typical kainate-induced seizures; however the associated neuronal cell death is attenuated in the hippocampus of these mice (Tomita et al., 2007a). γ -8 KO mice also show dramatic loss of AMPA receptor proteins and extrasynaptic AMPA receptors, with only a modest decrease in synaptic AMPA receptors. Stargazer mice, which lack γ -2, get their name from a characteristic upward gaze, caused by absence seizures (Adotevi and Leitch, 2016).

Pharmacological block of AMPA receptors with NBQX does not prevent the reduction in GluA2, suggesting that its mechanism of neuroprotection is by directly blocking modified AMPA receptor channels. NBQX is likely to remain in the system long enough to act on the new post-SE CP-AMPA receptors. However, overall block of AMPA receptor transmission

could act on AMPA receptors found on inhibitory interneurons, which would increase excitability.

1.4.4 Action of AEDs at the AMPA receptor

There is substantial interest in using AMPA receptor antagonists to control seizures but at present only one, the non-competitive antagonist perampanel, is clinically approved (Fig. 1.3). Perampanel can be given as an adjunct for refractory epilepsy, and has a high potency (IC_{50} of $0.093 \mu\text{M}$), compared to another non-competitive antagonist at AMPA receptors, GYKI-52466 (GYKI; IC_{50} of $12.5 \mu\text{M}$). Perampanel is moderately well tolerated but side effects of dizziness, fatigue, irritability, nausea, and weight gain have been commonly reported. NBQX shows anti-seizure but not antiepileptogenic effects in animal studies (Twele et al., 2015). GYKI also shows anti-convulsant effects in both slice seizure models and *in vivo* (Doczi et al., 1999; Yamaguchi et al., 1993). Decanoic acid, a major component of the MCT ketogenic diet acts on AMPA receptors in a non-competitive way, as discussed in section 1.2.3.2. It binds to all subunits, with a slight preference to GluA2/3 receptors (Chang et al., 2016).

Conversely, targeting other ionotropic glutamate receptors has little effect. In most *in vitro* seizure models, NMDA receptor antagonists alone fail to substantially suppress or eliminate epileptiform activity. Some AEDs acting at AMPA receptors have action at kainate too. However, these receptors contribute less to synaptic transmission than AMPA receptors (Frerking et al., 1998).

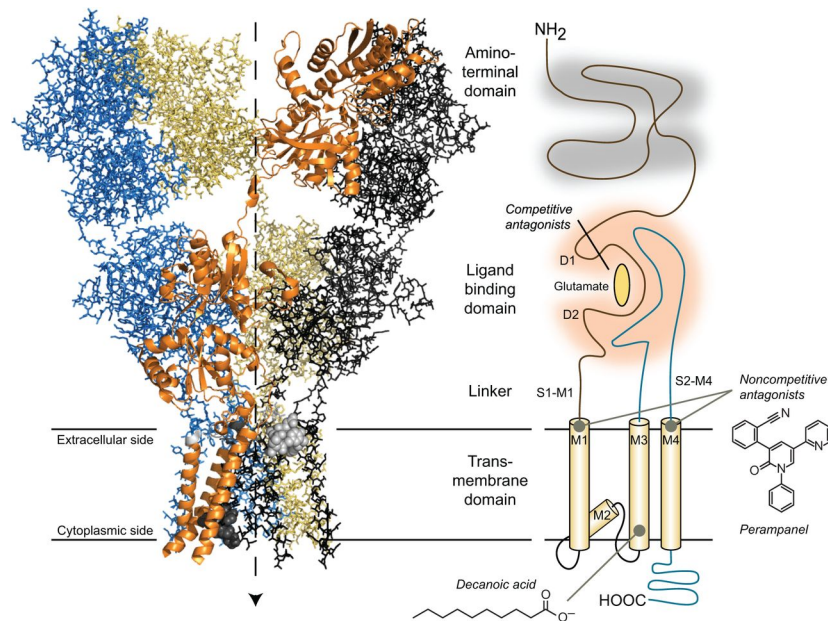


FIGURE 1.3: Binding sites of AEDs acting at the AMPA receptor

Crystallised structure of the AMPA receptor (left) was achieved by Sobolevsky et al. (2009). Schematic (right) showing AMPA receptor domains and the binding site of competitive antagonists, with the proposed binding sites of decanoic acid and perampanel. Adapted with permission from Rogawski (2016).

1.5 Sodium channels

A common target of AEDs are VG ion channels, which transmit synaptic potentials and action potentials along the dendrites and axons. Mutations within these channels are a cause of many genetic forms of epilepsy.

Voltage-gated sodium channels (VGSCs) are present in all excitable tissue, and a requirement for the fast-rising phase of action potentials. Neuronal sodium channels comprise one α -subunit, which may be associated with either one or two β -subunits. In mammalian cells, nine α -subunit isoforms ($\text{Na}_V1.1$ - $\text{Na}_V1.9$) are expressed, from which $\text{Na}_V1.1$, $\text{Na}_V1.2$, $\text{Na}_V1.3$ and $\text{Na}_V1.6$ are predominantly expressed in the CNS. The α -subunit contains four homologous domains containing six transmembrane segments each (S1-S6) as well as a pore-forming loop (Marban et al., 1998).

Much of our knowledge about sodium channels matches the m gates that underlie activation, and the h gate that mediates inactivation, as postulated by Hodgkin and Huxley (Hodgkin and Huxley, 1952). The Na^+ channel transitions through various conformational states in the process of opening, by cooperative action of the four S4 segments serving as the activation sensors. The voltage sensitivity comes from a positively charged S4 segment in each domain of the α -subunit (Yarov-Yarovoy et al., 2012), which moves in response to membrane depolarisation. Segments S5 and S6 form the channel pore and the extracellular loops between S5 and S6 are important for establishing the ion-selectivity of the channel, allowing sodium but not potassium or calcium ions to pass through (Payandeh et al., 2011). During maintained depolarisation, the channel shuts. The cytoplasmic loop between domains DIII-IV acts as a gate responsible for the fast inactivation of open sodium channels.

Sodium channel mediated currents have been studied in detail using neurotoxins. Tetrodotoxin (TTX) blocks Na^+ channels potently (at nM concentrations) in neuronal and skeletal muscle isoforms, but much higher concentrations (~ 5 - $10\mu\text{M}$) are required to block cardiac channels (Zimmer et al., 2014). The different states of sodium channel activation and inactivation can be measured by recording current responses to changes in the membrane voltage. The same channel can alter its gating to produce both transient (I_{NaT}) and persistent (I_{NaP}) currents.

I_{NaP} boosts distal synaptic potentials to allow them to reach the soma, and is important for behaviours such as autonomous pacemakers and fast spiking. These are not the only currents produced by the sodium channel. $Na_V1.6$ interacts with an auxiliary subunit, which is required for resurgent currents, when the channel moves from an open, inactive state to closed state. The axon initial segment and nodal membranes in many neurons express a high density of $Na_V1.6$ channels (Burbidge et al., 2002).

1.5.1 Sodium channels in epilepsy

Mutations in subunits of the sodium channel can cause epilepsy (O'Brien and Meisler, 2013). Mutations in the *SCN1A* gene, coding for $\alpha 1$ of $Na_V1.1$ have been associated with various types of epilepsy. 1200 different mutations in the *SCN1A* gene have been identified in studies using either knockin animal models or induced pluripotent stem cell (iPSC)-derived neurons from humans with the mutations. The β -subunit *SCN1B* was the first molecular link to be established in Generalised epilepsy with febrile seizures plus (GEFS+). Since this, it has been shown that in GEFS+ most mutations appear in the S4 voltage sensor region of *SCN1A*. A variety of functional defects, often missense mutations, have been found, including an increase in I_{NaP} (Uebachs et al., 2010; Agrawal et al., 2003).

In Dravet syndrome, one-third of children have mutations in *SCN1A*, the majority being frame-shift or missense, especially at the pore region (S5-S6). The type of mutation can map onto severity of the disease symptoms; nonsense mutations cause a more severe phenotype. The more debilitating mutations are *de novo*. Single amino acid mutations at different locations throughout the channel are likely to give rise to multiple distinct functional deficits, contributing to the varied clinical manifestation and severity of *SCN1A* epilepsy disorders. Single gene mutation diseases are good targets for gene therapy and modification studies, using new techniques such as clustered, regularly interspaced, short palindromic repeat (CRISPR) technology.

Anti-convulsants block voltage sensitive sodium channels to stop seizures (Ragsdale and Avoli, 1998; Mantegazza et al., 2010; Goldfarb, 2011; Colombo et al., 2013). Many AEDs act in an use- and voltage-dependent manner, which allows them to selectively prevent high frequency firing, with much less influence on normal action potentials and activity.

However, most drugs targeting sodium channels act on transient (sub- and supra-threshold) and persistent currents together. Phosphorylation of sodium channels changes kinetics of the channel and could alter effect of AEDs. For example, the effect of topiramate on I_{NaT} is reduced when the sodium channel is phosphorylated (Curia et al., 2007).

During epileptiform activity there is a reduction in the driving force for VG Na^+ channels. The significant shift in sodium reversal potential (+25mV from +55mV; Raimondo et al., 2015) reduces the driving force and alters action potential kinetics. This could reduce the ability of neighbouring VG Na^+ channels to recruit each other during the course of action potential generation. Interestingly, chronic epileptic-like activity can lead to upregulation of I_{NaP} (Chen et al., 2011), potentially constituting a positive feedback mechanism for triggering further seizures. It would be beneficial to find a way to just target persistent currents in epilepsy.

One day after induction of SE there was a 50% loss of the $Na_v1.1$ -positive interneurons (Qiao et al., 2013). $Na_v1.6$ immunoreactivity in the dendritic region of CA1, and CA3 was persistently reduced at all time-points during epileptogenesis (Blumenfeld et al., 2009). In layer 5 of the entorhinal cortex, the I_{NaP} was larger at a time point coinciding with the onset of spontaneous recurrent seizures (Agrawal et al., 2003). Although glia are non-excitabile cells which rarely express sodium channels, some astrocytes expressed $Na_v1.1$ and $Na_v1.6$ at 3 weeks after SE.

1.6 Circuits of the hippocampus

The hippocampus is where seizures initiate in mesial TLE, and is a well defined brain region important in epilepsy research. It is located in the medial temporal lobe and, along with the entorhinal cortex, subiculum, presubiculum, parasubiculum and the dentate gyrus, constitutes the hippocampal formation (Spiers, 2012). The hippocampus is required for the formation of new memories and for spatial navigation. Synapses in the hippocampus are highly plastic, and neuronal networks here can be synchronised to generate oscillations with varying frequencies and behavioural correlates. For instance the coupling of gamma and theta oscillations, produced by different neurons in the hippocampus, are vital to memory formation (Butler and Paulsen, 2015). These brain functions arise from networks in which individual neurons continuously receive synaptic inputs that are shaped by their intrinsic membrane properties.

The hippocampal formation mainly receives inputs from the entorhinal cortex, which goes via the perforant path to the dentate gyrus, CA3 and CA1. From the dentate gyrus, mossy fibres send axons to CA3, from which Schaffer collaterals send outputs to CA1. CA1 pyramidal neurons send projections to the subiculum or out to the entorhinal cortex, via the angular bundle (Andersen, 2007). The principal cells of the hippocampus are aligned in a densely packed single cell layer. These excitatory pyramidal neurons, which are multipolar as they form apical and basal dendrites extending in both directions from the cell body and have strictly laminated inputs. The dentate gyrus is full of densely packed, small granule cells (Andersen, 2007). The subgranular zone of the hippocampus is an area of adult neurogenesis proliferation, influenced by environmental factors and disturbed in epilepsy. The dentate hilar area usually contains a low density of neurons, but dentate granule cells disperse here in chronic epilepsy.

Throughout the hippocampus, there is a heterogeneous GABAergic interneuron population. These inhibitory neurons control excitation, and regulate the temporal precision of spiking. Interneurons can be distinguished electrophysiologically from principal neurons as they often have high rates of spontaneous activity and fire in relation to theta rhythm (Freund and Buzsaki, 1996). Interneurons can be categorised based on their subcellular targets on principle neurons; for example, somatostatin interneurons usually target the dendrites and

parvalbumin interneurons target the cell body of the same cells. Further, glial cells can be electrophysiologically distinguished from principle neurons as they are electrically passive. Glial cells influence synaptic transmission via release of gliotransmitters (glutamate, ATP, adenosine and cytokines) and regulation of the extracellular environment (such as by K^+ buffering). This regulation likely alters the survivability and functioning of newly formed connections (Ota et al., 2013).

One of the most common forms of epilepsy, temporal lobe epilepsy is characterised by seizures originating in the hippocampus. Animal research of this brain region important because in rodents, the hippocampus also readily generates epileptiform activity and has been instrumental in advancing our understanding of ictogenesis.

1.7 Models of temporal lobe epilepsy

1.7.1 Human resected tissue slices

Brain tissue removed in surgery for refractory epilepsy can be sliced and stored for several hours in artificial cerebrospinal fluid (aCSF). There is no control over the tissue received from surgical patients, so results can be very variable. Factors such as age of the patient, type of epilepsy, duration of seizures and current AED treatment profile would influence the network activity, and would ideally be controlled as is in animal studies.

Comparisons between rat and human neurons shows differences at the cellular and network level which should be taken into account when interpreting animals studies with relevance to humans. Human pyramidal neurons differ in their subcellular architecture and could have information processing capabilities distinct from rodent and macaque neurons (Mohan et al., 2015). Specifically, astrocytes and pyramidal neurons in the human temporal cortex are 23 times larger than rodents, and processes are 10 times more complex (Oberheim et al., 2009). There are neuron types in human which are not classified in rodents, as well as more diverse interneurons. Also, the absolute numbers and density of neurons, spines, and synapses are highly species-specific (DeFelipe et al., 2002); there are at least twice the number of synapses per pyramidal neuron in humans as in mice.

Histopathological studies comparing a number of clinical factors with neuronal architecture found no significant correlation between total dendrite length nor number of branch points when compared to the number of seizures, disease severity, or age of the patient (Mohan et al., 2015). However, there may be a more subtle change to neuron shape, or only certain neuronal types affected which would not have been apparent from this study.

1.7.2 Acute slices

In vitro models of epileptogenesis are useful to study the mechanism of molecular changes without the many confounding factors present in animal models. It can be useful to compare effects in multiple *in vitro* models, as inducers acting on specific receptors can cause specific outcomes. However, long range connections are cut in the production of acute slices and further the solutions used to store slices are artificial, which could dialyse important modulatory factors.

1.7.2.1 0-Mg²⁺

Epileptiform activity generated in aCSF with Mg²⁺ removed consists of bursts of action potentials riding on paroxysmal depolarising shifts. This leads to the development of synchronous, electrographic discharges (Mangan and Kapur, 2004). Bursting causes changes in the properties of GABA_A receptor similar to animals after 1h SE, including diminished mIPSC amplitude and decreased surface expression of GABA_A receptor subunit γ -2.

NMDA receptors are involved in the generation of epileptiform events, as these are blocked by D-AP5. Adding in a near-physiological concentration of Mg²⁺ (1mM) also completely and reversibly blocks recurrence of epileptiform activity. Activation of AMPA receptors is important for maintaining epileptiform activity; in addition, pathological discharges in this model depend on gap junction coupling of neurons and astrocytes. Since excessive activation of NMDA receptors in 0-Mg²⁺ aCSF could cause model specific changes in AMPA receptors, it is important to verify the findings using other epilepsy models.

1.7.2.2 PTZ

Application of pentylenetetrazol (PTZ) and increasing K⁺ concentration from 2.5mM to 6mM induces ictal and interictal activity in EC-hippocampal slices. PTZ is a GABA_A receptor antagonist, acting at the picrotoxin binding site (Huang et al., 2001). Activity is generated from the EC and the CA3, which is then sent onto CA1 and other areas. PTZ can also be used to develop both acute and chronic animal models of epilepsy, especially in pre-clinical drug studies.

1.7.3 *In vivo* models

In vivo models are used in the study of basic mechanisms of epilepsy in intact networks. They are also indispensable to test confounders which may impact the clinical outcome when using a particular drug, including bioavailability. Acute seizures are initiated by injection of chemoconvulsants, such as PTZ, or by electrical stimulation in the maximal electrical shock (MES) test. These models give useful information on seizure threshold and are good as a simple initial screen of anti-seizure potential. Chronic seizures are induced by chemical or electrical kindling, where multiple subthreshold doses eventually cause seizures after network changes within the animal's brain. Further, induced SE leads to

spontaneous seizures after injection of kainate or pilocarpine, or perforant path stimulation (PPS). Chronic models of epilepsy are used to compare seizure frequency and severity in differently treated groups of animals. They must be recorded continuously by video/EEG monitoring during this period for seizure monitoring (Loscher, 2011), and *ex vivo* brain tissue can be used for single cell electrophysiology and histochemistry. Finally, there are genetic models of epilepsy produced either from animals with a random mutation causing spontaneous seizures, or by genetic manipulation (e.g. stargazer mouse).

1.7.3.1 Perforant Path Stimulation

PPS is a post-SE model of epilepsy, induced by constant supra-threshold current pulses to the perforant path. Initially seizure activity depends entirely on ongoing stimulation; but then seizures becomes self-sustaining and no longer depend on the external stimuli. This second phase is refractory to treatment with standard anticonvulsants and may involve molecular alterations at GABA receptors, or long-term potentiation of excitatory synapses. Animals stimulated in such a way develop temporal lobe epilepsy with spontaneous seizures after a latent period of up to 3 weeks. Many AEDs are able to suppress seizures in PPS, so this model has pharmacological validity. However, as there is variability between TLE patients and epilepsy is not a static disorder, response rates to AEDs can change over time.

The neuropathological changes seen following PPS, such as patterns of sclerosis, match many patients with TLE. This contrasts with kainate- or pilocarpine-induced SE, which leads to more widespread damage to the brain (Loscher, 2011). Since PPS stimulation does not rely on exogenous application of a chemical agent, it has high validity. However, PPS is a technically difficult, expensive, and time-consuming model. This is a particularly important consideration when looking at chronic effects of treatments, as continuous seizure monitoring is required.

Thesis Aims

1. Explore whether excessive network activity causes a shift towards GluA2-lacking AMPA receptor expression on CA1 pyramidal neurons
2. Measure if this shift is blocked in the presence of NMDA receptor inhibitors
3. Determine if specific CP-AMPA receptor inhibitors block epileptiform activity in a similar way to general AMPA receptor inhibitors
4. Investigate whether AMPA receptor inhibition by decanoic acid can explain the success of the ketogenic diet
5. Explore if other neuronal targets of decanoic acid reduce network excitability
6. Determine if recordings from human neocortical neurons can be compared to results obtained in rats

Chapter 2

Materials and Methods

2.1 Animals

Wild type Sprague Dawley (SD) male rats were imported from Charles River, group housed and left to acclimatise for 1 week before use in experiments.

2.2 Acute rat hippocampal slices

P21-P26 SD rats were sacrificed by isoflurane anaesthesia (Henry Schein, UK) followed by cervical dislocation, in accordance with UK Animals (Scientific Procedures) Act 1986. The whole brain was quickly removed for dissection and placed in oxygenated ice-cold slicing solution containing (in mM): 87 NaCl, 12.5 NaHCO₃, 75 sucrose, 25 glucose, 2.5 KCl, 1.25 NaH₂PO₄, 7 MgCl₂, 0.5 CaCl₂, bubbled with 95% O₂/5% CO₂ to maintain pH at 7.4 (Osm:316mOsm).

For EC-hippocampus combined horizontal slices the cerebellum and forebrain were removed, and hemispheres were separated by cutting through the midbrain to expose the hippocampus (Fig. 2.1a). Each hemisphere was cut dorsally parallel to a prominent blood vessel (the "magic cut"; Fig. 2.1b; Bischofberger et al., 2006), glued to the platform and then immersed in oxygenated ice-cold sucrose solution in the slicing chamber of a vibrotome (Leica VT1200S, Milton Keynes UK). Slices (350 μ M thick) were obtained at a speed of 0.10-0.12mm/s and cutting frequency of 0.85.

Slices were allowed to recover at 35°C for 15 minutes before being transferred to a submerged

chamber (see Fig. 2.2) at room temperature for at least 30 minutes recovery in oxygenated aCSF containing (in mM): 125 NaCl, 2.5 KCl, 1 MgCl₂, 20 NaHCO₃, 1.25 NaH₂PO₄, 25 glucose, and 2 CaCl₂ (osmolarity 296 mOsm). Slices were then either transferred to a different incubation solution for at least one hour or left for a further 30 minutes before recording.

2.3 *Ex vivo* induction of epileptiform activity

At least one hour prior to recording, slices were transferred to an oxygenated interface chamber in a water-bath at 34°C (Fig. 2.2) containing either 0-Mg²⁺ aCSF (solution as above, with MgCl₂ excluded, KCl increased to 5mM, and 5mM Na-pyruvate), PTZ-aCSF (solution as above, with 2mM PTZ, KCl increased to 6mM, and 5mM Na-pyruvate) or control aCSF. Epileptiform discharges, recorded as population spikes consisting of positive field potentials, were recorded from stratum radiatum and appeared 5-30 minutes after incubation in the modified aCSF.

Interface style chambers (Fig. 2.2b) provide a humidified carbogenated atmosphere, which may provide a more "physiological-like" environment when compared to the submerged chambers. Slice viability and neuronal health based on the electrophysiological recordings obtained were improved by incubation in an interface chamber. Slices stored in the interface chamber stayed viable for up to eight hours after slicing. These chambers promote the induction of interictal and ictal activity in slice models of seizures, possibly due to the ability of the system to cope with increased metabolic demands (Hajos and Paulsen, 2009). Epileptiform activity could be generated by application of PTZ or 0-Mg²⁺ aCSF at room temperature, but was stronger and more consistent when induced at 34°C.

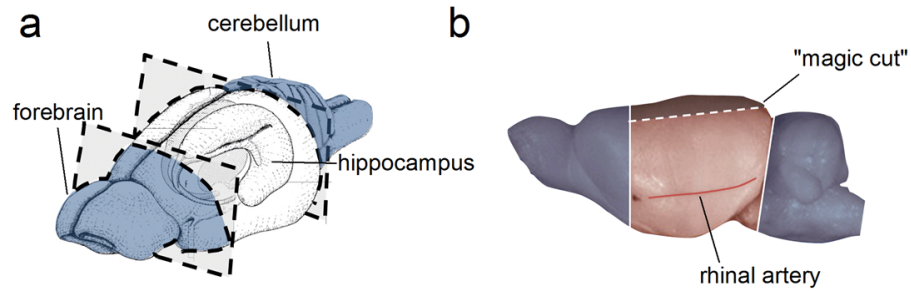


FIGURE 2.1: Brain dissection schematic for EC-hippocampal horizontal slices.

a) Dotted lines show cutting plane to remove forebrain and cerebellum (in blue) for horizontal hippocampal slices (an outline of the hippocampus is shown in the middle).
 b) Third cut to the whole brain is parallel to the rhinal artery. This provides a stable base to glue the brain and horizontal hippocampal slices at the correct orientation. (a) adapted from: Amaral DG, Witter MP. Hippocampal formation. In: Paxinos G, editor. *The Rat Nervous System*. Second. London, Academic Press; 1995. pp. 443-493.

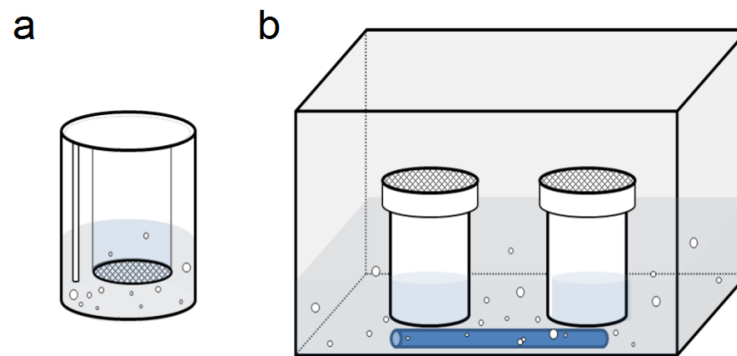


FIGURE 2.2: Submerged and interface chambers.

a) Submerged chamber. Slices were stored on nylon mesh, fully submerged in aCSF with carbogen gas (95% O₂ 5% CO₂) bubbled in the chamber to oxygenate slices. b) Gas-fluid interface chamber. Slices being incubated at 35°C were held in an interface chamber to increase viability. Slices were stored on nylon mesh, partially submerged in aCSF in a chamber filled with aCSF with carbogenated gas (95% O₂ 5% CO₂) bubbling through.

Compound	Conc.	Provider	Reference
4-AP	5mM	Sigma	Royeck et al. (2008)
4-BCCA	1mM	TCI Chemicals	Chang et al. (2015)
4-EOA	1mM	Chemos GmbH	Chang et al. (2015)
4-MNA	1mM	Alfa Aesar	Chang et al. (2015)
CdCl ₂	300 μ M	Sigma	Yue et al. (2005)
Decanoic acid	10-1000 μ M	Sigma	Chang et al. (2016)
D-AP5	50 μ M	Tocris	Zamanillo et al. (1999)
FK506	10mM	Tocris	Eckel et al. (2014)
GYKI-52466	50 μ M	Sigma	Donevan and Rogawski (1993)
LY-294002	20 μ M	Echelon	Chang et al. (2014)
Na-pyruvate	5mM	Sigma	Kovac et al. (2012)
NASPM	70 μ M	Alomone	Loweth et al. (2014)
NBQX	10 μ M	Alomone	Sanderson et al. (2012)
PTX	50 μ M	Sigma	Opazo et al. (2010)
PTZ	2mM	Sigma	Chang et al. (2014)
QX-314 Br	50 μ M	Alomone	Chen et al. (2011)
Spermine	100 μ M	Sigma	Zamanillo et al. (1999)
TC-2153	1 μ M	Sigma	Xu et al. (2014)
TEA-Cl	20mM	Sigma	Yue et al. (2005)
TTX	1 μ M	Alomone	Royeck et al. (2008)

TABLE 2.1: Compounds used in project, with standard concentration used.

2.4 Single cell electrophysiology

During single cell recording, hippocampal slices were placed on a double-sided, dual perfusion chamber and held in place with a handmade harp, consisting of a platinum wire bent into a horseshoe shape with single nylon threads from tights glued across. Slices were continuously perfused with oxygenated aCSF. Patch electrodes were prepared from filamented thick-walled borosilicate glass (World Precision Instruments, UK) pulled on a horizontal microelectrode puller (model P-97, Sutter Instruments, UK) using a two-stage pull protocol.

Whole-cell patch clamp recordings were made from the soma of CA1 pyramidal neurons, which were identified visually by their shape and physiological properties (Hamill et al., 1991). Neurons were visualised with an upright microscope (Olympus BX51WI) using a 40x water immersion objective, with a charge-coupled device (CCD) camera for viewing through a video monitor. A differential interference contrast (DIC) microscope was used to clearly visualise cells in deeper layers of the tissue, where the neurons are healthiest. Recordings were performed using an Multiclamp 700B amplifier (Molecular Devices, UK). The headstage was mounted on a PatchStar motorised micromanipulator (Scientifica, UK).

Whole-cell patch clamp configuration was achieved by patching in voltage clamp. Positive pressure was applied to the patch pipette to prevent clogging at the tip as it was lowered into the slice. The current transient elicited by a 5mV hyperpolarising voltage step was continually monitored during seal formation. When approaching a cell, an expanding dimple in the cell membrane was observed and the current transient decreased. After positive pressure was released, the seal became $G\Omega$ in resistance with the aid of negative pressure applied through the pipette tip, and changing the pipette potential from 0mV to -70mV. Pipette capacitance was corrected and then short, gentle ramps of negative pressure were applied to rupture the membrane and achieve whole-cell electrical access.

Ten minutes after access was established, series resistance compensation was applied between 55 and 80%, following whole-cell capacitance measurement. This is necessary to compensate resistance at the pipette tip, and is required to minimise errors in command voltage and to improve the accuracy of current kinetics. Access resistance was continually monitored by measuring the size of capacitance transients in response to a 5mV hyperpolarising step.

Recordings in which access resistance changed more than 20% were rejected. Cell input resistance was measured from steady-state currents in response to various depolarising steps. The currents were low-pass filtered at 5kHz and digitised at 20kHz using a PCI-6221 card A/D converter (National Instruments, UK) and recorded using LabVIEW software (National Instruments, UK). In all experiments, the recording chamber was maintained at 32°C using an inline heating system coupled with an automatic temperature controller (Scientifica, UK).

2.4.1 Voltage clamp

Voltage clamp was used to study the current-voltage ($I-V$) relationship of pharmacologically isolated VG ion channels or synaptic currents evoked by extracellular tissue stimulation.

2.4.1.1 Extracellular neuronal stimulation

Evoked EPSCs (eEPSCs) were obtained by stimulation of the Schaffer collaterals using a concentric bipolar platinum-iridium electrode (125 μ m, FHC, Bowdoin, ME) approximately 100-300 μ m from the recorded cell. Constant current pulses (200 μ s; 0.1 Hz) were administered to the slices using a constant current stimulus isolator (DS3, Digitmer, Hertfordshire, UK); the stimulus intensity was standardised at 1.5 times the minimum provoking EPSC response.

2.4.1.2 AMPA receptor-mediated currents

In CA1 pyramidal neurons voltage clamp is spatially limited (Bar-Yehuda and Korngreen, 2008). The injected current required to maintain the holding potential is filtered along axons and dendrites, and further currents originating from distal synapses are distorted kinetically by the time they reach the soma. To improve space clamp issues, a caesium-based internal solution, which blocks K⁺ leak channels was used, and series resistance was compensated as described above. As the response from many synapses is measured, the more proximal synapses with the greater clamp will be more influential in the response.

eEPSCs mediated by AMPA receptors were isolated by including 50 μ M PTX and 50 μ M D-AP5 in the recording solution, to block GABA_A and NMDA receptor currents respectively. As GABA_A receptor currents were blocked, a cut was made to separate CA3 from CA1

to block spontaneous activity generated here from contaminating recordings during these whole-cell voltage clamp recordings. Patch pipettes were filled with internal solution, filtered through a 22nm pore, containing (in mM): 125 cesium-methylsulphonate (Cs-MSF), 10 HEPES, 10 Na-phosphocreatine, 8 NaCl, 0.33 Na₃-GTP, 0.2 EGTA, 5 TEA-Cl, 4 ATP-Mg (buffered to pH 7.3 with CsOH; 315 mOsm) and had a final resistance of 2.5-4.5 MΩ. Liquid Junction Potential (LJP) is caused by the difference in mobility of ions through the tip of the pipette. LJP of 13 mV was taken into account before each recording (calculated *in silico* using LJP Calculator: JPCalcW). The internal solution contained spermine to compensate for the loss of endogenous cellular polyamines by dialysis of the cell contents and QX-314 Br (50μM) to block VG sodium channels and therefore abolish escape currents due to unclamped spikes.

The *I-V* relationship of AMPA receptor-mediated EPSCs was obtained by measuring the leak subtracted peak of 6-10 averaged eEPSCs at various holding potentials (-70 to +70 mV). Points were fitted with a linear relationship at negative potentials and this was either extrapolated into positive potentials, or positive potentials were fitted with a polynomial relationship to match the curved relationship (fitting used is indicated in each figure legend). As AMPA receptors are constitutively recycled from the synapse, all whole-cell recordings were initiated within 20 minutes of removal from the incubating solution.

The level of CP-AMPA receptor expression influences *I-V* relationships due to polyamine-dependent inward rectification. This can be measured using the Rectification Index (RI). RI was defined as:

$$RI = \frac{I_{+50mV}}{I_{-50mV}} \quad (2.1)$$

in all experiments (except in Fig. 3.4 and Fig. 3.6 where the holding potentials compared were +40 mV/-40 mV and +40 mV/-60 mV respectively, due to different voltage steps being recorded). RI is around 1 at a synapse containing only CI-AMPA receptors. In synapses containing only CP-AMPA receptors, the RI can be expected to be <0.25, and 0.7 is an arbitrary value used as a cut-off to guide when a combination of CP- and CI-AMPA receptors are present at the synapse (Wang and Gao, 2010).

Data were collected using LabVIEW and was analysed in LabVIEW, or using scripts written in Python. Statistical analysis was performed using SPSS (IBM, Portsmouth, UK), Origin 9.0 (OriginPro 9; MA, USA), or Python (Python Software Foundation). Cells with a RI calculated at >2 were discarded as outliers ($n=1$ cell). Each treatment group contained recordings in neurons from at least 3 separate animals. Treatment group sizes were chosen by performing a power calculation based on preliminary data (GPower 3.1). Mean eEPSCs recorded from both treatment groups were used to calculate RIs, which were then compared.

2.4.1.3 Voltage-gated sodium channel currents

To study VGSC currents in voltage clamp, CA1 pyramidal neurons were patched using an internal solution containing (in mM): 125 Cs-MSF, 10 HEPES, 10 Na-phosphocreatine, 8 NaCl, 0.33 Na₃-GTP, 0.2 EGTA, 5 TEA-Cl, 4 ATP-Mg (buffered to pH 7.3 with CsOH; 315 mOsm). LJP of 11 mV was compensated for before all recordings. To isolate sodium channel currents, 20mM TEA-Cl, 5mM 4AP and 0.3mM CdCl₂ were included in the extracellular recording solution to block VG potassium channels and calcium channels respectively.

To measure transient sodium currents, cells were held between -70 mV and +20 mV, at 10 mV steps. Three cycles of baseline currents were recorded, after which 300 μ M decanoic acid was washed in for three more cycles, followed by wash-in of 1 μ M TTX, as TTX is difficult to wash out of slices. Only one cell was recorded per slice for the same reason. Currents were averaged over 2 or 3 cycles per cell and traces made in TTX were subtracted for each holding voltage. During analysis of transient sodium currents, data was excluded if there was evidence of imperfect voltage clamp (ie. the peak was not within the first 20ms of the current response). Currents were then normalised to cell capacitance (pF) to control for changes in peak current and maximum conductance due to variations in cell size, and pA/pF was plotted against holding potential. Transient sodium channel currents were converted into conductances using Ohm's law (EQ. 2.2; Yue et al., 2005):

$$G_{(V)} = \frac{I_{(V)}}{(V - V_{Na})} \quad (2.2)$$

where $G_{(V)}$ is the conductance, $I_{(V)}$ the peak current recorded at test potential V , and V_{Na} is the sodium reversal potential estimated using the Nernst equation (EQ. 2.3; taken

as +55 mV in my experiments).

$$E = \frac{RT}{zF} \ln \frac{[X]_o}{[X]_i} \quad (2.3)$$

The activation curve (conductance-voltage relationship) was derived from the I - V curves obtained by plotting the peak current over voltage steps. Comparing conductance allowed me to look at voltage-dependence with differences in driving force taken into account. $G_{(V)}$ was then fitted with the following Boltzmann function:

$$G_{(V)} = \frac{G_{(max)}}{1 + \exp[(V_{50} - V)/k]} \quad (2.4)$$

where G_{max} is the maximal Na^+ conductance, V_{50} is the membrane voltage (V) at which $G_{(V)}$ is 50% of G_{max} , and k is the slope of the $G_{(V)}/V$ relationship at V_{50} .

To measure persistent sodium currents (I_{NaP}), the membrane potential was ramped from -80 mV to +20 mV over 50 seconds (2mV/s). This slow ramp speed is required to see persistent currents in CA1 pyramidal neurons (Park et al., 2013). Recordings were filtered at 4kHz and acquired at 10kHz, as the protocol was longer for these experiments and the time scale of the current of interest was slower than previous. Two recording cycles were collected for the baseline before 300 μ M decanoic acid was washed in for two more cycles, followed by wash-in of 1 μ M TTX. Currents were averaged over 2 or 3 cycles per cell and TTX subtracted.

I_{NaP} traces were converted to conductance traces using EQ. 2.2, and peak conductance was compared between control and decanoic acid by fitting a Boltzmann function using EQ. 2.4, as in Royeck et al. (2008). Peak conductance was normalised to baseline and compared to decanoic acid wash-in and TTX wash-in. Voltage of half-maximal activation (V_{50}) and the slope factor (k) of I_{NaP} were also compared.

2.4.2 Current clamp

Current clamp was used to record the number and shape of action potentials in response to increasing current injections, and the size of voltage response to current injections in the presence of TTX. Before recording, slices were incubated at room temperature in aCSF

or for 50 minutes with the phosphoinositide 3-kinase (PI3K) inhibitor, LY-294002 (20 μ M), added to the aCSF.

Whole-cell electrical access to CA1 pyramidal neurons was obtained in voltage clamp mode as described above, before switching to current clamp mode without current injection. Using whole-cell capacitance and access resistance estimates from voltage clamp mode, the bridge was balanced, and cell was left for 10 minutes. CA1 pyramidal neurons had a resting membrane potential of between -75 mV to -55 mV. Microelectrodes were filled with a K-gluconate based internal solution, containing (in mM): 140 K-gluconate, 10 HEPES, 10 Na₂-phosphocreatine, 8 NaCl, 0.33 Na₃-GTP, 0.2 EGTA, 2 ATP-Mg; and they had a final resistance of 2.5-4.5 M Ω . LJP was 8mV and was taken into account before all recordings. PTX (50 μ M), D-AP5 (50 μ M) and NBQX (10 μ M) were included in the recording solution to block GABA_A receptors, NMDA receptors and AMPA receptors respectively. TTX (1 μ M) was sometimes included in the recording solution to block VG sodium channel currents.

The sample frequency was initially set at 20kHz for counting the number of action potentials. It was then increased to 50kHz for analysis of action potential shape, with a Bessel filter of 8kHz. Voltage traces in response to 6-8 incrementing current steps of 25pA or 40pA were recorded using LabVIEW, with step size chosen in order to initiate action potentials on the 2nd-3rd step. Decanoic acid or BCCA were dissolved in dimethyl sulphoxide (DMSO) at 1000X stock, and volume matched decanoic acid or DMSO was washed into the recording solution to achieve a final concentration of 300 μ M.

Action potentials were counted by voltage threshold detection using Clampfit, and parameters were compared between treatment groups using a Python script. The change in number of action potentials at each current step was compared using area under the curve (AUC).

2.4.2.1 Analysis of action potentials

Limit cycle plots of dV/dt were drawn for traces recorded at 50kHz, with a Bessel filter of 8kHz. The differential of voltage over time was taken and plotted against voltage to give a representation of the kinetics of the action potential. From this the RMP, $V_{\text{repoliarise}}$, $V_{\text{threshold}}$ and V_{peak} could be determined and compared in treatment groups.

2.5 Extracellular recordings

Extracellular recordings were used to record network activity in response to extracellular stimulation or application of exogenous chemicals causing epileptiform activity. EC-hippocampal slices ($350\mu\text{M}$) were prepared because intact connections are required for PTZ-induced epileptiform activity, and recordings were made from the stratum radiatum of CA1. Recording electrodes were pulled from thick-walled borosilicate glass as previously described, filled with aCSF and had a resistance of $1\text{M}\Omega$. Electrode position determined the polarity and shape of population response (Fig. 2.3).

2.5.1 Epileptiform activity

Slices were placed in a dual-perfusion recording chamber, which allows perfusion on both sides of the slice, and were continuously perfused with PTZ-aCSF. Fatty acid derivatives were dissolved in DMSO at 1000X stock, then were added to the recording solution to achieve a final concentration of 1mM. The compounds tested were 4-methylnonanoic acid (MNA), 4-ethyloctanoic acid (EOA), trans-4-butylcyclohexane carboxylic acid (BCCA), 4-n-pentylphenylethanoic acid (PPEA) and 2-(4-pentylcyclohexyl) ethanoic acid (2PEA). All compounds were over 95% purity. Decanoic acid was dissolved in DMSO at 2000X stock, and GYKI was prepared at 1000X stock in distilled water. Field potentials were recorded for a stable 10 minute baseline before compound application. After 40 minutes recording with the compound in solution, drug washout was recorded using PTZ-aCSF for 30 minutes.

Spontaneous epileptiform discharges were recorded, digitised at 10kHz (4kHz filter, gain of 100), and analysed using WinEDR (Strathclyde Electrophysiology Software). An automated event detection program was used (WinEDR) and verified manually. The number of epileptiform events were binned into 5 minute intervals, normalised to baseline and averaged.

2.5.2 Synergy between decanoic acid and perampanel

After a stable 10 minute baseline field potential recording in PTZ-aCSF, perampanel was added to the bathing solution at the required concentration from a 50mM stock solution dissolved in DMSO. Decanoic acid was washed in at appropriate concentrations from a 600mM stock dissolved in DMSO. 100nM perampanel was the highest concentration that does not itself reduce epileptiform activity.

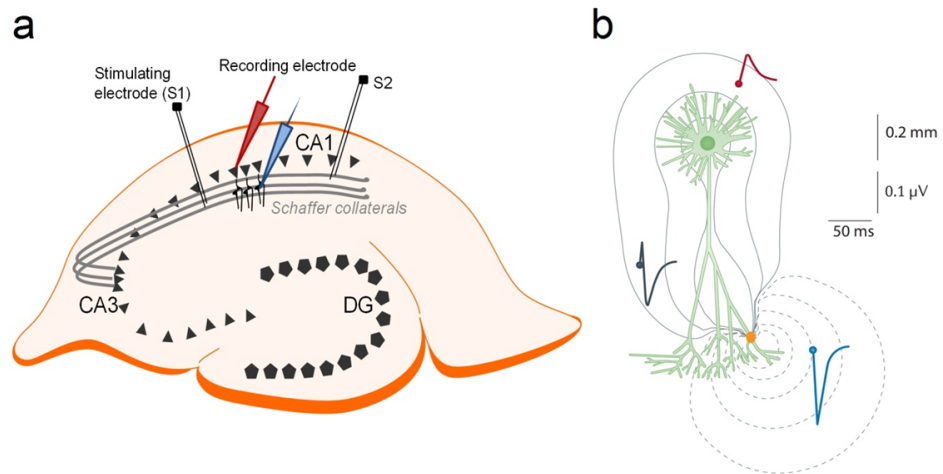


FIGURE 2.3: Position of stimulating electrodes and recording electrode in stratum radiatum of CA1, and the field response.

a) Two independent Schaffer collateral pathways were stimulated by electrodes placed on either side of a recording electrode in the CA1 st. radiatum. b) Dependence of the fEPSP shape, size and polarity on the recording electrode position. Recording a synaptic input (orange) from the electrode placed in st. radiatum (blue) during Schaffer collateral stimulation produces a negative-going fEPSP response (blue trace), whereas recording from the electrode placed in st. pyramidale (red) during Schaffer collateral stimulation produces a positive-going fEPSP response (red trace). Adapted with permission from Einevoll et al. (2013).

Epileptiform discharges were counted in one minute bins. The number of epileptiform discharges in each bin after seven minutes decanoic acid wash-in were averaged, and normalised to a perampanel-containing baseline. Hill functions were plotted for each slice and the concentration of decanoic acid that reduced epileptiform discharges by 50% was read off at normalised epileptiform discharges of 0.5.

2.5.3 Use-dependence

For use-dependence studies, field EPSPs (fEPSPs) were recorded in response to stimulation of two independent Schaffer collateral pathways. Two concentric bipolar platinum-iridium electrodes ($125\mu\text{m}$, FHC, Bowdoin, ME) were placed in the stratum radiatum at different depths either side of a recording electrode, which was also placed in the radiatum layer of CA1 (Fig. 2.3). AMPA receptor-mediated responses were pharmacologically isolated by including PTX ($50\mu\text{M}$) and D-AP5 ($50\mu\text{M}$) in the recording solution to block GABA_A receptor and NMDA receptor-mediated currents, respectively.

To confirm that the stimulation pathways activated independent populations of synapses, a paired pulse (PP) protocol (pulse width 1ms; pulse interval 100ms) was first executed in each pathway. During successive activation of independent pathways there was not expected to be any PP potentiation. The evoked current amplitude from each pathway did not differ from each other by $>10\%$. After pathway independence was confirmed, a stable ($<20\%$ change in the fEPSP amplitude over 15 minutes) baseline period was recorded. Constant current pulses (1ms; 0.025 Hz) were administered to the slice using a constant current stimulus isolator (DS3, Digitmer, UK). Subthreshold (e.g. half-maximal) stimulation was used to avoid saturation of the fEPSP response. If a population spike was seen in response to stimulation, then the recording electrode was moved to get a more appropriate response. After a baseline period, stimulation of one pathway was stopped and decanoic acid (in DMSO) was added to the recording solution, to achieve a final concentration of $300\mu\text{M}$. After 30 minutes, stimulation of the second pathway was resumed and fEPSP slopes in both pathways were compared. Recordings were collected using LabVIEW and exported as ASCII files for analysis in Python. During analysis, fEPSP responses were binned into groups of 2 consecutive recordings and the average was taken to reduce variation. Responses

were normalised to baseline.

2.6 Human surgically resected tissue

Informed written patient consent to use resected tissue for basic research was obtained prior to the surgery. Tissue was collected directly from the surgery theatre at the National Hospital for Neurology and Neurosurgery and immediately immersed in ice cold sucrose or choline-based aCSF containing (in mM): 110 CholineCl, 26 NaHCO₃, 7 MgCl₂, 2.5 KCl, 1.25 NaH₂PO₄, 0.5 CaCl₂, 10 glucose, 11.6 Na-ascorbate, 3.1 Na-pyruvate. The time from tissue removal to slicing procedure was approximately 15 minutes. The meninges were removed from the sample and areas damaged by removal were cut away. Then a suitable angle for cutting was chosen and the brain was glued to the tissue holder with a 2cm³ agar block glued behind for support. Slices (350 μ M or 450 μ M) were stored at 34°C for 15 minutes and then left in oxygenated aCSF in a submerged holding chamber at room temperature for at least 1 hour before use. Preparation and slicing of the human tissue samples was carried out by Dr Tom Jensen, Dr Ivan Pavlov or myself.

Neocortical pyramidal cells in layer 2-3 were targeted with the stimulating electrode placed in a region of cell fibres nearby. Data was collected using the same protocols and compound concentrations as in rodent experiments (described above).

2.7 Computational models

2.7.1 Quantitative modelling of Schaffer collateral-CA1 synapse

This model used a linear current-voltage relationship to simulate a synapse with 100% GluA2-containing AMPA receptors. Conversely, data from a kinetic model of kainate receptors (Bowie et al., 1998) built into a point process in NEURON (Carnevale and Hines, 2006) was used to simulate a synapse containing 100% GluA2-containing AMPA receptors. Data were collected using a Python script modelling activation of a synapse containing only AMPA receptors, tested at different holding potentials. The ratio of CP- to CI-AMPA receptors was varied to determine the proportion of CP-AMPA receptors required to detect using rectification index (<0.7 was chosen as the threshold to indicate synaptic CP-AMPA receptor presence).

2.7.2 Peak-scaled non stationary fluctuation analysis

Noise analysis of synaptic currents can be used to estimate the kinetics and conductance of a receptor (Benke et al., 2001). For this, evoked AMPA receptor-mediated currents from CA1 pyramidal cells were recorded in whole-cell configuration at a holding potential of -60 mV in response to external stimulation of Schaffer collateral fibres. >20 eEPSCs were collected at 20kHz for noise analysis as there was much variability between response amplitude and decay.

Recorded files were exported from LabVIEW as ASCII files and converted to CSV format. A Python script subtracted the average baseline, taken immediately before trigger of the extracellular stimuli, and then EPSCs were aligned by peak. The time points of interest were from peak of response to $6 \times t_{\text{decay}}$. Responses were normalised by scaling the average to each peak (Traynelis et al., 1993), however the peak amplitudes were fairly consistent between cycles as external stimulation likely activated all AMPA receptors from the stimulated fibres, onto the recorded cell. Mean current was binned into 50 groups based on current decay, and for each bin the variance was determined. Variance (σ^2) was plotted against mean peak scaled current (I). Single-channel current (i) was estimated by fitting the theoretical relationship for the peak scaled variance:

$$\sigma^2 = \sigma_s^2 + \left(i\bar{I} - \left(\frac{\bar{I}^2}{N} \right) \right) \quad (2.5)$$

to different fractions (50% and 100%) of the measured current-variance relationship. In this equation, N is the average number of channels open at the peak of the EPSC, as opposed to the number of channels in the postsynaptic membrane. When peak-scaling is used, the relationship is fitted to a modified equation, in which information on N is lost. The single-channel conductance (γ) can be calculated by:

$$\gamma = i/V \quad (2.6)$$

where V is the driving force (holding potential minus assumed reversal potential of 0mV). A holding potential of -60mV was used throughout the NSFA experiments. Therefore, the equation:

$$\gamma = i/ -0.06 \quad (2.7)$$

was used to estimate single-channel conductance.

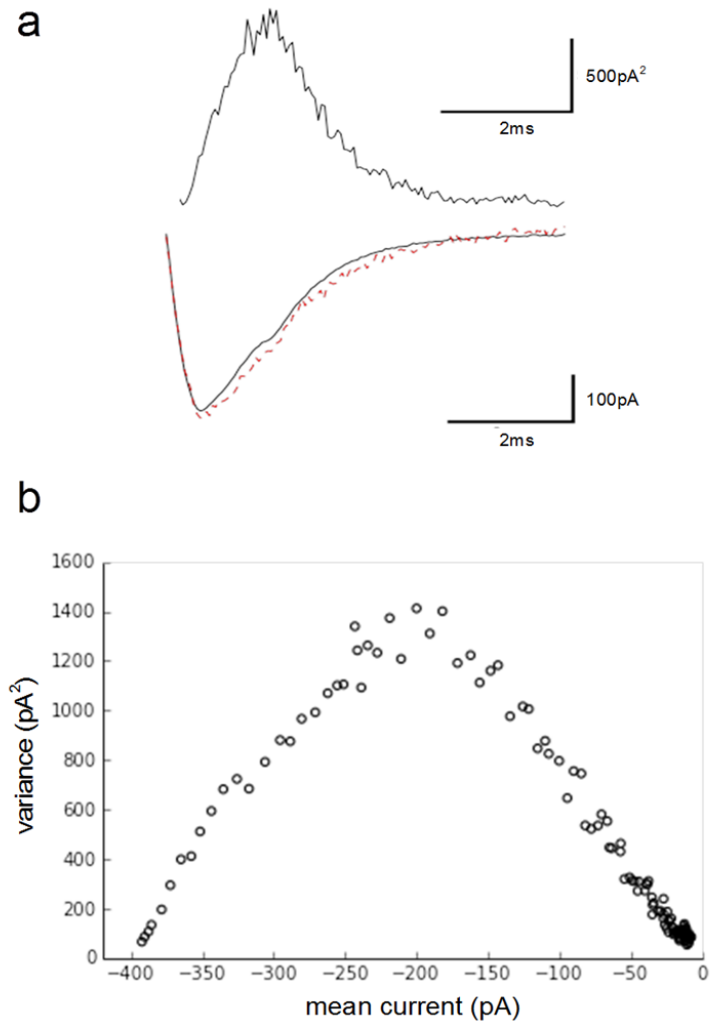


FIGURE 2.4: Estimation of single-channel conductance by peak scaled non-stationary fluctuation analysis

a) Example normalised AMPA receptor-mediated current (black line) with single sweep overlaid (red dotted line), and variance (top trace). b) Variance vs. mean current from 40 sweeps at -60 mV. Estimated of i from EQ. 2.5 is based on the initial gradient of the relationship.

2.8 Rodent model of epilepsy

2.8.1 Electrically-induced Status Epilepticus model

2.8.1.1 Animals

Male Sprague-Dawley rats (280-320g, Charles River, UK) were used throughout. Animals were housed individually with access to food and water *ad libitum* and maintained on a 12:12 hour light/dark cycle. All animal procedures had local ethical approval and followed the UK Home Office Animal (Scientific Procedures) Act, 1986.

2.8.1.2 Electrode preparation

Bipolar Teflon-coated stimulating electrodes were prepared from two intracranial electrodes wound tightly around each other by hand to prevent coating being removed from the remainder of the wire. Tips were kept ~ 0.7 mm apart to avoid short-circuiting. A scalpel blade was used to remove < 0.5 mm insulation to leave a conductive tip exposed. The unipolar Teflon-coated recording electrode was produced by removing < 0.5 mm insulation at the tip of the electrode. The reference electrode was produced from a 4cm silver wire soldered to a stainless steel gold plated socket contact. All electrodes used were from Plastics One Inc, Bilaney Consultants UK Ltd., UK.

2.8.1.3 Electrode implantation surgery

Rats were given 1 week to accommodate after arrival, then were weighted and checked for signs of ill health before the procedure. Rats were anaesthetised (5% isoflurane in 2L/min O₂) in an anaesthetic chamber, then their head area shaved with an electric shaver (Wella, UK) and cleaned with iodine (Videne, MidMeds Ltd., UK). The analgesic buprenorphine was administered (0.2mg/kg sc-40 minutes onset, 12 hour analgesia, Temgesic, Schering-Plough, UK) and gel drops were given to protect the eyeballs (Viscot Tears). The animal was then secured centrally in a stereotaxic frame (David Kopf Instruments, USA) with ear bars, incisor teeth bar and a nose bar to keep secure. The animal was placed on a heat mat with its tail tucked under to maintain optimum body temperature and enhance post-op recovery. Isoflurane delivery was reduced to 2-3% in 2L/min O₂ and monitored. Once there was no response to ear and toe pinch and breathing was satisfactory, skin was removed from the top of head (~ 1 cm²) and subcutaneous tissue cleared to reduce infection.

A stereotaxic drill (Model 1471, David Kopf Instruments, USA) attached to the stereotaxic frame was used to drill single burr holes through the skull for the bipolar stimulating electrode (right angular bundle, 4.4mm lat. and 8.1mm caud.) and recording electrode (right dentate gyrus, 2.5mm lat. and 4mm caud.), where coordinates were determined compared to Bregma; from Paxinos and Watson's rodent brain atlas (Paxinos et al., 1985). Three additional burr holes were drilled for screws to hold the dental fixture in place.

The reference electrode was wound around the front screw and 1cm tucked subcutaneously. Bipolar stimulating electrodes were placed in the angular bundle to target the perforant path projection from layer II/ III of entorhinal cortex (Stringer and Colbert, 1994). The recording electrode was placed in the dentate granule cell layer to pick up field potentials. Correct positioning of the electrodes was tested by recording the response to single test pulses. The recording electrode position was adjusted in the ventral plane until a maximal granule cell population spike amplitude was seen in response to a 3.5mA, 150 μ s single pulse stimulation (stimulating electrode lowered 3.5mm into the brain). Test pulses to the Perforant Path (PP) were initiated via a Neurolog system (Digitimer Ltd, Welwyn Garden City, UK) and stimulus isolator (Digitimer, UK) and the extracellular recordings from the dentate gyrus were amplified and bandpass-filtered (0.1-50 Hz) then digitised and recorded at 100 Hz using a CED micro 1401 and Spike 2 software (both CED, Cambridge, United Kingdom). A positive-going field potential with >2mV population spike was recorded when electrodes were in the correct position. The electrodes were mounted into a six-channel plastic pedestal (Plastics One, UK) and secured with dental cement (Kemdent, Swindon, UK). To improve recovery rates 2ml 0.9% w/v NaCl was administered subcutaneously and rats were monitored regularly.

2.8.1.4 Induction of self-sustaining status epilepticus

7-10 days after the initial surgery, rats that did not display >10% body weight loss were used to induce self-sustaining status epilepticus (SSSE). The pedestal was attached to a six-channel cable to a counterbalanced six-channel commutator (both Plastics One, UK) so that the animals were freely moving throughout. Stimulation of the perforant path was done using a Neurolog system and electrical signals were bandpass-filtered (0.1-500Hz), digitised

0	No signs
1	Facial movements
2	Wet dog shakes
3	Fore paw clonus
4	Rearing and both front paw clonus
5	Rearing and falling, wild jumping

TABLE 2.2: Racine score: Behavioural classification of seizure severity based on Racine (1972). Animals in SSSE all reached at least stage 4 severity.

at 1000Hz (CED micro 140; CED, Cambridge, UK) and recorded using Spike 2 software (CED, Cambridge, UK). After a 10 minute baseline recording, continuous stimulation consisting of trains of $50\mu\text{s}$ monopolar pulses at 20 Hz was applied for 2 hours. Stimulus intensity was adjusted to get 75% maximum population spike amplitude. Stimulation continued for 2 hours before electrically-induced SE was stopped and animals were monitored for up to 3 hours for development of SSSE. During stimulation and the subsequent recording period, the behaviour of awake freely moving rats was evaluated every 15 minutes. The severity of seizures were classified according to the Racine scale (Table 2.2) and particular behaviours such as blank gaze, chewing, focal clonus and wet dog shakes were noted down (Racine, 1972). All animals included in analysis reached at least stage 4 seizure severity during SSSE, which was considered induced if behavioural seizures or synchronous electrical events persisted for half an hour or longer, after stimulation. Animals displaying no behavioural seizures during PPS were excluded from analysis. After 30 minutes SSSE, either decanoic acid (400-600mg/kg, Sigma Aldrich) or a control vehicle DMSO (0.1ml) was injected intraperitoneally. At the end of the experiment, diazepam administered intraperitoneally (15mg/ kg) terminated seizure activity and 5ml 0.9% w/v NaCl subcutaneously (B. Braun, Germany) was given to rehydrate animals.

Spike frequency and electroencephalography (EEG) power were analysed offline using Spike 2 (CED Ltd.). EEG signals were band pass filtered in the gamma frequency range (20-70 Hz) to reduce noise contamination from movement artefacts while maintaining the signal in the frequency band associated with seizures in human and rat models (Lehmkuhle et al., 2009). Spike rate, EEG power, and integrated gamma power were compared between treatment

groups. EEG power was calculated as the ratio of root mean square (RMS) amplitude during seizure or with treatment to baseline, which has been used before to quantify seizure activity (Yang et al., 2003). Average waveforms of the unfiltered data were also compared before and after treatment. Event detection threshold was set as 7* baseline noise.

2.9 Statistics

Power calculations were performed online to determine sample size requirements, where preliminary data was available (G*Power). Electrophysiological data contained cells from at least 3 animals per experiment.

Non-parametric tests were only considered in experiments with $n=6$ or over (and $n<15$), where the Shapiro-Wilk test for normality showed that at least one data set in the comparison was not from a normal distribution (OriginPro). If normally distributed, the unpaired Student's *t*-test was used to compare two groups using different neurons/ slices/ animals, whereas paired Student's *t*-tests were used to compare the same group at different time points (for example after drug application). If the data set was reused, then significance level was Bonferroni corrected to account for multiple comparisons. When normality was rejected, a Mann-Whitney rank-sum test was the non-parametric test for unpaired data, whereas Wilcoxon signed-rank non-parametric test was used for paired datasets. Analysis of variance (ANOVA) was used to compare >2 groups, with a Tukey HSD *post-hoc* comparison of means to determine which specific groups differed from each other. A Dunnett's test was used to compare multiple treatments to a single control.

Data were presented as mean \pm SEM unless specified otherwise. The value, *n*, gives the number of cells (single cell experiments), slices (extracellular recordings), or animals (*in vivo* experiments) included. For all statistical tests, exact p-value was declared and significance with respect to the control is indicated on the figures using the following symbols: * $p < 0.05$, ** $p < 0.01$, and *** $p < 0.001$. All statistics were performed using SPSS (IBM, Portsmouth, UK), Origin 9.0 (OriginPro 9; MA, USA), or Python (Python Software Foundation).

Chapter 3

AMPA receptor properties are altered after *in vitro* SE

3.1 Summary

In this chapter I used *in vitro* models of prolonged seizure-like activity to determine changes to the properties of AMPA receptors following seizures.

AMPA receptor-mediated currents exhibit more marked inward rectification at CA1 pyramidal synapses following pilocarpine-induced seizures (Rajasekaran et al., 2012). Rectifying currents are a feature of calcium-permeable (CP)-AMPA receptors, so this indicates that following seizures there is a dynamic shift at these synapses from the normal expression of GluA2-containing AMPA receptors to expression of the GluA2-lacking subtype. In addition to more inwardly rectifying currents, CP-AMPA receptors have a higher single-channel conductance and a greatly increased permeability to divalent cations (Ca^{2+} and Zn^{2+}).

I aimed to reproduce these results in a slice model of seizures. Using whole-cell patch clamp I measured functional changes at the synapse. Electrophysiological data showed evidence for CP-AMPA receptor expression. This was supported by pharmacological analysis using a specific CP-AMPA receptor blocker. Determination of single-channel conductance using non-stationary fluctuation analysis, however, failed to support the insertion of higher conductance receptors, possibly due to confounds of the method used in neurons *in situ*.

Finally, I tested whether inhibiting only CP-AMPA receptors would be sufficient to block epileptiform activity in a slice model of persistent seizure-like activity. 1-naphthyl acetyl spermine (NASPM) had no effect on the frequency or amplitude of activity. This is probably because a low proportion of AMPA receptors are calcium-permeable and this subtype are also expressed at higher levels on seizure-controlling interneurons.

3.2 Introduction

There has been renewed interest in the role of AMPA receptors in epilepsy in part due to the recent approval of the AMPA receptor antagonist, perampanel, as an adjunctive treatment. Our understanding of the mechanism of epilepsy includes a clear role for glutamatergic activity cascading within networks of synaptically connected excitatory neurons.

There are contradictory findings regarding changes to AMPA receptors following seizures when looking at hippocampal mRNA and protein expression. CA1 pyramidal neuron synapses predominantly include GluA2-containing, CI-AMPA receptors in the healthy adult hippocampus (Lu et al., 2009). However CP-AMPA receptors are present in the immature brain (Rakhade et al., 2012; Talos et al., 2008), under certain pathological conditions, and after plasticity-inducing stimuli (Plant et al., 2006). One particular study has used whole-cell patch clamp and biotinylation to show that CP-AMPA receptors are present at CA1 pyramidal neuron synapses in slices from rats following pilocarpine-induced SE (Rajasekaran et al., 2012). Live cell imaging of hippocampal cultures shows GluA2 internalisation after 0-Mg^{2+} induced epileptiform activity (Rajasekaran et al., 2012).

Considerable evidence has accumulated showing a down-regulation of GluA2 expression in CA1 and CA3 of the hippocampus following kainate seizures (Friedman et al., 1994; Grooms et al., 2000; Condorelli et al., 1994), hypoxia-induced seizures (Sanchez et al., 2001) and lithium-pilocarpine status (Hu et al., 2012; Condorelli et al., 1994). This is not associated with either up- nor down-regulation of total AMPA receptor expression, but is consistent with increased CP-AMPA receptor expression. Down-regulation of GluA2 expression is also associated with cell layer patterns of neurodegeneration. However, this may vary according to the model used, the time window after seizures, or specific neuron types. For example, Russo et al. (2013) found decreased overall AMPA expression after 3 hours of lithium-pilocarpine seizures, but conversely found increased GluA2 protein. Seizures may also induce a rapid increase in the phosphorylation of GluA1 and GluA2 (Rakhade et al., 2012), or changes in RNA editing affecting the final AMPA receptor properties (Liu and Zukin, 2007; Krestel et al., 2004).

Humans studies determined the subunit composition of AMPA receptors in tissue extracted

during surgery for refractory epilepsy. Tissue from the neocortex has an increased GluA1 to GluA2 subunit ratio in patients, mainly due to a massive increase in GluA1 (Loddenkemper et al., 2014; Talos et al., 2008). In the hippocampus, there are reduced GluA2 levels in hippocampal areas with the most pronounced cell loss, but increased GluA2 levels within the dentate gyrus (Blumcke et al., 1996b).

The turnover rate of AMPA receptors is high, which allows a dynamic response to changes in the network activity level and is important for synaptic plasticity. Receptors move into and out of the synapse by lateral diffusion. Endocytosis and exocytosis of AMPA receptors occurs at extrasynaptic sites by separate constitutive and regulated pathways (Anggono and Huganir, 2012).

In this chapter I tested the following hypothesis:

- There is increased expression of CP-AMPA receptors in acute-hippocampal prolonged-seizure models, as has been seen in cell culture models and *ex vivo* slices from chronically epileptic animals

This will provide a basis for further investigation into the mechanism leading to a seizure-induced shift in synaptic AMPA receptor subtype.

3.3 Results

3.3.1 Theoretical relationship between proportion of CP-AMPA receptors and rectification index

CP-AMPA receptors - either GluA2-lacking or those expressing GluA2 in the unedited form - can be detected by their inwardly rectifying currents. They pass relatively small currents at positive holding potentials compared to negative voltages. This rectification is conferred by voltage-dependent block by endogenous or exogenous polyamines such as spermine. Channels from GluA2-lacking AMPA receptors show faster kinetics and larger single-channel conductance, and are uniquely sensitive to externally applied polyamine toxins such as 1-naphthyl acetyl spermine (NASPM). A useful method to estimate the contribution of CP-AMPA receptors to an EPSC is to measure the rectification index (see Chapter 2). The rectification index is 1 when currents have a linear relationship with voltage. It decreases towards zero when CP-AMPA receptors are contributing to the current, due to the polyamine-mediated ion channel block. Some groups use 0.7 as the index value at which CP-AMPA receptors begin to be detected (Wang and Gao, 2010), so I first compared the contribution of CP-AMPA receptors required to reach this detection threshold.

For this, I used a CA1 pyramidal neuron model built in NEURON. At a single point process, I expressed either CI- or CP-AMPA receptors (Fig. 3.1a). The CI-AMPA receptor was modelled with a linear $I-V$ relationship. The CP-AMPA receptor model was built in NEURON by Mr Jonathan Cornford using parameters from a model kainate receptor with $100\mu\text{M}$ spermine in the pipette (Bowie et al., 1998). Fig. 3.1b shows theoretical $I-V$ curves with different proportions of CP- to CI-AMPA receptors present at the synapse. $\sim 40\%$ CP-AMPA receptor expression is required for the RI to reach 0.7, which is the threshold often set for CP-AMPA receptor detection (Fig. 3.1c).

3.3.2 Comparison of epileptiform activity between *in vitro* models of seizure activity

I optimised the protocol of inducing epileptiform activity in hippocampal slices. An *in vitro* model in hippocampal slices was used as a compromise between simple hippocampal culture models and highly physiological *ex vivo* slices which are time consuming to prepare.

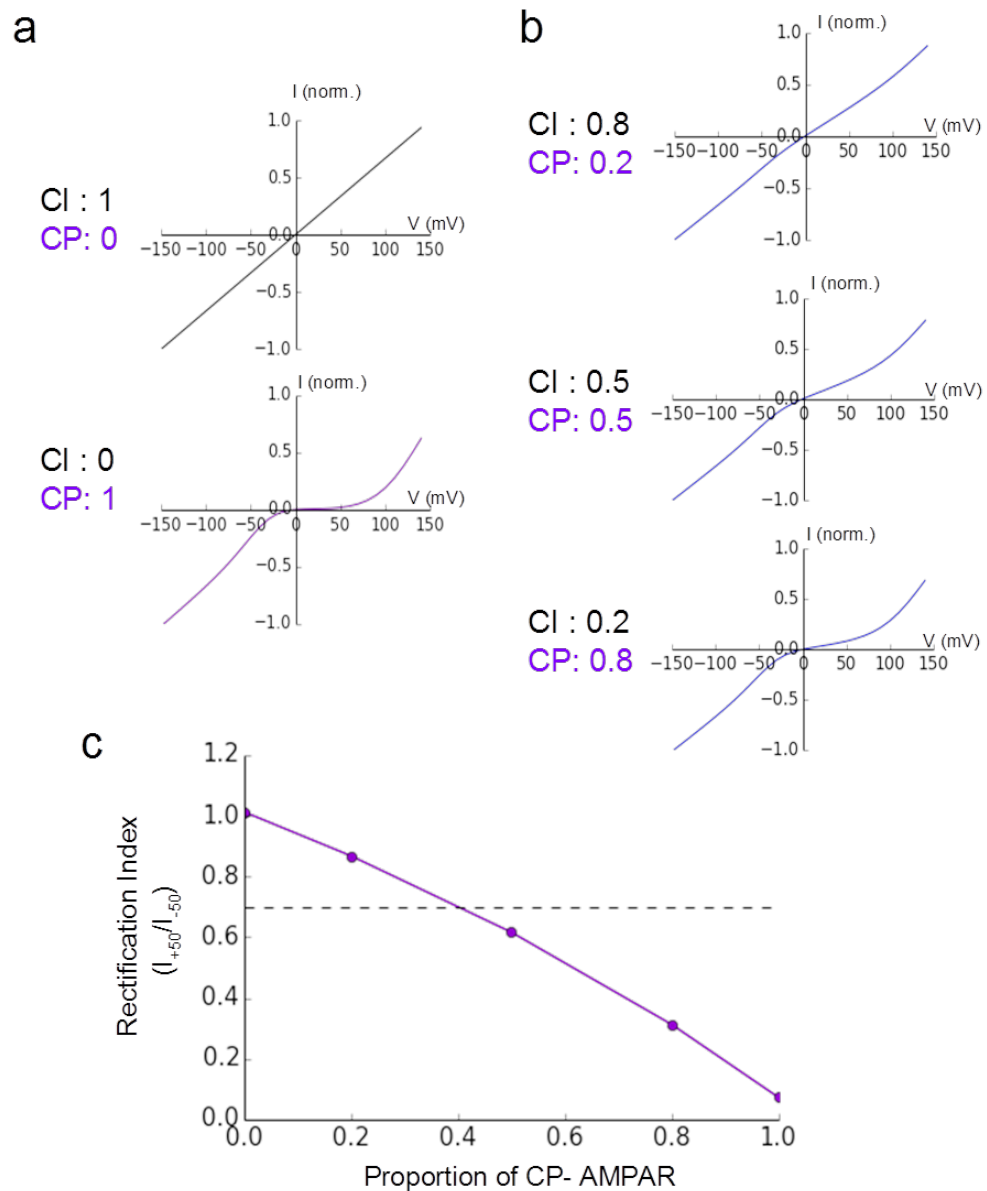


FIGURE 3.1: *In silico* models of the synapse show that CP-AMPA receptors must be present in high proportion to be detected by rectification index

a) The expected linear $I-V$ curve at a point process with no CP-AMPA receptors present, and with a rectification index (RI) of 1 [top]. A strongly inwardly rectifying $I-V$ curve when all AMPA receptors are calcium permeable and RI is 0.1 [lower]. b) As the proportion of CP-AMPA receptors included at the synapse increases, the amount of current rectification increases. c) Comparing the proportion of CP-AMPA receptors contributing to the overall current to the subsequent RI. Over 40% CP-AMPA receptors are required for RI to be below 0.7 and the mixed category given (dashed line marks 0.7 threshold).

As I planned to probe the mechanism leading to insertion of CP-AMPA receptors, it was important to use an appropriate model for their detection. In tissue from *in vivo* animal models, there is a model-dependence as to whether the effect is seen.

In extracellular recordings made from the stratum radiatum, epileptiform activity could be induced in both the 0-Mg²⁺ and 2 mM PTZ-aCSF slice models, in an interface chamber (Fig. 3.2). This was developed and sustained at both room temperature and 34°C. Epileptiform activity began sooner and was more pronounced after induction at 34°C, so this temperature induction was used for all experiments. Activity was larger amplitude and contained more ictal like bursts in 0-Mg²⁺ aCSF, but the pyramidal neurons were visually less healthy in this model. When 5mM pyruvate was included in the incubation solution it improved neuron health (Kovac et al., 2012) and did not alter network epileptiform activity. Recent findings show that pyruvate acts as an antagonist to AMPA receptors at 60mM (Pedersen et al., 2016), so this was not included in the solution during whole-cell patch clamp recordings.

After slicing, the slices recovered at room temperature for at least 40 minutes, before being incubated in the activity generating solutions. Slices were incubated in the epileptogenic solution for at least 60 minutes. At least one slice per animal was recorded from using an extracellular electrode, which confirmed that all slices produced epileptiform activity after 60 minutes of incubation. Under basal conditions roughly 15-25% surface AMPA receptors are internalised every 30 minutes (Ehlers, 2000), although expression of CP-AMPA receptors persisted for hours in a hippocampal culture model of ischemia (Blanco-Suarez and Hanley, 2014). Nonetheless, in my experiments I only included recordings in which whole-cell configuration was achieved within 20 minutes of removal from the incubation medium (Fig. 3.3).

3.3.3 0-Mg²⁺ aCSF induces rectifying AMPA receptor-mediated currents

I looked for evidence of CP-AMPA receptor expression in slice models of epilepsy by measuring the rectification index. Pyramidal neurons from the hippocampus CA1 were voltage clamped at holding potentials between -80mV and +60mV, at 20mV intervals. Neurons in the 0-Mg²⁺ treatment group had inwardly rectifying currents, and control neurons had a linear *I-V* relationship, as reported previously and consistent with predominant CI-AMPA receptor expression (Rozov et al., 2012; Mattison et al., 2014; Fig. 3.4a). The

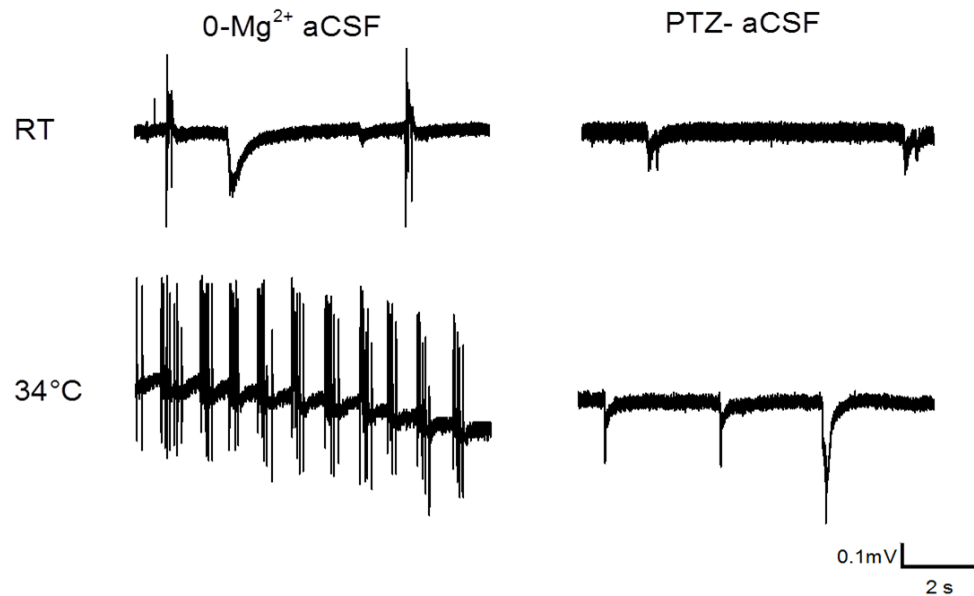


FIGURE 3.2: Representative extracellular recordings from stratum radiatum in CA1. Epileptiform activity is present after 60 minutes incubation in 0-Mg²⁺ or PTZ-aCSF at room temperature (RT), but is stronger and more sustained when generated at 34° C.

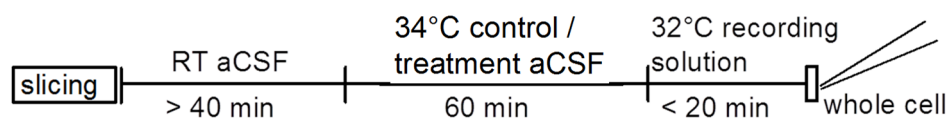


FIGURE 3.3: General experimental outline I employed, using *in vitro* slice models to compare AMPA receptor-mediated EPSCs.

rectification index was significantly lower in the 0-Mg²⁺ group than control (Fig. 3.4b-c; [control]: 1.07 ± 0.24 , n=7; [0-Mg²⁺]: 0.60 ± 0.14 , n=11. $p = 0.038$; Mann-Whitney U-test). In the 0-Mg²⁺ treated group, current reversal was shifted positively, although lines were fitted as reversing through 0mV, as assumed based on theory. Cell health was noticeably worse after incubation in 0-Mg²⁺ aCSF than control aCSF, and the addition of pyruvate was required to improve recording quality (observation not shown). There were no significant differences between treatment groups when comparing input resistance, cell size or leak currents (Supplementary Table 8.1). The quality of voltage clamp of the cell will depend on the health of cells patched, which could be a confounding factor. 0-Mg²⁺ treatment could reduce the clamp quality, but as there was no difference in input resistance, measured at -60mV, between treatment groups this should not be a significant factor.

3.3.4 PTZ-aCSF induces rectifying AMPA receptor-mediated currents

I next looked for evidence of CP-AMPA receptor expression in the PTZ slice model of seizures. Pyramidal neurons from the PTZ treatment group had inwardly rectifying currents, compared to the expected linear $I-V$ relationship measured in the control group (Fig. 3.5b-c; [control]: 0.93 ± 0.16 , n=10; [PTZ]: 0.57 ± 0.09 , n=11. $p = 0.029$, unpaired t -test with equal variance). AMPA receptor-mediated currents were sensitive to NBQX (Fig. 3.5a). The RI in the PTZ model was similar to that in the 0-Mg²⁺ model.

Cell health was similar in the PTZ-aCSF treatment group to control, and cells could be patched without including pyruvate in the incubation solution. There was no difference in rectification index between cells incubated in pyruvate and those not in pyruvate (not shown; [PTZ only]: 0.60 ± 0.13 , n=8; [PTZ-pyruvate]: 0.58 ± 0.07 , n=8. $p=0.44$, unpaired t -test).

3.3.5 Pharmacological detection of CP-AMPA receptors using NASPM

The effect of epileptiform activity on rectification index was apparent in both *in vitro* slice models of seizures. The cells were healthier in the PTZ model so I chose to continue using this treatment to induce seizure-activity throughout.

Next, I pharmacologically inhibited CP-AMPA receptors using NASPM, a polyamine and

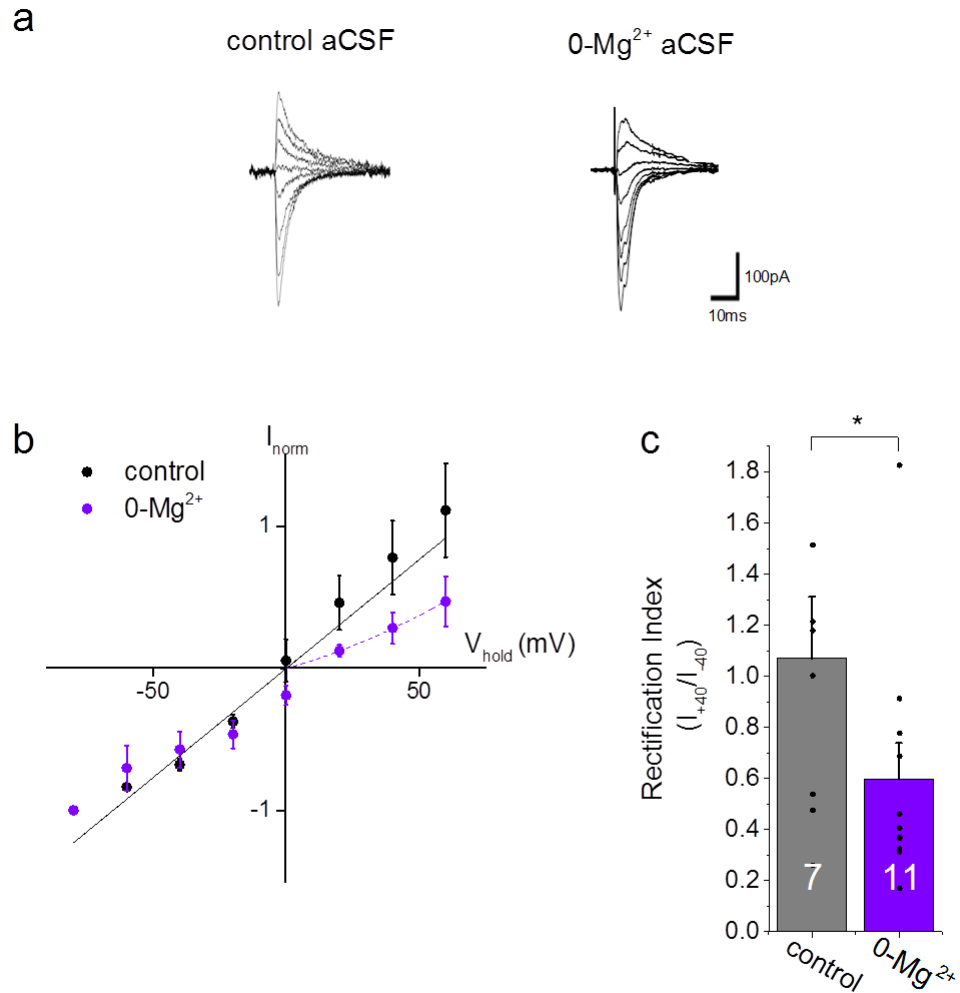


FIGURE 3.4: AMPA receptor-mediated currents are inwardly rectifying in the 0-Mg²⁺ slice model of seizures.

a) Example whole-cell voltage clamp recordings after incubation in control and 0-Mg²⁺ aCSF. b) Normalised $I-V$ curve in each treatment group. Black solid line is an extrapolation of a linear fit to the data in the control group at negative values. Purple dotted line is a polynomial fit to the 0-Mg²⁺ group at positive holding potentials only. c) Summary of RI, * $p < 0.05$, Mann-Whitney U-test.

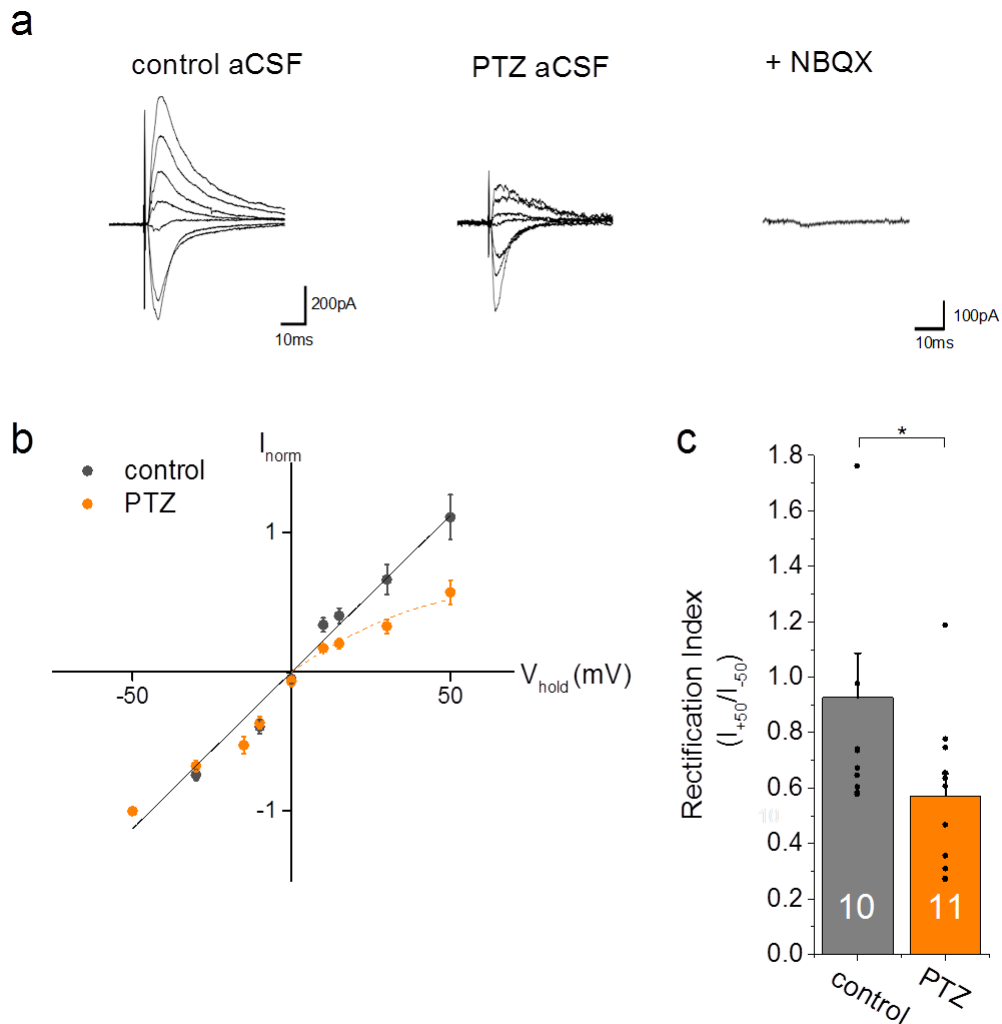


FIGURE 3.5: AMPA receptor-mediated currents are inward rectifying in the PTZ slice model of seizures.

a) Example whole-cell voltage clamp recordings in control and PTZ-aCSF the treatment groups. Blocking AMPA receptors with NBQX ($10\mu\text{M}$) eliminated eEPSCs at -60mV . b) Normalised $I-V$ curve is linear in the control group, and rectified in the PTZ group. Black solid line is a linear fit to the data in the control group, orange dotted line is fit to the PTZ group at positive holding potentials only. c) Summary of RI, $*p < 0.05$, t -test.

specific CP-AMPA receptor blocker, to confirm the presence of CP-AMPA receptors at CA1 pyramidal neuron synapses. Using more than one method for detection of CP-AMPA receptor is important as there are secondary reasons which could cause the same results on rectification index. For example, some CI-AMPA receptors have been shown to produce rectified AMPA receptor currents and auxiliary subunit interactions can enhance the polyamine block incurring inwardly rectifying currents. AMPA receptor-mediated currents at -60 mV significantly reduced in amplitude in the PTZ treatment group upon wash in of 70 μ M NASPM (Fig. 3.6a-b; n=11, currents reduced to 0.81 ± 0.06 [normalised]; p=0.05, paired *t*-test), and not in control slices (n=4, to 0.97 ± 0.04 [normalised]; p=0.15, paired *t*-test). This indicates that CP-AMPA receptors were present at the synapse, and were inhibited by NASPM.

Surprisingly, there was run-down in some recordings so the current amplitude at +40 mV was also reduced, and the RI decreased in the PTZ group after NASPM wash-in (Fig. 3.6c; 0.50 ± 0.09 to 0.39 ± 0.08 ; p=0.02, paired *t*-test), but did not in the control group (0.61 ± 0.23 to 0.60 ± 0.20 ; p=0.31, paired *t*-test). The contradictory finding that current amplitude decreased at positive potentials with the block of CP-AMPA receptors warrants further investigation.

3.3.6 Variance analysis for estimation of conductance of synaptic AMPA receptors

I next used analysis of variance to look for CP-AMPA receptors in the PTZ seizure model. Non-stationary fluctuation analysis (NSFA) is a method used to look at synaptic currents and to estimate the average number of channels open at the peak of the current (N), to determine the average single-channel conductance of these channels (γ). CP-AMPA receptors generally have a higher γ than GluA2-containing subtypes, although this can be dramatically altered by the association with auxiliary subunits (Swanson et al., 1997; Shelley et al., 2012).

The AMPA receptor-mediated current-variance relationship is parabolic, and fits to Equation 2.5 (see Chapter 2) where σ^2 is the variance, \bar{I} is the mean current, and i is the weighted-mean single-channel current. This shape can be explained as there is little variance at the peak

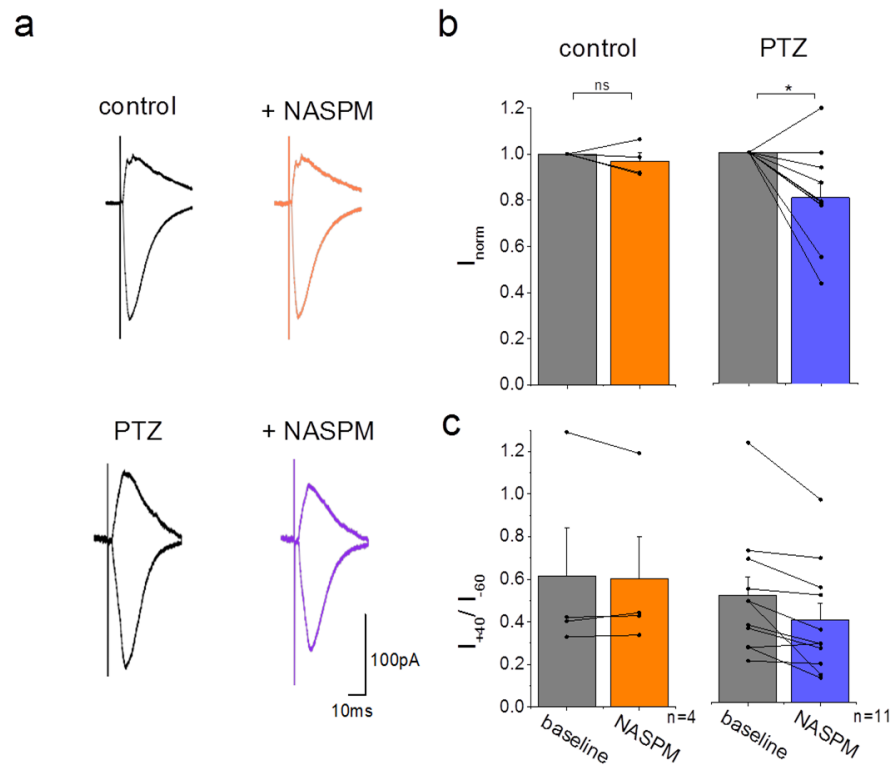


FIGURE 3.6: Pharmacological inhibition of CP-AMPA receptors in CA1 pyramidal neurons. a) Example AMPA receptor EPSCs before [black] and with NASPM [coloured] to inhibit currents from CP-AMPA receptors. Top traces are control conditions, lower traces after incubation in PTZ-aCSF. b) Peak current amplitude decreased with NASPM application [normalised]. c) Rectification index also decreased with NASPM. * $p < 0.05$, *t*-test.

current response (as all channels are open) and at very end of the current decay (as few channels remain open). Conversely, there is more variance during the current decay as the number of channels open varies between cycles.

My data were collected using a large extracellular stimulation electrode activating hundreds to thousands of fibres that synapse onto the patched pyramidal cell. The original method of NSFA has to be adapted for multi-synaptic responses (Traynelis et al., 1993). This peak scaling causes a loss of information about synaptic channel number (N) and peak open probability of channels (P_o). Multi-synaptic EPSCs have slower rise times and decays from dendritic filtering. Further, there is increased noise from asynchronous neurotransmitter release and overlap of different time constants of activation than mono-synaptic recordings. Sometimes a double response was generated from the stimulation, these responses could not be used for NSFA.

Single channel currents were not changed by the seizure model ([control]: 0.13 ± 0.05 pA, $n=5$, [PTZ]: 0.11 ± 0.07 pA, $n=5$; $p=0.80$, unpaired t -test, Fig. 3.7b), and single-channel conductance was 2.19 ± 0.09 pS [control] vs 1.81 ± 0.01 pS [PTZ], (Fig. 3.7b; $p=0.36$, unpaired t -test). These values are low compared to dendritically recorded CA1 EPSCs, and the PTZ group was expected to have a higher single-channel conductance (Smith et al., 2000; Benke et al., 1998). Variance was low at the peak and tail of the current, and the data points parabolic to fit Equation 2.5. However parabolas were skewed towards the peak currents, which could indicate that channels continue to open for the first time after the peak response. Another explanation is that kinetic properties of specific receptors can lead to a skewed variance vs. mean current relationship (Hartveit and Veruki, 2006).

3.3.7 Blocking CP-AMPA receptors with NASPM is insufficient to inhibit PTZ-induced epileptiform discharges

A simple way to monitor the excitability of a seizure network is to count the number of epileptiform events (Fig. 3.8a). I recorded activity extracellularly in the stratum radiatum; each event was composed of trains of spikes starting with a fast, large, negative spike and followed by smaller amplitude spikes in a slower downward phase (Fig. 3.8b). The event polarity depended on the cell layer the recording was taken from (Fig. 2.3).

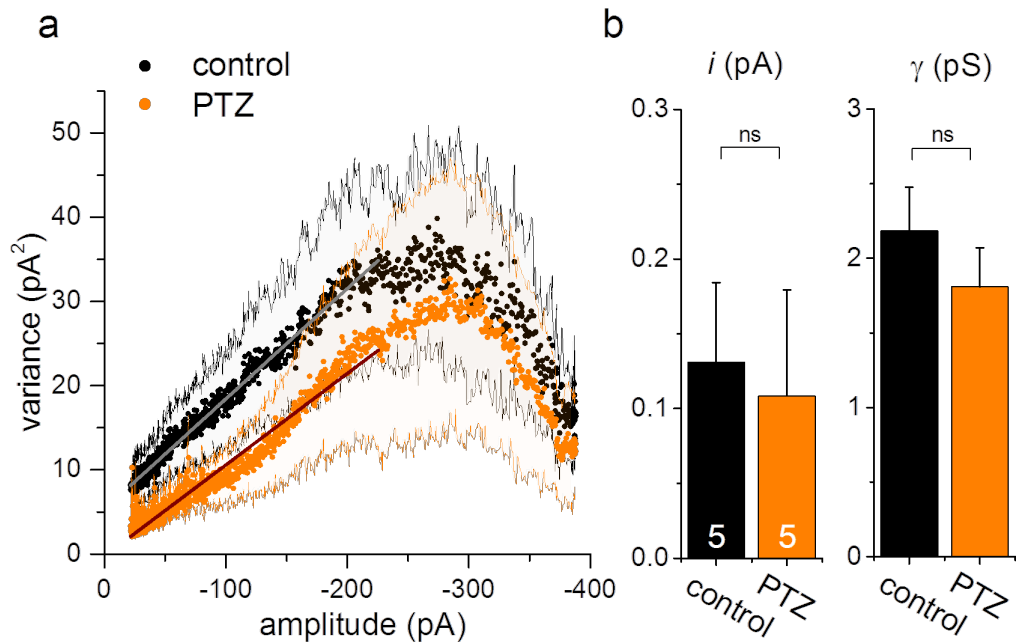


FIGURE 3.7: Estimation of single-channel conductance is lower in the seizure group than control, using peak-scaled NSFA.

a) Variance vs. mean evoked EPSC amplitude in control ($n=5$) and PTZ ($n=5$) treated groups. Variance and peak-scaled amplitude were averaged over treatment groups, shaded area denotes SEM. Grey and black solid lines are linear fits to 50% points in control and PTZ groups respectively. b) Single channel current (i) and single-channel conductance (γ) are not significantly different between groups, at a holding voltage of -60mV . ns: $p>0.05$, unpaired t -test.

If CP-AMPA receptor expression is increased at pyramidal neuron synapses under pathological conditions, then inhibiting these channels following seizures could have a functional impact. A CP-AMPA receptor blocker attenuated calcium bursts in hippocampal cultures incubated in 0-Mg²⁺ aCSF (Rajasekaran et al., 2012). Further, inhibiting CP-AMPA receptors protects hippocampal neurons against ischemia-induced cell death in an animal model (Noh et al., 2005). I recorded network activity in the slice model of seizures to test if CP-AMPA receptor inhibitors block epileptiform activity. I counted the number of epileptiform discharges, where each discharge contained poly-spikes (Fig. 3.8a-b). Specifically, blocking CP-AMPA receptors did not change the frequency of epileptiform activity (Fig. 3.8c; Number of epileptiform events per 5 minutes [normalised to baseline]: [control] = 1, [NASPM] = 0.99 ± 0.24, n=4; p=0.244, paired *t*-test; [washout] = 1.12 ± 0.24). Some slices showed ictal-like activity followed by long silent periods, so the binned event count was highly variable.

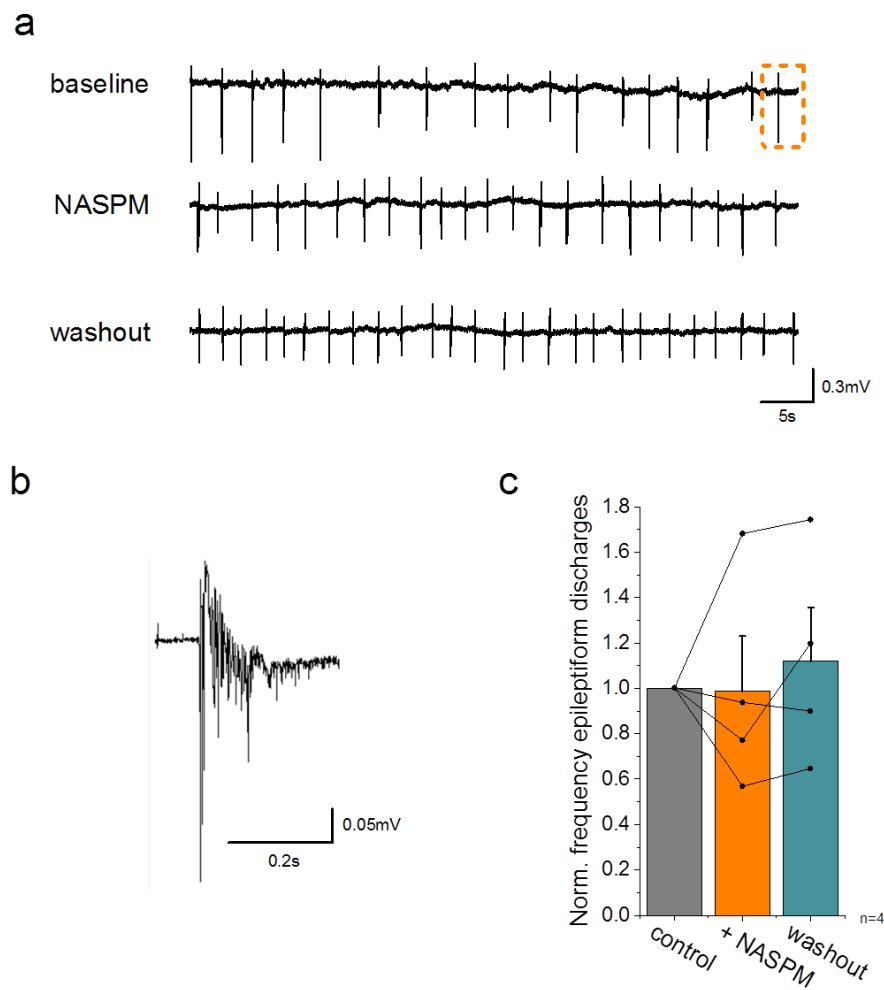


FIGURE 3.8: Inhibition of CP-AMPA receptors was not sufficient to inhibit epileptiform activity in a slice model of seizures

a) Example extracellular recordings after 1 hour in PTZ-aCSF [top], after application of a specific CP-AMPA receptor blocker [middle], and on wash out with PTZ-aCSF [lower].
 b) Close up of trace in (a) [orange box] showing a single epileptiform event, notice the large amplitude downward spike followed by smaller spikes phasically reducing.
 c) Normalised number of epileptiform events at with a CP-AMPA receptors blocker and wash out. [Control]= grey, average between -10 and 0 minutes, [NASPM] = orange, average between 25 and 35 minutes, [washout]= turquoise, average between 50 and 60 minutes.

3.4 Discussion

This chapter replicates previous findings, using an acute slice model of prolonged seizure activity, showing expression of CP-AMPA receptors after seizures. I showed rectification of $I-V$ curves in two *in vitro* models, which supports the presence of synaptic CP-AMPA receptors. Pyramidal neurons incubated in either 0-Mg²⁺ or PTZ-aCSF have decreased rectification indexes (Figs. 3.4- 3.5). There was a high variability in the rectification index between neurons in each group, and many factors are likely to influence the level of CP-AMPA receptor expression at the synapse. My theoretical calculations showed that 40% AMPA receptors may be required before the RI detects expression (Fig. 3.1). This simple calculation may exaggerate the ratio as CP-AMPA receptors have a greater single-channel conductance. If only over-active synapses express CP-AMPA receptors, then what proportion of synapses on a CA1 pyramidal neuron would be affected by this change? Further, there are CP-AMPA receptors which do not exhibit inward rectification (Bowie, 2012), and conversely some auxiliary subunits reduce the polyamine block of CP-AMPA receptors while enhancing calcium permeability (Jackson et al., 2011; Coombs et al., 2012). This led to the requirement of multiple experiments to test the presence of these receptors.

AMPA receptors are highly dynamic at synapses, so it was important for the measurement of CP-AMPA receptor presence to be within an appropriate time window after removal from the incubating solution. All recordings for the $I-V$ curves reached whole-cell configuration within 20 minutes of removal from the activity induction solution (0-Mg²⁺ or PTZ-aCSF). In Fig. 3.6, the specific CP-AMPA receptor blocker, NASPM, reduced AMPA receptor-mediated currents at -60mV. It also reduced the RI, which does not fit with results that should be obtained from the remaining CI-AMPA receptor currents. This may be from a problem with the specificity of the NASPM used, or a charging effect from the application of a high concentration of ionised polyamine to the recording solution affecting the driving force of Na⁺ and K⁺.

Next, the single-channel conductance was estimated by peak scaled NSFA. Single channel conductance (γ) was not found to be significantly different in the PTZ treated group compared to control, which did not match with the $I-V$ results. The analysis of many EPSCs was needed to account for variation in response shape from multi-synaptic activation. More

precise estimates could be achieved by recording from single channels, although access the CA1 synapses would not be possible with glass micro-pipettes. γ is altered by different mean opening times, and the estimation of γ is also affected by access resistance (R_A) so I ensured there was a $<10\%$ change in R_A throughout the recording (started $10.6\text{M}\Omega$ and ended $11.9\text{M}\Omega$; with $>60\%$ R_A compensation; Supplementary Table 8.1). The variance values were dependent on bin size, so I kept this consistent throughout analysis. Further, the recordings in Fig. 3.7 were made >40 minutes after removal from the induction solution; the experimental set-up was such that only the healthiest cells were kept to perform recordings for NSFA after the $I-V$ experiments. As synapses onto CA1 pyramidal neurons are susceptible to stimulation-induced changes in synaptic strength, the stimulation frequency did not exceed 0.1Hz and therefore the recordings took a long time to be completed. This selection bias may have meant that those with the least CP-AMPA receptors were included in NSFA experiments. These limitations did not allow reliable estimation of single-channel conductance from currents recorded in rat CA1 pyramidal neurons. However, this shows a proof of principle, although it may be that fewer recordings of $I-V$ curves are necessary before moving onto collecting the NSFA data. It would be beneficial to repeat the experiments in cells immediately removed from PTZ-aCSF.

My results provide evidence for the expression of CP-AMPA receptors at CA1 pyramidal cell synapses in a seizure model. GluA2-lacking AMPA receptors have markedly increased permeability to divalent cations such as Ca^{2+} as well as greater single-channel conductance and desensitisation rates. The increased single-channel conductance raises the risk of excitotoxicity for the cell, which could be a mechanism to mark the cell for apoptosis. The faster desensitisation rate reduces the time window for integration of synaptic inputs when CP-AMPA receptors are prevalent (Abrahamsson et al., 2012). This may be a mechanism to lower the probability for synaptic strengthening. Ca^{2+} entry into the cell is precisely controlled. The timing and intensity of intracellular Ca^{2+} elevation controls the direction of synaptic plasticity depending which intracellular proteins are activated: CaM kinase or calcineurin. Calcium entry can trigger further Ca^{2+} release from intracellular stores by Ca^{2+} -induced Ca^{2+} release (CICR). Initiation of this cascade will have consequences further than the activated synapse. Since calcium buffering is disrupted in epilepsy, CP-AMPA receptors may promote the initiation of apoptosis. The level of calbindin-D28k, a neuronal calcium binding protein, is halved in the hippocampus in a chronic *in vivo* model of epilepsy (Carter

et al., 2008).

Due to the polyamine block around V_{rev} , the largest influx of Ca^{2+} will occur when CP-AMPA receptors are activated at potentials closest to RMP, or even hyperpolarised potentials. Conversely, pyramidal neurons in epileptic tissue spike more frequently than pyramidal neurons in normal tissue, so are at the depolarised potentials of the peak of action potentials (around +40 mV; Sterratt et al., 2012) more often. Although they have a greater single-channel conductance, activation of CP-AMPA receptors carries reduced current when depolarised compared to GluA2-containing AMPA receptors, so increased synaptic CP-AMPA receptor expression may dampen the excitable network activity. Specific inhibition of CP-AMPA receptors by NASPM did not alter the frequency of epileptiform discharges. There is high expression of CP-AMPA receptors in interneurons in healthy tissue and epileptic tissue has reduced inhibitory drive, so blocking AMPA receptors on interneurons may increase epileptic network activity. It is unclear why my results contradict previous findings, but CP-AMPA receptor blockers could be expected to improve neuronal death by reducing apoptosis as a separate action to that on network activity.

These results do not shed light on whether CP-AMPA receptors are added to the existing complement of surface AMPA receptors, or whether they replace CI-AMPA receptors that are internalised via GluA2 endocytosis. Recent studies suggest that CP-AMPA receptors do replace CI-AMPA receptors at hippocampal synapses, at least in cell culture models of ischemia (Blanco-Suarez and Hanley, 2014). The mechanism for how CP-AMPA receptors become expressed at the hippocampal CA1 synapses is also not understood. In the following chapter, I look at some key pathways linked to the inclusion of CP-AMPA receptors at the synapse and look at the effect of pharmacologically blocking these.

Chapter 4

Investigation into the mechanism of expression of CP-AMPA receptors

4.1 Summary

In this chapter I investigated the mechanisms by which seizure-activity leads to increased expression of CP-AMPA receptors. I initially looked at the requirement of Ca^{2+} entry through the NMDA receptor for CP-AMPA receptor expression at CA1 pyramidal neuron synapses. Many dynamically regulated processes in cells are dependent on changes in calcium concentration and phosphorylation levels, as these signal a change in the network activity levels. As predicted, inhibiting NMDA receptors blocked the synaptic expression of CP-AMPA receptors in a slice model of seizures.

Then I looked at the requirement of a serine/threonine phosphatase and a tyrosine phosphatase for surface expression of CP-AMPA receptors. Inhibition of the serine/threonine phosphatase, calcineurin, but not the tyrosine phosphatase, STEP₆₁, occluded the effect of seizure activity. These results indicate that calcineurin activation via calcium entry through NMDA receptors mediates the shift from CI- to CP-AMPA receptors.

4.2 Introduction

The signalling pathway which leads to expression of CP-AMPA receptors at pyramidal neurons following seizures is not understood but is important to understanding their role in network changes and neuronal death following SE. The shift could be mediated by any candidate molecules in overlapping pathways, by inhibiting exocytosis of CI-AMPA receptors to the synapse or by promoting the production of AMPA receptor subunits with enhanced calcium permeability.

NMDA receptors respond to changes in network excitation as activation allows local Ca^{2+} influx, which reads out the activity of the synapse. Therefore, during a seizure there would be much greater Ca^{2+} influx through NMDA receptors. Ca^{2+} is buffered differently in nanodomains and microdomains, so excessive Ca^{2+} entry will therefore initiate different intracellular cascade proteins compared to physiological conditions, including activation of kinases and phosphatases (Alford et al., 1993). AMPA receptor phosphorylation by kinases can have a dramatic effect on surface expression on a fast time scale. This is ideal for dynamic responses to stimuli such as in synaptic plasticity. Depending on the site, phosphorylation can alter trafficking, stabilisation at the synapse and gating kinetics. Phosphorylation regulates with which proteins the receptor can associate. Phosphatase activation can also regulate AMPA receptor trafficking indirectly by altering the phosphorylation patterns of mediator proteins which interact with AMPA receptors to regulate their trafficking.

Calcineurin (CaN), a Ca^{2+} /calmodulin-dependent protein phosphatase, is activated by Ca^{2+} influx via NMDA receptors and is increased in the hippocampus following seizures (Kurz 2001). CaN has been implicated in activity-dependent regulation of GABAergic inhibition (Eckel et al., 2014) and AMPA receptors (Beattie et al., 2000). At the AMPA receptor CaN dephosphorylates serine 845 on the GluA1 subunit, which reverses PKA-induced increased channel open probability and internalises CP-AMPA receptors (Sanderson et al., 2012). Conversely, phosphorylation at S⁸⁴⁵ by PKA may stabilise CP-AMPA receptors at the perisynapse for activity-dependent trafficking (Derkach et al., 2007; Oh et al., 2006; Banke et al., 2000). Therefore this provides a balance between GluA1 insertion by kinases and removal by phosphatases in synapses.

Additionally, tyrosine phosphatases such as Striatal-enriched protein tyrosine phosphatase 61 (STEP₆₁) are also activated by NMDA receptors (Paul et al., 2003). STEP₆₁ specifically dephosphorylates tyrosine sites on the GluA2 AMPA receptor subunit and on NMDA receptor subunit GluN2B. GluA2 dephosphorylation at T⁸⁶⁹, T⁸⁷³, and T⁸⁷⁶ (3Tyr) causes AMPA receptor internalisation (Hayashi and Huganir, 2004). Genetic ablation of STEP₆₁ renders mice more resistant to pilocarpine-induced SE than WT (Briggs et al., 2011). STEP₆₁ is increased following prolonged activity in cultures incubated with GABA_A receptor inhibitor bicuculline. Further, acute induction of an electroconvulsive seizure increases STEP₆₁ and decreases tyrosine-phosphorylation in the hippocampus. However, chronic electroconvulsive seizures has no effect on STEP₆₁ levels (Jang et al., 2016). As STEP₆₁ reduces surface expression of AMPA receptors, STEP₆₁ upregulation may cause internalisation of extrasynaptic GluA2 to promote CP-AMPA receptor expression.

Altering the phosphorylation pattern on GluA2 subunits has a more complex effect than GluA1 subunits. GluA2 is not present in most CP-AMPA receptors, so phosphorylation will specifically affect CI-AMPA receptors. STEP₆₁ dephosphorylates amino acids at GluA2 without acting at GluA1.

Finally, auxiliary protein interactions have a major role in AMPA receptor trafficking and expression at synapses (Bats et al., 2013; Studniarczyk et al., 2013). They regulate AMPA receptor kinetics and, in some cases, the drug sensitivity of the receptor C-terminal protein interactions (Rouach et al., 2005). The most well categorised are TARPs; but more recently other families of auxiliary subunits have been established including cornichons, CKAMP44, GSG1L, synDIG1 (see section 1.3.2 for more information). Cornichons have a well defined role in the export of specific proteins from the ER (Brockie et al., 2013). Genetic knockout of $\gamma 2$ or $\gamma 8$ TARPs does not change which subtype reaches the synapse, but does influence the number of receptors there. TARPs also contain 9 phosphorylation sites which can further diversify the influence they have at AMPA receptors.

In this chapter I tested the following hypotheses:

- Expression of CP-AMPA receptors in pyramidal neurons following seizures is initiated

by NMDA receptor-dependent activity

- Downstream from Ca^{2+} entry through NMDA receptors, the phosphorylation patterns of AMPA receptors determines CP-AMPA receptor expression
- The phosphorylation patterns on AMPA receptor subunits can influence the amount of CP-AMPA receptor expression.

I aimed to determine the mechanism of subunit switch using acute hippocampal slices incubated in PTZ-aCSF. I included a specific blocker of the signalling molecule of interest in the induction medium throughout the entire induction period (>1 hour), and looked at the *I-V* relationship of isolated AMPA receptor-mediated currents in each condition to compare the contribution of CP-AMPA receptors.

4.3 Results

4.3.1 Inhibition of NMDA receptors blocks expression of CP-AMPA receptors in a seizure model

NMDA receptors are one of the main mechanisms of Ca^{2+} entry into cells. They are known as coincidence detectors as they require both a depolarised membrane potential, to remove the extracellular Mg^{2+} block, and activation by glutamate before they pass current. Strong neuronal depolarisations occur during epileptic activity, which can remove the Mg^{2+} block and increase NMDA receptor-mediated currents (Coan and Collingridge, 1985). Calcium entry through NMDA receptors is the initial step in intracellular signalling cascades having many effects at the synapse, including receptor trafficking. The NMDA receptor is key for a number of physiological processes, including different forms of plasticity.

NMDA receptor activity is not always necessary for burst generation. Spontaneous activity can be generated in the presence of NMDA receptor antagonists in kainic acid, high potassium or 4-AP models of epileptiform discharges (Neuman et al., 1988; Psarropoulou and Avoli, 1992). I first looked at the role of NMDA receptors in the PTZ slice model of seizures. Fig. 4.1a shows that in the PTZ model, NMDA receptors are not required for the maintenance nor the generation of epileptiform activity. The frequency of epileptiform discharges was not altered after application of $50\mu\text{M}$ D-AP5 (Fig. 4.1b; [PTZ]: 32.9 ± 10.9 events/min, [+D-AP5]: 27.4 ± 10.6 events/min; $n=4$, $p=0.18$, paired *t*-test). Further, the frequency of epileptiform discharges was the same when initiated in PTZ-aCSF alone or in PTZ-aCSF with $50\mu\text{M}$ D-AP5 (Fig. 4.1c; [PTZ]: 18.7 ± 1.8 events/min ($n=50$), [PTZ-D-AP5]: 19.4 ± 8.1 events/min ($n=5$); $p=0.17$, unpaired *t*-test). On the other hand, seizures alter NMDA receptor properties and one of the effects is an up-regulation of the NR2B subunit (Di Maio et al., 2011; Hardingham et al., 2002).

Activation of NMDA receptors is a trigger for receptor trafficking, as occurs in LTP and LTD. The NMDA receptor antagonist D-AP5 completely blocks the endocytosis of AMPA receptors in response to mild stimulation (Carroll et al., 1999). I found that after one hour of incubation in D-AP5, AMPA receptor-mediated currents showed no inward rectification in either the control aCSF nor the PTZ-aCSF group (Fig. 4.2a-b), indicating that D-AP5 blocked expression of CP-AMPA receptors. There was no difference in the RI between

groups (Fig. 4.2c; 0.71 ± 0.02 [control, n=4] vs. 0.78 ± 0.13 [PTZ, n=7]; $p=0.46$, unpaired *t*-test), indicating that D-AP5 blocks the seizure-induced change in rectification. This fits with previous data showing that NMDA receptors are required to trigger some forms of AMPA receptor trafficking.

Next, I looked at the pathway downstream of NMDA receptors. Ca^{2+} entry via NMDA receptors regulates phosphorylation of AMPA receptors by kinases and phosphatases.

4.3.2 Inhibiting calcineurin reduces seizure-induced rectification of AMPA receptor-mediated currents.

Calcineurin (protein phosphatase 2B; CaN) is a Ca^{2+} and calmodulin-dependent serine/threonine protein phosphatase that is distributed widely throughout the brain and can regulate the activity of several ligand-gated ion channels, including AMPA and GABA_A receptors. CaN works antagonistically with kinases in the cell by dephosphorylating proteins. CaN is anchored to the synapse with PKA by AKAP150, and internalises AMPA receptors by opposing phosphorylation of the GluA1 subunit by PKA at S⁸²⁵ (Beattie et al., 2000). Dephosphorylation at S⁸²⁵ increases mobility from the synapse; FK506 is a CaN blocker which strongly inhibits AMPA receptor endocytosis induced by either AMPA or NMDA application (Beattie et al., 2000). Further if the interaction between AKAP150 and CaN is disrupted then phosphorylation at GluA1 S⁸²⁵ is increased and AMPA receptors are incorporated both basally and during activity (Sanderson et al., 2012).

Basal and maximal activity of CaN is increased in SE *in vitro*, and is dependent on NMDA receptor activation (Kurz et al., 2001). CaN becomes truncated 24 hours after SE, possibly as it is activated irreversibly. Incubation with the AMPA receptor blocker GYKI-52466 (GYKI) for one hour also prevents seizure-induced increases in CaN activity after hypoxia-induced seizures (Sanchez et al., 2005). CaN regulates changes in GABA receptor subunits after seizures (Eckel et al., 2014). FK506 has been shown to have neuroprotective effects in a hippocampal slice culture, after 24 hours in kainic acid (Lee et al., 2010). Similarly FK506 has been shown to decrease the frequency of seizures, in a model of temporal lobe epilepsy (Nishimura et al., 2006). However, it is likely to have confounding results *in vitro* as it will act on both inhibitory and excitatory neurons.

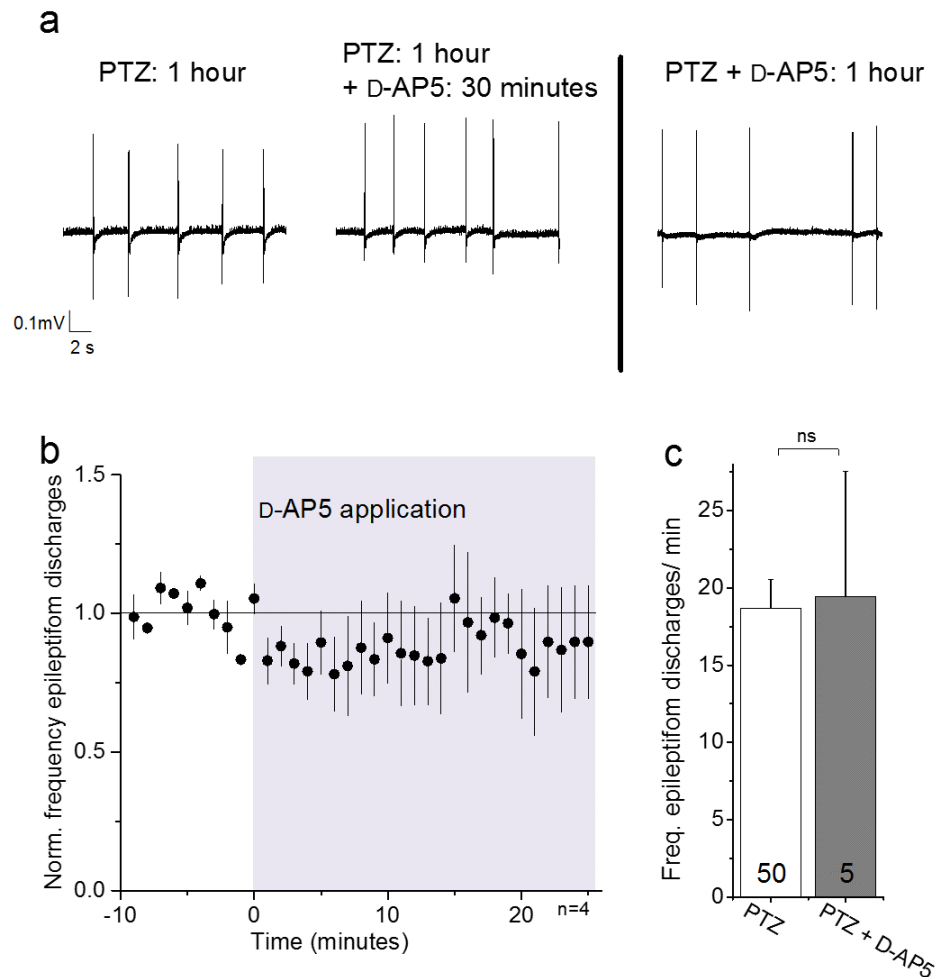


FIGURE 4.1: Epileptiform activity is both sustained and initiated in the presence of a NMDA receptor antagonist.

a) Example extracellular recordings show that PTZ-induced epileptiform activity [left] is sustained 30 minutes after application of D-AP5 [middle] and can be initiated after 1 hour in PTZ-aCSF in the presence of D-AP5 [right]. b) Application of D-AP5 does not alter the frequency of epileptiform discharges. c) Summary showing the frequency of epileptiform discharges was not altered when activity is initiated in the presence of D-AP5. ns: $p > 0.05$ (unpaired *t*-test).

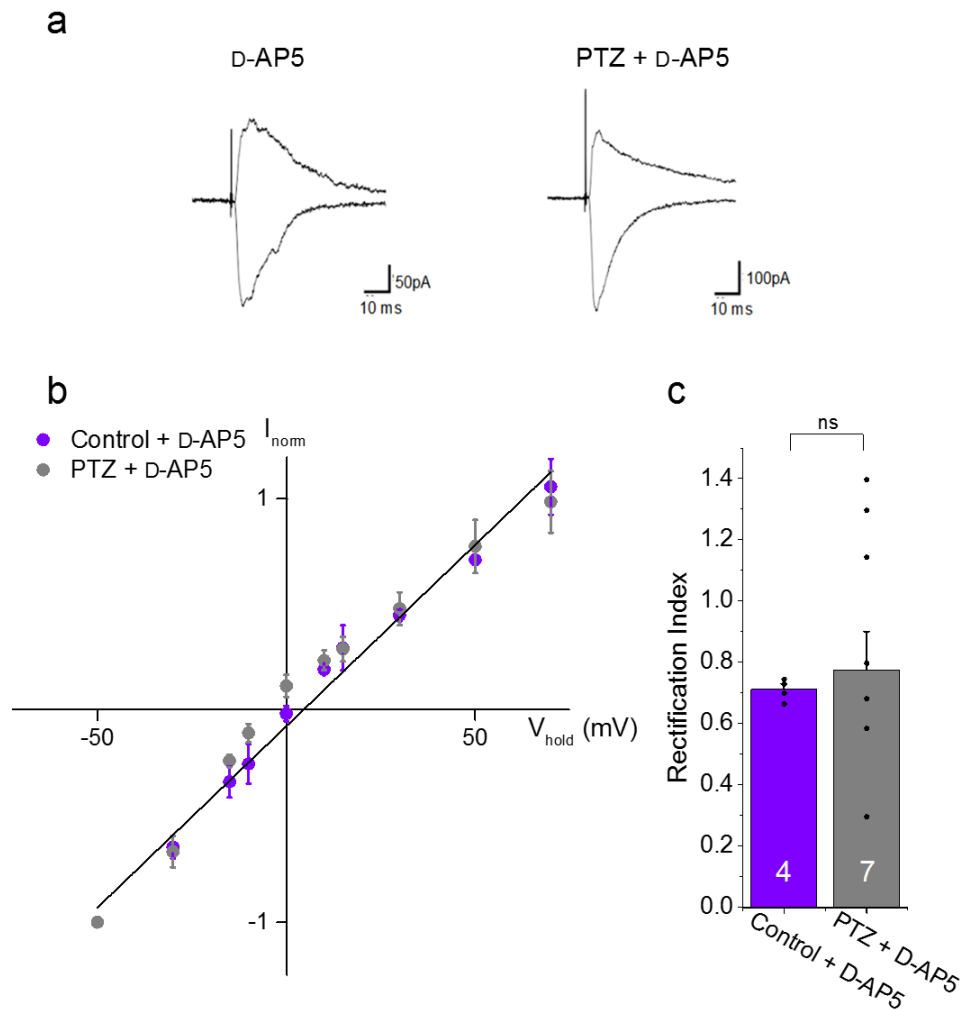


FIGURE 4.2: Inhibition of NMDA receptors blocks rectification of AMPA receptor-mediated currents in a slice model of seizures

a) Example whole-cell voltage clamp recordings (+50 mV and -50 mV) from pyramidal neurons incubated in D-AP5 with control [left] and PTZ-aCSF [right]. Example whole-cell voltage clamp recordings in control and PTZ-aCSF the treatment groups. b) Normalised I - V curve is linear in the control group, and in the PTZ group in the presence of NMDA receptor inhibitors. Black solid line is a linear fit to the data in the control group. c) Summary of RI and individual data values; ns: $p > 0.05$, unpaired t -test.

Blocking CaN enhances LTP, and conversely decreases the amplitude of LTD after low frequency stimulation (Wang and Kelly, 1996). Inhibition of CaN by FK506 may increase synaptic expression of CP-AMPA receptors by stabilising GluA1 phosphorylation, or it may block the internalisation of CI-AMPA receptors and therefore block expression of CP-AMPA receptors, so could prevent epilepsy-induced changes in AMPA receptor trafficking. CaN also dephosphorylates dynamin, synaptojanin, and the adaptor protein AP180, which are important in receptor endocytosis (Clayton et al., 2007).

Following one hour of incubation, FK506 did not inhibit epileptiform activity in PTZ-aCSF, and did not induce activity in control-aCSF (Fig. 4.3a). Currents did not show much inward rectification in either group (Fig. 4.3b-d), indicating there was little CP-AMPA receptor expression. There was no difference in the RI between groups (Fig. 4.3d; [control]: 0.73 ± 0.05 , $n=9$; [PTZ]: 0.67 ± 0.11 ; $n=8$; $p=0.08$, Mann-Whitney U-test), indicating that FK506 blocks the seizure-induced change in rectification. As the RI is still lower than one, its difficult to interpret CP-AMPA receptor expression with certainty.

4.3.3 Tyrosine phosphatase inhibition increases rectification in control slices to match the seizure model

The other phosphorylation target I considered was STEP₆₁, which works antagonistically with kinases by non-specifically dephosphorylating tyrosine residues on GluA2 AMPA receptor subunits and GluN2B NMDA receptor subunits, as well as other targets that are distinct from those of CaN. There are two splice variants of STEP: STEP₆₁ is an intrinsic membrane protein, and STEP₄₆ is cytosolic. STEP₆₁ is highly expressed in striatal neurons, is expressed in hippocampal neurons and is associated with the ER. Although the specific tyrosine residues on GluA2 regulated by STEP₆₁ are unknown, the GluA2 phosphorylation state at 3Tyr all regulate AMPA receptor trafficking. Tyrosine phosphorylation of GluA2 at T⁸⁷⁶ is by SRC family protein tyrosine kinases and is required for AMPA- and NMDA-induced internalisation of AMPA receptors as in LTD. Inhibiting this kinase blocks internalisation (Ahmadian et al., 2004; Hayashi and Huganir, 2004; Fox et al., 2007). Tyrosine phosphorylation of GluA2 regulates GluA2 binding to GRIP/ABP, but not to PICK1. This binding is also regulated by Ser880 phosphorylation by PKC, which allows multiple methods

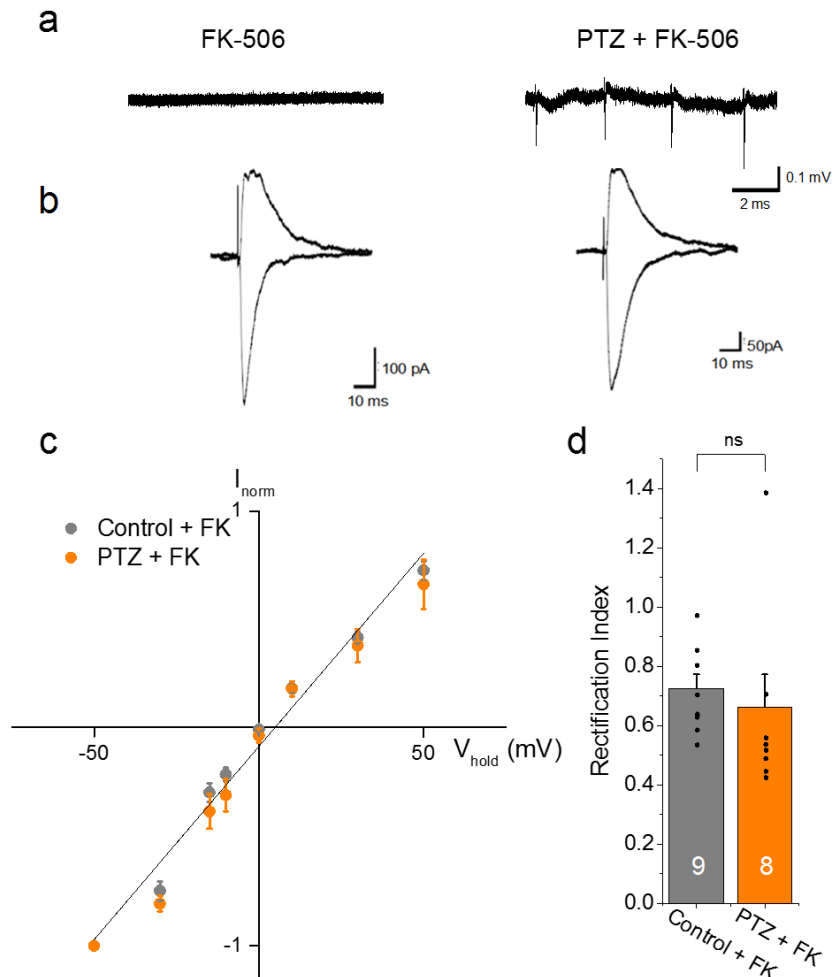


FIGURE 4.3: Inhibition of serine/threonine protein phosphatase, calcineurin, blocks rectification of AMPA receptor-mediated currents in a slice model of seizures

- a) Example extracellular recordings show that activity was not present after 1 hour in aCSF with CaN inhibited [left] and is sustained in PTZ-aCSF with calcineurin inhibited.
- b) Example whole-cell voltage clamp recordings (+50 mV and -50 mV) from pyramidal neurons incubated in FK506 with control [left] and PTZ-aCSF [right].
- c) Normalised $I-V$ curve is linear in the control group and the PTZ group in the presence of a CaN inhibitor. Black solid lines are a linear fit to the data in the control group and the PTZ group.
- d) Summary of RI; ns: $p > 0.05$, Mann-Whitney U-test

of regulating GluA2 release from GRIP. GRIP controls release of AMPA receptors to make them available for insertion into the synaptic membrane and for internalised receptors to be captured (Braithwaite et al., 2002; Matsuda et al., 2000). The specific subunit combinations of AMPA receptors regulated by this trafficking pathway has not been looked at.

STEP₆₁ is locally translated in dendrites after mGluR5 activation and is linked to mGluR-LTD (Zhang et al., 2008), whereas synaptic stimulation of NMDA receptors promotes STEP₆₁ ubiquitination and degradation after ERK1/2 activation (Xu et al., 2009). In neuronal cultures with increased activity, there is increased STEP₆₁ activity leading to reduced phosphorylation of tyrosine residues on GluA2, without affecting their total protein expression. Activity blockade by TTX reduced STEP₆₁ activity and increased AMPA receptor expression (Jang et al., 2015). Subunit specificity was not looked at in these experiments. STEP₆₁ is inactive when phosphorylated at Ser²²¹, and needs dephosphorylating to be activated (Kamceva et al., 2016).

TC-2153 is STEP₆₁ inhibitor which should leave tyrosine residues phosphorylated at GluA2. I looked at whether this would increase the incorporation of CP-AMPA receptors into synapses in the PTZ model. One hour of incubation with TC-2153 did not inhibit epileptiform activity in PTZ-aCSF, and did not initiate activity in control-aCSF (Fig. 4.4a). Surprisingly, currents showed inward rectification in both groups (Fig. 4.4b-c), indicating that there was expression of CP-AMPA receptors in both groups. Unexpectedly there was greater rectification in the control treatment group than in the PTZ group (Fig. 4.4d; [control]: 0.45 ± 0.03 , n=8; [PTZ]: 0.64 ± 0.08 , n=9; p=0.026, unpaired *t*-test). The reason for this should be investigated further, as it is possible that TC-2153 promotes synaptic CP-AMPA receptor expression in healthy pyramidal neurons.

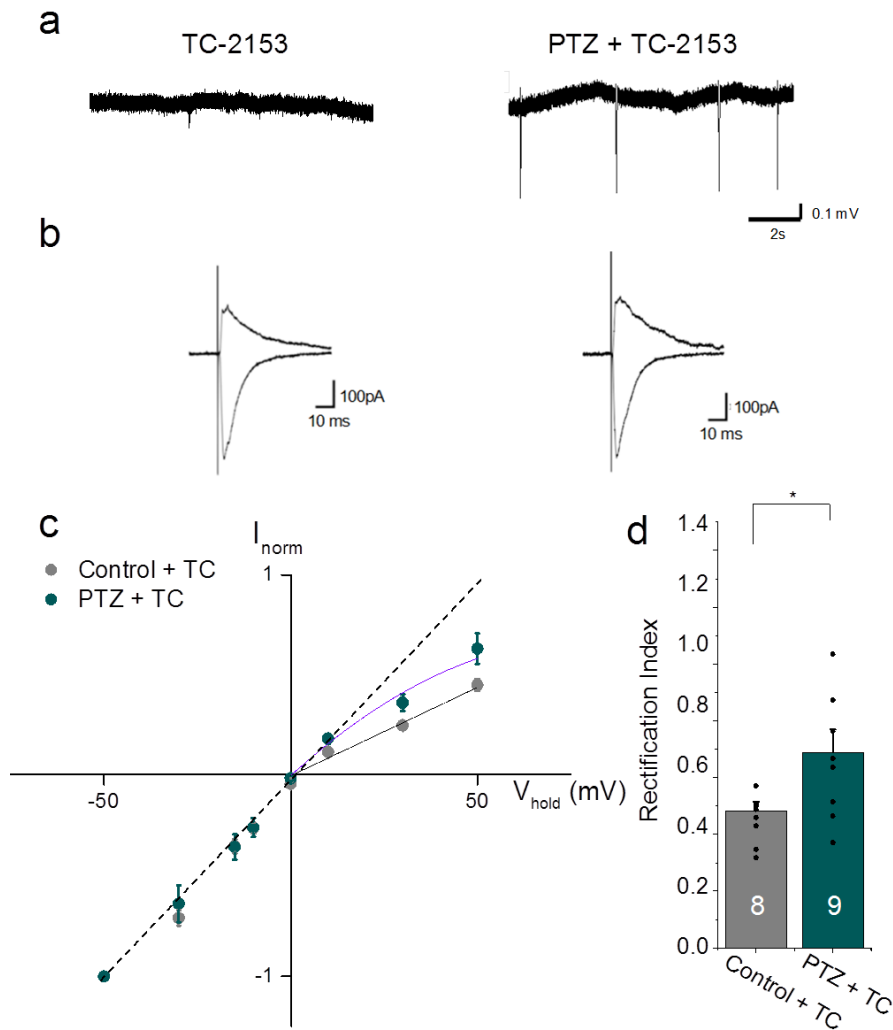


FIGURE 4.4: Inhibition of the tyrosine phosphatase, STEP₆₁, does not alter rectification after seizures and increases rectification in the non-seizure treatment group

a) Example extracellular recordings show that activity was not present after 1 hour in aCSF with tyrosine phosphatase inhibited [left] and is sustained in PTZ-aCSF with tyrosine phosphatase inhibited. b) Example whole-cell voltage clamp recordings from pyramidal neurons incubated in TC-2153 (+50mV and -50mV) with control [left] and PTZ-aCSF [right]. c) Normalised $I-V$ curve is rectified in the control group, and less rectifying in the PTZ group after incubation in a tyrosine phosphatase inhibitor. Black dotted line is a linear fit extrapolated from data at negative holding potentials in the control group; black solid line is fit to the control group at positive holding potentials, purple solid line is fit to the PTZ group at positive holding potentials. d) Summary of RI. * $p < 0.05$, unpaired t -test.

4.4 Discussion

In this chapter I investigated the relationship between NMDA receptor activation, subunit patterns of phosphorylation, and the expression of CP-AMPA receptors following seizure-like activity. PTZ-induced epileptiform activity was not altered in the presence of NMDA receptor blockers, but synaptic expression of CP-AMPA receptors was restricted by NMDA receptor blockade. Further, the calcium-dependent serine/threonine protein phosphatase, CaN, was also necessary for this expression. Conversely, the tyrosine phosphatase STEP₆₁ limits expression of CP-AMPA receptors, possibly by its action at NMDA receptors. However, this can not be confirmed by the experiments presented.

Activation of NMDA receptors causes activation of CaN as well as many other intracellular mediators. Calcium-dependent CaN activation leads to dephosphorylation and activation of STEP₆₁ at Ser221 (Paul et al., 2003). Phosphatases interact with intracellular signalling molecules as well as phosphorylating ion channels. The phosphorylation state of residues on AMPA receptors drives internalisation and lateral movement, for removal from the synapse (Fig. 4.5). Chen et al. (2013) showed that Ca²⁺-induced activation of CaN by NMDA receptors is required for CP-AMPA receptor expression after nerve injury in the spinal cord (Chen et al., 2013), which matches my results. FK506 is a non-specific CaN inhibitor which also acts as an immunosuppressant so it is possible, although very unlikely, that an off-target action is blocking expression of CP-AMPA receptors.

I found that TC-2153 promoted expression of CP-AMPA receptors. As TC-2153 has actions at both AMPA receptors and NMDA receptors, reducing STEP₆₁ dephosphorylation of GluN2B could enhance NMDA receptor activation to promote CP-AMPA receptor expression (Lee, 2006). Stimulation of NMDA receptors invokes proteolysis of STEP₆₁. Decreased STEP₆₁, as in the presence of TC-2153, increases phosphorylation of AMPA receptor GluA2 subunits and NMDA receptor subunit GluN2B. Increased phosphorylation of GluN2B at T¹⁵⁷² has been shown after febrile seizures (Chen et al., 2016). Phosphorylation of T¹³³⁶ and T¹⁴⁷² on GluN2B by the Src kinase, Fyn, enhances NMDA receptor-mediated currents and controls trafficking. T¹⁴⁷² phosphorylation enhances binding of GluN2B with PSD95, retaining NMDA receptors on synaptic membranes, and increasing LTP (Salter and Kalia, 2004; Nakazawa et al., 2001). Genetic deletion of STEP₆₁ improves cognitive function

in a mouse model of Alzheimer's disease, by restoring the number of AMPA receptors and enhancing LTP (Xu et al., 2014). Alternatively, phosphorylation at T¹³³⁶ results in translocation of GluN2B-containing NMDA receptors from synaptic to extrasynaptic membranes (Bi et al., 2000). STEP₆₁ is degraded by BDNF, which is increased following SE (Saavedra et al., 2015; Danzer et al., 2004), so this could explain why inhibiting STEP₆₁ has a greater effect in the control group. STEP₆₁ has a neuroprotective role by disrupting the p38 MAPK pathway (Deb et al., 2013), so it makes sense that inhibiting it will increase CP-AMPA receptor expression.

NMDA receptor antagonists do not alter epileptiform activity in slice models of seizure, but they have been shown to improve cell health *in vivo* (Meldrum, 1993). The AMPA receptor subunit switch detected after seizures might be induced by the deterioration in cell health which is evident in slice models of epilepsy. Reducing the excitotoxic influence on cells may slow the kinetics of intracellular pathways driving the subunit switch. If this is the case, then there may be CP-AMPA receptor expression after a longer incubation period than that looked at here.

There are different mechanisms regulating constitutive and activity-induced AMPA receptor. The pathways I have looked at may target receptor movement after seizures but not alter constitutive endocytosis. It would be interesting to track the movement of AMPA receptors in a seizure model by live cell imaging to see which pathways are important for CP-AMPA receptor movement into the synapse. Auxiliary subunits of AMPA receptors are involved in receptor trafficking and subunit composition (Bats et al., 2013; Kato et al., 2007; McGee et al., 2015). It would be interesting to see if the interaction between TARPs and AMPA receptors is altered following seizures.

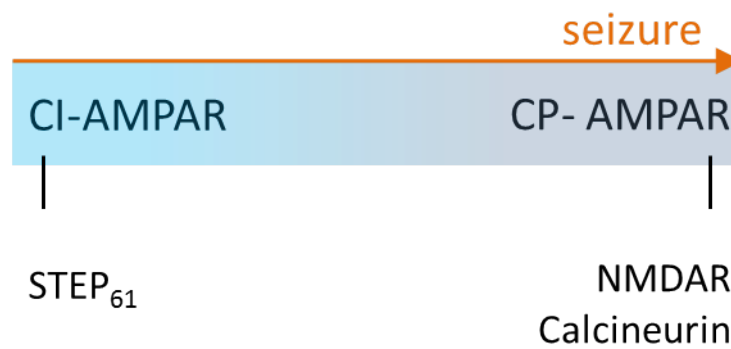


FIGURE 4.5: Summary of the key findings in this chapter. There is a scale of CP-AMPA receptor expression, which is increased after seizures. This is dependent of NMDA receptor activation and calcineurin. Activation of STEP₆₁ promotes expression of CI-AMPA receptors.

Chapter 5

The action of decanoic acid and other MCTs at AMPA receptors

5.1 Summary

In this chapter I looked at the inhibition of AMPA receptors by medium chain triglycerides (MCTs). Decanoic acid is a MCT and a key component of the MCT ketogenic diet. It exhibits anti-seizure properties *in vitro*, and non-competitively blocks isolated AMPA receptors in *Xenopus oocytes* and native AMPA receptors in the rodent brain (Chang et al., 2016).

I first investigated the anti-seizure effect of decanoic acid in acute hippocampal slices. In comparison to GYKI, another non-competitive AMPA receptor antagonist, decanoic acid had equivalent anti-seizure properties. This was at concentrations with comparable AMPA receptor antagonism, suggesting that AMPA receptor antagonism is sufficient to explain the anti-seizure properties of decanoic acid. Branched chain derivatives of medium chain triglycerides also inhibit epileptiform activity to a similar extent to decanoic acid, but may have favourable pharmacokinetics *in vivo*.

I next looked in further detail at the action of decanoic acid at AMPA receptors. AMPA receptor kinetics were not affected by decanoic acid. Perampanel and decanoic acid act synergistically at AMPA receptors to reduce epileptiform activity in a supra-linear way, even at a sub-therapeutic concentration of perampanel. Finally, I showed that AMPA receptor

block by decanoic acid was not use-dependent.

These data provide a more thorough understanding of how decanoic acid is acting at AMPA receptors to have anti-seizure properties, and suggest that this compound could be suitable as a treatment for epilepsy.

5.2 Introduction

Research into new treatments for epilepsy is particularly necessary as 30% of epilepsy patients have continued seizures despite treatment with current AEDs. Further, many patients on AEDs become refractory to treatment and have unacceptable side-effects on their present treatments. Alternative treatments such as neurosurgery and dietary intervention are options in epilepsy refractory to pharmacological treatment. The ketogenic diet is a successful method of seizure control, but compliance is low due to poor tolerability, associated side effects and metabolic consequences (Cross et al., 2010).

Decanoic acid is a 10 carbon saturated MCT and, along with 8 carbon octanoic acid, is a key component of the MCT ketogenic diet used clinically for the treatment of refractory epilepsy. The MCT ketogenic diet is a modification of the high fat, low carbohydrate classical ketogenic diet, which involves obtaining a high percentage of daily calorific intake from coconut oil. This version is less strict than the classic diet, but similarly effective. Decanoic acid crosses the blood-brain barrier and is increased in the brain plasma of those on the ketogenic diet (Haidukewych et al., 1982). It has been shown that decanoic acid is able to block PTZ-induced epileptiform activity more efficiently than octanoic acid *in vitro* (Chang et al., 2012).

Recently, decanoic acid has been shown to block AMPA receptor-mediated currents in *Xenopus oocytes*. In this study, decanoic acid was found to act non-competitively and in both a voltage-dependent and a dose-dependent way (Chang et al., 2016). Different AMPA receptor subunit compositions were tested, and decanoic acid was shown to be effective in both GluA2/3 heteromers and GluA1 homomeric channels but with differing potency at specific subunit combinations (Chang et al., 2016). Excitatory synapses are important in the synchronisation of neurons at seizure initiation and the propagation of seizures, and are therefore a promising target for anti-seizure therapies. In preclinical studies non-competitive AMPA receptor antagonists, including GYKI, have looked effective however many have frequent side effects *in vivo* affecting cognition and attention. Currently, the only clinically approved drug for use in refractory epilepsy which acts at the AMPA receptor is perampanel. This is a specific non-competitive AMPA receptor antagonist licensed for the adjunctive treatment of partial onset and primary generalised tonic-clonic seizures with or

without secondarily generalised seizures in people aged 12 years and older (Zwart et al., 2014; Frampton, 2015). However there are still side effects seen after treatment with perampanel which highlights the continuing need for novel compounds to be tested.

In this chapter I tested the following hypotheses:

- Decanoic acid's action at AMPA receptors is sufficient to explain its anti-seizure effects
- Branched derivatives of medium chain fatty acids show anti-seizure properties *in vitro*
- Decanoic acid stops status epilepticus *in vivo*
- The combination of perampanel and decanoic acid has a synergistic anti-seizure effect.

5.3 Results

5.3.1 The anti-seizure effect of decanoic acid can be explained by its action at AMPA receptors

Decanoic acid was compared to another AMPA receptor antagonist using the PTZ seizure model in hippocampal slices. GYKI is a benzodiazepine which acts as a non-competitive AMPA receptor antagonist and binds to a different site to the proposed decanoic acid binding site (Chang et al., 2016). It has a completely different structure to MCTs (Fig. 5.1a).

GYKI was used at $50\mu\text{M}$, a concentration that gives the same degree of AMPA receptor antagonism as 1mM decanoic acid. At lower concentrations, GYKI can potentiate AMPA receptor-mediated currents (Arai, 2001), however 1mM decanoic acid and $50\mu\text{M}$ GYKI both reduce all AMPA receptor-mediated current in hippocampal neurons by approximately 70% (Chang et al., 2016; Donevan and Rogawski, 1993). PTZ-induced spontaneous bursting activity was recorded from the stratum radiatum of rodent hippocampal CA1 extracellularly (Fig. 5.1b). This epileptiform activity was completely blocked by $50\mu\text{M}$ GYKI (Fig. 5.1b-d; from 83.1 ± 30.7 events per 5 minutes [baseline] to 0.6 ± 0.6 events [20 minutes in GYKI]; $n=4$, $p=0.036$, paired *t*-test), and returned upon washout. Epileptiform discharges were also blocked by 1mM decanoic acid (Fig. 5.1b-d; from 73.3 ± 16.7 events per 5 minutes [baseline] to 0 [20 minutes in decanoic acid]; $n=5$, $p=0.006$, paired *t*-test), and returned upon washout. Activity returned to $58.1 \pm 11.3\%$ of baseline in GYKI washout, and $72.6 \pm 14.6\%$ with decanoic acid washout (Fig. 5.1b-c).

5.3.2 Modification of epileptiform activity by derivatives of medium chain triglycerides

Previous studies, which compared different MCTs, showed that 10-carbon decanoic acid has greater anti-seizure effects *in vitro* than either longer or shorter straight-chained triglycerides (Chang et al., 2013). Decanoic acid is present at clinically relevant concentrations in the brain of those on the ketogenic diet (Haidukewych et al., 1982). Although a concentrated form of decanoic acid has strong anti-seizure effects *in vitro*, it may have limited action *in vivo* since MCTs accumulate in fatty tissue and undergo rapid metabolism before reaching the brain. In this section I examined derivatives of medium chain fatty acids, including

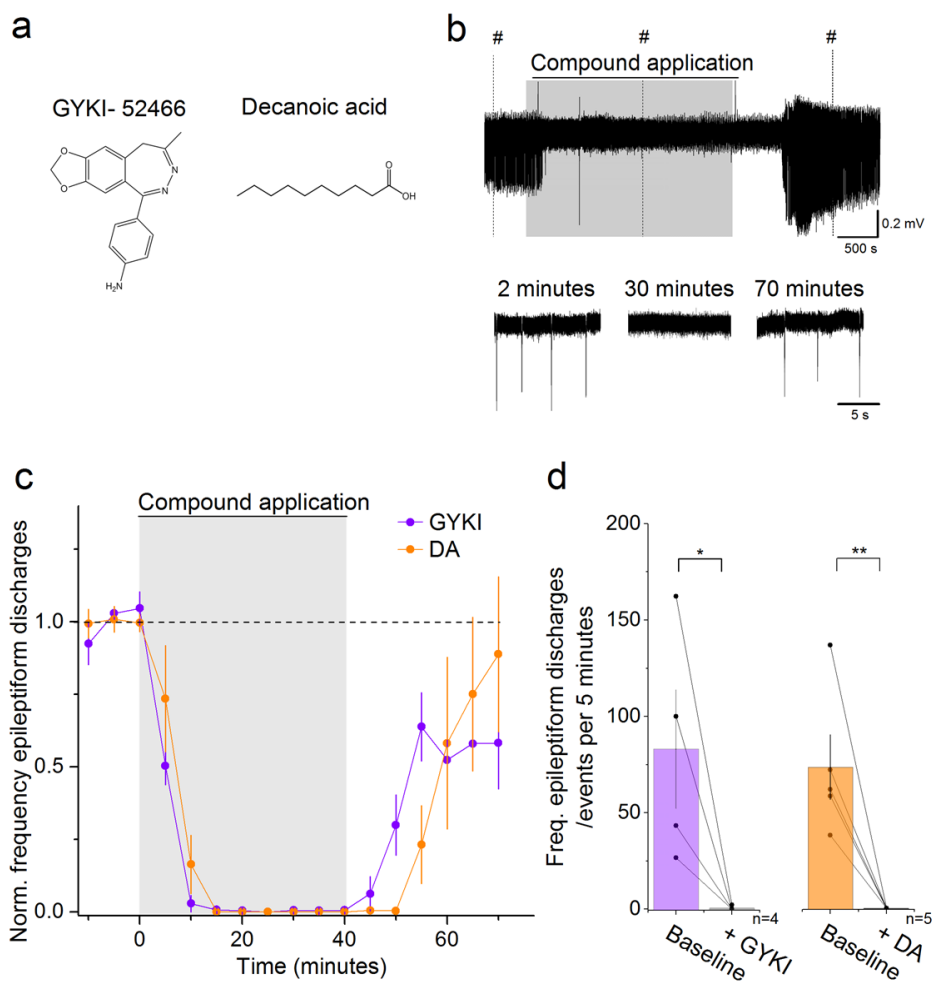


FIGURE 5.1: The effect of AMPA receptor antagonism on epileptiform activity: GYKI-52466 compared to decanoic acid

a) The chemical structure of GYKI is completely different to decanoic acid. b) Example extracellular recording from stratum radiatum of CA1 showing epileptiform activity induced by application of PTZ, which is stopped upon treatment with AMPA receptor antagonists [top], (#) expanded below. Example shown includes wash-in of decanoic acid. c) The effect of the selective AMPA receptor antagonist GYKI-52466 [purple] or decanoic acid [orange] on the frequency of epileptiform discharges. Bursts were binned into 5 minute intervals and normalised to the baseline frequency (mean \pm SEM). d) Absolute values from (c), showing epileptiform discharge frequency. Baseline: average over three bins [-10 to 0 minutes]; treatment: average over three bins [30 to 40 minutes]. * $p < 0.05$, ** $p < 0.01$, unpaired t -test.

octanoic acid, which has no anti-epileptic properties itself (Chang et al., 2013).

To test whether modifications to straight-chain fatty acids were effective at increasing its biological activity, derivatives were tested using the PTZ model in acute hippocampal slices (Fig. 5.2a). There was a significant reduction in the frequency of PTZ-induced epileptiform activity 30 minutes after administration of 4-methyl-nonanoic acid, (MNA: 0; $p=4.1E-8$, $n=5$), 4-ethyl-octanoic acid (EOA: 0.06 ± 0.05 ; $p=5.1E-8$, $n=5$), *trans*-4-butylcyclohexane carboxylic acid (BCCA: 0.08 ± 0.08 ; $p=4.3E-8$, $n=5$), 4-n-pentylphenyl-ethanoic acid (PPEA: 0.02 ± 0.01 ; $p=3.9E-8$, $n=6$), and 2-(4-pentylcyclohexyl) ethanoic acid (2PEA: 0.003 ± 0.003 ; $p=4.2E-8$, $n=5$), when compared to DMSO (Fig. 5.2b-c; 0.89 ± 0.18 ; ANOVA with Tukey post hoc test). Therefore, the addition of a methyl-branch, an ethyl-branch, a hexane ring or a phenyl ring structure decreased PTZ-induced activity to a similar extent as did the same concentration of decanoic acid did (Chang et al., 2015).

5.3.3 Decanoic acid can not block status epilepticus *in vivo*

Next I looked at the effect of acute administration of decanoic acid in an animal model of status epilepticus (SE). Self-sustaining status epilepticus (SSSE) was induced by 2 hours of perforant path stimulation (Fig. 5.3a). There was no difference in seizure severity monitored behaviourally in animals treated with decanoic acid (ip; 400-600mg/kg, $n=3$) and DMSO (volume matched to 0.1ml, $n=1$). Epileptic spikes tended to get smaller in amplitude, and less frequent after decanoic acid administration (Fig. 5.3b-d). However, the number of animals tested was not enough to detect significant differences. Gamma power increased during SSSE, and was not changed in either vehicle control nor treated animals (Fig. 5.3c).

5.3.4 Decanoic acid has no effect on the kinetics of AMPA receptor EPSCs

Decanoic acid is predicted to bind AMPA receptors at a novel site (Fig. 1.3; Chang et al., 2016). As with all fatty acids, decanoic acid favours binding in the lipid bilayer membrane and interacts with AMPA receptors from here. This suggests that as well as blocking the ion channel, this compound could have other effects on AMPA receptor kinetics. I began by measuring eEPSCs after decanoic acid application.

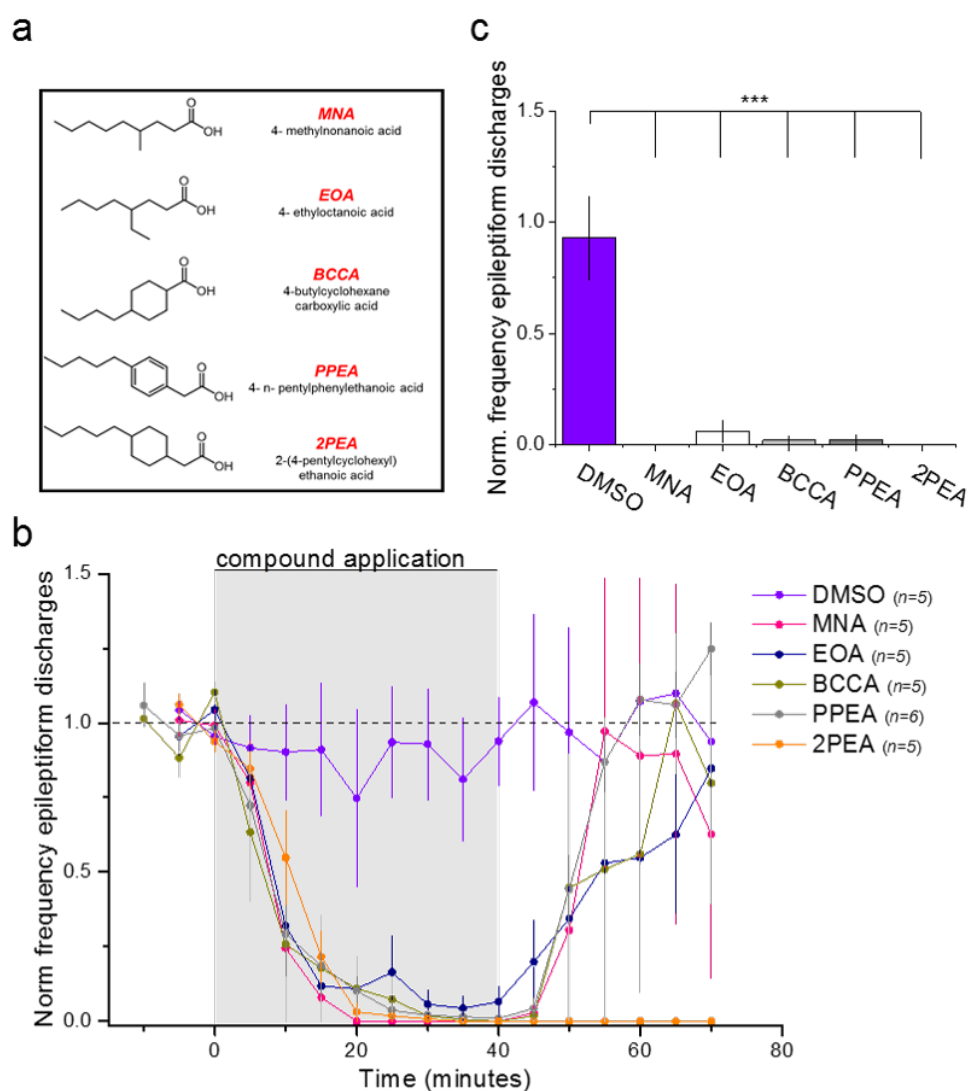


FIGURE 5.2: Modified methyl-octanoic acid derivatives have anti-seizure properties in an acute slice model of epileptiform activity

a) The structure of various fatty acids with modification on the fourth or fifth carbon. b) Summary of the change in frequency of PTZ-induced burst discharges in CA1, following application of MNA, EOA, BCCA, PPEA, 2PEA; all at 1mM. c) Comparative histogram of frequency of epileptiform discharges, taken 30 minutes after compound addition into PTZ-aCSF and normalised to baseline. *** <0.005 compared to DMSO, ANOVA with Tukey post hoc test for means comparison.

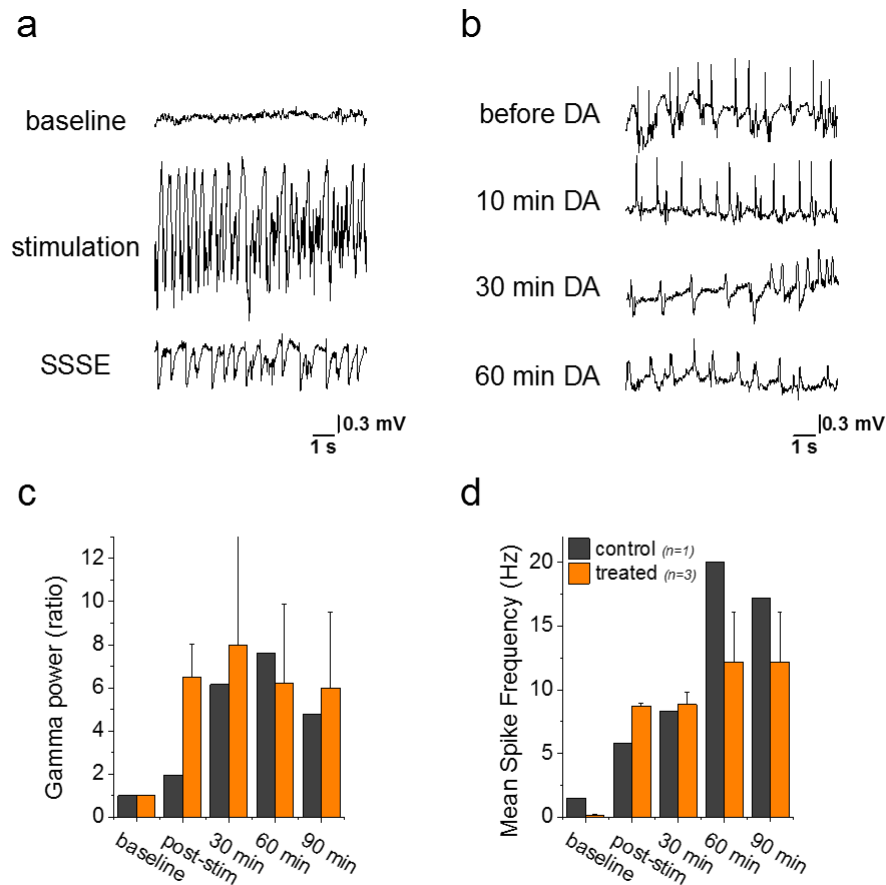


FIGURE 5.3: Acute treatment with decanoic acid does not suppress electrically-induced SE. a) Sample EEG traces recorded prior to, during, and 30 minutes after continuous PPS (2h) *in vivo*. b) Sample EEG traces recorded before injection of 600mg/kg decanoic acid (ip), and after 10 minutes, 30 minutes and 60 minutes. Traces are from the same animal and are representative of experiments where animals develop SSSE. c) EEG power in the gamma frequency band (20-70Hz) analysed in all animals that developed SSSE (n=1 control and n=3 treated). d) Spike frequency in EEG recordings from SSSE animals after 600mg/kg decanoic acid. Values are mean \pm SEM.

The amplitude of AMPA receptor-mediated currents was decreased upon 300 μ M decanoic acid wash-in (to 0.76 ± 0.03 [normalised amplitude], $n=5$; $p=0.0007$; paired t -test), and the single exponential decay constant (τ) was not changed (Fig. 5.4a-b; control: 8.6 ± 2.0 ms, decanoic acid: 9.7 ± 2.6 ms; $n=5$, $p=0.74$, paired t -test). τ is affected by the duration of receptor opening and level of desensitisation, so this indicates that decanoic acid does not change these AMPA receptor kinetics at a concentration that decreases the amplitude of AMPA receptor-mediated currents.

5.3.5 The action of decanoic acid at AMPA receptors was not use-dependent

Since the binding site on the AMPA receptors is likely to be near the pore region (Chang et al., 2016), I tested whether the effects of decanoic acid are use-dependent. If decanoic acid can bind only when the receptor is in its open state, then it will permit use-dependent inhibition. In this case, only those receptors that are activated (such as during a seizure) will be inhibited by decanoic acid.

To test this I recorded fEPSPs from two independent pathways (see Fig. 2.3). Stimulation of one pathway was stopped during application of 300 μ M decanoic acid, while stimulation of the other pathway was continued (Fig. 5.5a). After 30 minutes of drug application, stimulation of the second pathway was switched back on and fEPSPs from both pathways were compared. There was no difference in the magnitude of fEPSP suppression by decanoic acid between the two pathways (Fig. 5.5a-b; $n=5$; P1: 0.52 ± 0.11 , P2: 0.47 ± 0.14 [average 35-40 minutes]; $p=0.23$, unpaired t -test). Therefore, the effect of decanoic acid was not use-dependent, similar to the clinically approved AMPA receptor antagonist, perampanel.

5.3.6 Perampanel and decanoic acid act synergistically to reduce epileptiform discharges

In the clinical treatment of refractory epilepsy patients are commonly given multiple AEDs at the same time, often targeting different receptors to increase the overall effect. I looked at the combined action of perampanel and decanoic acid to see if they had a supra-linear effect on epileptiform discharges when applied together, as has been described for other combinations of AEDs (Russmann et al., 2016). Perampanel is also a non-competitive AMPA receptor antagonist with an IC_{50} of 60nM at hippocampal CA1 pyramidal neurons, but acts

at a different binding site to decanoic acid (Barygin, 2016; Chang et al., 2016). If both perampanel and decanoic acid preferentially bind to and stabilise the desensitised or closed state, then it would be expected that they would act synergistically (each one potentiating the action of the other) as the binding of one would promote the binding of the other.

Fitting a dose-response curve with the Hill equation allowed me to estimate the concentration of decanoic acid that reduced the frequency of epileptiform discharges by 50%, in each group. Applied without perampanel, decanoic acid dose-dependently decreased the frequency of epileptiform discharges (Fig. 5.6a-b; DMSO pre-treatment: 50% reduction at $314.5 \pm 65.7\mu\text{M}$; orange; n=8). When decanoic acid was applied with perampanel the effect on epileptiform discharges was enhanced, and 50% reduction was significantly different between groups when two different perampanel concentrations were compared to DMSO (F=4.27, p=0.028; one-way ANOVA).

Following application of a sub-effective concentration of 100nM perampanel ([baseline] 18.9 ± 3.1 events/min to [100nM perampanel] 18.3 ± 3.8 events/min), decanoic acid dose-dependently reduced the frequency of epileptiform discharges, and this reduction non-significantly tended to be at a higher rate than pre-treatment with DMSO alone (Fig. 5.6a-b; 100nM perampanel: 50% reduction = $159.1 \pm 30.1\mu\text{M}$; purple; n=7; p=0.074, *post-hoc* Dunnett's test). Further, when decanoic acid was washed in after application of a high concentration of perampanel (500nM; [baseline] 25.7 ± 6.5 events/min to [500nM perampanel] 20.4 ± 6.8 events/min), it significantly decreased the frequency of epileptiform discharges at a lower concentration (Fig. 5.6a-b; 500nM perampanel: 50% reduction = $125.3 \pm 41.7\mu\text{M}$; turquoise; n=8; p=0.023, *post-hoc* two-sided Dunnett's test). Perampanel and decanoic acid acted synergistically to reduce epileptiform discharges.

5.4 Discussion

Decanoic acid, a key component of the MCT ketogenic diet, has recently been shown to have acute anti-seizure properties, whilst ketones have no acute effect. In this chapter I looked at the action of decanoic acid on eEPSCs, and how AMPA receptor antagonism reduces epileptiform discharges in seizure models. I showed that the rate and extent of epileptiform discharge inhibition by decanoic acid was similar to that of an AMPA receptor antagonist with a different binding site. This means that the action of decanoic acid at AMPA receptors could fully explain its anti-seizure effect.

I also showed that other MCT derivatives have a similar anti-seizure effect *in vitro*. These results indicate that modifications to straight-chain molecules could be of interest when looking for treatments with improved side effects and safety *in vivo*. The short chain fatty acid valproic acid is a commonly used AED, but has been correlated with inhibition of histone deacetylase activity, hepatotoxicity, and sedative properties (Chang et al., 2013; Bojic et al., 1996). MCTs are promising candidates as different treatments for epilepsy without those secondary effects. In EC-hippocampal slices the application of PTZ can induce both ictal and interictal activity. This leads to high variability in spike frequency in 5 minute bins even over the baseline period. All the compounds tested, apart from 2PEA, had some return of epileptiform discharges upon washout. The washout period showed considerable variation in spontaneous activity, which in some cases exceeded baseline level in amplitude and frequency, occasionally becoming ictal, suggesting a rebound effect as has been described for some other AEDs (Marciani et al., 1985; Fig. 5.2a-b).

I looked at the action of decanoic acid *in vivo* in the PPS model and found it was unable to block SE. This is likely due to its pharmacokinetics as decanoic acid has high first-pass metabolism by the liver. In future experiments, chronic administration of decanoic acid either through multiple injections or presented in food may increase the concentration reaching the brain to have greater success at controlling seizures in chronic epilepsy *in vivo*. Orally ingested medium chain fatty acids are expected to be rapidly taken up in the liver (via the portal vein; St-Onge and Jones, 2002), and are quickly metabolised to produce carbon dioxide, acetate and ketone bodies (Huttenlocher et al., 1971; via co-enzyme A intermediates through β -oxidation and the citric acid cycle). In contrast, 4-methyloctanoic

acid is a branched chain derivative of octanoic acid which decreased spike frequency in the PPS model and terminated SE in all animals (Chang et al., 2013). Although decanoic acid does not seem to block SE *in vivo*, this may be because it does not reach the brain at an appropriate concentration in acute experiments. It will be worth seeing if the metabolically favourable compounds tested *in vitro* in section 5.3.2 are able to block SE. For example, BCCA blocks epileptiform discharges *in vitro* and has a central hexane ring which will reduce its metabolism *in vivo* compared to straight-chain compounds. It is important to see if decanoic acid has any benefit to the health of the post-SE brain. NeuN staining of paraformaldehyde (PFA)-fixed hippocampal slices from these animals could be used to compare neuron numbers to see if decanoic acid has neuroprotective properties.

Decanoic acid binding to AMPA receptors had a significant effect on the amplitude of eEPSCs but not on the shape. To measure the postsynaptic effects, isolated from presynaptic effects, I could measure mEPSCs in Sr^{2+} . If there was a difference here, I would be interested in seeing whether there was an effect of decanoic acid on deactivation or desensitisation of AMPA receptors. Further, binding of decanoic acid will be affected by auxiliary AMPA receptor subunits, such as TARPs, as these regulate many AMPA receptor properties (including trafficking). It is not known whether decanoic acid or other AMPA receptor antagonists including perampanel interact with TARPs (Rogawski and Hanada, 2013). A novel AMPA receptor antagonist which is dependent on TARP γ -8 has just been discovered which has anti-seizure efficacy against PTZ-induced convulsions *in vivo* (Gardinier et al., 2016; Maher et al., 2016). Decanoic acid has a synergistic anti-seizure effect with the clinically approved AED perampanel, via action through a different binding site on the AMPA receptors. This may be clinically relevant as it would predict synergy between perampanel and the MCT ketogenic diet. Further, it shows that decanoic acid may boost the actions of current AEDs.

In epilepsy patients the MCT ketogenic diet has diverse positive effects on brain function such as increased alertness, better cognitive functioning, and improved behaviour (Kinsman et al., 1992; Pulsifer et al., 2001). Decanoic acid is one of the main constituents in coconut oil so unlikely to have severe unwanted effects if given clinically. Supplements of decanoic acid may benefit those who show poor compliance to the stringent regimen necessary for the MCT ketogenic diet.

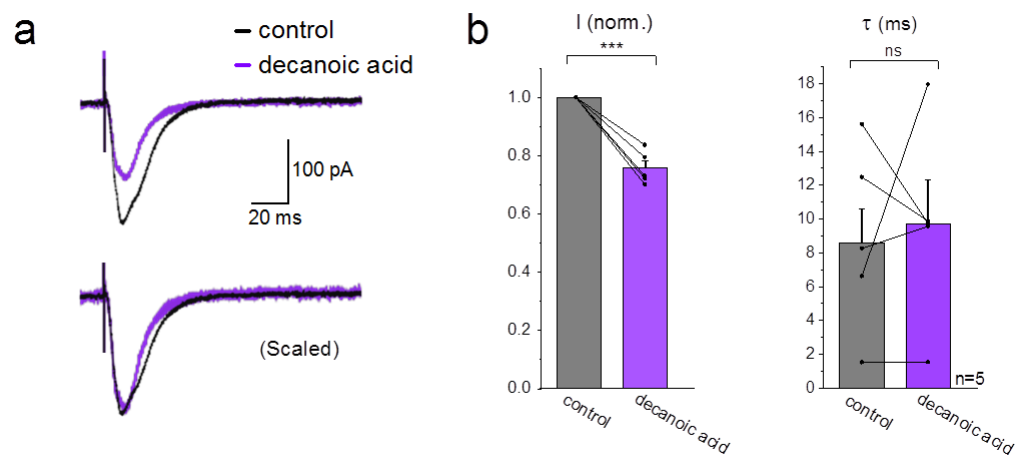


FIGURE 5.4: Decanoic acid reduces the AMPA receptor-mediated current but has no effect on eEPSC shape.

a) Example traces of evoked EPSCs before and after application of 300 μM decanoic acid [top]. Scaled responses demonstrate similar kinetics [below]. b) Peak AMPA receptor-mediated current is decreased, but kinetics were not affected after application of decanoic acid (n=5). ***p<0.005, ns: non-significant/p>0.05, paired *t*-test.

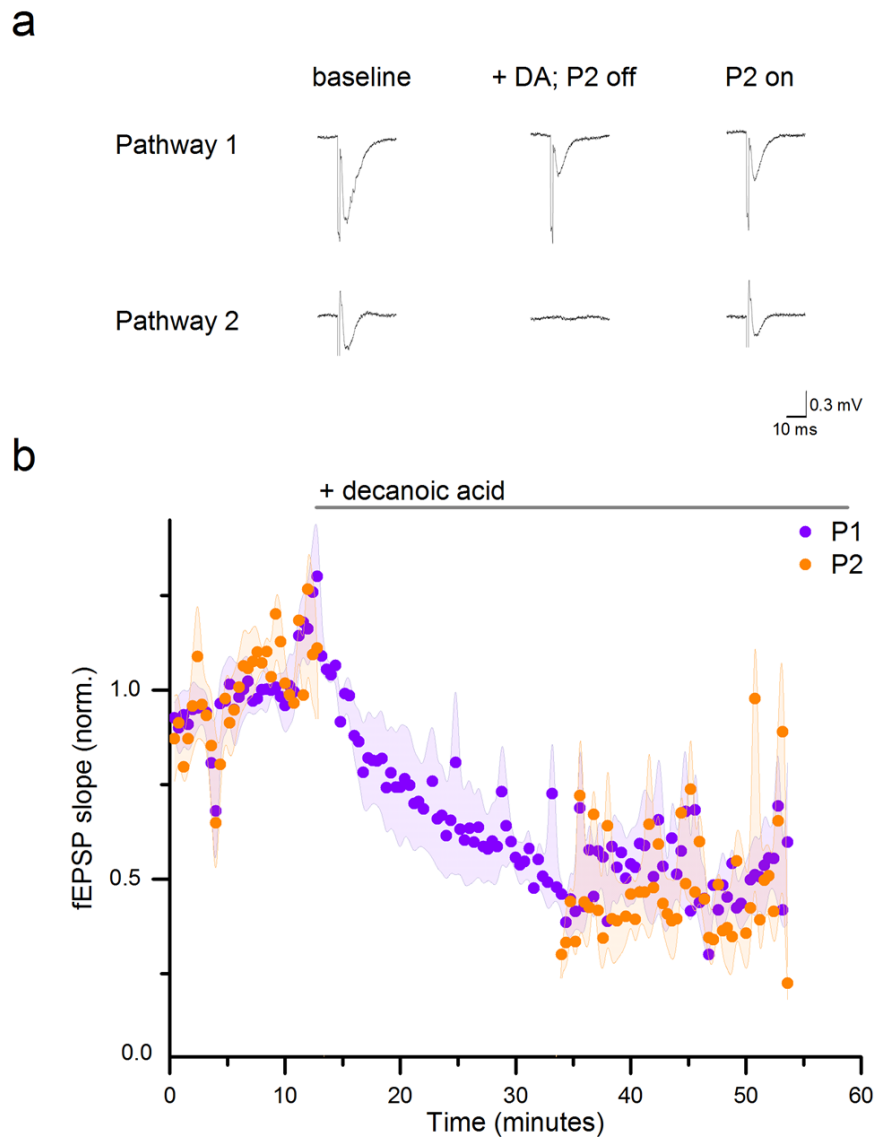


FIGURE 5.5: Decanoic acid does not act at AMPA receptors in a use-dependent way

a) Example fEPSP responses from independent Schaffer collateral pathways during baseline [left], with application of $300\mu\text{M}$ decanoic acid and only pathway 1 on [middle], and when pathway 2 is reactivated [right]. b) The time course of normalised slopes of AMPA receptor-mediated fEPSPs evoked by Schaffer collateral stimulation at 0.033Hz (recording electrode was placed in CA1 st. radiatum). Pathway 1 [purple] is activated throughout. Pathway 2 [orange] is switched off and $300\mu\text{M}$ decanoic acid washed in at 12 minutes, $n=5$ slices.

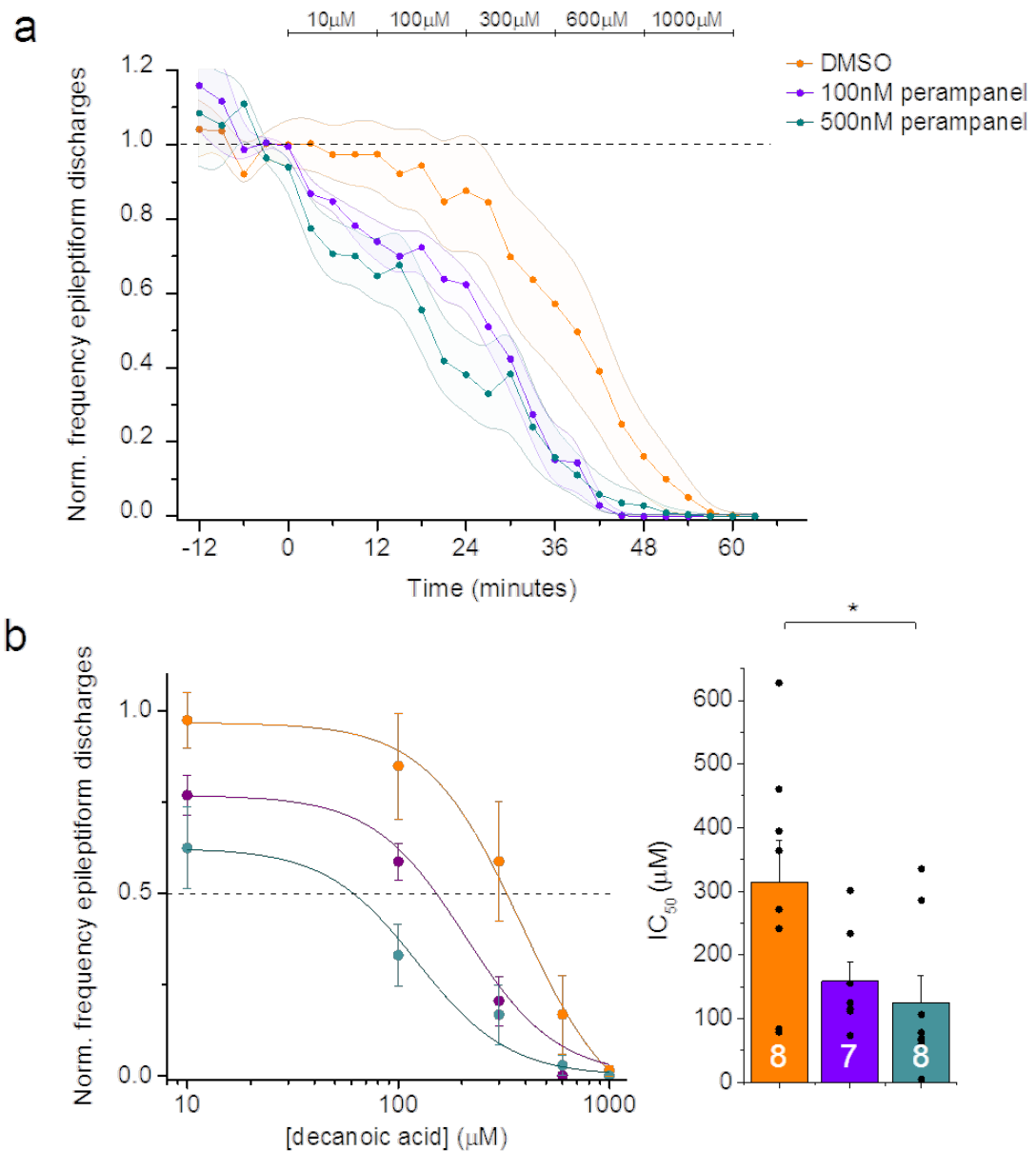


FIGURE 5.6: Decanoic acid and perampanel act synergistically to inhibit epileptiform activity in an acute slice model of epileptiform activity

a) Time course of response to increasing concentrations of decanoic acid. Application of 1 μ l DMSO (orange, n=8), 100nM perampanel (purple, n=7) or 500nM perampanel (turquoise, n=8) at -12 minutes. Grey region is SEM, and top bar shows concentration of decanoic acid.

b) Dose-response curve with a Hill equation fit [left], and concentration of decanoic acid that reduced the frequency of epileptiform discharges by 50%, in each treatment group [right; colour represent groups as above]. Frequency of epileptiform discharges is normalised to baseline in PTZ-aCSF with perampanel [-6 to 0 minutes]. Dashed line shows 0.5 frequency epileptiform discharges [norm.] used to measure 50% reduction.

Chapter 6

Novel actions of decanoic acid on neuronal excitability

6.1 Summary

Decanoic acid is one of the main constituents of the MCT ketogenic diet, which successfully reduces seizures in some patients who do not respond to common AEDs. In the previous chapter I looked at the anti-seizure action of decanoic acid at AMPA receptors. Previously, it has been shown that decanoic acid does not affect inhibitory neurotransmission (Chang et al., 2016). Here I asked whether it reduces the intrinsic excitability of neurons.

I found that decanoic acid increased the rheobase and reduced the number of action potentials initiated in response to a current injection. This action was not dependent on PI3 kinase, a previously determined target of medium chain fatty acids (Chang et al., 2014). In TTX, the voltage response to current injections did not change upon decanoic acid application. This led me to look in more detail at the action of decanoic acid at VG Na⁺ channels.

Decanoic acid did not reduce sodium channel-mediated transient currents in CA1 pyramidal neurons, but did reduce the persistent sodium current, which produces subcellular oscillations. Finally I showed that the branched chain derivative, BCCA, reduced the intrinsic excitability of CA1 pyramidal neurons, which is similar to decanoic acid. This dual action of decanoic acid at post-synaptic AMPA receptors and presynaptic axons may increase its anti-seizure potential.

6.2 Introduction

The previous chapter focused on the anti-seizure effects of decanoic acid, and its specific action at AMPA receptors. The MCT ketogenic diet is an effective treatment in many patients who do not achieve seizure freedom from typical AEDs alone, such as the AMPA receptor blocker perampanel. Here I have tested whether decanoic acid also affects other neuronal functions.

Other common targets of AEDs are synaptic receptors and VG ion channels (see section 1.2). Voltage-gated Na^+ channels (VGSCs) are closed at resting membrane potential, and depolarise the neuronal membrane when opened. They are responsible for the depolarising phase of action potentials. The actions of phenytoin and carbamazepine are attributed to their voltage- and frequency-dependent inhibition of VGSCs (Mantegazza et al., 2010). Several hundred VGSC gene mutations lead to inherited epileptic syndromes, many with gain of function, and hyper excitable effects. Therefore this ion channel is a good target to reduce neuronal excitability.

Voltage-gated K^+ channels (VGKCs) are responsible for the M-current which determines the threshold and rate of neuronal firing, and which modulates the somatic response to dendritic inputs. A selectivity filter in the channel blocks Na^+ flow. During action potentials, the delayed rectifier current (I_K) is crucial for returning the depolarised cell to a resting state. Retigabine is the only approved AED to act at K^+ channels; This K^+ channel opener acts at K_V7 , a delayed rectifier responsible for the M-current in the cell soma and AIS.

In this chapter I tested the following hypothesis:

- Decanoic acid and other MCTs do not alter the level of neuronal intrinsic excitability

I started by determining how decanoic acid altered action potentials, the main output of neurons.

6.3 Results

6.3.1 Neuronal intrinsic excitability is reduced by decanoic acid

My initial motivation to look at the action of decanoic acid on intrinsic excitability was to determine if the anti-seizure properties of decanoic acid were exclusively due to inhibiting AMPA receptors. The intrinsic excitability of a neuron is defined as the relationship between excitatory current input and action potential frequency output. To test the effect of decanoic acid on intrinsic excitability, I recorded hippocampal neurons in the current-clamp mode in the presence of synaptic blockers (50 μ M D-AP5, 50 μ M PTX, 10 μ M NBQX), and looked at the effect of decanoic acid on action potentials elicited by step current injections. In this way I eliminated presynaptic effects and the influence of other neurons on the target cell.

Decanoic acid significantly reduced neuronal output in response to progressive step current injections (Fig. 6.1a-c; reduced in decanoic acid to 0.52 ± 0.17 [normalised area under the curve]; n=8; p=0.0039, paired *t*-test). Decanoic acid has poor solubility in water, so was prepared at a 2000x stock in DMSO. DMSO alone has been shown to reduce action potentials at a concentration as low as 0.05% (Tamagnini et al., 2014). However, I found no change in intrinsic excitability after washing in 1/2000 DMSO (in DMSO to 1.02 ± 0.14 [normalised area under the curve]; n=5; p=0.44, paired *t*-test). Further, decanoic acid significantly reduced the number of action potentials in comparison to DMSO (comparing areas under the curve: p=0.012, unpaired *t*-test). This effect was reversed when decanoic acid was washed out.

Action potential kinetics can be studied by plotting the derivative of the membrane potential against the membrane potential (Fig. 6.2a). Figure. 6.2b is a phase plot comparing action potential kinetics after decanoic acid application. This allowed me to visualise where MCTs alter action potential kinetics, to help to see which currents are affected by MCTs such as decanoic acid and BCCA (Trombin et al., 2011). RMP was not changed following application of DMSO (Supplementary Table 8.2; RMP [control]: -63.0 ± 3.2 mV, [+DMSO]: -63.0 ± 3.3 mV; p=0.98, paired *t*-test) or decanoic acid (RMP [control]: -62.2 ± 2.0 mV, [+decanoic acid]: -63.4 ± 1.9 mV; p=0.66, paired *t*-test). There was also no statistically significant difference when comparing RMP between treatments (p=0.89, unpaired *t*-test). I found that voltage threshold ($V_{\text{threshold}}$) did not change when decanoic acid was washed

in (Fig. 6.2c-d: [control]: -46.6 ± 4.9 mV, [+decanoic acid]: -44.9 ± 3.6 mV, $p=0.24$ paired *t*-test; [washout]: -43.5 ± 3.7 mV). Further, repolarisation potential ($V_{\text{repolarisation}}$) was not affected by decanoic acid application ([control] -38.4 ± 1.8 mV, [+decanoic acid] -37.7 ± 2.0 mV, $p=0.24$ paired *t*-test; [washout] -36.2 ± 3.2 mV). Finally, maximum voltage (V_{max}) was not affected by decanoic acid wash-in ([control] 32.6 ± 12.4 mV, [+decanoic acid] 30.5 ± 12.3 mV, $p=0.72$ paired *t*-test; washout 38.4 ± 13.2 mV).

6.3.2 Branched derivatives of octanoic acid also reduce neuron intrinsic excitability

Next, I looked at the effect of the branched MCT derivative, BCCA (see Fig. 5.2a), on intrinsic excitability. Branched MCTs are as effective as decanoic acid at inhibiting epileptiform activity *in vitro* and have increased bioavailability. This fatty acid derivative had a similar effect on intrinsic excitability to decanoic acid. The number of action potentials significantly reduced upon BCCA application (Fig. 6.3a-b; in BCCA: 0.29 ± 0.16 [normalised area under the curve]; $n=5$, $p=0.011$, paired *t*-test) and returned during washout (0.88 ± 0.30 [normalised area under the curve]).

I used a phase plot to see if BCCA altered action potential kinetics. RMP was not altered by BCCA (Fig. 6.3c-d; [control]: -63.0 ± 3.4 mV, [+BCCA]: -62.8 ± 3.7 mV, $p=0.45$ paired *t*-test; [washout]: -60.7 ± 4.6 mV). Voltage threshold ($V_{\text{threshold}}$) was significantly increased in the presence of BCCA, ([control]: -44.0 ± 2.6 mV, [+BCCA]: -39.7 ± 3.0 mV, $p=0.014$ paired *t*-test; [washout]: -40.7 ± 0.7 mV). Further, the repolarisation potential ($V_{\text{repolarisation}}$) also tended to be increased after BCCA application, but this did not reach statistical significance ([control] -26.3 ± 4.5 mV, [+BCCA] -18.5 ± 5.5 mV, $p=0.054$ paired *t*-test; [washout] -19.5 ± 4.2 mV). Finally, maximum voltage (V_{max}) was not affected by BCCA wash-in ([control] 29.0 ± 2.9 mV, [+BCCA] 27.3 ± 1.6 mV, $p=0.37$ paired *t*-test; [washout] 33.6 ± 6.5 mV).

6.3.3 Decanoic acid does require activation of PI3 kinase to reduce intrinsic excitability

Valproic acid is a common AED and a short chain fatty acid. One of valproic acid's mechanisms of action is at phosphoinositide 3-kinase (PI3 kinase), to counter the seizure-

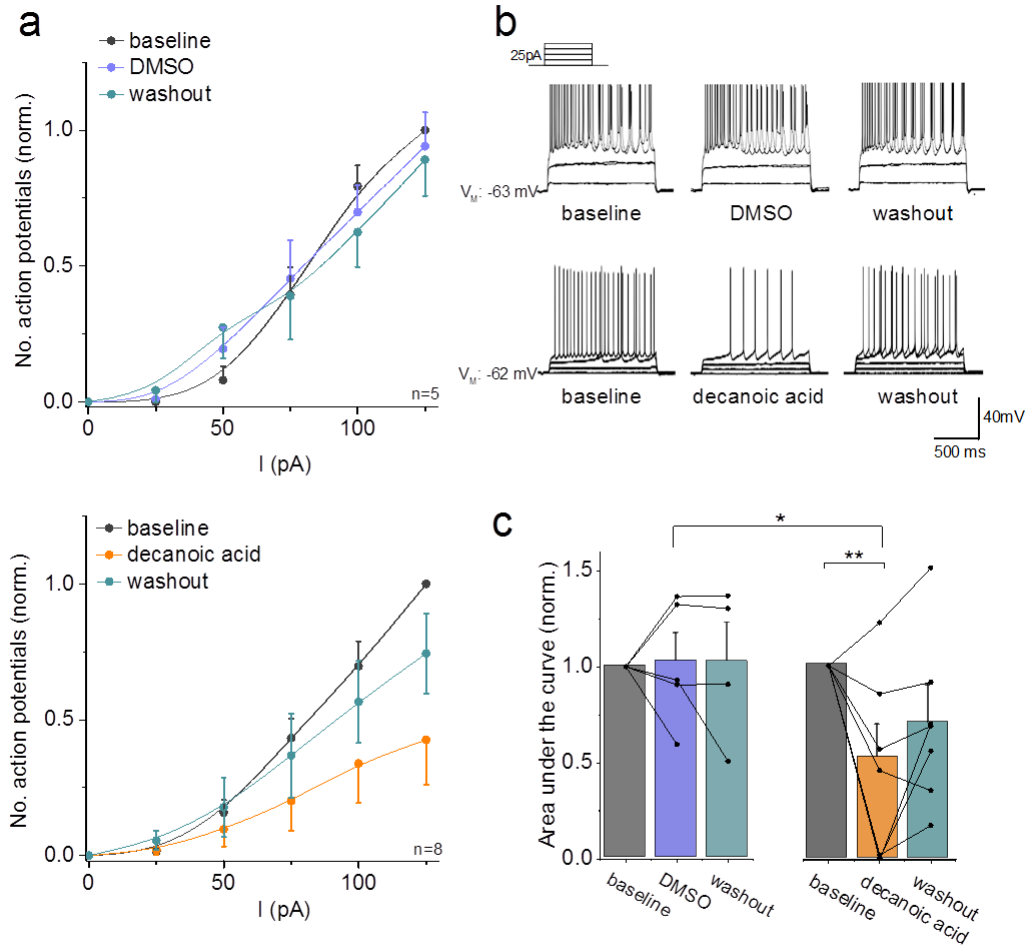


FIGURE 6.1: Decanoic acid reduces neuronal intrinsic excitability

a) Application of $300\mu\text{M}$ decanoic acid decreases the number of action potentials at each current step (lower), but the equivalent volume of DMSO alone has no effect (top). Lines are fitted to the data as a spline function. b) Representative recordings of action potentials (initiated by current injections at 25pA steps) at baseline, with treatment and during washout. c) Area under the curve (AUC) was used to quantify changes in intrinsic excitability with decanoic acid compared to DMSO control. * $p < 0.05$, ** $p < 0.01$. All recordings were performed in the presence of synaptic blockers.

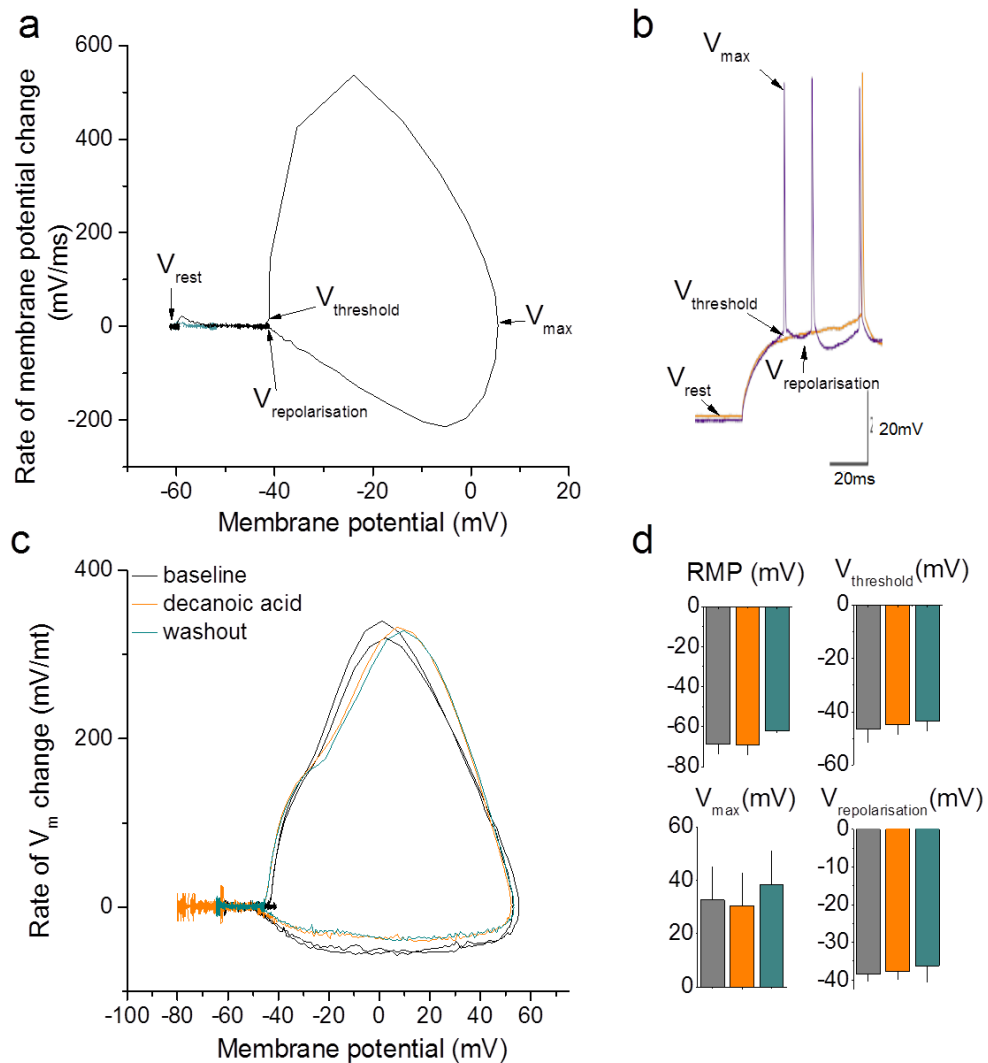


FIGURE 6.2: Phase plot showing that decanoic acid does not change the kinetics of action potentials.

a) Comparing the rate of membrane potential change against membrane potential can reveal differences in action potential kinetics. In recordings not containing action potentials, the phase plot stays around resting membrane potential (RMP; turquoise). In an action potential, phase plots reveal RMP (V_{rest}), action potential threshold ($V_{threshold}$), peak voltage (V_{peak}) and repolarisation potential ($V_{repoliarisation}$). b) Corresponding points are shown in a representative current trace in control conditions [purple] and upon application of decanoic acid [orange]. Notice the delay to the initial action potential. c) Application of decanoic acid reduces intrinsic excitability, but does not show gross changes in action potential kinetics. d) Summary graphs show trend in increase in voltage threshold (not significant) but no change in RMP or $V_{repoliarisation}$. $n=6$.

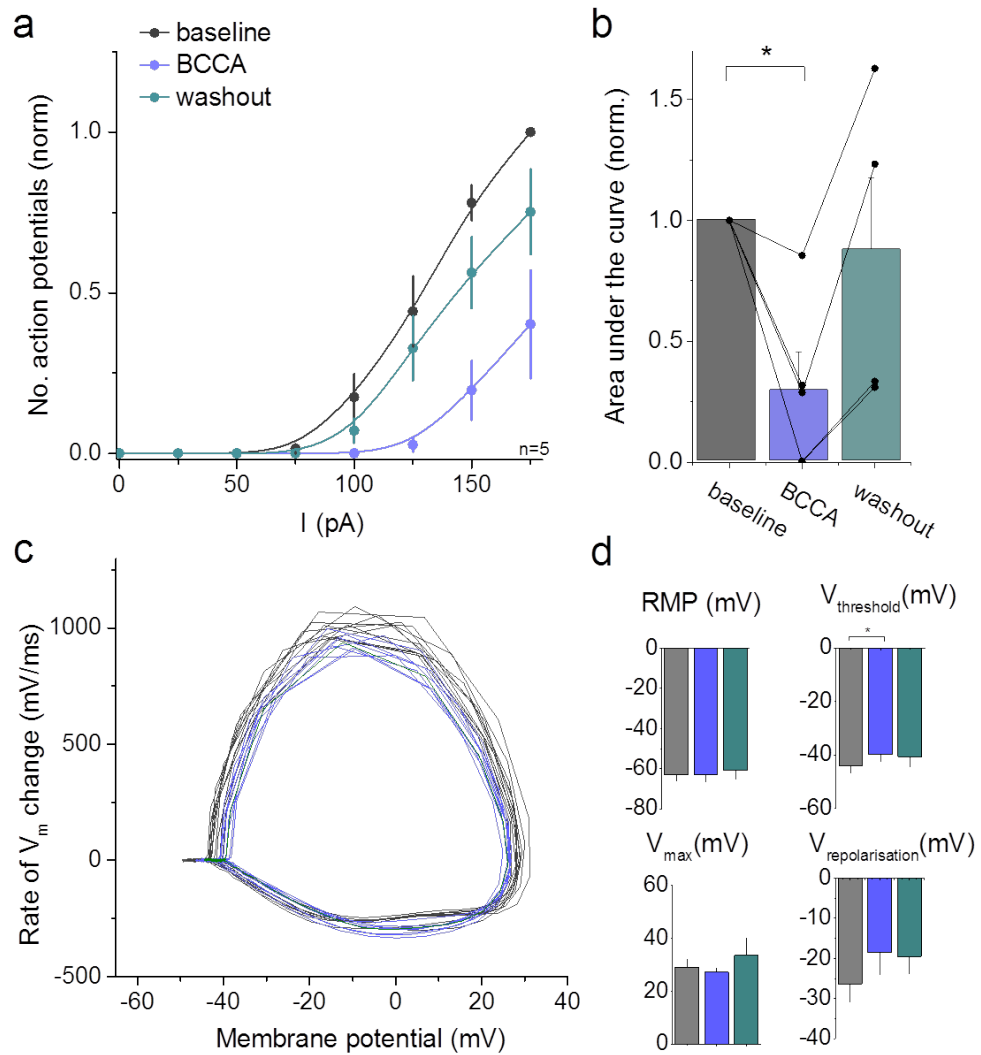


FIGURE 6.3: BCCA reduces neuronal intrinsic excitability

a) Application of $300\mu\text{M}$ BCCA acid decreases the number of action potentials at each current step. Lines are fitted to the data as a spline function. b) Area under the curve (AUC) was used to quantify changes in intrinsic excitability with BCCA. c) Phase plot shows no gross changes to action potential kinetics with application of BCCA. d) Threshold of action potential initiation was significantly altered by BCCA, but RMP, maximum voltage and repolarisation potential were not affected. $*p < 0.05$. All recordings were performed in the presence of synaptic blockers.

induced decrease in phosphatidylinositol-3,4,5-trisphosphate (PIP3; Chang et al., 2014). PI3 kinase phosphorylates PIP2 to produce PIP3, which is important for many cell functions including neurotransmission, receptor trafficking and membrane repair (Fig. 6.4a). PIP3 is also protective against oxidative stress, which is particularly relevant following seizures. PI3 kinase regulates VG K^+ , Na^+ and Ca^{2+} channels outside of the brain (Ballou et al., 2015). Further, PI3 kinase inhibition reduces the L-type calcium current (I_{CaL}), the delayed rectifier potassium currents (I_{Kr}), and the peak sodium current; whereas it increases the persistent sodium current (I_{NaP} ; Lu et al., 2013). Seizure-induced depletion of PIP3 would also interfere in homeostatic synaptic plasticity, which maintains basal synaptic activity (Wang et al., 2012).

I next used the PI3 kinase inhibitor LY294002 (Vlahos et al., 1994), to determine whether phosphorylation of PIP2 was required for the reduction in intrinsic excitability produced by decanoic acid. LY294002 ($20\mu M$) included in the recording solution did not change the effect of decanoic acid on neuronal input-output relationship (Fig. 6.4b-c; with decanoic acid to 0.29 ± 0.13 [normalised area under the curve]; $n=4$; $p=0.0055$, paired *t*-test). As above, DMSO in the presence of LY294002 had no effect on this parameter (with DMSO to 0.91 ± 0.20 [normalised area under the curve]; $n=4$; $p=0.35$, paired *t*-test). There was a significant difference between the number of action potentials when treated with decanoic acid compared to DMSO, in the presence of a PI3 kinase inhibitor (area under the curve: $p=0.021$, unpaired *t*-test).

When decanoic acid was compared in control aCSF and in aCSF with LY294022, there was no statistically significant difference (normalised AUC: $p=0.39$, unpaired *t*-test).

6.3.4 Actions of decanoic acid on intrinsic excitability are TTX-sensitive

Next I blocked VGSCs with TTX to distinguish the role of decanoic acid on input resistance and K^+ channels. Neuronal VGSCs comprise one central α -subunit and two auxiliary β -subunits that modulate α -subunit properties and are implicated in its subcellular targeting. The α -subunit forms the ion-conducting pore and the channel gate for activation and inactivation. It consists of four domains, each with six transmembrane segments. Pore loops between S5 and S6 in each of the four domains form the selectivity filter of the channel,

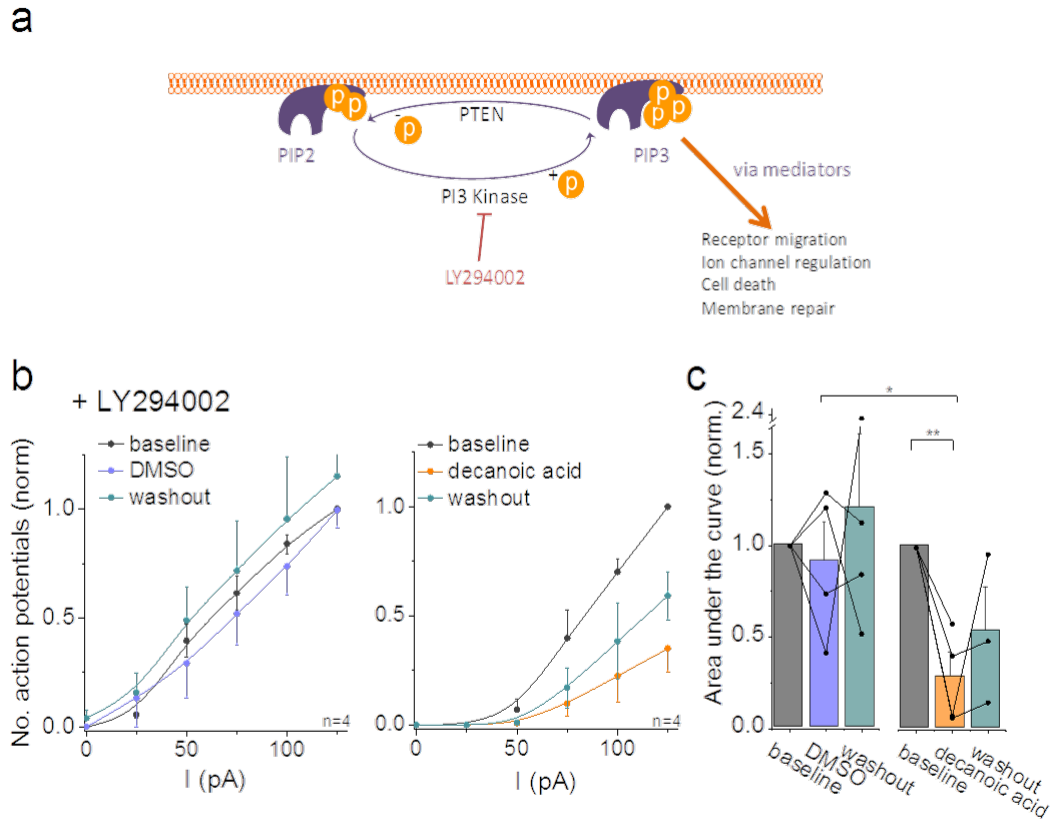


FIGURE 6.4: Decanoic acid continues to reduce intrinsic excitability of neurons with PI3 kinase blocked

a) Schematic diagram showing the role of PI3 kinase in PIP3 production, which has multiple downstream effects. b) In the presence of LY294002, application of 300 μ M decanoic acid decreases the number of action potentials at each current step [right], but the equivalent volume of DMSO has no effect alone [left]. Lines are fitted to the data as a spline function. c) Area under the curve (AUC) was used to quantify changes in intrinsic excitability with treatment by decanoic acid compared to control. * $p < 0.05$, ** $p < 0.01$. All recordings were performed in the presence of synaptic blockers and 20 μ M LY294002.

and the four S6 segments form the cytoplasmic end of the pore, which binds various types of therapeutically important pore-blocking compounds including local anaesthetics, anti-arrhythmic drugs and AEDs (Mantegazza et al., 2010).

TTX ($1\mu\text{M}$) was included in the recording solution to block VGSCs and, thus, prevent action potentials firing. Larger current steps than in the previous experiments (120 pA) were used here to maximise potential voltage differences in my whole-cell recordings. Small negative current injections (-40 pA) revealed no difference in neuronal input resistance upon application of decanoic acid (Fig. 6.5a-c; [baseline]: $123.1 \pm 24.2 \text{ M}\Omega$, [decanoic acid]: $134.6 \pm 28.7 \text{ M}\Omega$; $n=6$, $p=0.22$, paired t -test; [washout]: $133.5 \pm 33.6 \text{ M}\Omega$), or DMSO ([baseline]: $91.6 \pm 9.9 \text{ M}\Omega$, [DMSO]: $92.9 \pm 15.2 \text{ M}\Omega$; $n=5$, $p=0.42$, paired t -test; [washout]: $99.6 \pm 15.2 \text{ M}\Omega$). Large positive current steps did not reveal any decanoic acid, or DMSO-induced changes in input resistance either (Fig. 6.5a-c; [baseline]: $112.1 \pm 31.6 \text{ M}\Omega$, [DMSO]: $110.4 \pm 29.6 \text{ M}\Omega$; $p=0.35$, paired t -test; [washout]: $136.0 \pm 34.0 \text{ M}\Omega$; [baseline]: $130.7 \pm 35.6 \text{ M}\Omega$, [decanoic acid]: $121.4 \pm 30.8 \text{ M}\Omega$; $p=0.25$, paired t -test; [washout]: $118.1 \pm 42.6 \text{ M}\Omega$).

These results and those from the phase plot shown above lead me to investigate the action of decanoic acid at VGSC currents in more detail.

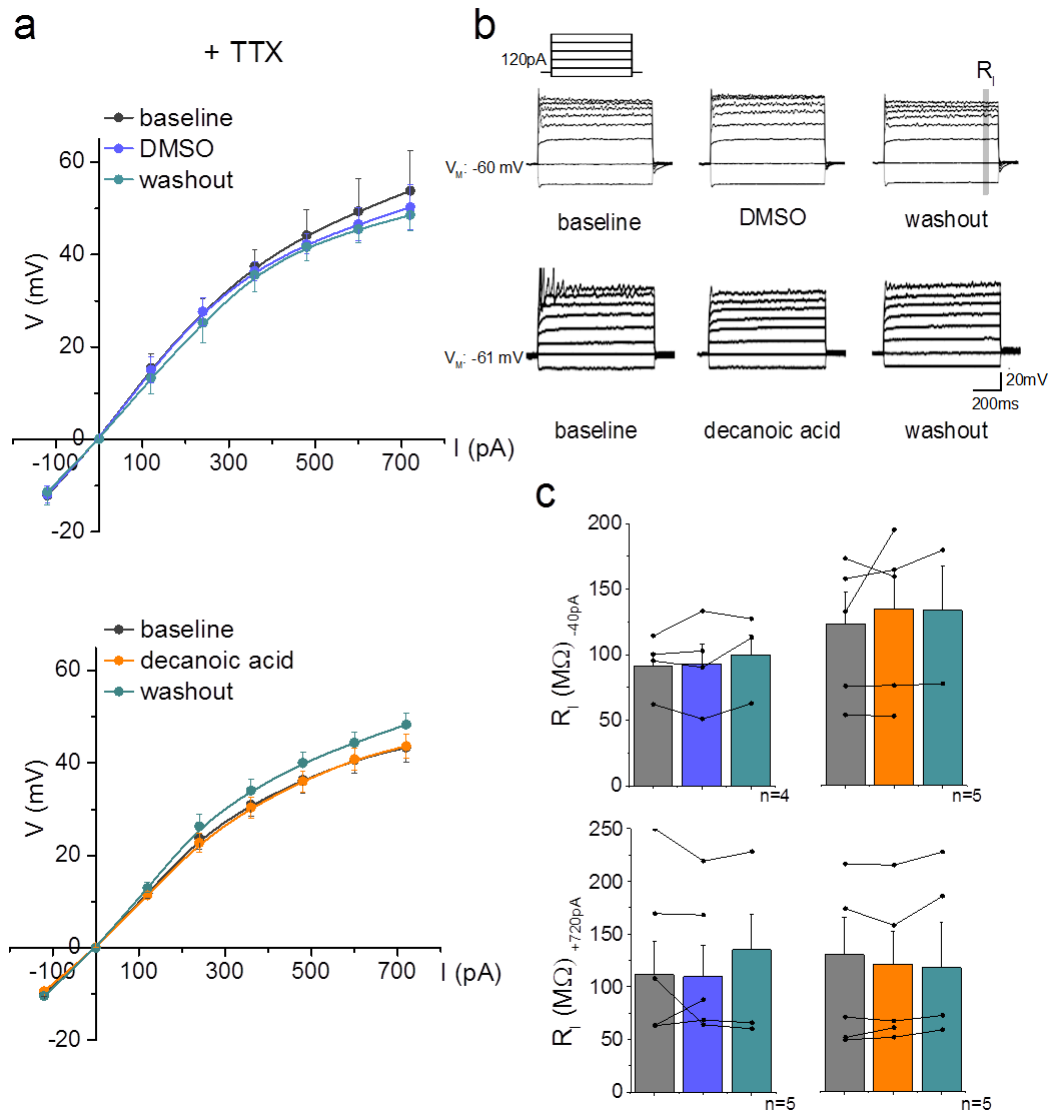


FIGURE 6.5: Decanoic acid does not affect neuronal input resistance

a) Application of $300\mu\text{M}$ decanoic acid in the presence of TTX does not alter the voltage response at each current step [lower], and nor does the equivalent volume of DMSO [upper]. Lines are fitted to the data as a spline function. b) Representative recordings of voltage responses to 120pA current steps in baseline, with treatment and during washout. Grey shaded box in top right trace is representative of the window used for calculation of resistance. c) Input resistance was determined from the voltage response to current injections. This was not altered by application of DMSO [left] or decanoic acid [right] after injection of -40pA [top] or $+720\text{pA}$ current [lower]. All recordings were performed in the presence of synaptic blockers, and TTX.

6.3.5 Decanoic acid did not change the transient sodium current

VGSCs produce multiple currents, as controlled by different gating modes. The transient Na^+ current (I_{NaT}) is a large, rapid activating and fast inactivating current which is TTX-sensitive and is initiated when the membrane voltage is depolarised above threshold (typically near -55mV to -50mV ; Carter et al., 2012). All known sodium channel α -subunits produce transient currents, I_{NaT} is present in all neurons and is necessary for action potential generation.

I looked at I_{NaT} at a range of voltage steps between -60mV and $+20\text{mV}$ (Fig. 6.6a). A plot of current density against step potential showed no difference in I_{NaT} upon decanoic acid application (Fig. 6.6b; peak current density in [control]: -156.6 ± 76.4 pA/pF, and in [$300\mu\text{M}$ decanoic acid]: -141.4 ± 43.2 pA/pF; $n=5$, $p=0.59$, paired t -test).

I converted the current trace to conductance using Ohm's law (EQ. 2.2), to see if decanoic acid affected conductance without the influence of driving force. I plotted conductance against membrane potential and fitted the relationship with a Boltzmann distribution (EQ. 2.4; Fig. 6.6c). Decanoic acid did not change peak conductance (G_{max}), voltage at which sodium current was half maximal (V_{50}), nor the slope factor (k ; Table 6.1). The values of G_{max} I measured fit with published values for CA1 pyramidal neurons (e.g. Royeck et al., 2008).

6.3.6 Decanoic acid reduced the persistent sodium current

Finally, I looked at the effect of decanoic acid on the persistent sodium current (I_{NaP}) which regulates the low threshold of activation and reduces inactivation during sustained membrane depolarisations (Crill, 1996). The persistent sodium current is much smaller than I_{NaT} , is dependent on the auxiliary β -subunit, and is present in $\text{Na}_V1.2$ and $\text{Na}_V1.6$ subtypes (the most numerous type in hippocampal pyramidal neurons; Chatelier et al., 2010). I_{NaP} is particularly important in subthreshold oscillations, spontaneous firing and burst generation as it is recruited in response to small membrane depolarisations (Magistretti and Alonso, 2002). Therefore, an increase of only a few percent can dramatically alter cell firing and facilitate hyper-excitability, as in seizure behaviour (Stafstrom, 2007).

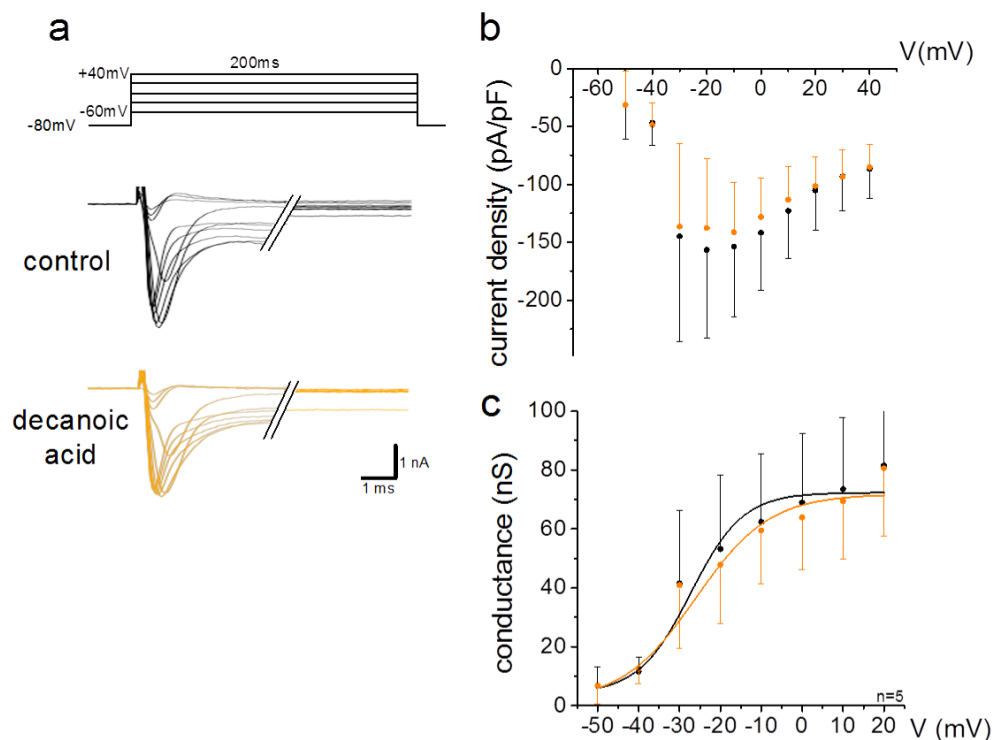


FIGURE 6.6: Decanoic acid does not change the transient sodium current.

a) Voltage protocol [top] evoked I_{NaT} lasting ~ 1 ms in control aCSF [black] and with decanoic acid application [orange]. Traces are TTX-subtracted. b) Current density plotted against step voltage showed no difference in amplitude of I_{NaT} after application of decanoic acid. c) Conductance-voltage relationships were fitted with a Boltzmann function (EQ. 2.4) and showed no difference with decanoic acid application.

	Control aCSF	+Decanoic acid	*p-value
G_{max} \	72.3 ± 3.3	71.8 ± 6.0	0.94
V_{50} \mV	-27.3 ± 2.5	-26.0 ± 3.4	0.77
k	6.4 ± 1.7	9.0 ± 2.9	0.44

TABLE 6.1: Application of decanoic acid does not alter G_{NaT} kinetics. Decanoic acid did not change peak conductance (G_{max}), half maximal sodium current (V_{50}), nor the slope factor (k). Values taken from fitting G_{NaT} (EQ. 2.2) values to a Boltzmann function (EQ. 2.4). *paired t -test; $n=5$.

I patched CA1 hippocampal pyramidal neurons in voltage clamp mode and evoked the I_{NaP} current with a slow voltage ramp from -80mV to 20mV, at a speed of 2mV/s. Recordings were filtered at 4kHz and acquired at 10kHz as high frequency components were not relevant to the measured response. The recording solution contained synaptic blockers (50 μ M D-AP5, 50 μ M PTX, 10 μ M NBQX), CdCl₂ (VG-Ca²⁺ channel blocker) and the internal solution contained Cs-MSF (to block leak K⁺ currents). Current traces obtained in TTX were subtracted to isolate I_{NaP} currents. The I_{NaP} was present from around -60mV to 0mV; the current peaked at around -40mV, and reached -183.1 ± 43.8 pA in control aCSF. Upon application of 300 μ M decanoic acid, the peak current amplitude significantly decreased to -115.7 ± 21.7 pA (maximum negative current minus baseline [grey dashed line]; Fig. 6.7a-b; n=5, p=0.031, paired *t*-test). Decanoic acid application decreased currents by $32.7 \pm 7.4\%$.

I next converted *I-V* traces to a conductance-voltage trace (Fig. 6.7c). Application of decanoic acid significantly reduced peak conductance (maximum conductance minus baseline [grey dashed line]; control: 1.9 ± 0.4 nS; decanoic acid: 1.2 ± 0.2 nS; n=5, p=0.021, paired *t*-test).

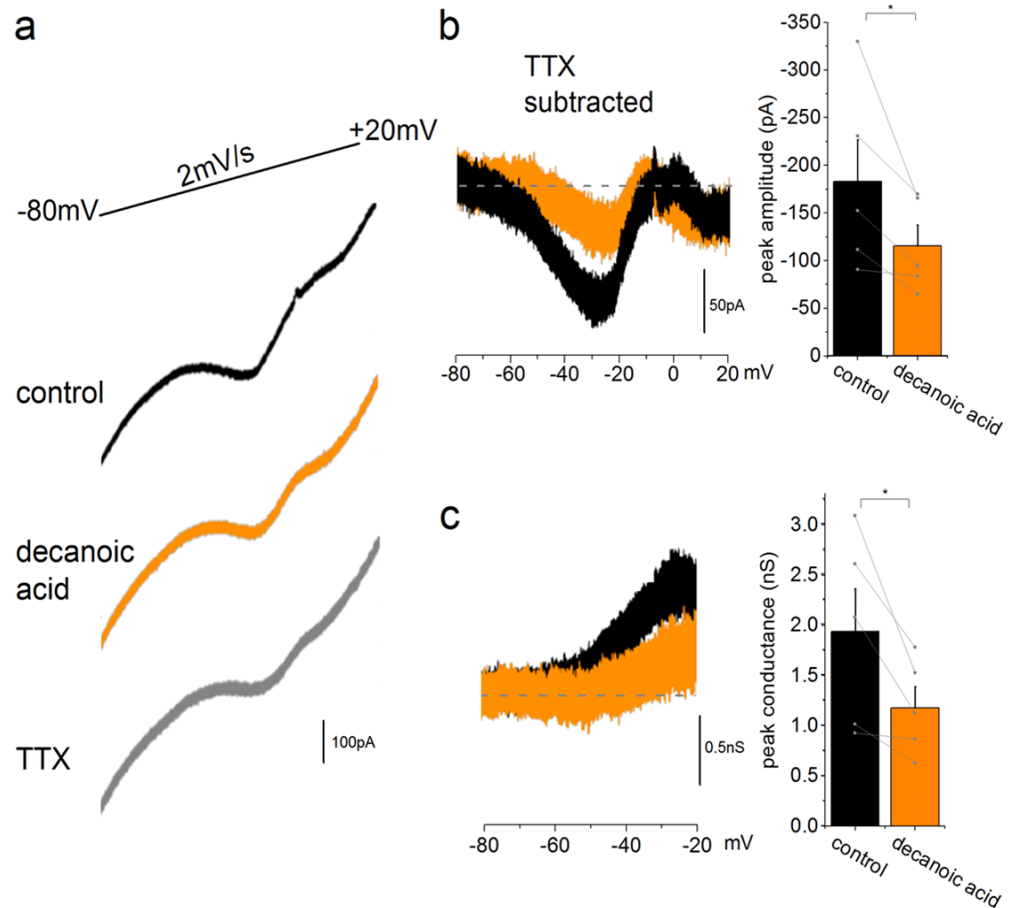


FIGURE 6.7: Decanoic acid reduces the persistent sodium current

a) I_{NaP} was evoked by a slow voltage ramp [top]. Current traces obtained in control aCSF [black], with decanoic acid [orange] and in TTX [grey]. b) Traces recorded in TTX were subtracted from those in control aCSF and in the presence of decanoic acid. [left] Example recording showing that I_{NaP} is reduced by application of $300 \mu\text{M}$ decanoic acid. [right] Peak I_{NaP} amplitude was reduced by decanoic acid. c) Conductance-voltage trace shows peak conductance is reduced by decanoic acid. $n=5$, $*p < 0.05$.

6.4 Discussion

In this chapter I looked at novel actions of decanoic acid and other medium chain fatty acids on neurons. I found that decanoic acid reduces the intrinsic excitability of neurons by actions at VGSCs. In the previous chapter, I focused on the action of decanoic acid as a non-competitive AMPA receptor antagonist. Decanoic acid and other MCTs are also known to increase mitochondrial citrate synthase and complex I activity, and to act as a peroxisome proliferator activator receptor- γ (PPAR- γ) agonist (Hughes et al., 2014). None of these actions would be expected to directly alter neuron intrinsic excitability.

When a square pulse of positive current is directly injected into a neuron it depolarises the membrane. If this depolarisation is sufficient to bring the membrane to $V_{\text{threshold}}$, then an action potential is initiated by the coordinated opening of VGSCs, followed by VGKCs. Upon application of decanoic acid or BCCA the same injection of current initiates fewer action potentials by increasing the rheobase and possibly increasing the voltage threshold. As these experiments were performed in the presence of synaptic blockers, this effect is distinct from the inhibition of AMPA receptors by decanoic acid. I used a phase plot to compare action potential kinetics in control aCSF and following application of BCCA. Phase plots require a high sampling frequency (at least 50kHz) for accurate comparison, so I could not interpret experiments with decanoic acid wash in as the sample rate was 20kHz. Further, phase plots are only useful in recordings which do not have a complete block of spikes upon BCCA wash-in, which may reduce the measured effect size.

In the presence of the VGSC blocker, TTX, application of decanoic acid has no effect on neuronal responses to current injections. As action potentials are blocked in TTX, I could not rule out the possibility that decanoic acid's effect was masked in TTX. Therefore I looked in further detail at the effect of decanoic acid on multiple currents produced by VGSCs. Decanoic acid did not alter I_{NaT} in CA1 pyramidal neurons, but did reduce the amplitude of I_{NaP} . The persistent current may provide a small but accelerated depolarising voltage ramp capable of triggering more efficient opening of other sodium channels.

To minimise the contribution of space-clamp errors to recordings of sodium channel currents, recordings with obvious space-clamp problems (such as increased delay to onset of an inward

current or insufficiently blocked K^+ currents) were not included in this study. A caesium-based internal solution improved the voltage clamp and methylsulphonate was used, as in previous experiments, which is more physiological than commonly used fluoride (Carter et al., 2012). The input resistance generally decreased with the duration of the recordings, so the TTX subtraction did not always remove all leak currents; but the persistent current could always be identified in control aCSF recordings. A very slow (2mV/s) voltage ramp protocol was used, which produces smaller I_{NaP} but was required for reducing escape transient sodium currents.

Sodium channels vary between three states: closed, open (activated), and inactivated. I_{NaT} has rapid kinetics, reaching its peak in less than one millisecond and declining back to baseline within a few more milliseconds. This current has an all-or-none threshold behaviour which makes it suited for action potential initiation. Conversely, I_{NaP} is localised on neuronal dendrites, where it boosts distal synaptic potentials to allow them to reach the soma. It is also present on the proximal axon, for spike initiation, and peripheral axons. The persistent current is important in subthreshold membrane oscillations which control spike patterning. Although the amplitude of persistent currents is typically $<1\%$ I_{NaT} (and around 3-4% in my recordings), it is activated 10mV negative to transient currents. Few VG channels are active here and input resistance is high so a change in voltage spreads further, which allows postsynaptic potentials in dendrites to get boosted toward threshold for action potential generation (Crill, 1996). Further, the voltage range in which I_{NaP} is activated is traversed in the interspike interval in an action potential train, so I_{NaP} can facilitate repetitive firing. Increased I_{NaP} has been implicated both in acquired (Agrawal et al., 2003; Vreugdenhil et al., 2004) and possibly in genetically determined epilepsy (Stafstrom, 2007), at a time point coinciding with the onset of spontaneous recurrent seizures. Several current AEDs have been found to reduce I_{NaP} at clinically appropriate doses, including phenytoin, valproic acid, topiramate, losigamone, lamotrigine, riluzole, and propofol (Colombo et al., 2013).

VGSC blockers that selectively target I_{NaP} could be effective at limiting pathological excitability and neurodegeneration. Decanoic acid shows dual action to reduce the excitability of neurons in epilepsy. This may explain the benefit of following a ketogenic diet in pharmaco-resistant epilepsy patients. The two decanoic acid targets may have a synergistic effect when targeted together. Decanoic acid is an attractive candidate molecule for the

treatments of epilepsy as it is naturally occurring in food, so these findings can easily be taken forwards to clinical trials. Finally, the effect of decanoic acid on intrinsic excitability was equivalent with BCCA treatment. I showed that BCCA inhibits epileptiform discharges in the previous chapter, and BCCA is also an AMPA receptor antagonist (K. Augustin, unpublished). In *Xenopus oocytes*, BCCA strongly inhibits GluA2/3 AMPA receptors (IC_{50} : $0.63 \pm 0.03mM$; $n=13$) and also inhibits GluA1/2 receptors (IC_{50} : $1.13 \pm 0.04mM$; $n=6$). This supports the use of metabolically favourable MCT derivatives for development as clinical treatments for seizure control.

Chapter 7

Comparison of experiments in rodent and human cortical tissue

7.1 Summary

In this chapter I used human brain slices obtained from resective epilepsy surgery to compare to data presented in previous chapters from rat hippocampal slices. In this physiologically relevant model I looked at the action of medium chain triglyceride's on network and single neuron function. I also examined the properties of AMPA receptors present at the synapse.

Network epileptiform activity was initiated by high potassium with GABAergic inhibition, and decanoic acid was able to reduce the frequency of epileptiform discharges. Decanoic acid blocked AMPA receptor-mediated currents in human cortical neurons, as it does in rat pyramidal neurons. Surprisingly, decanoic acid had no effect on the intrinsic excitability in human cortical neurons at a concentration which has a significant effect in rat neurons.

The $I-V$ relationship of AMPA receptors in cortical neurons from human surgically resected tissue was also investigated. These neurons were heterogeneous in their morphology and in their pathological background. Evoked EPSCs had a linear $I-V$ relationship and were not sensitive to NASPM. This suggests that the synapses contained only, or mainly, GluA2-containing AMPA receptors. This chapter provides a platform for the use of resected human tissue to be used for studies into network changes in epilepsy and the investigation into novel AEDs.

7.2 Introduction

The opportunity to compare rat with human neurons provides an important translational step in the treatment of chronic and pharmacoresistant epilepsy. Slices are prepared from surgically resected tissue and are viable for up to 36 hours in aCSF (Jones et al., 2016). The data are obtained from multiple brain regions with heterogeneous medical backgrounds and the tissue is from apparently normal brain, adjacent to epileptogenic cortex.

Both astrocytes and pyramidal neurons in the human temporal cortex are 2-3 times larger than those in rodents due to larger dendritic arborisation, and there are at least twice the number of synapses per pyramidal neuron in humans as there are in mice. There are neuron classes in human which are not seen in rodents, as well as more diversity in interneuronal classes. A recent study compared morphologies of human neurons to mouse and macaque neurons (Mohan et al., 2015). They found the total dendritic length and number of branch points were higher in human neurons and that there were distinct differences in dendrite morphologies. Further, processes are much more complex which hints toward differences in information processing in human neurons (Oberheim et al., 2009).

Neocortical tissue samples were collected from the National Hospital for Neurology and Neurosurgery in ice cold sucrose solution. Different collection solutions were tested including ice cold aCSF and choline-based aCSF, but sucrose-based aCSF was chosen as it produced consistently high quality slices and matched the protocol used for producing rat slices. The time from tissue resection to the slicer was < 15 minutes once the protocol and communication was established. There was delay in the initial preparation of the sample for slicing due to the additional step of removing the meninges and choosing a slicing angle from the unique samples. Once the tissue was positioned in the slicing chamber, the same slicing protocol was followed as for rat slices. The tissue samples obtained were $\sim 1.5\text{cm}^3$ and the slices produced were larger than horizontal EC-hippocampus rat slices. The benefit of this size slice is that larger intact networks could help initiate epileptiform activity. The size of slice made was limited by the size of the recording chamber on the rig, and slices had to be cut to fit sometimes. (See "Methods" for more details).

Slices from surgically resected human tissue can remain healthy at least 10-14 hours (Dossi

et al., 2014). The tissue can be used for multi-electrode recordings, preparation of organotypic cultures and calcium imaging, as well as extracellular and patch clamp recordings. Opportunities to collect human cortex samples were intermittent and infrequent, so the number of recordings was not enough to draw conclusions about correlations between recordings based on patient information (see Table 7.1). Individual differences in the age of the patient, duration of seizures and medication history will increase the variability between slices. Further, genetic variability is much greater between humans than between laboratory animals.

A table showing details of single neuron properties has been included in the appendix of this thesis (Supplementary Table 8.3).

In this chapter I tested the following hypotheses:

- Cortical tissue obtained from resective epilepsy surgery produces slices generates epileptiform discharges when the network is artificially pushed
- The pharmacology of decanoic acid at human neocortical neurons is similar to that in rodent hippocampal neurons
- Pyramidal neurons distant from the epileptic foci do not contain CP-AMPA receptors, but those in the epileptic foci do

Surgical area	Gender	Age	Onset	Seizure frequency	Pathology	AED
Frontal l.	M	NA	8yr	1.5/ month	cortical scar, prev. intracranial haemorrhage	GPN, LAC, CBZ, PHT, CLB
Temporal l.	F	NA	7yr	28/ week	SE (2 times), Type I/II + HS	CBZ, ZNS, CLB
Temporal l.	M	48yr	31yr	1/month -assoc. music	non specific neuron loss	LTG, PER
Temporal l.	F	49yr	16yr	2-7/ day	Pleomorphic Xanthoastrocytoma (tumour)	LAC, LVT
Temporal l.	M	30yr	15yr	10/day	Type II HC	LTG, LVT
Temporal l.	M	25yr	NA	NA	NA	NA
Frontal l.	M	NA	13yr	12.5/ month	SE and NAD	CBZ, PHT, ZNS

TABLE 7.1: Patient details of tissue included in this thesis. NA= No data available, HC= Hippocampal sclerosis, CBZ= Carbamazepine, CLB= Clobazam, GPN= Gabapentin, LAC= Lacosamide, LTG= Lamotrigine, LVT= Levetiracetam, PER = Perampanel, PHT= Phenytoin, ZNS= Zonisamide

7.3 Results

7.3.1 Epileptiform discharges are inhibited by decanoic acid in a slice from human temporal lobe

Cortical tissue obtained from epileptic patients has little spontaneous activity. There are a few reports of successfully recording interictal activity (Huberfeld et al., 2007; Roopun et al., 2010), and one of spontaneous ictal activity without modifying aCSF (Cunningham et al., 2012). It seems that this is only achieved in tissue from within the seizure onset zone (Simon et al., 2014). Further, pushing the network to a state in which spontaneous activity would be produced in rodent hippocampal slices also failed to induce epileptiform activity in human temporal lobe slices. It is not possible to know whether tissue outside the epileptogenic zone is less excitable than control temporal cortex would be. In rats, 4AP-induced activity is easier to generate in slices produced from control than from epileptic rats (Zahn et al., 2008). To promote the induction of epileptiform activity, the most important factors are slice orientation, perfusion rate, aCSF content and slice health (Husson et al., 2007). Differences in synaptic architecture or neuronal metabolism may also contribute to the high threshold for epileptic activity in human brain slices compared to rodent tissue. The density of neurons in the neocortex compared to hippocampus is lower, which would also reduce the ability for generation of spontaneous epileptiform activity (Jones et al., 2016). Inducing epileptiform activity in humans may be easiest to induce 4-5 hours after slicing (Remy et al., 2003).

Using 450 μ m slices, epileptiform activity was generated with 12mM K⁺ and 50 μ M PTX (Fig. 7.1a). The initiation of epileptiform activity in this slice required both pro-convulsive agents and pro-excitability changes in aCSF ion concentrations, however the activity was sustained and could be measured in both layer 2/3 and layer 5 within the same slice with a high perfusion rate (Morris et al., 2016). Activity in these two layers was synchronised and both responded to decanoic acid in the same way. Upon wash in of 300 μ M decanoic acid, activity was greatly reduced but did not stop (Fig. 7.1a). I used a concentration comparable to that observed in humans on the MCT diet. This is lower than that used in the rodent experiments. Activity reduced to 7.6% of control in the human slice (Fig. 7.1b), and returned when decanoic acid was washed out. Owing to the sporadic collection of human tissue samples and the difficulty in generating epileptiform activity, this graph contains data from

a single slice.

7.3.2 Decanoic acid reduces AMPA receptor-mediated currents in human neurons

Electrophysiological recordings were taken from visually identified pyramidal neurons in the neocortex of humans from tissue resected for epilepsy surgery (350 μ m slices; details on the patients are in Table 7.1). These neurons were more sparsely distributed than rat hippocampal cell layers, without clear cell body regions and fibre tracts. There was a greater density of unmyelinated axons in the human tissue. This may be a species difference related to the greater number of long range connections across the human brain, or just due to the age of the tissue from humans compared to the P21 rats used. During seal formation human cortical neurons took longer to reach gigaohm ($G\Omega$) resistance but upon reaching whole cell configuration cells were stable which allowed long recordings.

To record evoked EPSCs, the stimulating electrode was placed closer to the neuron being recorded from than in rat slices (\sim 500 μ m away). This is because there were no pronounced fibre tracts in the human neocortical tissue, compared to the hippocampus. Evoked responses were recorded in the presence of 50 μ M D-AP5 and 50 μ M PTX to block NMDA receptor and GABA_A receptor currents respectively (Fig. 7.2a), so that isolated AMPA receptor-mediated currents were recorded. Cells were patched using a caesium-methylsulphanate internal solution with 50 μ M QX-314, and the cell was held at -60mV for these recordings. Upon application of 600 μ M decanoic acid the amplitude of currents was reduced (Fig. 7.2b-c; $n=3$, [control]: -244.0 \pm 44.5pA; [+decanoic acid]: -95.1 \pm 16.9pA; $p=0.009$, paired t -test). This concentration was chosen to maximise the effect seen on AMPA receptor-mediated currents (Chang et al., 2016), as the collection of human tissue was infrequent. The time course of decanoic acid action in humans is similar to rat hippocampal slices, at a comparable slice thickness (Fig. 7.2c; Chang et al., 2016). A higher concentration of decanoic acid was used to show a significant difference with a small numbers of neurons.

There is high homology between rodent and human AMPA receptors (Traynelis et al., 1993); therefore it is unsurprising that decanoic acid has the same effect in human cells on AMPA receptor-mediated currents, as has been shown previously in rats. This is important,

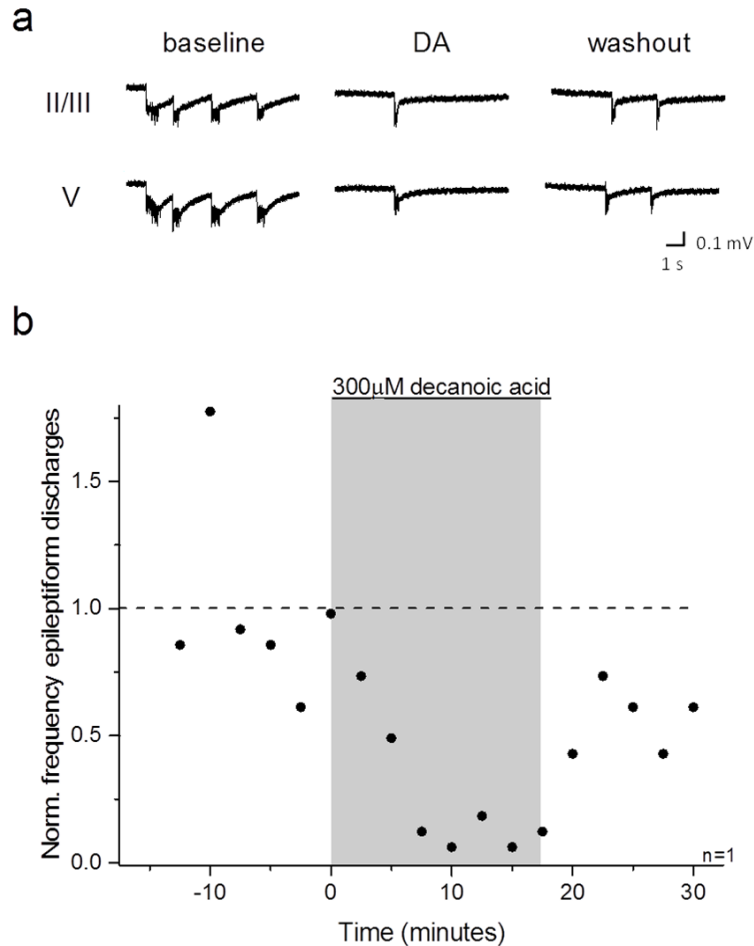


FIGURE 7.1: Epileptiform discharges are blocked by decanoic acid in one slice from human temporal lobe.

a) Application of 300 μM decanoic acid decreases the number of epileptiform events. Representative extracellular recordings of epileptiform activity initiated by raising K^+ to 12mM and adding 50 μM PTX. Recordings from layer 2/3 [upper] and layer V [lower] of the cortex are synchronised. b) Summary of number of events binned into 5 minute blocks. Grey area indicates presence of decanoic acid. Dashed line indicates baseline frequency. Event count is normalised to baseline (n=1); recording performed by Dr Gareth Morris.

as it shows decanoic acid will target AMPA receptor-mediated currents in human neurons, giving further support for its potential therapeutic benefit.

7.3.3 Decanoic acid does not reduce the intrinsic excitability of human neurons

Cells identified visually as cortical pyramidal neurons were patched with a K-gluconate internal solution. Current steps (50pA) were injected into neurons in the presence of ionotropic glutamate and GABA receptor antagonists (50 μ M PTX, 10 μ M NBQX, 50 μ M D-AP5) and voltage responses were recorded. Action potentials were very similar in shape and timing to those recorded from rat neurons (Fig. 7.3a-b). They were first initiated at -50mV to -40mV, and had a rheobase of 120pA to 200pA (see Supplementary Table 8.3 for all measured parameters).

300 μ M decanoic acid reduces the intrinsic excitability of rat hippocampal neurons via action on the persistent sodium channel current, as shown in Chapter 6. In this experiment, 300 μ M decanoic acid was applied to cortical human neurons and did not affect the intrinsic excitability, assessed by measuring the number of action potentials (Fig. 7.3c-d, n=2; area under the curve: [control]: 1589 ± 330 a.u., [decanoic acid]: 1567 ± 292 a.u.). Unfortunately, no washout of decanoic acid was achieved in these experiments.

7.3.4 No detection of CP-AMPA receptors at synapses on human cortical pyramidal neurons

Here, I investigated the presence of CP-AMPA receptors at the synapses onto pyramidal neurons in the neocortex. The resected tissue used in these experiments was taken from various sites during surgeries. Therefore some samples will likely have been obtained closer to the seizure foci than others, although no samples were obtained from within the seizure onset area.

In my experiments neurons were patched with a Cs-methylsulphanate internal solution containing QX-314 and spermine. Neurons were voltage clamped (-80mV to +60mV) in the presence of 50 μ M PTX and 50 μ M D-AP5, as in Chapter 3 for experiments using rodent slices. Fig. 7.4a shows an example trace of the eEPSCs recorded and average *I-V* relationship. The

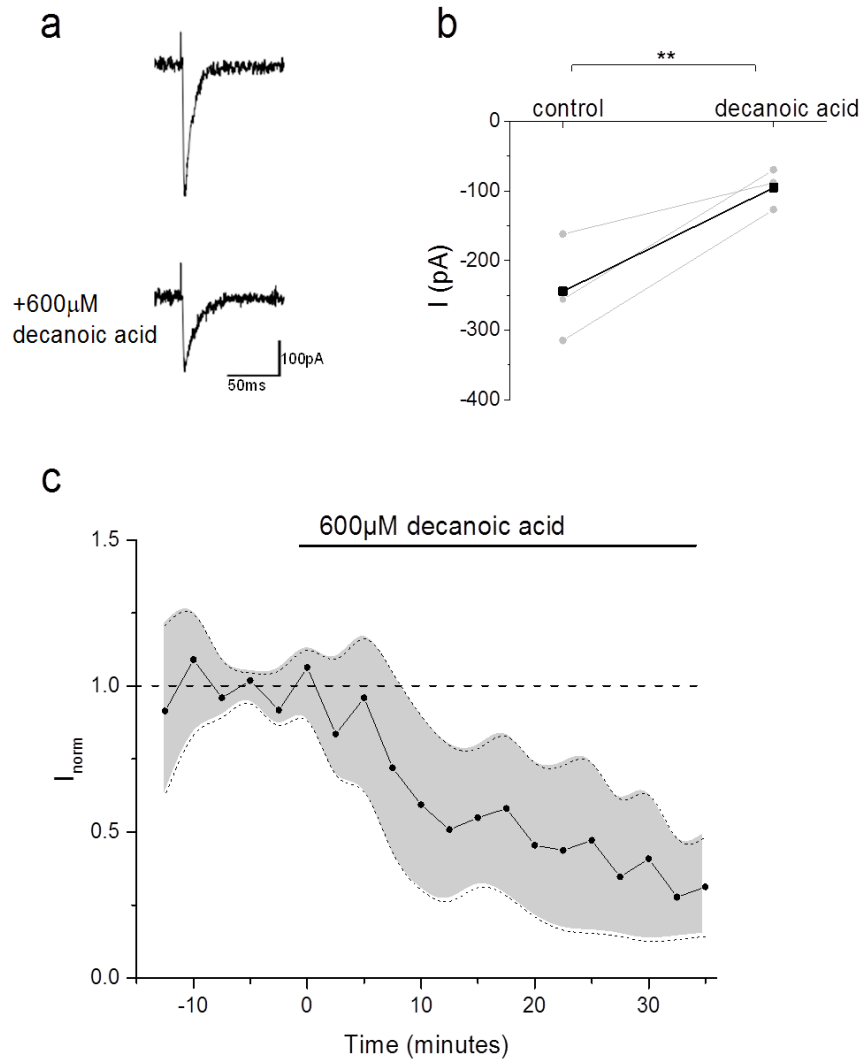


FIGURE 7.2: Decanoic acid decreases AMPA receptor-mediated currents in neurons from surgically excised human cortex.

a) Representative evoked AMPA receptor-mediated currents recorded from a pyramidal-like neuron in a cortical slice from a human. Control [top], and after application of 600 µM decanoic acid [lower]. Current traces are each averaged over 5 evoked EPSCs with the cell held at -60 mV. b) Summary of eEPSC amplitude change from wash in of 600 µM decanoic acid in human cortical neurons. Grey circles are individual cells, black squares are the average. **p < 0.01 (paired *t*-test). c) Normalised peak current amplitude obtained before and during application of 600 µM decanoic acid, showing time course of amplitude decrease. Black squares are mean; grey cloud shows ± SEM (n=3 cells).

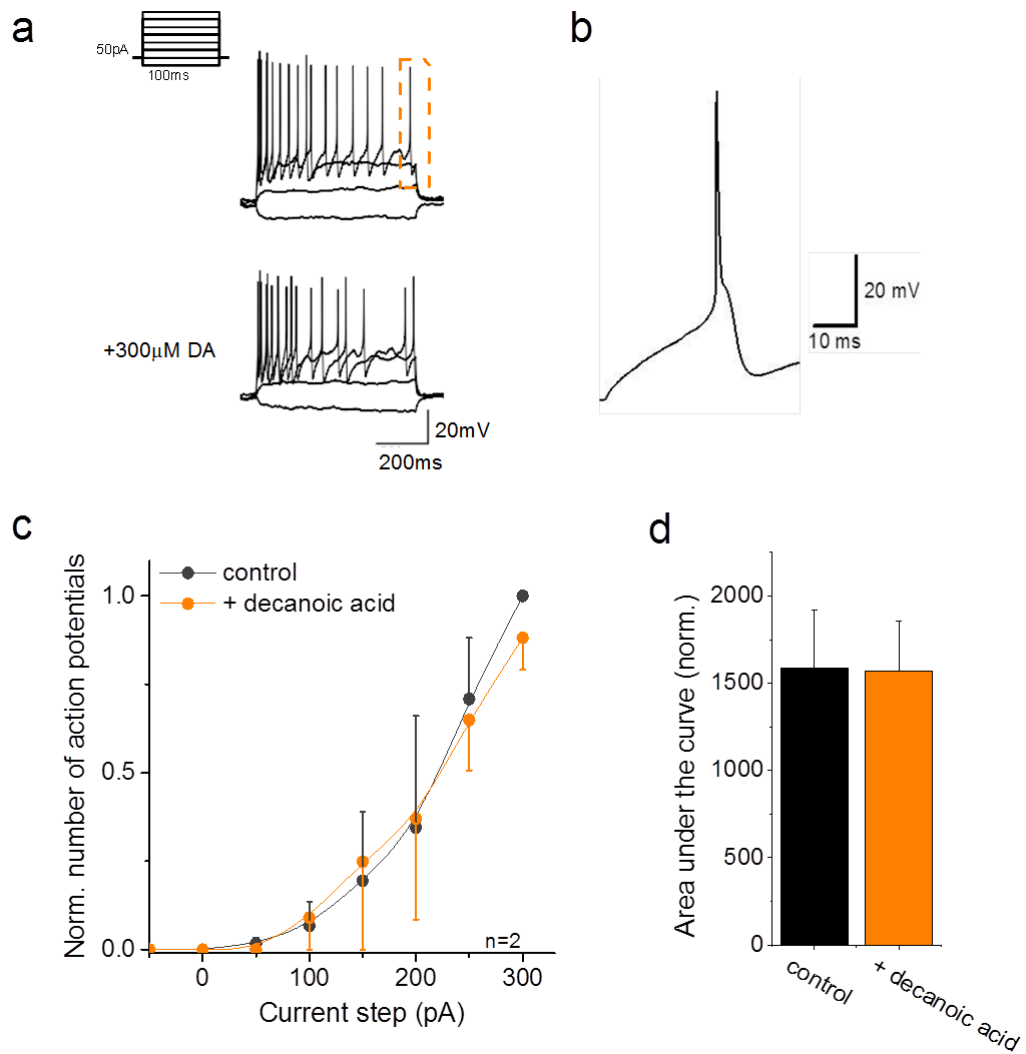


FIGURE 7.3: Decanoic acid does not affect the intrinsic excitability of human neurons

a) Representative recordings of action potentials initiated by 50pA current steps with 300µM decanoic acid treatment. b) Single action potential recorded from a human cortical neuron [enlarged from orange box in (a)]. c) The number of action potentials evoked by current injections were compared upon wash in of decanoic acid, to quantify changes in intrinsic excitability. Lines are fitted to the data as a spline function. d) Summary for (c): Area under the curve was not changed after decanoic acid wash-in. All recordings were performed in the presence of synaptic blockers, n=2.

I-V relationship was linear and averaged rectification index was 0.81 ± 0.19 (n=6), which indicated that the activated synapses predominantly contained CI-AMPA receptors. Upon application of the specific CP-AMPA receptor blocker NASPM ($70\mu\text{M}$) the peak current and rectification index did not change (Fig. 7.4b; [control]: 0.79, [+ NASPM]: 0.65; n=1). This further shows that there were no CP-AMPA receptors present at the synapses investigated.

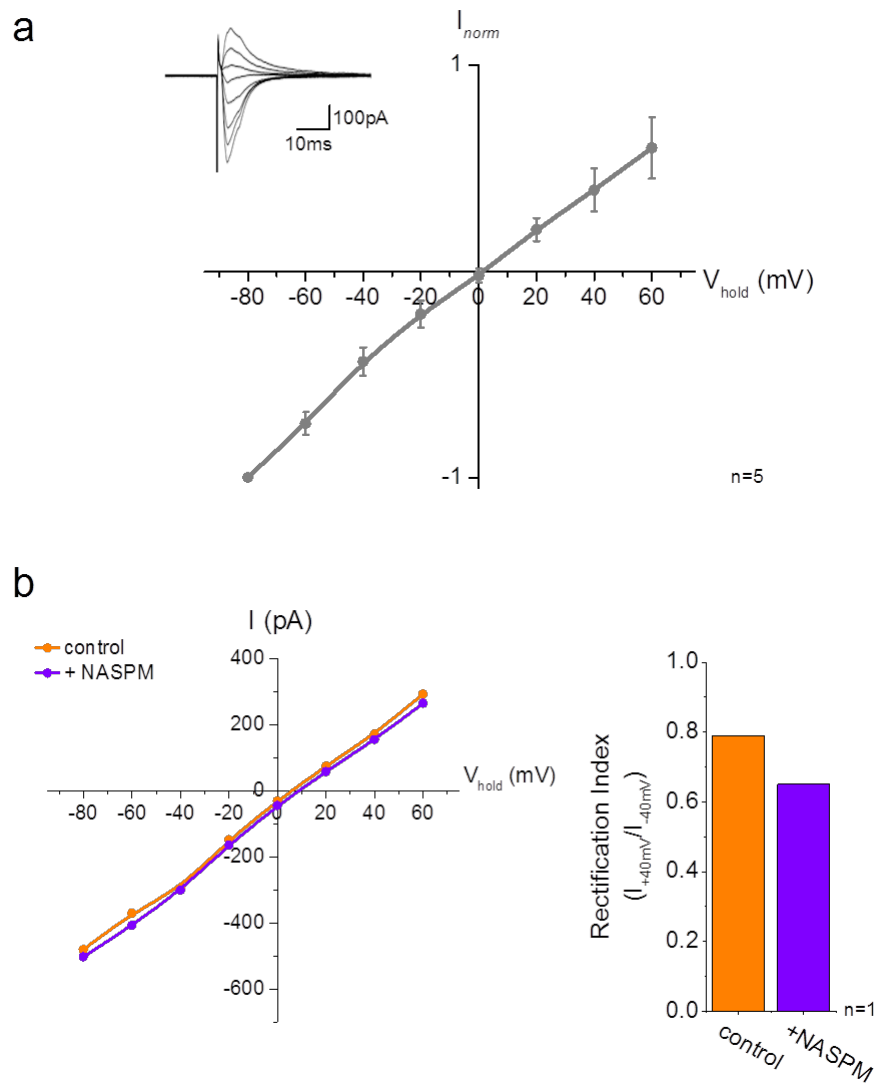


FIGURE 7.4: No CP-AMPA receptors were present in human cortical neurons outside the seizure onset zone, as the $I-V$ relationship is linear.

a) $I-V$ plot from human neocortical pyramidal neurons averaged (RI = 0.81 ± 0.19). [Inset] Representative eEPSCs at each step potential. b) $I-V$ plots comparing a neuron with application of the CP-AMPA receptor blocker, NASPM [left] and summary of rectification index with wash in of NASPM [right], $n=1$.

7.4 Discussion

In this chapter I used slices prepared from surgically resected cortical tissue in refractory epilepsy. Due to the limited tissue available, results from this chapter are preliminary. Nevertheless I was able to show that I could elicit epileptiform activity from human neocortex, and patch clamp neurons in *ex vivo* human tissue. This could offer an important step in translating results from rodent tissue to humans. I showed that decanoic acid is able to block induced epileptiform activity in a slice, and it reduces AMPA receptor-mediated currents. Tissue collected in surgery was from patients who were previously taking multiple AEDs without successful seizure control. Although the tissue used is from outside the seizure onset zone, the beneficial action of decanoic acid here raises the possibility that decanoic acid will work in cases when pharmacoresistant to typical AED.

Surprisingly, decanoic acid did not change intrinsic excitability in this preparation, as it does in rat hippocampal neurons. One explanation of these findings is that there is less persistent sodium current in human neocortical neurons compared to rat CA1 pyramidal cells. Mutations affecting the persistent sodium are a cause of human genetic epilepsy (Stafstrom, 2007), and the persistent sodium currents has been measured in layer V pyramidal neurons in the human neocortex (Aracri et al., 2006). The persistent sodium current contributes a smaller component compared to the fast component in humans (1.3%) compared to rat (1.6% in mature rat and 2% in immature rat neocortex; Cummins et al., 1994). It could be interesting to compare the action of decanoic acid on intrinsic excitability in rodent hippocampal pyramidal neurons to its action at rodent cortical pyramidal neurons. Also, the number of sodium channels needed for action potential initiation could be different in human neurons, and a higher concentration of decanoic acid is needed to block these. A dose-response experiment would allow me to find out if this is the reason for the species difference. Input resistance was $134.0 \pm 22.7\text{M}\Omega$ and membrane capacitance was $19.0 \pm 3.7\text{pF}$, which is comparable to cortical neurons (Supplementary Table 8.3). Another key difference between the slices prepared from rats and those from humans is that rats are anaesthetised under isoflurane for minutes before dissection, whereas human surgical patients may have been under anaesthesia for hours. General anaesthetics act at sodium channels, so the effect of decanoic acid at sodium channels may be altered by the actions of general anaesthetics.

I also looked at the I - V relationship in neurons from human slices outside of the seizure foci. These neurons did not have rectifying AMPA receptor-mediated currents, and were not affected by the CP-AMPA receptor blocker, NASPM. This suggests that the activated synapses did not contain CP-AMPA receptors. Importantly, the tissue obtained was not from the seizure foci, as this tissue was required by the clinical pathology team. The distance from foci varied between specimens, and this could be a confounding factor. As these recordings were taken from outside the seizure zone, it would be interesting to see whether there is CP-AMPA receptor expression at synapses within the trigger zone. Histopathological studies comparing a number of clinical factors with neuronal architecture found no significant correlation between total dendrite length nor number of branch points when compared to the number of seizures, disease severity, or age of the patient (Mohan et al., 2015). However, there may be a more subtle change to neuron morphology, or a change which only affects certain neuronal types which would not be noticed by this study. Previous studies using fixed tissue from the brains of patients with refractory TLE have compared the expression of AMPA receptor subunits and found reduced protein GluA2 levels in hippocampal areas with the most pronounced cell loss, but increased GluA2 levels within the dentate gyrus (Blumcke et al., 1996b).

Non-invasive whole brain recordings (EEG, fMRI, PET) are taken as part of the pre-surgery assessment. There could be an interesting correlation between excitability measured here and recordings taken from slices of tissue from these brains. Perhaps this may predict which slices would exhibit spontaneous epileptiform activity, and even which would have CP-AMPA receptor expression.

Given the limited quantity of tissue obtained it is difficult to draw definitive conclusions from the data. However, the action of decanoic acid on epileptiform activity from pharmacoresistant cases seem clear, which provides more evidence for the ability of decanoic acid to control seizures. To summarise, this chapter provides proof of principle for the use of resected human tissue to be used for studies into network changes in epilepsy and the investigation into novel AEDs.

Chapter 8

General Discussion

The principal focus of this thesis was to investigate the effect of excessive network activity on AMPA receptor expression and also the inhibition of epileptiform discharges by medium chain fatty acids and their derivatives, which are non-competitive AMPA receptor antagonists. AMPA receptors drive the spread of seizure activity through networks and are increasingly being looked at as an important target for seizure control.

In Chapters 3-4, I used *in vitro* seizure models and demonstrated that there is CP-AMPA receptor expression at CA1 pyramidal neuron synapses following excessive activity, and this is dependent on both NMDA receptors and calcineurin activation. In Chapter 5, I compared medium chain fatty acids, including decanoic acid, with other AMPA receptor antagonists at inhibiting epileptiform activity. I found that the action of decanoic acid at AMPA receptors does not affect receptor kinetics, and was not use-dependent. I also showed that decanoic acid acts synergistically with perampanel at inhibiting epileptiform discharges. In Chapter 6, I looked into other actions of decanoic acid, and showed that it reduces intrinsic excitability via decreasing the persistent sodium current. Finally, I tested some of these findings in experiments using human surgically resected tissue in Chapter 7, and provided preliminary evidence for the use of this in mechanistic and pharmacological studies for epilepsy treatment.

I will first discuss how data recorded in this thesis relate to previously published data and then I will discuss the physiological impact of my findings. I will address each of my hypotheses in turn.

8.1 Excessive network activity causes a shift towards GluA2-lacking AMPA receptor expression at CA1 pyramidal neurons

There is an elevation of $[Ca^{2+}]_i$ to around three times that at control levels, following excessive network activity (such as during SE; measured using $^{45}CaCl_2$ autoradiography and Fura 2AM Ca^{2+} imaging), which is sustained until after SE is over (Pal et al., 1999; Friedman et al., 2008). Ca^{2+} entry via VGCCs, NMDA receptors and AMPA receptors can trigger cascades causing apoptosis in cells without sufficient calcium buffering proteins, such as CA1 pyramidal neurons. CP-AMPA receptor expression provides an additional means for Ca^{2+} entry into the neuron during excessive network activation.

The experiments presented in Chapter 3 show evidence for increased expression of CP-AMPA receptors. Incubation of hippocampal slices in 0-Mg $^{2+}$ or PTZ-aCSF produced rectifying AMPA receptor-mediated currents. Rectification was used as a measure of the proportion of CP-AMPA receptors at the synapse, since CP-AMPA receptors are subject to voltage-dependent inhibition by polyamines. I further confirmed my findings by pharmacology and used variance analysis to determine if there is an increase in conductance as would be predicted by CP-AMPA receptor expression.

My results are in line with previous immunohistochemical and electrophysiological findings. In fixed tissue from the brains of patients with TLE, there is reduced GluA2 in hippocampal areas with the most pronounced cell loss, but increased GluA2 levels within the dentate gyrus (Blumcke et al., 1996b). In rats, transient CP-AMPA receptor expression has been shown up to one month after kindling by PTZ (Ekonomou et al., 2001), and has been shown in slices from SE models (Rajasekaran et al., 2012; Friedman et al., 2008). A recent study found increased CP-AMPA receptor expression following hypoxia-induced seizures in the immature brain, caused by reduced GluA2 expression at the synapse. This results in impaired LTD, which requires GluA2-containing AMPA receptors (Lippman-Bell et al., 2016).

CP-AMPA receptor expression at pyramidal cells may also alter classical NMDA receptor-

dependent LTP. This process relies on Ca^{2+} entry through the NMDA receptor for coincidence detection, and therefore Ca^{2+} entry through CP-AMPA receptors when the cell has not been previously depolarised could disrupt the specificity of coincidence detection in synapse strengthening. A critical question is whether plasticity can be induced with NMDA receptors blocked, due to calcium entry through synaptic CP-AMPA receptors on pyramidal neurons in these seizure models. CP-AMPA receptors are important for inducing other forms of plasticity, with high temporal precision and favouring strengthening at hyperpolarising potentials in interneurons (Lamsa et al., 2007).

My experiments were carried out using *in vitro* models of epileptiform discharges in hippocampal slices. This was a compromise which allowed simple pharmacological manipulation and was less labour intensive compared to *ex vivo* preparation from animals with induced epilepsy. Using slices allowed me to look at an identified set of synaptic connections in the well-categorised hippocampal network, which could not be achieved in cultures. The experiments looked at a single time point to compare slice models of seizures, so only acute effects were looked at. It would be useful to track the duration of this increase in CP-AMPA receptor expression, as an acute switch may induce apoptosis of damaged cells whereas a chronic switch may promote epileptogenic network generation. A recent study showed there is CP-AMPA receptor expression in rat *ex vivo* slices after systemic pilocarpine-induced SE (Malkin et al., 2016). The group showed that expression was transient, with the greatest CP-AMPA receptor expression three days after SE, and baseline expression returned after seven days. It may be that expression is only during the latent period, before development of TLE (Malkin et al., 2016).

8.2 The shift toward CP-AMPA receptor expression is blocked in the presence of NMDA receptor inhibitors

Under physiological conditions, CP-AMPA receptors are only transiently expressed in response to synaptic activity (Plant et al., 2006; Hou et al., 2008) so expression and trafficking must be tightly regulated. To answer the question of how CP-AMPA receptors become functionally expressed at the synapse, I started by asking whether the process is NMDA receptor-dependent. NMDA receptor activation is a necessary step in the initiation of numerous cellular processes, including LTP and apoptosis. Activation signals an increase

in network activity, since the membrane must be already depolarised from previous activity for glutamate binding to allow the channel to open. NMDA receptor activation further depolarises the membrane and increases $[Ca^{2+}]_i$ to trigger intracellular messenger cascades (Nowak et al., 1984).

I found that NMDA receptor activation was required for synaptic CP-AMPA receptor expression, as AMPA receptor-mediated currents were not rectifying if D-AP5 was included in the PTZ-induction medium (Chapter 4). It is likely that Ca^{2+} entry through NMDA receptors triggers a cascade favouring synaptic insertion of GluA2-lacking AMPA receptors. Based on this result, I looked at which protein phosphatases could be involved in CP-AMPA receptor expression by dephosphorylating AMPA receptor subunits and found that CP-AMPA receptor expression was calcineurin (CaN) dependent, but not STEP₆₁ dependent. CaN is a direct transducer of NMDA receptor signalling, as it is Ca^{2+} activated; it is therefore also activated by CP-AMPA receptors (Sanchez et al., 2005). CaN is found in a complex with kinases (PKA and PKC) and is assembled by AKAP79/150, which is targeted to the C-termini of AMPA receptors and NMDA receptors. This puts it in an ideal location to respond to NMDA receptor-mediated Ca^{2+} influx and regulate AMPA receptor trafficking. F-actin filaments are organised in a CaN-dependent way to traffic AMPA receptors to the PSD (Halpain et al., 1998). Further, CaN interacts directly with the TARPs γ -8, which modulates AMPA receptor trafficking and kinetics (Itakura et al., 2014).

CaN and PKA mediate the transient expression of CP-AMPA receptors following LTD (Sanderson et al., 2012, 2016). PKA was required for insertion, whereas CaN removed CP-AMPA receptors from the synaptic membrane. Expression of these proteins acutely increases after hippocampal sclerosis in P10 rats (Rakhade et al., 2008; Sanchez et al., 2005). The direction of CaN-mediated trafficking may be dependent on the pattern of Ca^{2+} influx by NMDA receptors, by restricting which phosphorylation sites CaN acts at. It may also be age-dependent, as expression of CP-AMPA receptors at pyramidal neuron synapses following LTP initiation has been described to be. The control of bidirectional plasticity by CaN allows dynamic regulation, as is seen in oligodendrocyte precursor cells (Zonouzi et al., 2011). It has recently been shown that phosphorylation of Elk-1 by ERK can have opposing effects depending on the site of phosphorylation (Mylona et al., 2016), which hints

at the complexity of interactions between protein regulators. This shows that multisite modification events do not act unidirectionally and phosphatases may not always produce the reverse effect to kinases.

AMPA receptor antagonists (such as NBQX) also block the enhanced Ca^{2+} response and NASPM sensitivity after hypoxia (Lippman-Bell et al., 2016). AMPA receptors mediate the bulk of excitatory synaptic transmission for the maintenance and spread of seizure-activity through the network, including the paroxysmal depolarisation shift (the basis of the EEG spike) and the electrographic seizure discharge (Rogawski, 2016). It appears that activation of AMPA receptors is required for CP-AMPA receptor expression. In the presence of NBQX there was no difference in CP-AMPA receptor-mediated Ca^{2+} responses in hippocampal CA1 neurons in epileptic compared to control non-epileptic animals. Further, NBQX blocked the post-seizure decrease in synaptic GluA2 expression (Lippman-Bell et al., 2016). However, this study was in immature brains, so the results could be specific for that particular developmental stage. NBQX does not have anti-epileptogenic effects in adults, but it is not known whether it inhibits the switch to CP-AMPA receptor expression in adults too (Twele et al., 2015).

The reason for expression of CP-AMPA receptors following seizures is not understood. NMDA receptors are extensively activated in epilepsy. Increased Ca^{2+} entry through NMDA receptors could trigger further $[\text{Ca}^{2+}]_i$ elevation due to calcium-induced Ca^{2+} release (CICR; Alford et al., 1993). If Ca^{2+} entry also allows synaptic expression of CP-AMPA receptors, then the different kinetics of Ca^{2+} -entry through AMPA receptors may induce non-overlapping intracellular processes. Many SE models report increased Ca^{2+} -dynamics in CA1 pyramidal neurons with similar patterns in cell death, thus studies can not resolve whether changes in Ca^{2+} permeability are a product of excitotoxicity pathways, or of epileptogenesis pathways. I next looked at whether inhibition of CP-AMPA receptors alters epileptiform activity.

8.3 Specific CP-AMPA receptor inhibitors block epileptiform activity in a similar way to general AMPA receptor inhibitors

The most potent and clinically well-tolerated AMPA receptor inhibitors act via a non-competitive mechanism, but many potential new AEDs produce adverse side effects. Non-competitive inhibitors stabilise the inactive receptor, preventing conformation changes leading to the ion channel opening (Yelshanskaya et al., 2016). Perampanel is a non-competitive AMPA receptor blocker, which is an approved AED but has CNS-related side effects of dizziness, somnolence, fatigue and irritability (Frampton, 2015). I asked whether specifically inhibiting CP-AMPA receptors, which have less widespread expression, would block epileptiform discharges.

Nascent CP-AMPA receptors are expressed at synapses following excessive network activity. If this is in addition to CI-AMPA receptors, then specifically blocking nascent CP-AMPA receptors could be beneficial. Previous studies have shown that selective CP-AMPA receptor block decreases excessive Ca^{2+} activity (Rajasekaran et al., 2012; Lippman-Bell et al., 2016), whereas NMDA receptor or L-type Ca^{2+} channel inhibition did not prevent seizure-induced increases in Ca^{2+} responses in hippocampal slices. In contrast to these findings, I found that NASPM did not reduce epileptiform discharges in the PTZ slice model of seizures.

Although NASPM did not alter the frequency of epileptiform discharges, there could be a benefit to long term NASPM administration for cell viability, if excessive Ca^{2+} entry through CP-AMPA receptors contributes to cell death.

8.4 AMPA receptor inhibition by decanoic acid can explain the success of the ketogenic diet

The ketogenic diet is successfully used for seizure control in refractory epilepsy, particularly in children (Cross et al., 2010). In patients, a long-term ketogenic diet postpones epilepsy disease progression and in a mouse model it prolongs life expectancy. Those on the MCT ketogenic diet have appreciable levels of MCTs in the circulation and the brain (Sills et al., 1986).

Decanoic acid is a key component of the MCT ketogenic diet, which inhibits epileptiform activity and acts as a non-competitive AMPA receptor antagonist. Similarly to other anti-seizure compounds, (such as GYKI and perampanel), decanoic acid acts as a non-competitive AMPA receptor antagonist. Receptor block by competitive antagonists can be removed if there is excessive glutamate at the synaptic (such as during a seizure), whereas the action of non-competitive antagonists is independent of the concentration of glutamate. This block could have effects on physiological synapse functioning, which I investigated further in Chapter 5. The hypothesised location of decanoic acid binding on AMPA receptors, based on modelling, suggested that it may influence the kinetics of AMPA receptor-mediated currents (Chang et al., 2016). However, I found that it does not affect AMPA receptor current kinetics. If the eEPSC tail current duration was reduced by decanoic acid, this would shorten the time window for LTP induction which is a key neuronal process for learning and memory.

Decanoic acid does not inhibit AMPA receptors in a use-dependent way. Use-dependent inhibition occurs when the binding site of the compound is inside the receptor pore, so it can only access here when the receptor is activated and channel open. Use-dependent inhibitors would preferentially inhibit overactive synapses in a seizure, however they may also be less effective at synapses which have a high AMPA receptor turn over rate. Perampanel does not block AMPA receptors in a use-dependent way, whereas polyamines use-dependently block certain subtype configurations of AMPA receptor.

Synergistic relationships between AEDs and AMPA receptor antagonists are often noted (Citraro et al., 2014). I found that perampanel enhanced decanoic acid's anti-seizure effects in the PTZ slice model. Similarly, GYKI enhances conventional AEDs action against maximal electric shock (MES)-induced seizures at a sub-therapeutic dose (Yamaguchi et al., 1993).

8.5 Other neuronal targets of decanoic acid reduce network excitability

Although decanoic acid acts at AMPA receptors, until now it has been unclear whether it is specific or, like many AEDs, has multiple targets. I showed that decanoic acid reduced

neuron intrinsic excitability by actions at VGSCs, including inhibition of I_{NaP} .

VGSCs are a common target of AEDs, including those with multiple targets. Sodium channel blockers have the highest affinity for binding to the inactivated state, which slows the conformational re-activating process. This produces a voltage- and frequency-dependent reduction in channel conductance, and limits repetitive neuronal firing (Sills and Brodie, 2001). Phenytoin, carbamazepine and lamotrigine all inhibit I_{NaP} more than I_{NaT} but none are specific I_{NaP} inhibitors. The polypharmacology of phenytoin includes actions at the Na-K-ATPase, the GABA_A receptor complex, ionotropic glutamate receptors, and calcium channels (Tunnicliff, 1996).

There are other known targets of decanoic acid which indicate it is neuroprotective and could improve cognition (e.g. in Alzheimer's patients; Henderson et al., 2009). Decanoic acid activates PPAR- γ receptors, which decreases inflammation after seizures in the hippocampus of mice (Jeong et al., 2011). MCTs, including decanoic acid, improve cognition in multiple memory tests in rats. Decanoic acid decreases many immediate early genes related to synaptic renovation and protein synthesis following LTP (e.g. activity-regulated cytoskeleton-associated protein Arc/Arg3.1, the transcription factor jun-B, and early growth response 2 *egr2*), but increases Akt phosphorylation and expression of proteins involved in synaptic maintenance (Wang and Mitchell, 2016).

Further, MCTs are metabolised into ketones which also have effects on excitability (Ma et al., 2007) and neuroprotection (Kim et al., 2015a, 2007); although there is a poor correlation between serum ketones and seizure control (Likhodii et al., 2000; Thavendiranathan et al., 2000). The success of the ketogenic diet may be from the multiple targets by decanoic acid and its metabolites.

8.6 Recordings from human neocortical neurons can be compared to results obtained in rats

Human tissue obtained during epileptic foci resection surgery gives a unique insight into pharmacoresistant epilepsy. Decanoic acid reduced epileptiform discharges when induced in slices of human cortical tissue peripheral to the seizure onset zone. I looked at the

mechanism of action of decanoic acid at human neurons. I also looked for evidence of CP-AMPA receptor expression by looking at the $I-V$ relationship at cortical pyramidal neurons. I showed the potential use of human slices for both pharmacological studies and to look at the underlying mechanism of seizures.

As this tissue was not from the seizure foci, but from tissue adjacent to the foci, there were no spontaneously produced epileptic discharges. Further, there would be minimal receptor and network epileptogenic changes compared to the seizure-onset zone. For future experiments, it would be useful to fill cells with biocytin during recording to see precisely which neuron type is being recorded from. Moreover, with more data collected it would be possible to correlate slice recordings with patient details, such as seizure frequency and which AEDs were prescribed.

Preliminary results in human tissue give further evidence that decanoic acid will inhibit seizures in humans as in rodents, which is essential for a compound being developed for clinical treatment. Decanoic acid inhibited AMPA receptor-mediated currents in human neurons, but did not reduce intrinsic excitability as shown in rodent neurons in Chapter 6. The lack of an effect on intrinsic excitability may be due to a lack of persistent sodium currents in the cells from which I recorded- this needs to be investigated further.

8.7 Future Directions

Following the first section of this thesis—looking at the expression of CP-AMPA receptors at CA1 pyramidal neurons after seizures— it is important to work out why this receptor type becomes expressed at the synapse, and the time period of this expression. Ca^{2+} imaging would allow me to see when there is increased Ca^{2+} influx and how long this lasts. I could patch neurons at different time points after SE in *ex vivo* slices, and see when the *I-V* relationship becomes linear.

CP-AMPA receptors could drive some of the epileptogenic network changes following the initial insult. There is evidence that CP-AMPA receptors do not lead to cell death (Lippman-Bell et al., 2016). The mechanism by which CaN activation leads to expression of CP-AMPA receptors is not known, but the pattern of Ca^{2+} influx is important for determining whether there is CP-AMPA receptor expression. Since CaN is required for expression of CP-AMPA receptors, it would be important to see if reversing the change in AMPA receptors using clinically available CaN inhibitors has an impact on the outcome of SE.

For the second section of my results, it will be interesting to determine the specific target of decanoic acid at VGSCs, using HEK cells transfected with both α - and β -subunits of sodium channels. If decanoic acid is beneficial in patients with refractory epilepsy, then it may be looked at as a treatment in other neurological conditions. The MCT ketogenic diet has potential to reduce clinical and cellular symptoms in other neurological disorders characterised by neuronal cell death (Rho and Stafstrom, 2012), such as Alzheimer’s disease (Reger et al., 2004; Henderson et al., 2009) and Parkinson disease (Vanitallie et al., 2005). A ketogenic diet increased serum BHB (ketone) levels and reduced β -amyloid plaques in a mouse model of Alzheimers disease models, with no changes in behaviour (Van der Auwera et al., 2005). Finally, the MCT ketogenic diet may be beneficial in ischemia by reducing oxidative stress, excitotoxicity and apoptosis (Shaafi et al., 2014). Future research into the use of MCTs for these conditions may provide important advances in therapy for neurological diseases and cancers. There have been 11 clinical trials of the ketogenic diet in cancer, and multiple pre-clinical studies showing delayed tumour growth using *in vivo* models of glioma, colon cancer, liver cancer, gastric cancer and prostate cancer (Hao et al., 2015; Cay et al., 1992; Otto et al., 2008). The first trial using MCT oil for two children with advanced

stage astrocytomas showed a reduction in glucose uptake at the tumour site; and disease progression was halted in one patient, even after 12 months (Nebeling et al., 1995). This may be beneficial by a different mechanism to the seizure-inhibiting actions of MCT oil, such as by reducing the energy supply to cancer cells.

8.8 Conclusions and Perspectives

AMPA receptors are crucial for the spread of seizures. Excessive activity dynamically alters synaptic expression of AMPA receptors at pyramidal neuron synapses by allowing transient expression of CP-AMPA receptors after NMDA receptor activation.

Inhibition of CP-AMPA receptors alone is not able to inhibit epileptiform discharges in a slice model. However, fatty acid molecules based on the MCT ketogenic diet are able to inhibit seizure-like activity and act as non-competitive AMPA receptor antagonists. These compounds show polypharmacology, as is common among antiepileptic agents, and also reduce intrinsic excitability by reducing I_{NaP} .

“Sounded like a load of waffle to me.”

“There was some important stuff hidden in the waffle.”

- JK Rowling, *Harry Potter and the Order of the Phoenix*

Appendix

	control aCSF (n=9)	0-Mg ²⁺ aCSF (n=11)	control aCSF (n=10)	PTZ-aCSF (n=11)
Bath temperature/ ° C	31.9 ± 0.1	29.1 ± 1.2	31.8 ± 0.1	32.3 ± 0.3
Membrane capacitance/ pF	25.3 ± 3.6	23.7 ± 2.7	26.6 ± 3.2	19.0 ± 1.6
Stimulation intensity/ pA	195 ± 103	180 ± 82	86 ± 36	56 ± 33
Series resistance/ MΩ	11.5 ± 1.6	13.0 ± 1.2	10.6 ± 0.7	11.2 ± 1.2
Series resistance compensation/ %	66 ± 2	28 ± 8	73 ± 3	61 ± 7
Input resistance/ MΩ	166 ± 30	145 ± 10	145 ± 33	214 ± 41
Reversal potential/ mV	0.06 ± 1.3	7.3 ± 2.5	0.1 ± 0.8	2.4 ± 1.0

TABLE 8.1: Supplementary information: Neuronal properties compared between treatment groups in slice models of status epilepticus.

	control aCSF	+ DMSO	washout	AB sig. (p<0.05)
RMP /mV	-63.0 ± 3.2	-63.0 ± 3.3	-64.0 ± 4.7	-
Rheobase /norm.	1	0.93 ± 0.16	0.93 ± 0.16	-
Spike amplitude /mV	92.5 ± 5.3	93.6 ± 4.7	91.9 ± 3.7	-
Inter-event interval /ms	30.4 ± 7.4	35.0 ± 10.3	35.3 ± 9.8	-
R _{input} /norm.	1	1.07 ± 0.13	1.18 ± 0.29	-
Rise time /ms	0.93 ± 0.08	0.93 ± 0.08	0.91 ± 0.10	-
Half width /norm.	1	1.13 ± 0.15	0.88 ± 0.24	-
Decay time /ms	1	1.12 ± 0.07	0.91 ± 0.25	-

	control aCSF	+ decanoic acid	washout	AB sig. (p<0.05)
RMP /mV	-62.2 ± 2.0	-63.4 ± 1.9	-62.4 ± 1.5	-
Rheobase /norm.	1	1.9 ± 0.5	1.4 ± 0.2	+
Spike amplitude /mV	96.9 ± 2.5	96.8 ± 1.4	95.0 ± 1.3	-
Inter-event interval /ms	43.6 ± 11.6	48.6 ± 10.9	40.4 ± 10.6	-
R _{input} /norm.	1	0.99 ± 0.11	1.02 ± 0.06	-
Rise time /ms	1.01 ± 0.01	1.01 ± 0.01	1.00 ± 0.01	-
Half width /norm.	1	1.43 ± 0.27	1.27 ± 0.16	+
Decay time /ms	1	1.31 ± 0.12	1.31 ± 0.16	-

TABLE 8.2: Supplementary information: Neuron properties and action potentials compared in the presence of decanoic acid

Significant change in rheobase and half width with 300 μ M decanoic acid compared to control. RMP = resting membrane potential (mV), rheobase = current injection to reach action potential threshold (pA), R_{input} = Input resistance (M Ω)

Cell no.	R_{access} (M Ω)	C_m (pF)	R_{input} (M Ω)	RMP (mV)	AP threshold (mV)	Rheobase (pA)	V_{peak} (mV)
1	8.3	30.2	120				
2	8.2	42	122				
3	7.75	12.12	200				
4	8.2	17.4	166				
5	12.4	10.7	166				
6	12.8	6.5	71				
7	16	13.8	250				
8	9.7	19.34	133.9	-72.8			
9	9	18.9	40	-74.7	-55	200	32
10	11.9	18.45	71				
11	11		200	-67	-40	120	22
12	10.3		125	-83			

TABLE 8.3: Supplementary information: Properties of neurons patched from human surgically resected tissue.

R_{access} = access resistance (M Ω), C_m = membrane capacitance (pF) gives an indication of cell size, R_{input} = input resistance (M Ω), RMP = resting membrane potential (mV), rheobase = current injection to reach action potential voltage threshold (pA)

References

- Abraham, W. C. and Bear, M. F. (1996). Metaplasticity: the plasticity of synaptic plasticity. *Trends in Neurosciences*, 19(4):126–130.
- Abrahamsson, T., Cathala, L., Matsui, K., Shigemoto, R., and Digregorio, D. A. (2012). Thin dendrites of cerebellar interneurons confer sublinear synaptic integration and a gradient of short-term plasticity. *Neuron*, 73(6):1159–1172.
- Adotevi, N. K. and Leitch, B. (2016). Alterations in AMPA receptor subunit expression in cortical inhibitory interneurons in the epileptic stargazer mutant mouse. *Neuroscience*, 339:124–138.
- Agrawal, N., Alonso, A., and Ragsdale, D. S. (2003). Increased persistent sodium currents in rat entorhinal cortex layer v neurons in a poststatus epilepticus model of temporal lobe epilepsy. *Epilepsia*, 44(12):1601–1604.
- Ahmadian, G., Ju, W., Liu, L., Wyszynski, M., Lee, S. H., Dunah, A. W., Taghibiglou, C., Wang, Y., Lu, J., Wong, T. P., Sheng, M., and Wang, Y. T. (2004). Tyrosine phosphorylation of GluR2 is required for insulin-stimulated AMPA receptor endocytosis and LTD. *The EMBO Journal*, 23(5):1040–1050.
- Alford, S., Frenguelli, B. G., Schofield, J. G., and Collingridge, G. L. (1993). Characterization of Ca^{2+} signals induced in hippocampal CA1 neurones by the synaptic activation of NMDA receptors. *The Journal of Physiology*, 469:693–716.
- Ambros-Ingerson, J., Xiao, P., Larson, J., and Lynch, G. (1993). Waveform analysis suggests that LTP alters the kinetics of synaptic receptor channels. *Brain Research*, 620(2):237–244.
- Andersen, P. (2007). *The Hippocampus Book*. Oxford Neuroscience Series. Oxford University Press, USA.

- Anggono, V. and Huganir, R. L. (2012). Regulation of AMPA receptor trafficking and synaptic plasticity. *Current Opinion in Neurobiology*, 22(3):461–469.
- Aracri, P., Colombo, E., Mantegazza, M., Scalmani, P., Curia, G., Avanzini, G., and Franceschetti, S. (2006). Layer-specific properties of the persistent sodium current in sensorimotor cortex. *Journal of Neurophysiology*, 95(6):3460–3468.
- Arai, A. C. (2001). GYKI 52466 has positive modulatory effects on AMPA receptors. *Brain Research*, 892(2):396–400.
- Araki, Y., Lin, D.-T., and Huganir, R. L. (2010). Plasma membrane insertion of the AMPA receptor GluA2 subunit is regulated by NSF binding and Q/R editing of the ion pore. *Proceedings of the National Academy of Sciences of the United States of America*, 107(24):11080–11085.
- Asrar, S., Zhou, Z., Ren, W., and Jia, Z. (2009). Ca⁽²⁺⁾ permeable AMPA receptor induced long-term potentiation requires PI3/MAP kinases but not Ca/CaM-dependent kinase II. *PLOS One*, 4(2):243–339.
- Ballou, L. M., Lin, R. Z., and Cohen, I. S. (2015). Control of cardiac repolarization by phosphoinositide 3-kinase signaling to ion channels. *Circulation Research*, 116(1):127–137.
- Banke, T. G., Bowie, D., Lee, H., Huganir, R. L., Schousboe, A., and Traynelis, S. F. (2000). Control of GluR1 AMPA receptor function by cAMP-dependent protein kinase. *The Journal of Neuroscience*, 20(1):89–102.
- Bar-Yehuda, D. and Korngreen, A. (2008). Space-clamp problems when voltage clamping neurons expressing voltage-gated conductances. *Journal of Neurophysiology*, 99(3):1127–1136.
- Barad, Z., Shevtsova, O., Arbuthnott, G. W., and Leitch, B. (2012). Selective loss of AMPA receptors at corticothalamic synapses in the epileptic stargazer mouse. *Neuroscience*, 217:19–31.
- Barygin, O. I. (2016). Inhibition of calcium-permeable and calcium-impermeable AMPA receptors by perampanel in rat brain neurons. *Neuroscience Letters*, 633:146–151.

- Basello, D. A. and Scovassi, A. I. (2015). Poly(ADP-ribosylation) and neurodegenerative disorders. *Mitochondrion*, 24:56–63.
- Bats, C., Farrant, M., and Cull-Candy, S. G. (2013). A role of TARPs in the expression and plasticity of calcium-permeable AMPARs: Evidence from cerebellar neurons and glia. *Neuropharmacology*, 74:76–85.
- Beattie, E. C., Carroll, R. C., Yu, X., Morishita, W., Yasuda, H., von Zastrow, M., and Malenka, R. C. (2000). Regulation of AMPA receptor endocytosis by a signaling mechanism shared with LTD. *Nature Neuroscience*, 3(12):1291–1300.
- Behr, J., Lyson, K. J., and Mody, I. (1998). Enhanced propagation of epileptiform activity through the kindled dentate gyrus. *Journal of Neurophysiology*, 79(4):1726–1732.
- Beique, J.-C., Na, Y., Kuhl, D., Worley, P. F., and Huganir, R. L. (2011). Arc-dependent synapse-specific homeostatic plasticity. *Proceedings of the National Academy of Sciences of the United States of America*, 108(2):816–821.
- Bengzon, J., Kokaia, Z., Elmr, E., Nanobashvili, A., Kokaia, M., and Lindvall, O. (1997). Apoptosis and proliferation of dentate gyrus neurons after single and intermittent limbic seizures. *Proceedings of the National Academy of Sciences of the United States of America*, 94(19):10432–10437.
- Benke, T. A., Luthi, A., Isaac, J. T. R., and Collingridge, G. L. (1998). Modulation of AMPA receptor unitary conductance by synaptic activity. *Nature*, 393(6687):793–797.
- Benke, T. A., luthi, A., Palmer, M. J., Wikstrom, M. A., Anderson, W. W., Isaac, J. T., and Collingridge, G. L. (2001). Mathematical modelling of non-stationary fluctuation analysis for studying channel properties of synaptic AMPA receptors. *The Journal of Physiology*, 537(Pt 2):407–420.
- Bi, R., Rong, Y., Bernard, A., Khrestchatisky, M., and Baudry, M. (2000). Src-mediated tyrosine phosphorylation of NR2 subunits of N-methyl-D-aspartate receptors protects from calpain-mediated truncation of their C-terminal domains. *The Journal of Biological Chemistry*, 275(34):26477–26483.
- Bialer, M. and White, H. S. (2010). Key factors in the discovery and development of new antiepileptic drugs. *Nature Reviews. Drug Discovery*, 9(1):68–82.

- Binder, D. K. and Steinhuser, C. (2006). Functional changes in astroglial cells in epilepsy. *Glia*, 54(5):358–368.
- Bischofberger, J., Engel, D., Li, L., Geiger, J. R., and Jonas, P. (2006). Patch-clamp recording from mossy fiber terminals in hippocampal slices. *Nature Protocols*, 1(4):2075–2081.
- Blanco-Suarez, E. and Hanley, J. G. (2014). Distinct subunit-specific α -Amino-3-hydroxy-5-methyl-4-isoxazolepropionic acid (AMPA) receptor trafficking mechanisms in cultured cortical and hippocampal neurons in response to oxygen and glucose deprivation. *Journal of Biological Chemistry*, 289(8):4644–4651.
- Blumcke, I., Beck, H., Nitsch, R., Eickhoff, C., Scheffler, B., Celio, M. R., Schramm, J., Elger, C. E., Wolf, H. K., and Wiestler, O. D. (1996a). Preservation of calretinin-immunoreactive neurons in the hippocampus of epilepsy patients with Ammon’s horn sclerosis. *Journal of Neuropathology and Experimental Neurology*, 55(3):329–341.
- Blumcke, I., Beck, H., Scheffler, B., Hof, P. R., Morrison, J. H., Wolf, H. K., Schramm, J., Elger, C. E., and Wiestler, O. D. (1996b). Altered distribution of the α -amino-3-hydroxy-5-methyl-4-isoxazole propionate receptor subunit GluR2(4) and the N-methyl-D-aspartate receptor subunit NMDAR1 in the hippocampus of patients with temporal lobe epilepsy. *Acta Neuropathologica*, 92(6):576–587.
- Blumcke, I., Schewe, J. C., Normann, S., Brustle, O., Schramm, J., Elger, C. E., and Wiestler, O. D. (2001). Increase of nestin-immunoreactive neural precursor cells in the dentate gyrus of pediatric patients with early-onset temporal lobe epilepsy. *Hippocampus*, 11(3):311–321.
- Blumenfeld, H., Lampert, A., Klein, J. P., Mission, J., Chen, M. C., Rivera, M., Dib-Hajj, S., Brennan, A. R., Hains, B. C., and Waxman, S. G. (2009). Role of hippocampal sodium channel Na_v1.6 in kindling epileptogenesis. *Epilepsia*, 50(1):44–55.
- Bojic, U., Elmazar, M. M., Hauck, R. S., and Nau, H. (1996). Further branching of valproate-related carboxylic acids reduces the teratogenic activity, but not the anticonvulsant effect. *Chemical Research in Toxicology*, 9(5):866–870.
- Bowie, D. (2012). Redefining the classification of AMPA-selective ionotropic glutamate receptors. *The Journal of Physiology*, 590(1):49–61.

- Bowie, D., Lange, G. D., and Mayer, M. L. (1998). Activity-dependent modulation of glutamate receptors by polyamines. *The Journal of Neuroscience*, 18(20):8175–8185.
- Braithwaite, S. P., Xia, H., and Malenka, R. C. (2002). Differential roles for NSF and GRIP/ABP in AMPA receptor cycling. *Proceedings of the National Academy of Sciences of the United States of America*, 99(10):7096–7101.
- Bredt, D. S. and Nicoll, R. A. (2003). AMPA receptor trafficking at excitatory synapses. *Neuron*, 40(2):361–379.
- Briggs, S. W., Walker, J., Asik, K., Lombroso, P., Naegele, J., and Aaron, G. (2011). STEP regulation of seizure thresholds in the hippocampus. *Epilepsia*, 52(3):497–506.
- Brockie, P. J., Jensen, M., Mellem, J. E., Jensen, E., Yamasaki, T., Wang, R., Maxfield, D., Thacker, C., Hoerndli, F., Dunn, P. J., Tomita, S., Madsen, D. M., and Maricq, A. V. (2013). Cornichons control ER export of AMPA receptors to regulate synaptic excitability. *Neuron*, 80(1):129–142.
- Burbidge, S. A., Dale, T. J., Powell, A. J., Whitaker, W. R. J., Xie, X. M., Romanos, M. A., and Clare, J. J. (2002). Molecular cloning, distribution and functional analysis of the Na_v1.6 voltage-gated sodium channel from human brain. *Brain Research. Molecular Brain Research*, 103(1-2):80–90.
- Butler, J. L. and Paulsen, O. (2015). Hippocampal network oscillations- recent insights from in vitro experiments. *Current Opinion in Neurobiology*, 31:40–44.
- Carnevale, N. and Hines, M. (2006). *The NEURON book*. Cambridge University Press, Cambridge, UK.
- Carroll, R. C., Beattie, E. C., Xia, H., Luscher, C., Altschuler, Y., Nicoll, R. A., Malenka, R. C., and von Zastrow, M. (1999). Dynamin-dependent endocytosis of ionotropic glutamate receptors. *Proceedings of the National Academy of Sciences of the United States of America*, 96(24):14112–14117.
- Carter, B. C., Giessel, A. J., Sabatini, B. L., and Bean, B. P. (2012). Transient sodium current at subthreshold voltages: activation by EPSP waveforms. *Neuron*, 75(6):1081–1093.

- Carter, D. S., Harrison, A. J., Falenski, K. W., Blair, R. E., and DeLorenzo, R. J. (2008). Long-term decrease in calbindin-D28k expression in the hippocampus of epileptic rats following pilocarpine-induced status epilepticus. *Epilepsy Research*, 79(2-3):213–223.
- Cay, O., Radnell, M., Jeppsson, B., Ahrn, B., and Bengmark, S. (1992). Inhibitory effect of 2-deoxy-D-glucose on liver tumor growth in rats. *Cancer Research*, 52(20):5794–5796.
- Chang, P., Augustin, K., Boddum, K., Williams, S., Sun, M., Terschak, J. A., Hardege, J. D., Chen, P. E., Walker, M. C., and Williams, R. S. B. (2016). Seizure control by decanoic acid through direct AMPA receptor inhibition. *Brain: A Journal of Neurology*, 139(Pt 2):431–443.
- Chang, P., Orabi, B., Deranieh, R. M., Dham, M., Hoeller, O., Shimshoni, J. A., Yagen, B., Bialer, M., Greenberg, M. L., Walker, M. C., and Williams, R. S. B. (2012). The antiepileptic drug valproic acid and other medium-chain fatty acids acutely reduce phosphoinositide levels independently of inositol in Dictyostelium. *Disease Models & Mechanisms*, 5(1):115–124.
- Chang, P., Terbach, N., Plant, N., Chen, P. E., Walker, M. C., and Williams, R. S. (2013). Seizure control by ketogenic diet-associated medium chain fatty acids. *Neuropharmacology*, 69(100):105–114.
- Chang, P., Walker, M. C., and Williams, R. S. B. (2014). Seizure-induced reduction in PIP3 levels contributes to seizure-activity and is rescued by valproic acid. *Neurobiology of Disease*, 62:296–306.
- Chang, P., Zuckermann, A. M. E., Williams, S., Close, A. J., Cano-Jaimez, M., McEvoy, J. P., Spencer, J., Walker, M. C., and Williams, R. S. B. (2015). Seizure control by derivatives of medium chain fatty acids associated with the ketogenic diet show novel branching-point structure for enhanced potency. *Journal of Pharmacology and Experimental Therapeutics*, 352(1):43–52.
- Chatelier, A., Zhao, J., Bois, P., and Chahine, M. (2010). Biophysical characterisation of the persistent sodium current of the Na_v1.6 neuronal sodium channel: a single-channel analysis. *Pflügers Archiv: European Journal of Physiology*, 460(1):77–86.
- Chen, B., Feng, B., Tang, Y., You, Y., Wang, Y., Hou, W., Hu, W., and Chen, Z. (2016). Blocking GluN2b subunits reverses the enhanced seizure susceptibility after prolonged

- febrile seizures with a wide therapeutic time-window. *Experimental Neurology*, 283(Pt A):29–38.
- Chen, L., El-Husseini, A., Tomita, S., Bredt, D. S., and Nicoll, R. A. (2003). Stargazin differentially controls the trafficking of α -amino-3-hydroxyl-5-methyl-4-isoxazolepropionate and kainate receptors. *Molecular Pharmacology*, 64(3):703–706.
- Chen, R.-Q., Wang, S.-H., Yao, W., Wang, J.-J., Ji, F., Yan, J.-Z., Ren, S.-Q., Chen, Z., Liu, S.-Y., and Lu, W. (2011). Role of glycine receptors in glycine-induced LTD in hippocampal CA1 pyramidal neurons. *Neuropsychopharmacology*, 36(9):1948–1958.
- Chen, S.-R., Zhou, H.-Y., Byun, H. S., and Pan, H.-L. (2013). Nerve injury increases GluA2-lacking AMPA receptor prevalence in spinal cords: functional significance and signaling mechanisms. *Journal of Pharmacology and Experimental Therapeutics*, 347(3):765–772.
- Chung, H. J., Xia, J., Scannevin, R. H., Zhang, X., and Huganir, R. L. (2000). Phosphorylation of the AMPA receptor subunit GluR2 differentially regulates its interaction with PDZ domain-containing proteins. *The Journal of Neuroscience*, 20(19):7258–7267.
- Citraro, R., Aiello, R., Franco, V., Sarro, G. D., and Russo, E. (2014). Targeting α -amino-3-hydroxyl-5-methyl-4-isoxazole-propionate receptors in epilepsy. *Expert Opinion on Therapeutic Targets*, 18(3):319–334.
- Clayton, E. L., Evans, G. J. O., and Cousin, M. A. (2007). Activity-dependent control of bulk endocytosis by protein dephosphorylation in central nerve terminals. *The Journal of Physiology*, 585(Pt 3):687–691.
- Clem, R. L. and Barth, A. (2006). Pathway-specific trafficking of native AMPARs by in vivo experience. *Neuron*, 49(5):663–670.
- Coan, E. J. and Collingridge, G. L. (1985). Magnesium ions block an N-methyl-D-aspartate receptor-mediated component of synaptic transmission in rat hippocampus. *Neuroscience Letters*, 53(1):21–26.
- Collingridge, G. L., Isaac, J. T. R., and Wang, Y. T. (2004). Receptor trafficking and synaptic plasticity. *Nature Reviews Neuroscience*, 5(12):952–962.

- Colom, L. V. and Saggau, P. (1994). Spontaneous interictal-like activity originates in multiple areas of the CA2-CA3 region of hippocampal slices. *Journal of Neurophysiology*, 71(4):1574–1585.
- Colombo, E., Franceschetti, S., Avanzini, G., and Mantegazza, M. (2013). Phenytoin inhibits the persistent sodium current in neocortical neurons by modifying its inactivation properties. *PLOS One*, 8(1):e55329.
- Condorelli, D. F., Belluardo, N., Mud, G., Dell’Albani, P., Jiang, X., and Giuffrida-Stella, A. M. (1994). Changes in gene expression of AMPA-selective glutamate receptor subunits induced by status epilepticus in rat brain. *Neurochemistry International*, 25(4):367–376.
- Constals, A., Penn, A. C., Compans, B., Toulm, E., Phillipat, A., Marais, S., Retailleau, N., Hafner, A.-S., Coussen, F., Hosy, E., and Choquet, D. (2015). Glutamate-induced AMPA receptor desensitization increases their mobility and modulates short-term plasticity through unbinding from Stargazin. *Neuron*, 85(4):787–803.
- Coombs, I. D., Soto, D., Zonouzi, M., Renzi, M., Shelley, C., Farrant, M., and Cull-Candy, S. G. (2012). Cornichons modify channel properties of recombinant and glial AMPA receptors. *The Journal of Neuroscience*, 32(29):9796–9804.
- Cossart, R., Bernard, C., and Ben-Ari, Y. (2005). Multiple facets of GABAergic neurons and synapses: multiple fates of GABA signalling in epilepsies. *Trends in Neurosciences*, 28(2):108–115.
- Crill, W. E. (1996). Persistent sodium current in mammalian central neurons. *Annual Review of Physiology*, 58:349–362.
- Cross, J. H., McLellan, A., Neal, E. G., Philip, S., Williams, E., and Williams, R. E. (2010). The ketogenic diet in childhood epilepsy: where are we now? *Archives of Disease in Childhood*, 95(7):550–553.
- Cuadra, A. E., Kuo, S.-H., Kawasaki, Y., Brecht, D. S., and Chetkovich, D. M. (2004). AMPA receptor synaptic targeting regulated by stargazin interactions with the Golgi-resident PDZ protein nPIST. *The Journal of Neuroscience*, 24(34):7491–7502.
- Cui, J., Zhang, M., Zhang, Y.-Q., and Xu, Z.-H. (2007). JNK pathway: diseases and therapeutic potential. *Acta Pharmacologica Sinica*, 28(5):601–608.

- Cull-Candy, S., Kelly, L., and Farrant, M. (2006). Regulation of Ca²⁺-permeable AMPA receptors: synaptic plasticity and beyond. *Current Opinion in Neurobiology*, 16(3):288–297.
- Cummins, T. R., Xia, Y., and Haddad, G. G. (1994). Functional properties of rat and human neocortical voltage-sensitive sodium currents. *Journal of Neurophysiology*, 71(3):1052–1064.
- Cunningham, M. O., Roopun, A., Schofield, I. S., Whittaker, R. G., Duncan, R., Russell, A., Jenkins, A., Nicholson, C., Whittington, M. A., and Traub, R. D. (2012). Glissandi: transient fast electrocorticographic oscillations of steadily increasing frequency, explained by temporally increasing gap junction conductance. *Epilepsia*, 53(7):1205–1214.
- Curia, G., Aracri, P., Colombo, E., Scalmani, P., Mantegazza, M., Avanzini, G., and Franceschetti, S. (2007). Phosphorylation of sodium channels mediated by protein kinase-C modulates inhibition by topiramate of tetrodotoxin-sensitive transient sodium current. *British Journal of Pharmacology*, 150(6):792–797.
- Danzer, S. C., He, X., and McNamara, J. O. (2004). Ontogeny of seizure-induced increases in BDNF immunoreactivity and TrkB receptor activation in rat hippocampus. *Hippocampus*, 14(3):345–355.
- de Curtis, M., Jefferys, J. G. R., and Avoli, M. (2012). Interictal epileptiform discharges in partial epilepsy: complex neurobiological mechanisms based on experimental and clinical evidence. In Noebels, J. L., Avoli, M., Rogawski, M. A., Olsen, R. W., and Delgado-Escueta, A. V., editors, *Jasper’s Basic Mechanisms of the Epilepsies*. National Center for Biotechnology Information (US), Bethesda (MD), 4th edition.
- Deb, I., Manhas, N., Poddar, R., Rajagopal, S., Allan, A. M., Lombroso, P. J., Rosenberg, G. A., Candelario-Jalil, E., and Paul, S. (2013). Neuroprotective role of a brain-enriched tyrosine phosphatase, STEP, in focal cerebral ischemia. *The Journal of Neuroscience*, 33(45):17814–17826.
- DeFelipe, J., Alonso-Nanclares, L., and Arellano, J. I. (2002). Microstructure of the neocortex: Comparative aspects. *Journal of Neurocytology*, 31(3-5):299–316.
- Delgado, J. Y., Coba, M., Anderson, C. N. G., Thompson, K. R., Gray, E. E., Heusner, C. L., Martin, K. C., Grant, S. G. N., and O’Dell, T. J. (2007). NMDA receptor activation

- dephosphorylates AMPA receptor glutamate receptor 1 subunits at Threonine 840. *The Journal of Neuroscience*, 27(48):13210–13221.
- Derkach, V., Barria, A., and Soderling, T. R. (1999). Ca^{2+} /calmodulin-kinase II enhances channel conductance of α -amino-3-hydroxy-5-methyl-4-isoxazolepropionate type glutamate receptors. *Proceedings of the National Academy of Sciences of the United States of America*, 96(6):3269–3274.
- Derkach, V. A., Oh, M. C., Guire, E. S., and Soderling, T. R. (2007). Regulatory mechanisms of AMPA receptors in synaptic plasticity. *Nature Reviews Neuroscience*, 8(2):101–113.
- Di Maio, R., Mastroberardino, P. G., Hu, X., Montero, L., and Greenamyre, J. T. (2011). Pilocarpine alters NMDA receptor expression and function in hippocampal neurons: NADPH oxidase and ERK1/2 mechanisms. *Neurobiology of Disease*, 42(3):482–495.
- Dias, R. B., Rombo, D. M., Ribeiro, J. A., and Sebastiao, A. M. (2013). Ischemia-induced synaptic plasticity drives sustained expression of calcium-permeable AMPA receptors in the hippocampus. *Neuropharmacology*, 65:114–122.
- Dineley, K. E., Votyakova, T. V., and Reynolds, I. J. (2003). Zinc inhibition of cellular energy production: implications for mitochondria and neurodegeneration. *Journal of Neurochemistry*, 85(3):563–570.
- Doczi, J., Banczerowski-Pelyhe, I., Barna, B., and Vilagi, I. (1999). Effect of a glutamate receptor antagonist (GYKI 52466) on 4-aminopyridine-induced seizure activity developed in rat cortical slices. *Brain Research Bulletin*, 49(6):435–440.
- Dogini, D. B., Avansini, S., Schwambach Vieira, A., and Lopes-Cendes, I. (2013). MicroRNA regulation and dysregulation in epilepsy. *Frontiers in Cellular Neuroscience*, 7:172.
- Donevan, S. D. and Rogawski, M. A. (1993). GYKI 52466, a 2,3-benzodiazepine, is a highly selective, noncompetitive antagonist of AMPA/kainate receptor responses. *Neuron*, 10(1):51–59.
- Dossi, E., Blauwblomme, T., Nabbout, R., Huberfeld, G., and Rouach, N. (2014). Multi-electrode array recordings of human epileptic postoperative cortical tissue. *Journal of Visualized Experiments : JoVE*, (92).

- Dutta, R., Chomyk, A. M., Chang, A., Ribaldo, M. V., Deckard, S. A., Doud, M. K., Edberg, D. D., Bai, B., Li, M., Baranzini, S. E., Fox, R. J., Staugaitis, S. M., Macklin, W. B., and Trapp, B. D. (2013). Hippocampal demyelination and memory dysfunction are associated with increased levels of the neuronal microRNA miR-124 and reduced AMPA receptors. *Annals of Neurology*, 73(5):637–645.
- Eckel, R., Szulc, B., Walker, M. C., and Kittler, J. T. (2014). Activation of calcineurin underlies altered trafficking of $\alpha 2$ subunit containing GABA_A receptors during prolonged epileptiform activity. *Neuropharmacology*, 88:82–90.
- Ehlers, M. D. (2000). Reinsertion or degradation of AMPA receptors determined by activity-dependent endocytic sorting. *Neuron*, 28(2):511–525.
- Einevoll, G. T., Kayser, C., Logothetis, N. K., and Panzeri, S. (2013). Modelling and analysis of local field potentials for studying the function of cortical circuits. *Nature Reviews. Neuroscience*, 14(11):770–785.
- Ekonomou, A., Smith, A. L., and Angelatou, F. (2001). Changes in AMPA receptor binding and subunit messenger RNA expression in hippocampus and cortex in the pentylenetetrazole-induced 'kindling' model of epilepsy. *Brain Research. Molecular Brain Research*, 95(1-2):27–35.
- Fox, C., Russell, K., Titterness, A., Yu, T., and Christie, B. (2007). Tyrosine phosphorylation of the GluR2 subunit is required for long-term depression of synaptic efficacy in young animals in vivo. *Hippocampus*, 17(8):600–605.
- Frampton, J. E. (2015). Perampanel: A review in drug-resistant epilepsy. *Drugs*, 75(14):1657–1668.
- Francis, J., Jugloff, D. G., Mingo, N. S., Wallace, M. C., Jones, O. T., Burnham, W. M., and Eubanks, J. H. (1997). Kainic acid-induced generalized seizures alter the regional hippocampal expression of the rat K_v4.2 potassium channel gene. *Neuroscience Letters*, 232(2):91–94.
- Frerking, M., Malenka, R. C., and Nicoll, R. A. (1998). Synaptic activation of kainate receptors on hippocampal interneurons. *Nature Neuroscience*, 1(6):479–486.

- Freund, T. and Buzsaki, G. (1996). Interneurons of the hippocampus. *Hippocampus*, 6(4):347–470.
- Friedman, L. K. (2006). Calcium: a role for neuroprotection and sustained adaptation. *Molecular Interventions*, 6(6):315–329.
- Friedman, L. K., Pellegrini-Giampietro, D. E., Sperber, E. F., Bennett, M. V., Mosh, S. L., and Zukin, R. S. (1994). Kainate-induced status epilepticus alters glutamate and GABA_A receptor gene expression in adult rat hippocampus: an in situ hybridization study. *The Journal of Neuroscience*, 14(5 Pt 1):2697–2707.
- Friedman, L. K., Saghyan, A., Peinado, A., and Keeseey, R. (2008). Age- and region-dependent patterns of Ca²⁺ accumulations following status epilepticus. *International Journal of Developmental Neuroscience: The Official Journal of the International Society for Developmental Neuroscience*, 26(7):779–790.
- Fritsch, G. (1870). *Ueber Die Elektrische Erregbarkeit Des Grosshirns*, volume 37. Arch Anat Physiol Wissen.
- Gan, Q., Salussolia, C. L., and Wollmuth, L. P. (2014). Assembly of AMPA receptors: mechanisms and regulation. *The Journal of Physiology*, 593(Pt 1):39–48.
- Gano, L. B., Patel, M., and Rho, J. M. (2014). Ketogenic diets, mitochondria, and neurological diseases. *Journal of Lipid Research*, 55(11):2211–2228.
- Gardinier, K. M., Gernert, D. L., Porter, W. J., Reel, J. K., Ornstein, P. L., Spinazze, P., Stevens, F. C., Hahn, P., Hollinshead, S. P., Mayhugh, D., Schkeryantz, J., Khilevich, A., De Frutos, O., Gleason, S. D., Kato, A. S., Luffer-Atlas, D., Desai, P. V., Swanson, S., Burris, K. D., Ding, C., Heinz, B. A., Need, A. B., Barth, V. N., Stephenson, G. A., Diseroad, B. A., Woods, T. A., Yu, H., Breddt, D., and Witkin, J. M. (2016). Discovery of the first α -amino-3-hydroxy-5-methyl-4-isoxazolepropionic acid (AMPA) receptor antagonist dependent upon transmembrane AMPA receptor regulatory protein (TARP) γ -8. *Journal of Medicinal Chemistry*, 59(10):4753–4768.
- Gardner, S. M., Takamiya, K., Xia, J., Suh, J.-G., Johnson, R., Yu, S., and Haganir, R. L. (2005). Calcium-permeable AMPA receptor plasticity is mediated by subunit-specific interactions with PICK1 and NSF. *Neuron*, 45(6):903–915.

- Geiger, J. R., Melcher, T., Koh, D. S., Sakmann, B., Seeburg, P. H., Jonas, P., and Monyer, H. (1995). Relative abundance of subunit mRNAs determines gating and Ca^{2+} permeability of AMPA receptors in principal neurons and interneurons in rat CNS. *Neuron*, 15(1):193–204.
- Gerace, E., Masi, A., Resta, F., Felici, R., Landucci, E., Mello, T., Pellegrini-Giampietro, D. E., Mannaioni, G., and Moroni, F. (2014). PARP-1 activation causes neuronal death in the hippocampal CA1 region by increasing the expression of Ca^{2+} -permeable AMPA receptors. *Neurobiology of Disease*, 70:43–52.
- Goldfarb, M. (2011). Voltage-gated sodium channel-associated proteins and alternative mechanisms of inactivation and block. *Cellular and Molecular Life Sciences*, 69(7):1067–1076.
- Gorter, J. A., Petrozzino, J. J., Aronica, E. M., Rosenbaum, D. M., Opitz, T., Bennett, M. V., Connor, J. A., and Zukin, R. S. (1997). Global ischemia induces downregulation of Glur2 mRNA and increases AMPA receptor-mediated Ca^{2+} influx in hippocampal CA1 neurons of gerbil. *The Journal of Neuroscience*, 17(16):6179–6188.
- Gray, E. E., Fink, A. E., Sariana, J., Vissel, B., and O’Dell, T. J. (2007). Long-term potentiation in the hippocampal CA1 region does not require insertion and activation of GluR2-lacking AMPA receptors. *Journal of Neurophysiology*, 98(4):2488–2492.
- Greco, T., Glenn, T. C., Hovda, D. A., and Prins, M. L. (2015). Ketogenic diet decreases oxidative stress and improves mitochondrial respiratory complex activity. *Journal of Cerebral Blood Flow and Metabolism*, 36(9):1603–1613.
- Grooms, S. Y., Opitz, T., Bennett, M. V. L., and Zukin, R. S. (2000). Status epilepticus decreases glutamate receptor 2 mRNA and protein expression in hippocampal pyramidal cells before neuronal death. *Proceedings of the National Academy of Sciences of the United States of America*, 97(7):3631–3636.
- Guire, E. S., Oh, M. C., Soderling, T. R., and Derkach, V. A. (2008). Recruitment of calcium-permeable AMPA receptors during synaptic potentiation is regulated by CaM-Kinase I. *The Journal of Neuroscience*, 28(23):6000–6009.
- Haidukewych, D., Forsythe, W. I., and Sills, M. (1982). Monitoring octanoic and decanoic

- acids in plasma from children with intractable epilepsy treated with medium-chain triglyceride diet. *Clinical Chemistry*, 28(4 Pt 1):642–645.
- Hainmuller, T., Kriegstein, K., Kulik, A., and Bartos, M. (2014). Joint CP-AMPA and group I mGlu receptor activation is required for synaptic plasticity in dentate gyrus fast-spiking interneurons. *Proceedings of the National Academy of Sciences of the United States of America*, 111(36):13211–13216.
- Hajos, N. and Paulsen, O. (2009). Network mechanisms of gamma oscillations in the CA3 region of the hippocampus. *Neural Networks: The Official Journal of the International Neural Network Society*, 22(8):1113–1119.
- Halpain, S., Hipolito, A., and Saffer, L. (1998). Regulation of F-actin stability in dendritic spines by glutamate receptors and calcineurin. *The Journal of Neuroscience*, 18(23):9835–9844.
- Hamill, O., Huguenard, J., and Prince, D. (1991). Patch-clamp studies of voltage-gated currents in identified neurons of the rat cerebral cortex. *Cerebral Cortex*, 1(1):48–61.
- Hanada, T., Hashizume, Y., Tokuhara, N., Takenaka, O., Kohmura, N., Ogasawara, A., Hatakeyama, S., Ohgoh, M., Ueno, M., and Nishizawa, Y. (2011). Perampanel: a novel, orally active, noncompetitive AMPA-receptor antagonist that reduces seizure activity in rodent models of epilepsy. *Epilepsia*, 52(7):1331–1340.
- Hanley, J. G. (2008). PICK1: a multi-talented modulator of AMPA receptor trafficking. *Pharmacology & Therapeutics*, 118(1):152–160.
- Hanley, J. G., Khatri, L., Hanson, P. I., and Ziff, E. B. (2002). NSF ATPase and α -/ β -SNAPs disassemble the AMPA receptor-PICK1 complex. *Neuron*, 34(1):53–67.
- Hao, G.-W., Chen, Y.-S., He, D.-M., Wang, H.-Y., Wu, G.-H., and Zhang, B. (2015). Growth of human colon cancer cells in nude mice is delayed by ketogenic diet with or without omega-3 fatty acids and medium-chain triglycerides. *Asian Pacific Journal of Cancer Prevention*, 16(5):2061–2068.
- Hardingham, G. E., Fukunaga, Y., and Bading, H. (2002). Extrasynaptic NMDARs oppose synaptic NMDARs by triggering CREB shut-off and cell death pathways. *Nature Neuroscience*, 5(5):405–414.

- Hartveit, E. and Veruki, M. L. (2006). Studying properties of neurotransmitter receptors by non-stationary noise analysis of spontaneous synaptic currents. *The Journal of Physiology*, 574(3):751–785.
- Hayashi, T. and Huganir, R. L. (2004). Tyrosine phosphorylation and regulation of the AMPA receptor by Src family tyrosine kinases. *The Journal of Neuroscience*, 24(27):6152–6160.
- Hayashi, Y., Shi, S. H., Esteban, J. A., Piccini, A., Poncer, J. C., and Malinow, R. (2000). Driving AMPA receptors into synapses by LTP and CaMKII: requirement for GluR1 and PDZ domain interaction. *Science (New York, N.Y.)*, 287(5461):2262–2267.
- He, K., Song, L., Cummings, L. W., Goldman, J., Huganir, R. L., and Lee, H.-K. (2009). Stabilization of Ca²⁺-permeable AMPA receptors at perisynaptic sites by GluR1-S845 phosphorylation. *Proceedings of the National Academy of Sciences of the United States of America*, 106(47):20033–20038.
- Henderson, S. T., Vogel, J. L., Barr, L. J., Garvin, F., Jones, J. J., and Costantini, L. C. (2009). Study of the ketogenic agent AC-1202 in mild to moderate Alzheimer’s disease: a randomized, double-blind, placebo-controlled, multicenter trial. *Nutrition & Metabolism*, 6:31.
- Herguedas, B., Garca-Nafra, J., Cais, O., Fernandez-Leiro, R., Krieger, J., Ho, H., and Greger, I. H. (2016). Structure and organization of heteromeric AMPA-type glutamate receptors. *Science (New York, N.Y.)*, 352(6285).
- Ho, M. T.-W., Pelkey, K. A., Topolnik, L., Petralia, R. S., Takamiya, K., Xia, J., Huganir, R. L., Lacaille, J.-C., and McBain, C. J. (2007). Developmental expression of Ca²⁺-permeable AMPA receptors underlies depolarization-induced long-term depression at mossy fiber CA3 pyramid synapses. *The Journal of Neuroscience*, 27(43):11651–11662.
- Hodgkin, A. L. and Huxley, A. F. (1952). A quantitative description of membrane current and its application to conduction and excitation in nerve. *The Journal of Physiology*, 117(4):500–544.
- Hou, Q., Zhang, D., Jarzylo, L., Huganir, R. L., and Man, H.-Y. (2008). Homeostatic regulation of AMPA receptor expression at single hippocampal synapses. *Proceedings of the National Academy of Sciences of the United States of America*, 105(2):775–780.

- Houser, C. R. (1990). Granule cell dispersion in the dentate gyrus of humans with temporal lobe epilepsy. *Brain Research*, 535(2):195–204.
- Howard, M. A., Elias, G. M., Elias, L. A. B., Swat, W., and Nicoll, R. A. (2010). The role of SAP97 in synaptic glutamate receptor dynamics. *Proceedings of the National Academy of Sciences of the United States of America*, 107(8):3805–3810.
- Hu, Y., Jiang, L., Chen, H., and Zhang, X. (2012). Expression of AMPA receptor subunits in hippocampus after status convulsion. *Child's Nervous System*, 28(6):911–918.
- Huang, R. Q., Bell-Horner, C. L., Dibas, M. I., Covey, D. F., Drewe, J. A., and Dillon, G. H. (2001). Pentylentetrazole-induced inhibition of recombinant gamma-aminobutyric acid type A (GABA_A) receptors: mechanism and site of action. *The Journal of Pharmacology and Experimental Therapeutics*, 298(3):986–995.
- Huberfeld, G., Menendez de la Prida, L., Pallud, J., Cohen, I., Le Van Quyen, M., Adam, C., Clemenceau, S., Baulac, M., and Miles, R. (2011). Glutamatergic pre-ictal discharges emerge at the transition to seizure in human epilepsy. *Nature Neuroscience*, 14(5):627–634.
- Huberfeld, G., Wittner, L., Clemenceau, S., Baulac, M., Kaila, K., Miles, R., and Rivera, C. (2007). Perturbed chloride homeostasis and GABAergic signaling in human temporal lobe epilepsy. *The Journal of Neuroscience*, 27(37):9866–9873.
- Hughes, S. D., Kanabus, M., Anderson, G., Hargreaves, I. P., Rutherford, T., Donnell, M. O., Cross, J. H., Rahman, S., Eaton, S., and Heales, S. J. R. (2014). The ketogenic diet component decanoic acid increases mitochondrial citrate synthase and complex I activity in neuronal cells. *Journal of Neurochemistry*, 129(3):426–433.
- Huie, J. R., Stuck, E. D., Lee, K. H., Irvine, K.-A., Beattie, M. S., Bresnahan, J. C., Grau, J. W., and Ferguson, A. R. (2015). AMPA receptor phosphorylation and synaptic colocalization on motor neurons drive maladaptive plasticity below complete spinal cord injury. *eneuro*, 2(5).
- Hume, R. I., Dingledine, R., and Heinemann, S. F. (1991). Identification of a site in glutamate receptor subunits that controls calcium permeability. *Science (New York, N.Y.)*, 253(5023):1028–1031.

- Husson, T. R., Mallik, A. K., Zhang, J. X., and Issa, N. P. (2007). Functional imaging of primary visual cortex using flavoprotein autofluorescence. *The Journal of Neuroscience*, 27(32):8665–8675.
- Huttenlocher, P. R., Wilbourn, A. J., and Signore, J. M. (1971). Medium-chain triglycerides as a therapy for intractable childhood epilepsy. *Neurology*, 21(11):1097–1103.
- Itakura, M., Watanabe, I., Sugaya, T., and Takahashi, M. (2014). Direct association of the unique C-terminal tail of transmembrane AMPA receptor regulatory protein γ -8 with calcineurin. *FEBS Journal*, 281(5):1366–1378.
- Jackson, A. C., Milstein, A. D., Soto, D., Farrant, M., Cull-Candy, S. G., and Nicoll, R. A. (2011). Probing TARP modulation of AMPA receptor conductance with polyamine toxins. *The Journal of Neuroscience*, 31(20):7511–7520.
- Jang, S.-S., Royston, S. E., Lee, G., Wang, S., and Chung, H. J. (2016). Seizure-induced regulations of Amyloid- β , STEP₆₁, and STEP₆₁ substrates involved in hippocampal synaptic plasticity. *Neural Plasticity*, 2016:2123748.
- Jang, S.-S., Royston, S. E., Xu, J., Cavaretta, J. P., Vest, M. O., Lee, K. Y., Lee, S., Jeong, H. G., Lombroso, P. J., and Chung, H. J. (2015). Regulation of STEP₆₁ and tyrosine-phosphorylation of NMDA and AMPA receptors during homeostatic synaptic plasticity. *Molecular Brain*, 8:55.
- Jeong, E. A., Jeon, B. T., Shin, H. J., Kim, N., Lee, D. H., Kim, H. J., Kang, S. S., Cho, G. J., Choi, W. S., and Roh, G. S. (2011). Ketogenic diet-induced peroxisome proliferator-activated receptor- activation decreases neuroinflammation in the mouse hippocampus after kainic acid-induced seizures. *Experimental Neurology*, 232(2):195–202.
- Jones, R. S. G., da Silva, A. B., Whittaker, R. G., Woodhall, G. L., and Cunningham, M. O. (2016). Human brain slices for epilepsy research: Pitfalls, solutions and future challenges. *Journal of Neuroscience Methods*, 260:221–232.
- Ju, W., Morishita, W., Tsui, J., Gaietta, G., Deerinck, T. J., Adams, S. R., Garner, C. C., Tsien, R. Y., Ellisman, M. H., and Malenka, R. C. (2004). Activity-dependent regulation of dendritic synthesis and trafficking of AMPA receptors. *Nature Neuroscience*, 7(3):244–253.

- Kamceva, M., Benedict, J., Nairn, A. C., Lombroso, P. J., Kamceva, M., Benedict, J., Nairn, A. C., and Lombroso, P. J. (2016). Role of striatal-enriched tyrosine phosphatase in neuronal function. *Neural Plasticity, Neural Plasticity*, 2016, 2016:e8136925.
- Kato, A. S., Gill, M. B., Ho, M. T., Yu, H., Tu, Y., Siuda, E. R., Wang, H., Qian, Y.-W., Nisenbaum, E. S., Tomita, S., and Brecht, D. S. (2010). Hippocampal AMPA receptor gating controlled by both TARP and cornichon proteins. *Neuron*, 68(6):1082–1096.
- Kato, A. S., Zhou, W., Milstein, A. D., Knierman, M. D., Siuda, E. R., Dotzlaw, J. E., Yu, H., Hale, J. E., Nisenbaum, E. S., Nicoll, R. A., and Brecht, D. S. (2007). New transmembrane AMPA receptor regulatory protein isoform, γ -7, differentially regulates AMPA receptors. *The Journal of Neuroscience*, 27(18):4969–4977.
- Khosravani, H., Bladen, C., Parker, D. B., Snutch, T. P., McRory, J. E., and Zamponi, G. W. (2005). Effects of Cav3.2 channel mutations linked to idiopathic generalized epilepsy. *Annals of Neurology*, 57(5):745–749.
- Kim, D. Y., Davis, L. M., Sullivan, P. G., Maalouf, M., Simeone, T. A., Brederode, J. v., and Rho, J. M. (2007). Ketone bodies are protective against oxidative stress in neocortical neurons. *Journal of Neurochemistry*, 101(5):1316–1326.
- Kim, D. Y., Simeone, K. A., Simeone, T. A., Pandya, J. D., Wilke, J. C., Ahn, Y., Geddes, J. W., Sullivan, P. G., and Rho, J. M. (2015a). Ketone bodies mediate antiseizure effects through mitochondrial permeability transition. *Annals of Neurology*, 78(1):77–87.
- Kim, J.-E., Kim, Y.-J., Kim, J. Y., and Kang, T.-C. (2014). PARP1 activation/expression modulates regional-specific neuronal and glial responses to seizure in a hemodynamic-independent manner. *Cell Death & Disease*, 5(8):e1362.
- Kim, S., Titcombe, R. F., Zhang, H., Khatri, L., Girma, H. K., Hofmann, F., Arancio, O., and Ziff, E. B. (2015b). Network compensation of cyclic GMP-dependent protein kinase II knockout in the hippocampus by Ca²⁺-permeable AMPA receptors. *Proceedings of the National Academy of Sciences of the United States of America*.
- Kim, S. and Ziff, E. B. (2014). Calcineurin mediates synaptic scaling via synaptic trafficking of Ca²⁺-permeable AMPA receptors. *PLoS biology*, 12(7):e1001900.

- Kinsman, S. L., Vining, E. P., Quaskey, S. A., Mellits, D., and Freeman, J. M. (1992). Efficacy of the ketogenic diet for intractable seizure disorders: review of 58 cases. *Epilepsia*, 33(6):1132–1136.
- Kobayashi, E., Li, L. M., Lopes-Cendes, I., and Cendes, F. (2002). Magnetic resonance imaging evidence of hippocampal sclerosis in asymptomatic, first-degree relatives of patients with familial mesial temporal lobe epilepsy. *Archives of Neurology*, 59(12):1891–1894.
- Kott, S., Sager, C., Tapken, D., Werner, M., and Hollmann, M. (2009). Comparative analysis of the pharmacology of GluR1 in complex with transmembrane AMPA receptor regulatory proteins γ -2, γ -3, γ -4, and γ -8. *Neuroscience*, 158(1):78–88.
- Kovac, S., Domijan, A.-M., Walker, M. C., and Abramov, A. Y. (2012). Prolonged seizure activity impairs mitochondrial bioenergetics and induces cell death. *Journal of Cell Science*, 125(Pt 7):1796–1806.
- Kovac, S., Domijan, A.-M., Walker, M. C., and Abramov, A. Y. (2014). Seizure activity results in calcium- and mitochondria-independent ROS production via NADPH and xanthine oxidase activation. *Cell Death & Disease*, 5:e1442.
- Krestel, H. E., Shimshek, D. R., Jensen, V., Nevian, T., Kim, J., Geng, Y., Bast, T., Depaulis, A., Schonig, K., Schwenk, F., Bujard, H., Hvalby, i., Sprengel, R., and Seeburg, P. H. (2004). A genetic switch for epilepsy in adult mice. *The Journal of Neuroscience*, 24(46):10568–10578.
- Kumar, S. S., Bacci, A., Kharazia, V., and Huguenard, J. R. (2002). A developmental switch of AMPA receptor subunits in neocortical pyramidal neurons. *The Journal of Neuroscience*, 22(8):3005–3015.
- Kurz, J. E., Sheets, D., Parsons, J. T., Rana, A., Delorenzo, R. J., and Churn, S. B. (2001). A significant increase in both basal and maximal calcineurin activity in the rat pilocarpine model of status epilepticus. *Journal of Neurochemistry*, 78(2):304–315.
- Lamsa, K. P., Heeroma, J. H., Somogyi, P., Rusakov, D. A., and Kullmann, D. M. (2007). Anti-Hebbian long-term potentiation in the hippocampal feedback inhibitory circuit. *Science (New York, N.Y.)*, 315(5816):1262–1266.

- Laschet, J., Trottier, S., Leviel, V., Guibert, B., Bansard, J. Y., Chauvel, P., and Bureau, M. (1999). Heterogeneous distribution of polyamines in temporal lobe epilepsy. *Epilepsy Research*, 35(2):161–172.
- Lee, H.-K. (2006). AMPA receptor phosphorylation in synaptic plasticity: insights from knockin mice. In Kittler, J. T. and Moss, S. J., editors, *The Dynamic Synapse: Molecular Methods in Ionotropic Receptor Biology*, Frontiers in Neuroscience. CRC Press/Taylor & Francis, Boca Raton (FL).
- Lee, K. H., Won, R., Kim, U. J., Kim, G. M., Chung, M.-A., Sohn, J.-H., and Lee, B. H. (2010). Neuroprotective effects of FK506 against excitotoxicity in organotypic hippocampal slice culture. *Neuroscience Letters*, 474(3):126–130.
- Lehmkuhle, M. J., Thomson, K. E., Scheerlinck, P., Pouliot, W., Greger, B., and Dudek, F. E. (2009). A simple quantitative method for analyzing electrographic status epilepticus in rats. *Journal of Neurophysiology*, 101(3):1660–1670.
- Lennox, W. G. and Cobb, S. (1928). Epilepsy: From the standpoint of physiology and treatment. *Medicine*, 7(2):105–290.
- Li, W., Xu, X., and Pozzo-Miller, L. (2016). Excitatory synapses are stronger in the hippocampus of Rett syndrome mice due to altered synaptic trafficking of AMPA-type glutamate receptors. *Proceedings of the National Academy of Sciences of the United States of America*, page 201517244.
- Likhodii, S. S., Musa, K., Mendonca, A., Dell, C., Burnham, W. M., and Cunnane, S. C. (2000). Dietary fat, ketosis, and seizure resistance in rats on the ketogenic diet. *Epilepsia*, 41(11):1400–1410.
- Lin, D.-T., Makino, Y., Sharma, K., Hayashi, T., Neve, R., Takamiya, K., and Huganir, R. L. (2009). Regulation of AMPA receptor extrasynaptic insertion by 4.1n, phosphorylation and palmitoylation. *Nature Neuroscience*, 12(7):879–887.
- Lippman-Bell, J. J., Zhou, C., Sun, H., Feske, J. S., and Jensen, F. E. (2016). Early-life seizures alter synaptic calcium-permeable AMPA receptor function and plasticity. *Molecular and Cellular Neurosciences*, 76:11–20.

- Liu, S. J. and Zukin, R. S. (2007). Ca^{2+} -permeable AMPA receptors in synaptic plasticity and neuronal death. *Trends in Neurosciences*, 30(3):126–134.
- Liu, S.-Q. J. and Cull-Candy, S. G. (2000). Synaptic activity at calcium-permeable AMPA receptors induces a switch in receptor subtype. *Nature*, 405(6785):454–458.
- Liu, Y.-m. C. (2008). Medium-chain triglyceride (MCT) ketogenic therapy. *Epilepsia*, 49 Suppl 8:33–36.
- Loddenkemper, T., Talos, D. M., Cleary, R. T., Joseph, A., Snchez Fernndez, I., Alexopoulos, A., Kotagal, P., Najm, I., and Jensen, F. E. (2014). Subunit composition of glutamate and γ -aminobutyric acid receptors in status epilepticus. *Epilepsy Research*, 108(4):605–615.
- Loscher, W. (2011). Critical review of current animal models of seizures and epilepsy used in the discovery and development of new antiepileptic drugs. *Seizure*, 20(5):359–368.
- Loscher, W., Klitgaard, H., Twyman, R. E., and Schmidt, D. (2013). New avenues for anti-epileptic drug discovery and development. *Nature Reviews. Drug Discovery*, 12(10):757–776.
- Loweth, J. A., Scheyer, A. F., Milovanovic, M., LaCrosse, A. L., Flores-Barrera, E., Werner, C. T., Li, X., Ford, K. A., Le, T., Olive, M. F., Szumlinski, K. K., Tseng, K. Y., and Wolf, M. E. (2014). Synaptic depression via mGluR1 positive allosteric modulation suppresses cue-induced cocaine craving. *Nature Neuroscience*, 17(1):73–80.
- Lu, W., Isozaki, K., Roche, K. W., and Nicoll, R. A. (2010). Synaptic targeting of AMPA receptors is regulated by a CaMKII site in the first intracellular loop of GluA1. *Proceedings of the National Academy of Sciences of the United States of America*, 107(51):22266–22271.
- Lu, W. and Roche, K. W. (2012). Posttranslational regulation of AMPA receptor trafficking and function. *Current Opinion in Neurobiology*, 22(3):470–479.
- Lu, W., Shi, Y., Jackson, A. C., Bjorgan, K., During, M. J., Sprengel, R., Seeburg, P. H., and Nicoll, R. A. (2009). Subunit composition of synaptic AMPA receptors revealed by a single-cell genetic approach. *Neuron*, 62(2):254–268.

- Lu, Y., Zhong, C., Wang, L., Wei, P., He, W., Huang, K., Zhang, Y., Zhan, Y., Feng, G., and Wang, L. (2016). Optogenetic dissection of ictal propagation in the hippocampal-entorhinal cortex structures. *Nature Communications*, 7:10962.
- Lu, Z., Jiang, Y.-P., Wu, C.-Y. C., Ballou, L. M., Liu, S., Carpenter, E. S., Rosen, M. R., Cohen, I. S., and Lin, R. Z. (2013). Increased persistent sodium current due to decreased PI3k signaling contributes to QT prolongation in the diabetic heart. *Diabetes*, 62(12):4257–4265.
- Lutas, A. and Yellen, G. (2013). The ketogenic diet: metabolic influences on brain excitability and epilepsy. *Trends in Neurosciences*, 36(1):32–40.
- Ma, W., Berg, J., and Yellen, G. (2007). Ketogenic diet metabolites reduce firing in central neurons by opening K(ATP) channels. *The Journal of Neuroscience*, 27(14):3618–3625.
- Magiorkinis, E., Diamantis, A., Sidiropoulou, K., Panteliadis, C., Magiorkinis, E., Diamantis, A., Sidiropoulou, K., and Panteliadis, C. (2014). Highlights in the history of epilepsy: The last 200 years, highlights in the history of epilepsy: The last 200 years. *Epilepsy Research and Treatment, Epilepsy Research and Treatment*, 2014, 2014:e582039.
- Magistretti, J. and Alonso, A. (2002). Fine gating properties of channels responsible for persistent sodium current generation in entorhinal cortex neurons. *The Journal of General Physiology*, 120(6):855–873.
- Maher, M. P., Wu, N., Ravula, S., Ameriks, M. K., Savall, B. M., Liu, C., Lord, B., Wyatt, R. M., Matta, J. A., Dugovic, C., Yun, S., Donck, L. V., Steckler, T., Wickenden, A. D., Carruthers, N. I., and Lovenberg, T. W. (2016). Discovery and characterization of AMPA receptor modulators selective for TARP γ -8. *Journal of Pharmacology and Experimental Therapeutics*, 357(2):394–414.
- Malkin, S. L., Amakhin, D. V., Veniaminova, E. A., Kim, K. K., Zubareva, O. E., Magazanik, L. G., and Zaitsev, A. V. (2016). Changes of AMPA receptor properties in the neocortex and hippocampus following pilocarpine-induced status epilepticus in rats. *Neuroscience*, 327:146–155.
- Mangan, P. S. and Kapur, J. (2004). Factors underlying bursting behavior in a network of cultured hippocampal neurons exposed to zero magnesium. *Journal of Neurophysiology*, 91(2):946–957.

- Mantegazza, M., Curia, G., Biagini, G., Ragsdale, D. S., and Avoli, M. (2010). Voltage-gated sodium channels as therapeutic targets in epilepsy and other neurological disorders. *The Lancet. Neurology*, 9(4):413–424.
- Marban, E., Yamagishi, T., and Tomaselli, G. F. (1998). Structure and function of voltage-gated sodium channels. *The Journal of Physiology*, 508(Pt 3):647–657.
- Marciani, M. G., Gotman, J., Andermann, F., and Olivier, A. (1985). Patterns of seizure activation after withdrawal of antiepileptic medication. *Neurology*, 35(11):1537–1543.
- Matsuda, S., Launey, T., Mikawa, S., and Hirai, H. (2000). Disruption of AMPA receptor GluR2 clusters following long-term depression induction in cerebellar Purkinje neurons. *The EMBO Journal*, 19(12):2765–2774.
- Mattison, H., Bagal, A., Mohammadi, M., Pulimood, N., Reich, C., Alger, B., Kao, J., and Thompson, S. (2014). Evidence of calcium-permeable AMPA receptors in dendritic spines of CA1 pyramidal neurons. *Journal of Neurophysiology*, 112(2):263–275.
- McGee, T. P., Bats, C., Farrant, M., and Cull-Candy, S. G. (2015). Auxiliary subunit GSG11 acts to suppress calcium-permeable AMPA receptor function. *The Journal of Neuroscience*, 35(49):16171–16179.
- Meldrum, B. S. (1993). Excitotoxicity and selective neuronal loss in epilepsy. *Brain Pathology (Zurich, Switzerland)*, 3(4):405–412.
- Meldrum, B. S. and Rogawski, M. A. (2007). Molecular targets for antiepileptic drug development. *Neurotherapeutics: The Journal of the American Society for Experimental Neurotherapeutics*, 4(1):18–61.
- Menuz, K., Stroud, R. M., Nicoll, R. A., and Hays, F. A. (2007). TARP auxiliary subunits switch AMPA receptor antagonists into partial agonists. *Science*, 318(5851):815–817.
- Mohan, H., Verhoog, M. B., Doreswamy, K. K., Eyal, G., Aardse, R., Lodder, B. N., Goriounova, N. A., Asamoah, B., Brakspear, A. B. C. B., Groot, C., Sluis, S. v. d., Testa-Silva, G., Obermayer, J., Boudewijns, Z. S. R. M., Narayanan, R. T., Baayen, J. C., Segev, I., Mansvelder, H. D., and Kock, C. P. J. d. (2015). Dendritic and axonal architecture of individual pyramidal neurons across layers of adult human neocortex. *Cerebral Cortex*, 25(12):4839–4853.

- Morace, R., DI Gennaro, G., Quarato, P., D’Aniello, A., Mascia, A., Grammaldo, L., DE Risi, M., Sparano, A., DE Angelis, M., DI Cola, F., Solari, D., and Esposito, V. (2016). Deep brain stimulation for intractable epilepsy. *Journal of Neurosurgical Sciences*, 60(2).
- Morita, D., Rah, J., and Isaac, J. (2014). Incorporation of inwardly rectifying AMPA receptors at silent synapses during hippocampal long-term potentiation. *Philosophical Transactions of the Royal Society B: Biological Sciences*, 369(1633):20130156.
- Morris, G., Jiruska, P., Jefferys, J. G. R., and Powell, A. D. (2016). A New Approach of Modified Submerged Patch Clamp Recording Reveals Interneuronal Dynamics during Epileptiform Oscillations. *Frontiers in Neuroscience*, 10:519.
- Mosbacher, J., Schoepfer, R., Monyer, H., Burnashev, N., Seeburg, P. H., and Ruppersberg, J. P. (1994). A molecular determinant for submillisecond desensitization in glutamate receptors. *Science (New York, N.Y.)*, 266(5187):1059–1062.
- Mylona, A., Theillet, F.-X., Foster, C., Cheng, T. M., Miralles, F., Bates, P. A., Selenko, P., and Treisman, R. (2016). Opposing effects of Elk-1 multisite phosphorylation shape its response to ERK activation. *Science*, 354(6309):233–237.
- Nakazawa, T., Komai, S., Tezuka, T., Hisatsune, C., Umemori, H., Semba, K., Mishina, M., Manabe, T., and Yamamoto, T. (2001). Characterization of Fyn-mediated tyrosine phosphorylation sites on glur2 (NR2b) subunit of the N-methyl-D-aspartate receptor. *The Journal of Biological Chemistry*, 276(1):693–699.
- Nebeling, L. C., Miraldi, F., Shurin, S. B., and Lerner, E. (1995). Effects of a ketogenic diet on tumor metabolism and nutritional status in pediatric oncology patients: two case reports. *Journal of the American College of Nutrition*, 14(2):202–208.
- Neuman, R., Cherubini, E., and Ben-Ari, Y. (1988). Epileptiform bursts elicited in CA3 hippocampal neurons by a variety of convulsants are not blocked by N-methyl-D-aspartate antagonists. *Brain Research*, 459(2):265–274.
- Nishimura, T., Imai, H., Minabe, Y., Sawa, A., and Kato, N. (2006). Beneficial effects of FK506 for experimental temporal lobe epilepsy. *Neuroscience Research*, 56(4):386–390.

- Noh, K.-M., Hwang, J.-Y., Follenzi, A., Athanasiadou, R., Miyawaki, T., Grealia, J. M., Bennett, M. V. L., and Zukin, R. S. (2012). Repressor element-1 silencing transcription factor (REST)-dependent epigenetic remodeling is critical to ischemia-induced neuronal death. *Proceedings of the National Academy of Sciences of the United States of America*, 109(16):962–971.
- Noh, K.-M., Yokota, H., Mashiko, T., Castillo, P. E., Zukin, R. S., and Bennett, M. V. L. (2005). Blockade of calcium-permeable AMPA receptors protects hippocampal neurons against global ischemia-induced death. *Proceedings of the National Academy of Sciences of the United States of America*, 102(34):12230–12235.
- Nowak, L., Bregestovski, P., Ascher, P., Herbet, A., and Prochiantz, A. (1984). Magnesium gates glutamate-activated channels in mouse central neurones. *Nature*, 307(5950):462–465.
- Oberheim, N. A., Takano, T., Han, X., He, W., Lin, J. H. C., Wang, F., Xu, Q., Wyatt, J. D., Pilcher, W., Ojemann, J. G., Ransom, B. R., Goldman, S. A., and Nedergaard, M. (2009). Uniquely hominid features of adult human astrocytes. *The Journal of Neuroscience*, 29(10):3276–3287.
- O’Brien, J. E. and Meisler, M. H. (2013). Sodium channel SCN8a (Nav1.6): properties and de novo mutations in epileptic encephalopathy and intellectual disability. *Behavioral and Psychiatric Genetics*, 4:213.
- Ogoshi, F., Yin, H. Z., Kuppumbatti, Y., Song, B., Amindari, S., and Weiss, J. H. (2005). Tumor necrosis-factor-alpha (TNF- α) induces rapid insertion of Ca²⁺-permeable α -amino-3-hydroxyl-5-methyl-4-isoxazole-propionate (AMPA)/kainate (Ca-A/K) channels in a subset of hippocampal pyramidal neurons. *Experimental Neurology*, 193(2):384–393.
- Oh, M. C., Derkach, V. A., Guire, E. S., and Soderling, T. R. (2006). Extrasynaptic membrane trafficking regulated by GluR1 serine 845 phosphorylation primes AMPA receptors for long-term potentiation. *The Journal of Biological Chemistry*, 281(2):752–758.
- Opazo, P., Labrecque, S., Tigaret, C. M., Frouin, A., Wiseman, P. W., De Koninck, P., and Choquet, D. (2010). CaMKII triggers the diffusional trapping of surface AMPARs through phosphorylation of stargazin. *Neuron*, 67(2):239–252.

- Ota, Y., Zanetti, A. T., Hallock, R. M., Ota, Y., Zanetti, A. T., and Hallock, R. M. (2013). The role of astrocytes in the regulation of synaptic plasticity and memory formation, the role of astrocytes in the regulation of synaptic plasticity and memory formation. *Neural Plasticity, Neural Plasticity*, 2013, 2013:e185463.
- Otto, C., Kaemmerer, U., Illert, B., Muehling, B., Pfetzer, N., Wittig, R., Voelker, H. U., Thiede, A., and Coy, J. F. (2008). Growth of human gastric cancer cells in nude mice is delayed by a ketogenic diet supplemented with omega-3 fatty acids and medium-chain triglycerides. *BMC Cancer*, 8:122.
- Pal, S., Sombati, S., Limbrick Jr., D. D., and DeLorenzo, R. J. (1999). In vitro status epilepticus causes sustained elevation of intracellular calcium levels in hippocampal neurons. *Brain Research*, 851(12):20–31.
- Pandey, S. P., Rai, R., Gaur, P., and Prasad, S. (2015). Development- and age-related alterations in the expression of AMPA receptor subunit GluR2 and its trafficking proteins in the hippocampus of male mouse brain. *Biogerontology*, 16(3):317–328.
- Parent, J. M., Janumpalli, S., McNamara, J. O., and Lowenstein, D. H. (1998). Increased dentate granule cell neurogenesis following amygdala kindling in the adult rat. *Neuroscience Letters*, 247(1):9–12.
- Park, P., Sanderson, T. M., Amici, M., Choi, S.-L., Bortolotto, Z. A., Zhuo, M., Kaang, B.-K., and Collingridge, G. L. (2016). Calcium-permeable AMPA receptors mediate the induction of the protein kinase A-dependent component of long-term potentiation in the hippocampus. *The Journal of Neuroscience*, 36(2):622–631.
- Park, Y. Y., Johnston, D., and Gray, R. (2013). Slowly inactivating component of Na⁺ current in peri-somatic region of hippocampal CA1 pyramidal neurons. *Journal of Neurophysiology*, 109(5):1378–1390.
- Passafaro, M., Pich, V., and Sheng, M. (2001). Subunit-specific temporal and spatial patterns of AMPA receptor exocytosis in hippocampal neurons. *Nature Neuroscience*, 4(9):917–926.
- Paul, S., Nairn, A. C., Wang, P., and Lombroso, P. J. (2003). NMDA-mediated activation of the tyrosine phosphatase STEP regulates the duration of ERK signaling. *Nature Neuroscience*, 6(1):34–42.

- Paxinos, G., Watson, C., Pennisi, M., and Topple, A. (1985). Bregma, lambda and the interaural midpoint in stereotaxic surgery with rats of different sex, strain and weight. *Journal of Neuroscience Methods*, 13(2):139–143.
- Payandeh, J., Scheuer, T., Zheng, N., and Catterall, W. A. (2011). The crystal structure of a voltage-gated sodium channel. *Nature*, 475(7356):353–358.
- Payne, N. E., Cross, J. H., Sander, J. W., and Sisodiya, S. M. (2011). The ketogenic and related diets in adolescents and adults A review. *Epilepsia*, 52(11):1941–1948.
- Pedersen, S., Kvist, T., Rathje, M., Bruner-Osborne, H., Andreassen, T., and Madsen, K. (2016). Novel combination of calcium and pH biosensors reveals pyruvate as an inhibitor of ionotropic glutamate receptors. In *FENS abstract book*.
- Peng, P. L., Zhong, X., Tu, W., Soundarapandian, M. M., Molner, P., Zhu, D., Lau, L., Liu, S., Liu, F., and Lu, Y. (2006). ADAR2-dependent RNA editing of AMPA receptor subunit GluR2 determines vulnerability of neurons in forebrain ischemia. *Neuron*, 49(5):719–733.
- Plant, K., Pelkey, K. A., Bortolotto, Z. A., Morita, D., Terashima, A., McBain, C. J., Collingridge, G. L., and Isaac, J. T. R. (2006). Transient incorporation of native GluR2-lacking AMPA receptors during hippocampal long-term potentiation. *Nature Neuroscience*, 9(5):602–604.
- Poon, M. M. and Chen, L. (2008). Retinoic acid-gated sequence-specific translational control by RAR α . *Proceedings of the National Academy of Sciences of the United States of America*, 105(51):20303–20308.
- Psarropoulou, C. and Avoli, M. (1992). CPP, an NMDA-receptor antagonist, blocks 4-aminopyridine-induced spreading depression episodes but not epileptiform activity in immature rat hippocampal slices. *Neuroscience Letters*, 135(1):139–143.
- Pulsifer, M. B., Gordon, J. M., Brandt, J., Vining, E. P., and Freeman, J. M. (2001). Effects of ketogenic diet on development and behaviour: preliminary report of a prospective study. *Developmental Medicine and Child Neurology*, 43(5):301–306.
- Qiao, X., Werkman, T. R., Gorter, J. A., Wadman, W. J., and van Vliet, E. A. (2013). Expression of sodium channel α subunits 1.1, 1.2 and 1.6 in rat hippocampus after kainic acid-induced epilepsy. *Epilepsy Research*, 106(12):17–28.

- Quirk, J. C., Siuda, E. R., and Nisenbaum, E. S. (2004). Molecular determinants responsible for differences in desensitization kinetics of AMPA receptor splice variants. *The Journal of Neuroscience*, 24(50):11416–11420.
- Racine, R. J. (1972). Modification of seizure activity by electrical stimulation. I. After-discharge threshold. *Electroencephalography and Clinical Neurophysiology*, 32(3):269–279.
- Ragsdale, D. S. and Avoli, M. (1998). Sodium channels as molecular targets for antiepileptic drugs. *Brain Research Reviews*, 26(1):16–28.
- Raimondo, J. V., Burman, R. J., Katz, A. A., and Akerman, C. J. (2015). Ion dynamics during seizures. *Frontiers in Cellular Neuroscience*, 9:419.
- Rajasekaran, K., Todorovic, M., and Kapur, J. (2012). Calcium-permeable AMPA receptors are expressed in a rodent model of status epilepticus. *Annals of Neurology*, 72(1):91–102.
- Rakhade, S. N., Fitzgerald, E. F., Klein, P. M., Zhou, C., Sun, H., Huganir, R. L., and Jensen, F. E. (2012). Glutamate receptor 1 phosphorylation at Serine 831 and 845 modulates seizure susceptibility and hippocampal hyperexcitability after early life seizures. *Journal of Neuroscience*, 32(49):17800–17812.
- Rakhade, S. N., Zhou, C., Aujla, P. K., Fishman, R., Sucher, N. J., and Jensen, F. E. (2008). Early alterations of AMPA receptors mediate synaptic potentiation induced by neonatal seizures. *The Journal of Neuroscience*, 28(32):7979–7990.
- Reger, M. A., Henderson, S. T., Hale, C., Cholerton, B., Baker, L. D., Watson, G. S., Hyde, K., Chapman, D., and Craft, S. (2004). Effects of β -hydroxybutyrate on cognition in memory-impaired adults. *Neurobiology of Aging*, 25(3):311–314.
- Remy, S., Gabriel, S., Urban, B. W., Dietrich, D., Lehmann, T. N., Elger, C. E., Heinemann, U., and Beck, H. (2003). A novel mechanism underlying drug resistance in chronic epilepsy. *Annals of Neurology*, 53(4):469–479.
- Rho, J. M. and Stafstrom, C. E. (2012). The ketogenic diet as a treatment paradigm for diverse neurological disorders. *Neuropharmacology*, 3:59.
- Rogawski, M. A. (2013). AMPA receptors as a molecular target in epilepsy therapy. *Acta Neurologica Scandinavica*, 127:9–18.

- Rogawski, M. A. (2016). A fatty acid in the MCT ketogenic diet for epilepsy treatment blocks AMPA receptors. *Brain*, 139(2):306–309.
- Rogawski, M. A. and Hanada, T. (2013). Preclinical pharmacology of perampanel, a selective non-competitive AMPA receptor antagonist. *Acta neurologica Scandinavica. Supplementum*, (197):19–24.
- Roopun, A. K., Simonotto, J. D., Pierce, M. L., Jenkins, A., Nicholson, C., Schofield, I. S., Whittaker, R. G., Kaiser, M., Whittington, M. A., Traub, R. D., and Cunningham, M. O. (2010). A nonsynaptic mechanism underlying interictal discharges in human epileptic neocortex. *Proceedings of the National Academy of Sciences of the United States of America*, 107(1):338–343.
- Rouach, N., Byrd, K., Petralia, R. S., Elias, G. M., Adesnik, H., Tomita, S., Karimzadegan, S., Kealey, C., Brecht, D. S., and Nicoll, R. A. (2005). TARP γ -8 controls hippocampal AMPA receptor number, distribution and synaptic plasticity. *Nature Neuroscience*, 8(11):1525–1533.
- Royeck, M., Horstmann, M.-T., Remy, S., Reitze, M., Yaari, Y., and Beck, H. (2008). Role of axonal Nav1.6 sodium channels in action potential initiation of CA1 pyramidal neurons. *Journal of Neurophysiology*, 100(4):2361–2380.
- Rozov, A. and Burnashev, N. (1999). Polyamine-dependent facilitation of postsynaptic AMPA receptors counteracts paired-pulse depression. *Nature*, 401(6753):594–598.
- Rozov, A., Sprengel, R., and Seeburg, P. H. (2012). GluA2-lacking AMPA receptors in hippocampal CA1 cell synapses: evidence from gene-targeted mice. *Frontiers in Molecular Neuroscience*, 5:22.
- Russmann, V., Salvamoser, J. D., Rettenbeck, M. L., Komori, T., and Potschka, H. (2016). Synergism of perampanel and zonisamide in the rat amygdala kindling model of temporal lobe epilepsy. *Epilepsia*, 57(4):638–647.
- Russo, I., Bonini, D., Via, L. L., Barlati, S., and Barbon, A. (2013). AMPA receptor properties are modulated in the early stages following pilocarpine-induced status epilepticus. *Neuromolecular Medicine*, 15(2):324–338.

- Saavedra, A., Puigdemvol, M., Tyebji, S., Kurup, P., Xu, J., Gins, S., Alberch, J., Lombroso, P. J., and Prez-Navarro, E. (2015). BDNF induces striatal-enriched protein tyrosine phosphatase 61 degradation through the proteasome. *Molecular Neurobiology*, 53(6):4261–4273.
- Salter, M. W. and Kalia, L. V. (2004). Src kinases: a hub for NMDA receptor regulation. *Nature Reviews. Neuroscience*, 5(4):317–328.
- Sanchez, R. M., Dai, W., Levada, R. E., Lippman, J. J., and Jensen, F. E. (2005). AMPA/kainate receptor-mediated downregulation of GABAergic synaptic transmission by calcineurin after seizures in the developing rat brain. *The Journal of Neuroscience*, 25(13):3442–3451.
- Sanchez, R. M., Koh, S., Rio, C., Wang, C., Lamperti, E. D., Sharma, D., Corfas, G., and Jensen, F. E. (2001). Decreased glutamate receptor 2 expression and enhanced epileptogenesis in immature rat hippocampus after perinatal hypoxia-induced seizures. *The Journal of Neuroscience*, 21(20):8154–8163.
- Sanderson, J. L., Gorski, J. A., and Dell’Acqua, M. L. (2016). NMDA receptor-dependent LTD requires transient synaptic incorporation of Ca^{2+} -permeable AMPARs mediated by AKAP150-anchored PKA and calcineurin. *Neuron*, 89(5):1000–1015.
- Sanderson, J. L., Gorski, J. A., Gibson, E. S., Lam, P., Freund, R. K., Chick, W. S., and Dell’Acqua, M. L. (2012). AKAP150-anchored calcineurin regulates synaptic plasticity by limiting synaptic incorporation of Ca^{2+} -permeable AMPA receptors. *The Journal of Neuroscience*, 32(43):15036–15052.
- Schubert, M., Siegmund, H., Pape, H.-C., and Albrecht, D. (2005). Kindling-induced changes in plasticity of the rat amygdala and hippocampus. *Learning & Memory (Cold Spring Harbor, N.Y.)*, 12(5):520–526.
- Schwenk, J., Baehrens, D., Haupt, A., Bildl, W., Boudkazi, S., Roeper, J., Fakler, B., and Schulte, U. (2014). Regional diversity and developmental dynamics of the AMPA-receptor proteome in the mammalian brain. *Neuron*, 84(1):41–54.
- Schwenk, J., Harmel, N., Zolles, G., Bildl, W., Kulik, A., Heimrich, B., Chisaka, O., Jonas, P., Schulte, U., Fakler, B., and Klocker, N. (2009). Functional proteomics identify

- cornichon proteins as auxiliary subunits of AMPA receptors. *Science (New York, N.Y.)*, 323(5919):1313–1319.
- Sepkuty, J. P., Cohen, A. S., Eccles, C., Rafiq, A., Behar, K., Ganel, R., Coulter, D. A., and Rothstein, J. D. (2002). A neuronal glutamate transporter contributes to neurotransmitter GABA synthesis and epilepsy. *The Journal of Neuroscience*, 22(15):6372–6379.
- Setou, M., Seog, D.-H., Tanaka, Y., Kanai, Y., Takei, Y., Kawagishi, M., and Hirokawa, N. (2002). Glutamate-receptor-interacting protein GRIP1 directly steers kinesin to dendrites. *Nature*, 417(6884):83–87.
- Shaafi, S., Mahmoudi, J., Pashapour, A., Farhoudi, M., Sadigh-Eteghad, S., and Akbari, H. (2014). Ketogenic diet provides neuroprotective effects against ischemic stroke neuronal damages. *Advanced Pharmaceutical Bulletin*, 4(Suppl 2):479–481.
- Shah, M. M., Anderson, A. E., Leung, V., Lin, X., and Johnston, D. (2004). Seizure-induced plasticity of h channels in entorhinal cortical layer III pyramidal neurons. *Neuron*, 44(3):495–508.
- Shelley, C., Farrant, M., and Cull-Candy, S. G. (2012). TARP-associated AMPA receptors display an increased maximum channel conductance and multiple kinetically distinct open states. *The Journal of Physiology*, 590(Pt 22):5723–5738.
- Shepherd, J. D., Rumbaugh, G., Wu, J., Chowdhury, S., Plath, N., Kuhl, D., Huganir, R. L., and Worley, P. F. (2006). Arc/Arg3.1 mediates homeostatic synaptic scaling of AMPA receptors. *Neuron*, 52(3):475–484.
- Sills, G. J. and Brodie, M. J. (2001). Update on the mechanisms of action of antiepileptic drugs. *Epileptic Disorders: International Epilepsy Journal with Videotape*, 3(4):165–172.
- Sills, M. A., Forsythe, W. I., and Haidukewych, D. (1986). Role of octanoic and decanoic acids in the control of seizures. *Archives of Disease in Childhood*, 61(12):1173–1177.
- Simon, A., Traub, R. D., Vladimirov, N., Jenkins, A., Nicholson, C., Whittaker, R. G., Schofield, I., Clowry, G. J., Cunningham, M. O., and Whittington, M. A. (2014). Gap junction networks can generate both ripple-like and fast ripple-like oscillations. *The European Journal of Neuroscience*, 39(1):46–60.

- Sisodiya, S. M. (2003). Mechanisms of antiepileptic drug resistance. *Current Opinion in Neurology*, 16(2):197–201.
- Sloviter, R. S., Dean, E., Sollas, A. L., and Goodman, J. H. (1996). Apoptosis and necrosis induced in different hippocampal neuron populations by repetitive perforant path stimulation in the rat. *Journal of Comparative Neurology*, 366(3):516–533.
- Smith, T. C., Wang, L. Y., and Howe, J. R. (2000). Heterogeneous conductance levels of native AMPA receptors. *The Journal of Neuroscience*, 20(6):2073–2085.
- Sobolevsky, A. I., Rosconi, M. P., and Gouaux, E. (2009). X-ray structure, symmetry and mechanism of an AMPA-subtype glutamate receptor. *Nature*, 462(7274):745–756.
- Sommer, B., Kohler, M., Sprengel, R., and Seeburg, P. H. (1991). RNA editing in brain controls a determinant of ion flow in glutamate-gated channels. *Cell*, 67(1):11–19.
- Song, I. and Huganir, R. L. (2002). Regulation of AMPA receptors during synaptic plasticity. *Trends in Neurosciences*, 25(11):578–588.
- Song, I., Kamboj, S., Xia, J., Dong, H., Liao, D., and Huganir, R. L. (1998). Interaction of the N-ethylmaleimide-sensitive factor with AMPA receptors. *Neuron*, 21(2):393–400.
- Soto, D., Coombs, I. D., Gratacs-Batlle, E., Farrant, M., and Cull-Candy, S. G. (2014). Molecular mechanisms contributing to TARP regulation of channel conductance and polyamine block of calcium-permeable AMPA receptors. *The Journal of Neuroscience*, 34(35):11673–11683.
- Soto, D., Coombs, I. D., Kelly, L., Farrant, M., and Cull-Candy, S. G. (2007). Stargazin attenuates intracellular polyamine block of calcium-permeable AMPA receptors. *Nature Neuroscience*, 10(10):1260–1267.
- Spiers, H. J. (2012). Hippocampal formation. *The Encyclopedia of Human Behaviour*, 2:297–304.
- Spruston, N. (2008). Pyramidal neurons: dendritic structure and synaptic integration. *Nature Reviews. Neuroscience*, 9(3):206–221.
- St-Onge, M.-P. and Jones, P. J. H. (2002). Physiological effects of medium-chain triglycerides: potential agents in the prevention of obesity. *The Journal of Nutrition*, 132(3):329–332.

- Stafstrom, C. E. (2007). Persistent sodium current and its role in epilepsy. *Epilepsy Currents*, 7(1):15–22.
- Sterratt, D. C., Groen, M. R., Meredith, R. M., and van Ooyen, A. (2012). Spine calcium transients induced by synaptically-evoked action potentials can predict synapse location and establish synaptic democracy. *PLoS computational biology*, 8(6):e1002545.
- Steward, O., Wallace, C. S., Lyford, G. L., and Worley, P. F. (1998). Synaptic activation causes the mRNA for the IEG Arc to localize selectively near activated postsynaptic sites on dendrites. *Neuron*, 21(4):741–751.
- Stringer, J. L. and Colbert, C. M. (1994). Analysis of field potentials evoked in CA1 by angular bundle stimulation in the rat. *Brain Research*, 641(2):289–294.
- Studniarczyk, D., Coombs, I., Cull-Candy, S. G., and Farrant, M. (2013). TARP γ -7 selectively enhances synaptic expression of calcium-permeable AMPARs. *Nature Neuroscience*, 16(9):1266–1274.
- Sullivan, P. G., Rippey, N. A., Dorenbos, K., Concepcion, R. C., Agarwal, A. K., and Rho, J. M. (2004). The ketogenic diet increases mitochondrial uncoupling protein levels and activity. *Annals of Neurology*, 55(4):576–580.
- Sun, W., Mao, W., Meng, X., Wang, D., Qiao, L., Tao, W., Li, L., Jia, X., Han, C., Fu, M., Tong, X., Wu, X., and Wang, Y. (2012). Low-frequency repetitive transcranial magnetic stimulation for the treatment of refractory partial epilepsy: a controlled clinical study. *Epilepsia*, 53(10):1782–1789.
- Swanson, G. T., Kamboj, S. K., and Cull-Candy, S. G. (1997). Single-channel properties of recombinant AMPA receptors depend on RNA editing, splice variation, and subunit composition. *The Journal of Neuroscience*, 17(1):58–69.
- Tada, H., Koide, M., Ara, W., Shibata, Y., Funabashi, T., Suyama, K., Goto, T., and Takahashi, T. (2015). Estrous cycle-dependent phasic changes in the stoichiometry of hippocampal synaptic AMPA receptors in rats. *PLOS One*, 10(6):e0131359.
- Talos, D. M., Kwiatkowski, D. J., Cordero, K., Black, P. M., and Jensen, F. E. (2008). Cell-specific alterations of glutamate receptor expression in tuberous sclerosis complex cortical tubers. *Annals of Neurology*, 63(4):454–465.

- Tamagnini, F., Scullion, S., Brown, J. T., and Randall, A. D. (2014). Low concentrations of the solvent dimethyl sulphoxide alter intrinsic excitability properties of cortical and hippocampal pyramidal cells. *PLoS One*, 9(3):e92557.
- Teber, I., Kohling, R., Speckmann, E.-J., Barnekow, A., and Kremerskothen, J. (2004). Muscarinic acetylcholine receptor stimulation induces expression of the activity-regulated cytoskeleton-associated gene (ARC). *Brain Research. Molecular Brain Research*, 121(1-2):131–136.
- Terashima, A., Cotton, L., Dev, K. K., Meyer, G., Zaman, S., Duprat, F., Henley, J. M., Collingridge, G. L., and Isaac, J. T. R. (2004). Regulation of synaptic strength and AMPA receptor subunit composition by PICK1. *The Journal of Neuroscience*, 24(23):5381–5390.
- Terashima, A., Pelkey, K. A., Rah, J.-C., Suh, Y. H., Roche, K. W., Collingridge, G. L., McBain, C. J., and Isaac, J. T. R. (2008). An essential role for PICK1 in NMDA receptor-dependent bidirectional synaptic plasticity. *Neuron*, 57(6):872–882.
- Thavendiranathan, P., Mendonca, A., Dell, C., Likhodii, S. S., Musa, K., Iracleous, C., Cunnane, S. C., and Burnham, W. M. (2000). The MCT ketogenic diet: effects on animal seizure models. *Experimental Neurology*, 161(2):696–703.
- Thiagarajan, T. C., Lindskog, M., and Tsien, R. W. (2005). Adaptation to synaptic inactivity in hippocampal neurons. *Neuron*, 47(5):725–737.
- Tigerholm, J., Borjesson, S. I., Lundberg, L., Elinder, F., and Fransn, E. (2012). Dampening of hyperexcitability in CA1 pyramidal neurons by polyunsaturated fatty acids acting on voltage-gated ion channels. *PLoS One*, 7(9):e44388.
- Tomita, S., Byrd, R. K., Rouach, N., Bellone, C., Venegas, A., O'Brien, J. L., Kim, K. S., Olsen, O., Nicoll, R. A., and Brecht, D. S. (2007a). AMPA receptors and stargazin-like transmembrane AMPA receptor-regulatory proteins mediate hippocampal kainate neurotoxicity. *Proceedings of the National Academy of Sciences of the United States of America*, 104(47):18784–18788.
- Tomita, S., Shenoy, A., Fukata, Y., Nicoll, R. A., and Brecht, D. S. (2007b). Stargazin interacts functionally with the AMPA receptor glutamate-binding module. *Neuropharmacology*, 52(1):87–91.

- Traynelis, S. F., Silver, R. A., and Cull-Candy, S. G. (1993). Estimated conductance of glutamate receptor channels activated during EPSCs at the cerebellar mossy fiber-granule cell synapse. *Neuron*, 11(2):279–289.
- Traynelis, S. F., Wollmuth, L. P., McBain, C. J., Menniti, F. S., Vance, K. M., Ogden, K. K., Hansen, K. B., Yuan, H., Myers, S. J., and Dingledine, R. (2010). Glutamate receptor ion channels: Structure, regulation, and function. *Pharmacological Reviews*, 62(3):405–496.
- Trombin, F., Gnatkovsky, V., and Curtis, M. d. (2011). Changes in action potential features during focal seizure discharges in the entorhinal cortex of the in vitro isolated guinea pig brain. *Journal of Neurophysiology*, 106(3):1411–1423.
- Tunnicliff, G. (1996). Basis of the antiseizure action of phenytoin. *General Pharmacology*, 27(7):1091–1097.
- Turrigiano, G. G., Leslie, K. R., Desai, N. S., Rutherford, L. C., and Nelson, S. B. (1998). Activity-dependent scaling of quantal amplitude in neocortical neurons. *Nature*, 391(6670):892–896.
- Twele, F., Bankstahl, M., Klein, S., Romermann, K., and Loscher, W. (2015). The AMPA receptor antagonist NBQX exerts anti-seizure but not antiepileptogenic effects in the intrahippocampal kainate mouse model of mesial temporal lobe epilepsy. *Neuropharmacology*, 95:234–242.
- Uebachs, M., Opitz, T., Royeck, M., Dickhof, G., Horstmann, M.-T., Isom, L. L., and Beck, H. (2010). Efficacy loss of the anticonvulsant carbamazepine in mice lacking sodium channel β subunits via paradoxical effects on persistent sodium currents. *The Journal of Neuroscience*, 30(25):8489–8501.
- Uysal, H., Cevik, I. U., Soylemezoglu, F., Elibol, B., Ozdemir, Y. G., Evrenkaya, T., Saygi, S., and Dalkara, T. (2003). Is the cell death in mesial temporal sclerosis apoptotic? *Epilepsia*, 44(6):778–784.
- Van der Auwera, I., Wera, S., Van Leuven, F., and Henderson, S. T. (2005). A ketogenic diet reduces amyloid β 40 and 42 in a mouse model of Alzheimer’s disease. *Nutrition & Metabolism*, 2:28.

- Vanitallie, T. B., Nonas, C., Di Rocco, A., Boyar, K., Hyams, K., and Heymsfield, S. B. (2005). Treatment of Parkinson disease with diet-induced hyperketonemia: a feasibility study. *Neurology*, 64(4):728–730.
- Vieira, M., Fernandes, J., Burgeiro, A., Thomas, G. M., Haganir, R. L., Duarte, C. B., Carvalho, A. L., and Santos, A. E. (2010). Excitotoxicity through Ca^{2+} -permeable AMPA receptors requires Ca^{2+} -dependent JNK activation. *Neurobiology of Disease*, 40(3):645–655.
- Vlahos, C. J., Matter, W. F., Hui, K. Y., and Brown, R. F. (1994). A specific inhibitor of phosphatidylinositol 3-kinase, 2-(4-morpholinyl)-8-phenyl-4h-1-benzopyran-4-one (LY294002). *Journal of Biological Chemistry*, 269(7):5241–5248.
- Vreugdenhil, M., Hoogland, G., van Veelen, C. W. M., and Wadman, W. J. (2004). Persistent sodium current in subicular neurons isolated from patients with temporal lobe epilepsy. *The European Journal of Neuroscience*, 19(10):2769–2778.
- Vyazovskiy, V. V., Cirelli, C., Pfister-Genskow, M., Faraguna, U., and Tononi, G. (2008). Molecular and electrophysiological evidence for net synaptic potentiation in wake and depression in sleep. *Nature Neuroscience*, 11(2):200–208.
- Wagenaar, D. A., Pine, J., and Potter, S. M. (2006). Searching for plasticity in dissociated cortical cultures on multi-electrode arrays. *Journal of Negative Results in BioMedicine*, 5:16.
- Walker, M. C., White, H. S., and Sander, J. W. a. S. (2002). Disease modification in partial epilepsy. *Brain: A Journal of Neurology*, 125(Pt 9):1937–1950.
- Wang, D. and Mitchell, E. S. (2016). Cognition and synaptic-plasticity related changes in aged rats supplemented with 8- and 10-carbon medium chain triglycerides. *PLOS One*, 11(8):e0160159.
- Wang, G., Gilbert, J., and Man, H.-Y. (2012). AMPA receptor trafficking in homeostatic synaptic plasticity: functional molecules and signaling cascades. *Neural Plasticity*, 2012:e825364.
- Wang, H.-X. and Gao, W.-J. (2010). Development of calcium-permeable AMPA receptors

- and their correlation with NMDA receptors in fast-spiking interneurons of rat prefrontal cortex. *The Journal of Physiology*, 588(Pt 15):2823–2838.
- Wang, J. H. and Kelly, P. T. (1996). Regulation of synaptic facilitation by postsynaptic Ca^{2+} /CaM pathways in hippocampal CA1 neurons. *Journal of Neurophysiology*, 76(1):276–286.
- Wenthold, R., Petralia, R., Blahos, I., and Niedzielski, A. (1996). Evidence for multiple AMPA receptor complexes in hippocampal CA1/CA2 neurons. *Journal of Neuroscience*, 16(6):1982–1989.
- Wieser, H. (2004). Mesial temporal lobe epilepsy with hippocampal sclerosis. *Epilepsia*, 45(6):695–714.
- Williams, S., Hamil, N., Abramov, A. Y., Walker, M. C., and Kovac, S. (2015). Status epilepticus results in persistent overproduction of reactive oxygen species, inhibition of which is neuroprotective. *Neuroscience*, 303:160–165.
- Wiltgen, B. J., Royle, G. A., Gray, E. E., Abdipranoto, A., Thangthaeng, N., Jacobs, N., Saab, F., Tonegawa, S., Heinemann, S. F., O’Dell, T. J., Fanselow, M. S., and Vissel, B. (2010). A role for calcium-permeable AMPA receptors in synaptic plasticity and learning. *PLOS One*, 5(9):e12818.
- Wlacz, P., Socaa, K., Nieocz, D., arnowski, T., Zarnowska, I., Czuczwar, S. J., and Gasior, M. (2015). Acute anticonvulsant effects of capric acid in seizure tests in mice. *Progress in Neuro-Psychopharmacology & Biological Psychiatry*, 57:110–116.
- Xie, X., Liaw, J. S., Baudry, M., and Berger, T. W. (1997). Novel expression mechanism for synaptic potentiation: alignment of presynaptic release site and postsynaptic receptor. *Proceedings of the National Academy of Sciences of the United States of America*, 94(13):6983–6988.
- Xu, J., Chatterjee, M., Baguley, T. D., Brouillette, J., Kurup, P., Ghosh, D., Kanyo, J., Zhang, Y., Seyb, K., Ononenyi, C., Foscue, E., Anderson, G. M., Gresack, J., Cuny, G. D., Glicksman, M. A., Greengard, P., Lam, T. T., Tautz, L., Nairn, A. C., Ellman, J. A., and Lombroso, P. J. (2014). Inhibitor of the tyrosine phosphatase STEP reverses cognitive deficits in a mouse model of Alzheimer’s disease. *PLoS Biol*, 12(8):e1001923.

- Xu, J., Kurup, P., Zhang, Y., Goebel-Goody, S. M., Wu, P. H., Hawasli, A. H., Baum, M. L., Bibb, J. A., and Lombroso, P. J. (2009). Extrasynaptic NMDA receptors couple preferentially to excitotoxicity via calpain-mediated cleavage of STEP. *The Journal of Neuroscience*, 29(29):9330–9343.
- Yamaguchi, S., Donevan, S. D., and Rogawski, M. A. (1993). Anticonvulsant activity of AMPA/kainate antagonists: comparison of GYKI 52466 and NBOB in maximal electroshock and chemoconvulsant seizure models. *Epilepsy Research*, 15(3):179–184.
- Yang, G., Xiong, W., Kojic, L., and Cynader, M. S. (2009). Subunit-selective palmitoylation regulates the intracellular trafficking of AMPA receptor. *European Journal of Neuroscience*, 30(1):35–46.
- Yang, J., Peng, C., and Wu, B. (2003). [Advance in signal analysis of auditory evoked potential]. *Sheng Wu Yi Xue Gong Cheng Xue Za Zhi = Journal of Biomedical Engineering = Shengwu Yixue Gongchengxue Zazhi*, 20(3):563–566.
- Yarov-Yarovoy, V., DeCaen, P. G., Westenbroek, R. E., Pan, C.-Y., Scheuer, T., Baker, D., and Catterall, W. A. (2012). Structural basis for gating charge movement in the voltage sensor of a sodium channel. *Proceedings of the National Academy of Sciences of the United States of America*, 109(2):E93–E102.
- Yelshanskaya, M. V., Singh, A. K., Sampson, J. M., Narangoda, C., Kurnikova, M., and Sobolevsky, A. I. (2016). Structural bases of noncompetitive inhibition of AMPA-subtype ionotropic glutamate receptors by antiepileptic drugs. *Neuron*, 91(6).
- Ying, Z., Babb, T. L., Comair, Y. G., Bushey, M., and Touhalisky, K. (1998). Increased densities of AMPA GluR1 subunit proteins and presynaptic mossy fiber sprouting in the fascia dentata of human hippocampal epilepsy. *Brain Research*, 798(1-2):239–246.
- Yue, C., Remy, S., Su, H., Beck, H., and Yaari, Y. (2005). Proximal persistent Na⁺ channels drive spike afterdepolarizations and associated bursting in adult CA1 pyramidal cells. *The Journal of Neuroscience*, 25(42):9704–9720.
- Zahn, R. K., Tolner, E. A., Derst, C., Gruber, C., Veh, R. W., and Heinemann, U. (2008). Reduced ictogenic potential of 4-aminopyridine in the perirhinal and entorhinal cortex of kainate-treated chronic epileptic rats. *Neurobiology of Disease*, 29(2):186–200.

- Zamanillo, D., Sprengel, R., Hvalby, i., Jensen, V., Burnashev, N., Rozov, A., Kaiser, K. M. M., Koster, H. J., Borchardt, T., Worley, P., Lubke, J., Frotscher, M., Kelly, P. H., Sommer, B., Andersen, P., Seeburg, P. H., and Sakmann, B. (1999). Importance of AMPA receptors for hippocampal synaptic plasticity but not for spatial learning. *Science*, 284(5421):1805–1811.
- Zhang, L. and Luo, X.-P. (2011). Plasticity and metaplasticity of lateral perforant path in hippocampal dentate gyrus in a rat model of febrile seizure. *Sheng li xue bao: [Acta physiologica Sinica]*, 63(2):124–130.
- Zhang, Y., Venkitaramani, D. V., Gladding, C. M., Zhang, Y., Kurup, P., Molnar, E., Collingridge, G. L., and Lombroso, P. J. (2008). The tyrosine phosphatase STEP mediates AMPA receptor endocytosis after metabotropic glutamate receptor stimulation. *The Journal of Neuroscience*, 28(42):10561–10566.
- Zimmer, T., Haufe, V., and Blechschmidt, S. (2014). Voltage-gated sodium channels in the mammalian heart. *Global Cardiology Science & Practice*, 2014(4):449–463.
- Zonouzi, M., Renzi, M., Farrant, M., and Cull-Candy, S. G. (2011). Bidirectional plasticity of calcium-permeable AMPA receptors in oligodendrocyte lineage cells. *Nature Neuroscience*, 14(11):1430–1438.
- Zwart, R., Sher, E., Ping, X., Jin, X., Sims, J. R., Chappell, A. S., Gleason, S. D., Hahn, P. J., Gardinier, K., Gernert, D. L., Hobbs, J., Smith, J. L., Valli, S. N., and Witkin, J. M. (2014). Perampanel, an antagonist of α -Amino-3-Hydroxy-5-Methyl-4-Isoxazolepropionic acid receptors, for the treatment of epilepsy: Studies in human epileptic brain and nonepileptic brain and in rodent models. *Journal of Pharmacology and Experimental Therapeutics*, 351(1):124–133.